Developing a model for designing self-compacting concrete mixes incorporating a blend of rice husk ash and calcined clay

Abubakar Muhammad

Vollständiger Abdruck der von der Fakultät für Bauingenieurwesen und Umweltwissenschaften der Universität der Bundeswehr München zur Erlangung des akademischen Grades eines

Doktor-Ingenieurs (Dr.-Ing.)

angenommenen Dissertation.

Gutachter/Gutachterin:

1. Univ.-Prof. Dr.-Ing. Karl-Christian Thienel
2. Univ.-Prof. Dr.-Ing. Harald Garrecht

Die Dissertation wurde am 16.10.2023 bei der Universität der Bundeswehr München eingereicht und durch die Fakultät für Bauingenieurwesen und Umweltwissenschaften am 16.12.2023 angenommen. Die mündliche Prüfung fand am 19.12.2023 statt.

Acknowledgement

This research project is funded by the German Academic Exchange Service (DAAD) and the Nigerian Petroleum Technology Development Fund (PTDF) under the Nigerian-German Postgraduate Training Programme PhD, 2019. I gratefully acknowledge the financial support from these institutions. I would like to acknowledge the financial support, provision of conducive learning environment, and technical support from the Universität der Bundeswehr München as the host university, where the research activities are conducted. I would also acknowledge the Fellowship support I received from Abubakar Tafawa Balewa University Bauchi, Nigeria.

I would like to express my deepest gratitude to my PhD supervisor and head of the institute of construction materials, Univ.-Prof. Dr.-Ing. Karl-Christian Thienel, for his continuous mentorship, guidance, patience, and prompt feedback on all my submissions. Vielen Dank!

I am also grateful to all my colleagues, the technical laboratory staff, and the head of laboratory of the institute of construction materials in person of Dr.-Ing. Nancy Beuntner, for their support and guidance throughout the research period.

Last but not least, I would like to thank my family and friends for their understanding and support throughout the research program.

Zusammenfassung

Mit dem Bevölkerungswachstum in den afrikanischen Ländern südlich der Sahara steigt auch die Nachfrage nach Wohnraum und Infrastrukturprojekten für die Beton benötigt wird, was zu einem erhöhten Bedarf an Zement für dessen Herstellung führt. Nigeria - das bevölkerungsreichste Land in der afrikanischen Region - hat einen massiven Ausbau der Infrastruktur eingeleitet, um unter anderem den durch die rasche Verstädterung und das hohe jährliche Bevölkerungswachstum verursachten Bedarf an Wohnraum zu decken. Die Herstellung von Zement, einem wesentlichen Bestandteil von Beton, stellt zwei große Herausforderungen dar. Erstens wird für die Herstellung und das Mahlen von Zement eine große Menge an Energie benötigt. Dies ist vor allem in Entwicklungsländern ein Problem, das den Zement verteuert. Zweitens ist die Zementherstellung für etwa 6 % bis 10 % der weltweiten Kohlenstoffdioxidemissionen verantwortlich. Die Kohlenstoffdioxidemissionen aus der Zementherstellung könnten durch eine kreislauforientierte Kohlenstoffwirtschaft mit Reduzierung, Wiederverwendung, Recycling und Beseitigung von CO_2 verringert werden.

Diese Studie befasst sich mit der Möglichkeit, die CO_2-Emissionen durch den teilweisen Ersatz von Zement durch einen Zementersatz bzw. Betonzusatzstoff (Supplementary cementitious material (SCM)) zu senken. Die Leistungsfähigkeit zweier in Nigeria lokal verfügbarer SCMs, kalziniertem Ton (calcined clay (CC)) und Reisschalenasche (Rice husk ash ((RHA)), als teilweiser Ersatz für Zement in Mörtel und Beton wurde bestimmt. Der erste Teil befasst sich mit der Bestimmung des puzzolanischen Potenzials von nigerianischen kalzinierten Tonen (NCC) im Vergleich zu einem deutschen kalzinierten Ton und RHA als Teilersatz für Zement im Allgemeinen. Zu diesem Zweck wurden vier natürlich vorkommende Tonproben (zwei kaolinitreiche und zwei smektitreiche) aus verschiedenen Gebieten in der Nähe des Zementwerks Ashaka im nigerianischen Bundesstaat Gombe gesammelt und in einem Labor kalziniert. Die mineralogische Charakterisierung der Tone erfolgte mittels XRD. Die Hydratationskinetik der kalzinierten Ton-Zement-Systeme wurde durch isothermische Kalorimetrie überwacht. Die Verarbeitbarkeit wurde mit Hilfe des Fließmaßes bestimmt. Die Reaktivität der kalzinierten Tone wurde anhand der Löslichkeit von Si- und Al-Ionen und des Festigkeitsaktivitätsindex (SAI) bestimmt. Die erzielten Ergebnisse wurden dann mit dem deutschen CC für die spätere Verwendung bei der Herstellung von Beton verglichen, da die erforderliche Menge für die Versuche nur schwer aus Nigeria nach Deutschland zu transportieren ist.

Reishülsen aus der Umgebung von Zaria im Bundesstaat Kaduna, Nigeria, wurden in einem Elektroofen kalziniert, um RHA zu erhalten und mit einer Labormühle gemahlen. Das RHA-Pulver wurde mit den für die CCs verwendeten Methoden charakterisiert und anschließend bewertet.

Für die Anwendung der oben beschriebenen CC und RHA in Beton sieht das Versuchsprogramm dieser Studie die Verwendung von selbstverdichtendem Beton (SCC) vor, um einen dauerhaften Beton herzustellen, der zudem einen guten Widerstand gegen das Eindringen von Chloridionen aufweist. Dies liegt daran, dass sowohl CC als auch RHA im Vergleich zu Zement einen höheren Wasserbedarf und eine größere spezifische Oberfläche (SSA) haben, was ihre Verwendung als teilweiser Ersatz für Zement in SCC kritischer macht. Ziel ist es, die anspruchsvollen physikalischen Eigenschaften von CC und RHA zu berücksichtigen und einen Pulver-Typ SCC mit einem niedrigeren Anteil an Portlandzement (OPC) zu entwickeln, um einen ökoeffizienten und dauerhaften SCC zu erhalten. Daher wird

zunächst der OPC zunächst teilweise durch 15 Vol.-% Kalksteinmehl (LP) ersetzt, was zu einem Portlandkalksteinzement (PLC) führt. Nachfolgend werden bis zu 40 Vol.-% des PLC in binären und ternären Mischungen durch CC und/oder RHA ersetzt. Für den Entwurf der SCC wird ein empirisches Verfahren verwendet. Der Bindemittelleim des SCC wurde zunächst unter Berücksichtigung der physikalischen Eigenschaften von CC und RHA entwickelt. Dieser Bindemittelleim bildet zusammen mit der feinen Gesteinskörnung (FA) einen selbstverdichtenden Mörtel (SC-M). Schließlich wurde der SC-M zusammen mit der gröberen Gesteinskörnung (CA) zum gewünschten SCC kombiniert.

Zwei volumetrische Wasser-Pulver-Verhältnisse (V_w/V_p) wurden unter Berücksichtigung der physikalischen Eigenschaften von CC und RHA verwendet, zunächst Vw/Vp = 0,875 für die Referenzmischungen (PLC-SCC) und SCC-Mischungen, die in binären Systemen bis zu 40 Vol.-% CC als teilweisen Ersatz für PLC in SCC enthalten. Für die Verwendung von RHA in SCC wurde ein individuelles Vw/Vp für jede Stufe des PLC-Ersatzes durch RHA verwendet. Für den Vergleich von Referenz-SCC und SCC, der mit binären und ternären Mischungen von CC und RHA hergestellt wurde, wurde ein Vw/Vp = 1,275 verwendet. Die Auswirkungen des teilweisen Ersatzes von PLC durch CC und RHA auf die Frischbetoneigenschaften des SCC wurden in einer Reihe von Tests untersucht.

Alle untersuchten CCs und die RHA erfüllten die Anforderungen der ASTM C618 für die Verwendung natürlicher Puzzolane als Teilersatz für Zement. Die Eigenschaften der deutschen CC ähneln denen der metasmektitischen nigerianischen Tone (eingestuft als 2:1 CC). Die metasmektitischen Tone wiesen eine größere SSA, einen höheren Wasserbedarf und weniger reaktive Si- und Al-Ionen auf als die metakaolinitischen Tone (klassifiziert als 1:1 CC). Die beiden CC-Gruppen erfordern die Zugabe von Fließmittel (SP), um eine ähnliche Verarbeitbarkeit wie das OPC-Mörtelsystem zu erreichen. Sie können als Ersatz für OPC mit einem Anteil von bis zu 45 % in Kombination mit LP verwendet werden, wodurch mindestens eine Reduzierung der Treibhausgasemissionen der Stufe 1 erreicht wird. Auch RHA hat im Vergleich zu CC einen hohen Wasserbedarf und SSA und kann als Ersatz für bis zu 40 Vol-% Zement in SCC verwendet werden.

Sowohl CC als auch RHA haben einen höheren Wasserbedarf als PLC, wobei der Wasserbedarf von CC um ein Drittel höher ist als der von PLC und nur eine Anpassung von SP erforderlich ist, um eine Viskosität zu erreichen, die mit der des Referenz-SCC vergleichbar ist. Hierfür wurde ein Vw/Vp = 0,875 sogar bis zu einem teilweisen Ersatz von 40 Vol.-% CC verwendet. Die führte allerdings zu einer erhöhten Viskosität. Die Verwendung von RHA als teilweiser Ersatz für PLC in SCC ist kritischer, da sein Wasserbedarf mehr als dreimal so hoch ist und im Gegensatz zum CC-SCC-System die Fließmittelanpassung nicht ausreicht, um das RHA-SCC-System fließfähig zu halten. Ein teilweiser Ersatz von PLC durch RHA bis zu 40 Vol.-% ist ebenfalls möglich, wenn ein erhöhtes Vw/Vp ≥ 1,575 verwendet wird. Bei einem V_w/V_p = 1,275 waren alle SCC-Proben kurzfristigen stabil ohne sich zu entmischen. Selbst SCC, der mit 20 Vol.-% RHA als teilweisem PLC-Ersatz hergestellt wurde, behielt seine Fließfähigkeit bis zu 30 Minuten nach dem Mischen. Für die Bewertung der Fließfähigkeit wird die Verwendung von 20 Vol.-% RHA als teilweiser Ersatz für PLC als kritisch angesehen, da diese SCC-Mischung 30 Minuten nach dem Mischen derart ansteifte, dass sie ihre Selbstverdichtbarkeit verlor.

SCC, der mit 20 Vol.-% CC hergestellt wurde, kann sowohl für die Herstellung von Fertigteilen als auch von Fertigbeton verwendet werden. Die Verwendung von 20 Vol.-% RHA und der

ternären Mischung aus 10 Vol.-% CC und 10 Vol.-% RHA führte jedoch zu einem hohen Fließwiderstand und einem schnellen Verlust der Fließfähigkeit nach 30 Minuten Mischzeit. Daher muss ihre Fließfähigkeit für Anwendungen über 30 Minuten hinaus verbessert werden.

Bei einem niedrigeren Vw/Vp = 0,875 erhöhte ein teilweiser Ersatz von PLC durch 20 und 40 Vol.-% CC die Druckfestigkeit von SCC geringfügig und steigerte seinen Chloridmigrations-widerstand, wodurch sich die SCC-Qualität in Bezug auf den Chloridwiderstand von "Normal" auf "Gut" änderte und eine CO_2-Einsparung von 32 % erzielt wurde. Die Erhöhung des Vw/Vp auf 1,275 führte zu einer Vergrößerung des durchschnittlichen Porendurchmessers von SCC und SCC, der mit 20 Vol.-% CC hergestellt wurde, wodurch sich die ursprüngliche Einstufung von SCC mit 20 Vol.-% CC von "Gut" auf "Normal" änderte. Während der mit RHA hergestellte SCC und die Mischung aus CC und RHA mit einem Vw/Vp = 1,275 die 28-Tage-Druckfestigkeit von SCC leicht erhöhte. Der Chloridmigrationswiderstand von 20 Vol.-% RHA ist dreimal so hoch wie der von SCC, der nur mit PLC hergestellt wurde und ist bei der ternären Mischung 10 Vol.-% CC + 10 Vol.-% RHA noch doppelt so hoch. RHA ist in der Lage, den Chloridmigrationswiderstand von SCC zu verbessern und sollte zur Verbesserung der Mikrostruktur von SCC verwendet werden, der nur mit PLC hergestellt wurde.

Abstract

As the population of sub-Saharan Africa grows, so does the demand for housing and other infrastructure that requires concrete, leading to an increased need for cement for its production. Nigeria - the most populous country in the African region – has embarked on a massive infrastructural development to meet among others the demand for housing caused by rapid urbanization and a high annual population growth. The production of cement, an essential component of concrete, presents two major challenges. First, a large amount of energy is required for its production and grinding. This is a problem especially in developing countries, making cement more expensive. Second, cement production accounts for about 6 % to 10 % of global carbon dioxide emissions. It's already well established that carbon dioxide (CO_2) emission from cement production could be reduced through a circular carbon economy of reducing, reusing, recycling, and or removing CO_2.

This study considers the option of reducing CO_2 emission by partial replacement of cement with a supplementary cementitious material (SCM). The performance of two SCMs locally available in Nigeria, calcined clay (CC) and rice husk ash (RHA), as partial replacements for cement in mortar and concrete was determined. The first part deals with the determination of the pozzolanic potential of Nigerian calcined clays (NCC) relative to German calcined clay and RHA as partial substitutes for cement in general. For this purpose, four naturally occurring clay samples (two kaolinite-rich and two smectite-rich) were collected from different areas in the vicinity of the Ashaka cement plant in Gombe State, Nigeria, and calcined in a laboratory. Mineralogical characterization of the clays was carried out by XRD. The hydration kinetics of the calcined clay–cement systems were monitored by isothermal calorimetry. Workability was determined using the flow table method. The reactivity of the CCs was determined by the solubility of Si and Al ions and the strength activity index (SAI). The results obtained were then compared with the German CC for later use in the production of concrete, since such a quantity needed for the concrete batches is difficult to transport from Nigeria.

Rice husks from the vicinity of Zaria in Kaduna State, Nigeria, were calcined in an electric furnace to obtain the RHA and ground with a laboratory-scale mill. The RHA powder was characterized and subsequently evaluated.

For the application of the CC and RHA characterized above in concrete, the experimental program of this study considers the use of self-compacting concrete (SCC) to produce durable concrete that has good resistance to chloride ions penetration. This is because both CC and RHA have higher water demand and specific surface area (SSA) compared to cement, which makes their use as a partial replacement for cement in SCC more critical. The objective is to consider the challenging physical properties of CC and RHA and design a powder type of SCC, with a higher replacement level of ordinary Portland cement (OPC) to achieve an eco-efficient and durable SCC. Therefore, first, the OPC is partially replaced by 15 vol-% limestone powder (LP), resulting in a Portland limestone cement (PLC), and up to 40 vol-% of the PLC is replaced by binary and ternary blends of CC and RHA. A rational mix design procedure for SCC was used for proportioning the quantities of SCC. The paste phase of the SCC was first designed considering the physical properties of CC and RHA and used as a medium to embed the fine aggregate (FA), which forms a self-compacting mortar (SC-M). Finally, the SC-M was considered as a medium for embedding the coarser aggregate (CA) that forms the SCC.

Two volumetric water-to-powder ratios (V_w/V_p) were used considering the physical properties of CC and RHA, first V_w/V_p = 0.875 for the reference mixtures (PLC-SCC) and SCC mixtures

containing up to 40 vol-% CC as partial replacement to PLC in SCC. For the use of RHA in SCC, an individual V_w/V_p was used for each level of PLC replacement by RHA. For comparison of the reference SCC, and SCC produced with binary and ternary blends of CC and RHA, a V_w/V_p = 1.275 was used. The effect of partially replacing PLC with CC and RHA on the fresh properties of the SCC was investigated using a variety of tests.

All the CCs and RHA studied met the requirements of ASTM C618 for the use of natural pozzolans as a partial replacement for hydraulic cement. The properties of the German CC are similar to those of the metasmectite Nigerian clays (classified as 2:1 CC). The metasmectitic clays exhibited greater SSA, higher water demand, and less reactive Si and Al ions than the metakaolinitic clays (classified as 1:1 CC). The two CC groups require the addition of a superplasticizer (SP) to achieve a similar workability class to the OPC mortar system. They can be used to replace OPC at replacement levels of up to 45 %, in combination with LP, there by achieving at least a “Level 1” reduction in greenhouse gas emissions. Similarly, RHA is characterized as having high water demand and SSA compared to CC and can be used to replace up to 40 vol-% of cement in SCC.

Both CC and RHA have a higher water demand than PLC, with the water demand value of CC being one-third higher than that of PLC which required only an adjustment of SP to achieve a degree of deformability comparable to the reference SCC. Using a V_w/V_p = 0.875 made even a partial replacement up to 40 vol-% CC possible although with an increased viscosity. The use of RHA as a partial replacement for PLC in SCC is more critical because its water demand is more than three times higher and, unlike the CC-SCC system, the SP adjustment is not sufficient to deform the RHA-SCC system. Partial replacement of PLC with RHA up to 40 vol-% is also possible if an increased $V_w/V_p \geq 1.575$ is used. Using a V_w/V_p = 1.275, all the SCC specimens achieved the short-term segregation resistance of SCC, and even SCC produced with 20 vol-% RHA as PLC partial replacement retained its flowability up to 30 min after mixing. For the flowability retention evaluation, the use of 20 vol-% RHA as a partial replacement to PLC is considered critical because the excess mixing water was absorbed after 30 min of mixing, making the SCC mix stiffer and rapidly losing its flowability. Therefore, SCC produced with 20 vol-% CC can be used to produce both precast and ready-mix SCC. However, the use of 20 vol-% RHA and the ternary blend 10 vol-% CC + 10 vol-% RHA developed high flow resistance and showed rapid loss of flowability after 30 min of mixing. Therefore, their flowability retention needs to be improved for applications beyond 30 minutes.

At a lower V_w/V_p = 0.875, partial replacement of PLC with 20 and 40 vol-% CC slightly increased the compressive strength of SCC and its chloride migration resistance, changing the SCC quality in terms of chloride resistance from “Normal” to “Good” and resulting in a CO_2 savings of 32 %. The increase of the V_w/V_p to 1.275 increased the average pore diameter of the reference SCC and SCC produced with 20 vol-% CC, which changed the initial grade of SCC with 20 vol-% CC from “Good” to “Normal” classification. While the SCC produced with RHA and the blend of CC and RHA with a V_w/V_p = 1.275 slightly increased the 28-day compressive strength of SCC. The chloride migration resistance of 20 vol-% RHA is 3 times that of SCC produced with only PLC, while that of the ternary blend 10 vol-% CC + 10 vol-% RHA is twice that of SCC produced with PLC only. RHA is capable of improving the chloride migration resistance of SCC and should be used to improve the microstructural densification of SCC produced with only PLC.

Content

List of general abbreviations

AFm	Monophases, C_4AXHn
AFt	Ettringite
ASTM	American Society for Testing and Materials
ATR-FTIR	Attenuated total reflection – Fourier transformed infrared spectroscopy
BET	Brunauer Emmett Teller
$CaCO_3$	Calcium carbonate
CH	Calcium hydroxide, portlandite
$CO_{2\text{-eq}}$	CO_2 equivalent
CVC	conventional vibrated concrete
C_3A	Tricalcium aluminate
C_3S	Tricalcium silicate, alite
C-(A)-S-H	Calcium-(aluminate)-silicate-hydrate
DIN	Deutsches Institut für Normierung
DTA	Differential thermal analysis
EE	Embodied energy
EN	European Standard
GWP	Global-warming potential
ICP-OES	Inductively coupled plasma – optical emission spectroscopy
LC^3	Limestone calcined clay cement
M_{RCM}	Chloride migration coefficient
MIP	Mercury intrusion porosimetry
NaOH	sodium hydroxide
OPC	Ordinary Portland cement
PAI	Pozzolanic activity index
PJ	Passing ability class for the J-ring-test
PLC	Portland limestone cement
PSD	Particle size distribution
RHA	Rice husk ash
SAI	Strength activity index
SCC	Self-compacting concrete
SCM(s)	Supplementary cementitious material(s)
SF	Slump-flow class
SP	Superplasticizer
SR	Segregation resistance class
SSA	Specific surface area
TG	Thermogravimetry
t_{500}	Time in seconds to flow to a diameter of 500 mm in a slump-flow test
VF	Viscosity class for the V-funnel test
VMA(s)	Viscosity modifying Agent(s)
VS	Viscosity class for the t_{500} test
w/b	Water-to-binder ratio
w/p	Water-to-powder ratio
XRD	X-ray diffraction

List of self-assigned abbreviations

CA	Coarse aggregate
CC	Calcined clay
CT7	German calcined clay
FA	Fine aggregate, sand
NCC	Nigerian calcined clays
NRC	Raw Nigerian clay
RCT7	Raw German clay
SCP	Self-compacting paste
SC-M	Self-compacting mortar
V_a	Volume of air in self-compacting concrete
V_s	Volume of the fine aggregate, sand
V_w/V_p	Volumetric water-to-powder ratio

List of Figures

.

1 Introduction

Global demand for housing and other concrete-based infrastructures has increased tremendously, especially in emerging economies worldwide [1, 2] leading to an increased need for cement to produce them. For instance, in Nigeria - the most populous country in the African region - demand for shelters and other civil engineering infrastructure has recently increased due to rapid urbanization and a high annual population growth rate [3]. To meet the country's infrastructural requirements, the Federal Government of Nigeria in partnership with private investors embarked on massive infrastructural development, such as the construction of the Abuja world trade center, Eko Atlantic, and Lekki free trade zone. These projects and others ongoing in the country consume a large quantity of cement annually. Another reason for the increasing demand for cement is the need to maintain existing concrete structures and bring them in line with recent developments [4].

Concrete and reinforced concrete usually remain the most widely used construction material to provide the needed infrastructures [4]. In reinforced concrete, a sufficient concrete cover usually serves to protect the reinforcement from adverse weather effects, harmful substances, and to improve durability. A dense microstructure can only be achieved if the concrete flows properly and embeds the reinforcement closely, filling all gaps and corners of the formwork without any kind of obstruction [5]. The integrity and ease of handling concrete determine its lifespan and application. Self-compacting concrete (SCC) is the concreting technique developed to provide durable and self-deformable concrete without the need for external compaction [6, 7]. In this concreting technique, the proportion of the coarse aggregate is reduced while the fine aggregate (FA) is increased to ease the rate of deformability of the concrete. Increasing the proportion of fines (powder) or the use of viscosity modifying admixtures can improve the segregation resistance of the SCC [6-8]. Consequently, higher amounts of cement in SCC lead to more cement consumption and hence increase the greenhouse gas emissions related to cement production. Despite its technological advantages, the market share of SCC is small due to some obstacles especially in developing countries [9, 10]. First, SCC mixes are more sensitive even to a minor variation in constituent's proportions [10, 11], change in materials properties [12, 13], and the production method adopted [10, 14]. Secondly, and eventually, the most important concern of SCC, is the high cost of its production due to the use of high dosages of chemical admixtures and the higher binder content [15].

The production of cement, an essential component of SCC, presents two major challenges. First, a large amount of energy is needed for its production and grinding. This is a problem especially in developing countries, making cement more expensive [16]. Second, cement production accounts for about 6% to 10% of the global carbon dioxide emissions [17]. Although the total per capita carbon dioxide emissions of sub-Saharan Africa in 2018 were only 0.81 kt, below the 2.7 kt threshold for limiting global warming to below 2 °C by 2050 [18], the rate of urbanization in the region is increasing rapidly compared to the rest of the world, leading to an increase in demand for shelter and other concrete infrastructure, with a consequently higher demand for cement [3]. For example, the cement production capacity of Nigeria was only 21 Mt in 2015, but increased to 28 Mt by 2020, and it is expected to reach 53 Mt in 2040 [19]. Although total carbon dioxide emissions from cement production were estimated at 11 $MtCO_2e$ in 2015, they increased to 15 $MtCO_2e$ in 2020 and are expected to reach 28 $MtCO_2e$ in 2040 [19].

Carbon dioxide emission from cement production could be reduced through a circular carbon dioxide economy of reducing, reusing, recycling and or removing CO_2. Technologies such as carbon dioxide capture, CO_2 sequestering, concrete carbon dioxide-steam curing, clinker efficient cement are also widely adopted [20]. One of the potential pathways to decarbonize SCC is to use less clinker, as clinker is the main driver of embodied carbon dioxide in SCC. However, the main challenge is how to continue to benefit from the use of SCC with less clinker while ensuring its technical properties such as workability, strength and durability. Therefore, partial replacement of cement with SCMs that require less energy for production and release less CO_2 is essential to reduce the cost of SCC and help limit global warming [21].

The SCMs used as partial substitute to cement in SCC include among others fly ash [22, 23], silica fume [23, 24], blast furnace slag [25, 26], rice husk ash (RHA) [27, 28] and metakaolin [29, 30]. These materials yielded positive results at optimal dosage levels. The use of fly ash and silica fume, especially at higher cement replacement rates, will no longer be possible in the near future; this is because, first, fly ash production declines with the reduction of coal-combustion which is enforced to limit the global CO_2 release. Right now, it is already hardly available in Africa or South America [31]. Second, the replacement-level of silica fume is limited due to its high-water demand and portlandite consumption as well as for economic reasons. Calcined clays and RHA could be alternative sources of SCMs for SCC production to sub-Saharan Africa.

Therefore, the current research is directed towards establishing the pozzolanic potentials of CC and RHA, and optimizing SCC mixes incorporating the binary and ternary blend of CC and RHA as partial replacement to cement. Four samples of naturally occurring clays in the vicinity of the Ashaka cement plant in Nigeria were analyzed for their potential use as partial substitutes for cement in concrete. These clays were analyzed from mineralogical, physical, and chemical points of view and compared with clay from southern Germany. The essence is to use the latter for the production of self-compacting paste, mortar, and concrete as quantities needed for all samples will be difficult to be transported from Nigeria. The first part of the study deals with the characterization of CCs and RHA as potential SCMs that can be used as partial replacement for cement in concrete generally. The scope of the work was then narrowed down to the development of self-compacting paste (SCP), mortar, and concrete with CC from southern Germany, and its fresh and hardening properties were tested. New workability windows/thresholds were proposed for self-compacting mortars (SC-M) produced with a high volume of CC as PLC partial replacement. The influence of RHA on the deformability characteristic of SC-M was also investigated, here the V_w/V_p necessary to deform different RHA substitution ratios up to 40 vol-% and its consequences on fresh and hardened properties of SC-M were established. Finally, mix design for binary and ternary blends of CC and RHA as partial replacement for PLC in SCC was developed. At this stage, the influence of CC and RHA on the rheological, flowability retention, hardened, and durability properties of SCC was determined. An estimate of the CO_2 savings to be achieved by the partial replacement of PLC with the binary and ternary blends of CC and RHA is presented.

2 State of the art

2.1 Global population and demand for housing and concrete infrastructure

Rapid urbanization and a higher annual population growth rate increase the demand for housing and other concrete-based infrastructures, especially in emerging economies worldwide [1, 2]. The world population was 2.5 billion in 1950 and increased to 6.15 billion by 2020. According to the United Nations World Population Projections (2022), it will continue to rise, reaching 9.71 billion in 2050, with the largest increase coming from Asia and sub-Saharan Africa. Sub-Saharan Africa in particular is projected to lead the world in urban growth by the end of 2050 [32], as both urban and rural populations increase [3], although at different rates. Sub-Saharan Africa urban is experiencing a surge in population growth owing to an increase in rural-to-urban migration in search of economic opportunities and access to basic services, leading to an increase demand for housing and other civil engineering infrastructure for economic growth and development. Housing and access to basic services are central to urbanization, but the majority of urban residents in the sub-Saharan Africa region face housing deficit, and live in poor housing conditions [32].

Nigeria, the most populous country in the sub-Saharan Africa region, is experiencing rapid population growth and urbanization compared to other sub-Saharan Africa countries, resulting in the need for over 17 million housing units to reduce the housing deficit [33]. The Nigerian government established the National Housing Policy in 1991, and the Federal Mortgage Bank in 1989, and also embarked on massive infrastructural development in partnership with private investors, such as a new housing scheme to build 121,000 housing units in Kado Estate Abuja, the construction of Abuja World Trade Center, Eko Atlantic, the Lekki Free Trade Zone and the construction of 18,500 housing units in each state of the federation. All of these were initiated to ensure adequate and affordable housing for all Nigerians, but the housing deficit is still increasing, especially due to rapid population growth, low incomes, high-interest rates on mortgage loans, and high cost of building materials [33, 34].

Most housing in Nigeria is privately owned, and this continues to be the case as the government and/or private investors do not provide adequate housing. The few available homes are purchased by a privileged few residents, most of whom have formal employment [35]. Due to the high cost of construction materials and low per capita income, building houses is becoming increasingly unaffordable [15]. Lack of access to quality building materials and affordable mortgage credit also increased the housing deficit and led to the use of non-durable building materials, resulting in early structural defects and collapses. Cement is the most commonly used material for the production of building elements and concrete. To make housing more affordable to Nigerians, a greater proportion of cement (up to 50 %) can be replaced by a SCM, which requires less activation energy compared to cement, as previously studied by [16, 36].

It is obvious that SCMs can reduce the cost of cement and CO_2 emissions, but the main challenge is to what extent we can replace cement with these materials and whether we can use them for special concreting methods such as self-compacting concrete (SCC). The next sections will explain the benefits of using SCMs in concrete as one of the partial pathways to reduce CO_2 emission and what can be achieve from them will be made clear.

2.2 Potential pathways to reduce CO_2 emission from cement production

Global demand for concrete infrastructures is expected to continue increasing to accommodate rapid urbanization and increasing population growth in developing countries and to maintain existing concrete structures and bring them in line with recent developments in an already developed part of the globe [3, 4]. Concrete constituents are usually naturally sourced from the environment and processed at different levels, with coarse and fine aggregates requiring light processing compared to cement and other additives. In general, cement production requires a huge amount of energy for calcination and grinding, and up to 90 % of the greenhouse gas emissions associated with concrete production are from cement [37]. The cement industry currently contributes about 6 % to 10 % of global CO_2 emissions [17]. This value is already high and is expected to increase if appropriate measures are not taken.

One of the potential pathways to decarbonize concrete is to use less clinker per m^3 of concrete, as clinker is the main driver of embodied carbon in concrete [4, 38, 39]. The research trend in the cement industry is currently geared toward establishing the potential of blended cement produced with the use of inert, hydraulic, or pozzolanic SCMs as a substitute for cement. Limestone powder, fly ash, slag cement, silica fume, natural pozzolans, and heat-treated agro-waste are the most commonly used SCMs as partial substitutes for cement [22, 23, 28]. The use of some conventional SCMs in concrete, especially at higher cement replacement rates, will no longer be possible in the near future. For example, the production of fly ash is decreasing with the reduction of coal combustion, slag cement is not readily available, especially in countries with less industrial development, and the cement replacement by silica fume is also limited due to its high water demand [5].

On the other hand, the use of CC, especially in combination with limestone powder (LP), has recently gained importance in the cement industry [40, 41] and could be an alternative source of SCM to Nigeria. Vast deposits of kaolinite and illite clay minerals are available in Nigeria and unlike other sub-Saharan African regions, Nigeria has a deposit of limestone across its six geopolitical regions as previously reported by [42]. With the use of CEM II/C-M (Q-LL), the clinker phase of the cement can be reduced by 50%, while at the same time achieving a similar 28-day compressive strength as OPC [40, 41]. Greenhouse gas emission reduction of at least “Level 1” could be achieved by ternary blending CC and LP as partial replacement of OPC in concrete as already published in [16]. Additionally, the fact that agriculture is one of the leading economic sectors of sub-Saharan Africa, agricultural waste such as RHA, palm oil fuel ash, cassava ash, bagasse ash, bamboo leaf ash, and corn cob ash, are another viable source of SCM present in a significant amount to be used in concrete [3, 15, 43, 44].

It is evident that the use of SCMs as partial replacement to cement reduced CO_2 emissions. However, the main challenge is how to continue to benefit from the use of concrete with less clinker while ensuring its technical properties such as workability, strength, and durability. The open questions at this point are whether we can also achieve the same durability class as OPC if we reduce the clinker by 50 % and whether this type of cement is suitable for special concrete production technologies such as self-compacting concrete (SCC).

2.3 Self-compacting concrete

In reinforced concrete, a sufficient concrete cover usually serves to protect the reinforcement from adverse weather effects, harmful substances, and to improve durability. A dense microstructure can only be achieved if the concrete flows properly and embeds the

reinforcement closely, fills all gaps and corners of formwork without any kind of obstruction. To achieve these attributes, concrete that requires very little compaction was first produced and used in Europe in the early 1970s [45]. At that time, the concept of SCC — without the application of external vibration or compaction — was still an imaginary vision. It was first proposed in 1986 and produced at the University of Tokyo, Japan, in 1988 [6-8]. More so, the need to reduce noise on the construction site, save energy, and compensate for the lack of labor, leads to the self-compacting method of concrete production. SCC is considered a high-performance concrete that differs from conventional vibrated concrete (CVC) in its fresh properties, i.e. SCC deforms under the influence of gravity without the need for external compaction. SCC microstructure is considered dense and the method is environmentally friendly, as the noise caused by vibration is eliminated. The optimization of mix design towards self-compacting properties leads to superior qualities over CVC [8]. The modified flowing properties and segregation resistance both yield high homogeneity [28], a reduction of voids and higher early strength values [28, 46], an improved interfacial transition zone and hence higher durability [26, 47]. Also, the use of SCC improves the construction environment as the absence of concrete vibrators reduces noise pollution [45].

The flow of SCC, measured as the total spread of the mixture particles purely under the influence of gravity, is normally achieved by controlling the w/p and applying high range water-reducing admixtures (HRWR) [48]. Besides the w/p, the proportion of finer and coarser particles and the application of viscosity modifying agents (VMAs) in the mix design is decisive for the segregation resistance of SCC [6, 49]. The mix design of SCC can be classified into three types. The powder type: here, the fluidity of SCC is achieved by a reduction in coarser aggregate (CA) content and the addition of HRWR. While the segregation resistance is achieved by increasing the percentage of fines [6, 7, 50]. This type is usually adopted for higher grades of SCC with a w/p of as low as 0.35. The VMA type: in this method, viscosity modifying agents are applied to provide the required segregation resistance of the SCC. Also, a small amount of HRWR is added to provide fluidity for the mixture [7, 51, 52]. This method is suitable for low grades of SCC with a w/p of 0.45. The combined type: this combines the use of VMA and increasing the percentage of powder, in controlling the segregation and fluidity of SCC. The combined type is usually employed for medium grades of SCC with a w/p of 0.40 [28, 51].

Unlike the CVC, SCC has no standardized method for its mix design due to its susceptibility to nuances in material characteristics and other environmental factors. The empirical method was initially adopted to produce SCC [6, 7]. In this method, the w/p as well as the dosage of SP are both adjusted to achieve the required degree of deformability, followed by the determination of the volume of fine aggregate (FA) required to produce a self-compacting mortar (SC-M). Finally, the required volume of CA is determined. Other methods used to achieve self-consolidation include the yield stress and plastic viscosity method (rheometer method) and aggregate packing method [48, 53, 54]. Various limits have been set to achieve the desired deformability, viscosity, and segregation resistance of SCC based on the empirical design method [6, 7].

Despite its technological advantages, the market share of SCC is small due to some obstacles especially in developing countries [9, 10]. First, SCC mixes are more sensitive even to a minor variation in constituent's proportions [10], change in materials properties [13], and the production method adopted [14]. Secondly, and eventually, the most important concern of SCC, is the high cost of its production due to the use of high dosages of chemical admixtures and the higher binder content [15]. The cost of materials in SCC exceeds approximately 20 –

50 % of those for CVC [9]. Although, this can be partially compensated by rapid and easy placing [55]. The mix design of SCC, as discussed earlier, entails either a large reduction of CA and increased powder content or a small reduction in the CA content and the addition of VMAs. From a technological point of view, a lower content of CA in SCC might result in a lower modulus of elasticity, which may affect negatively the time-dependent deformation (creep and shrinkage) of SCC [56]. Higher binder content also increases the environmental impact. The method to achieve SCC with small changes in the coarse aggregate and the use of VMA, instead, leads to altered mechanical properties of the concrete [56]. To provide solutions to these problems, researchers have focused on the potential of SCMs in SCC production. The most commonly used SCM in SCC production includes fly ash [22], silica fume [23], blast furnace slag [57] rice husk ash [28, 58], and metakaolin [29, 30]. These materials yielded positive results at optimal dosage levels. Fly ash, blast furnace slag and silica fume will not be considered in this study due to the issues earlier pointed out. The use of CC and RHA as partial replacements for cement in SCC is considered due to their availability in Nigeria.

2.3.1 Potentials of calcined clays as a pozzolan in concrete

Calcined clays are dehydroxylated aluminosilicate pozzolanic materials that can partially replace cement at high proportions and improve the strength and durability of concrete. The great potential of CC is based on physical effects such as the filler effect [59, 60] and the adsorption of ions from the pore solution [61], as well as on the release of silicon and aluminum ions at early time of hydration [62, 63]. This is evidenced by a strong influence of the early clinker hydration in CC blended systems [64, 65]. Metakaolinite, as the most famous representative of CC, is the metaphase of the phyllosilicate kaolinite after calcination. The calcination temperature (500 – 650 °C) is chosen based on the dehydroxylation temperature of kaolinite. Kaolinite is a 1:1 phyllosilicate consisting of (SiO_4) tetrahedral and (AlO_6) octahedral sheets that are connected via OH-groups and aluminum cations [66, 67]. By dehydroxylation, the structure of metakaolinite becomes x-ray amorphous. Metakaolinite is the most reactive CC in concrete and mortar since it yields higher early strength when used as SCM compared to other CCs [5, 68, 69]. It reacts faster than other CCs and promotes in addition to the silicate the aluminate reaction especially in the presence of $CaCO_3$, thereby stabilizing AFt and promoting the precipitation of hemi/monocarboaluminate AFm phases instead of monosulfates [70]. Cement can be partially replaced with up to 45 wt-% of a blend of CC and limestone (LC^3 (limestone calcined clay cement) or CEM II/C-M (Q-LL)) without an adverse effect on its strength.

When metakaolinite is used as a partial replacement for cement, it consumes high amounts of portlandite (CH) from cement hydration and forms more C-S-H due to its pozzolanic reactivity, which densifies the pore structure of SCC, resulting in a reduction of interconnected pores by creating more C-A-H and decreasing the diffusion rate of SCC [71, 72]. This increases the resistance to the ingress of harmful substances and improves the freeze-thaw resistance of concrete [73]. However, it decreases the deformability of SCC and increases its viscosity [5, 30]. This is due to its higher water demand and higher specific surface area compared to cement [5, 74] and leads to the use of high dosages of SP to liquify the system and to keep the viscosity within the specified limit. Furthermore, unlike cement particles, CC particles have an overall negatively charged surface that can cause flocculation when added to the heterogeneously charged cement, thus requiring more SP to deflocculate the blended cementitious system [74, 75].

In addition, the use of metakaolinite as a partial replacement for cement in large proportions is not economical. Metakaolinite is an expensive material due to its frequent use in other competing industries, as the price of pure metakaolinite is almost two to three times the price of cement in many countries [41]. Besides metakaolinite, the suitability of calcined common clays — with various types of 2:1 phyllosilicates and further inert components — as SCM has been investigated within the last few years [76, 77]. Although their application in CVC has been investigated in recent years, by [16, 78, 79], it should also be extended to SCC.

2.3.2 Potentials of rice husk ash as a pozzolan in concrete

Rice husk is a by-product of rice milling and consists of cellulose (50 %), lignin (25 % - 30 %), silica (15 % - 20 %), and moisture (10 % - 15 %) [80]. Calcination of rice husks removes cellulose and lignin, leaving a silica ash called RHA. The calcination temperature is maintained between 600 and 700 °C to keep the ash in the amorphous phase [27, 81, 82]. RHA consists of microporous, regular, and angular particles, having large specific surface area particle micromorphology [83-85] and contains a high amount of amorphous silica, designating it as pozzolanic material according to [86]. Its mesoporous structure absorbed a considerable amount of aqueous phase from the free water content of the paste, leading to an increase in viscosity. RHA derives its pozzolanicity from the optimization of proper calcination and grinding [27, 81, 82] and can be used as a viscosity modifying agent or as a partial replacement to cement in SCC [28, 87].

The hydration mechanism of RHA in SCC is related to the consumption of CH and enhancement of precipitation of C-S-H due to its pozzolanic reactivity, which may lead to the refinement of pore size and densification of the binder matrix [88, 89]. These attributes make it possible to partially substitute cement with RHA up to 20 wt-% without an adverse effect on its strength and or durability [27, 58, 90]. Another possible reason for this could be caused by the ability of RHA to behave like an internal curing agent, whereby it continuously releases the absorbed free water from its mesoporous cellular structure for hydration, which facilitates the precipitation of more C-S-H in the system and densifies SCC microstructure [85, 91].

The major concern in using RHA as a partial replacement for cement in SCC lies in its peculiar physical properties. Its specific surface area and water demand exceed those of cement and metakaolin [5, 72]. Therefore, similar to silica fume, its use in SCC is limited due to its negative effect on the deformability characteristics of SCC.

2.3.3 Influence of CC and RHA on SCC mix design

Various methods have been developed for the design of SCC since, unlike CVC, SCC is susceptible to nuances in material properties and other environmental factors. First, Okamura and Ozawa [7] used an empirical design method to achieve self-compactability. In this method, both CA and FA are kept constant. The V_w/V_p and SP amounts are adjusted to achieve the desired degree of self-compactability. This method eliminates repeatability during SCC production. However, it is considered too complicated for practical application [48], and the V_w/V_p cannot be fixed based on strength, but rather on the self-compactability requirement. Later, methods based on rheometer tests were developed to characterize the yield stress and plastic viscosity of SCC [53]. Just like the previous method, this method does not take compressive strength as a determinant factor in designing SCC mixes and requires more sophisticated tools to measure the rheology. Su et al. [48] used the aggregate packing method to achieve self-compactability. Although this method simplifies the SCC grades, it yields the

required mix proportion for only medium to high strength concrete. Kheder and Jadiri [92] factored in compressive strength as a determinant in designing self-compacting mixes. Their method determines the water-to-binder ratio based on maximum aggregate size and compressive strength requirement. Similarly, Dinakar [93, 94] achieved self-compactability by considering the efficiency of pozzolanic materials added to SCC. With this method, even low-grade SCC can be achieved, although it requires adjustment to all concrete constituents in case of a minute change. Moreover, Xie et al. [95] further considered even the fraction of the key oxides of a particular SCM to model both fresh and hardened properties of SCC. Their method permits achieving, both self-compactability and strength by knowing the exact characteristics of the SCC binder.

The same mix design methods described above were adopted when cement is replaced with CC and RHA. For instance, CC can replace up to 20% of the cement in SCC at a low w/p of ≤ 0.32 by simply increasing the SP dosage to properly deform the SCC-CC systems and achieve a similar workability class to SCC-cement systems [30, 96, 97]. The strength and durability of such concrete are improved by the pozzolanic reactivity of CC, although the viscosity increases. RHA-SCC systems, on the other hand, require an adjustment of the w/p value to achieve similar deformation properties as SCC-cement systems due to the high water demand and specific surface area of RHA. Typically, increasing the SP dosage is not sufficient to deform SCC-RHA systems. To achieve the self-compactability, the w/p is increased to 0.41 at the RHA replacement ratio of 15 % [27], and higher replacement ratios > 20 % require an increase in v/p to 0.55 to achieve self-compactability [72]. Both metakaolin and RHA were found to provide sufficient segregation resistance required in SCC mixes and therefore, eliminate the use of VMAs [28, 30]. Although the use of binary and ternary blends of CC and RHA as partial replacements for cement has been investigated in previous research, some questions regarding their influence on the fresh and durability properties of SCC remain unanswered.

2.3.4 Research gap

The present investigation started with a literature review on the suitability of blends of RHA and CC for the preparation of SCC, a review paper titled “Suitability of blending rice husk ash and calcined clay for the production of self-compacting concrete: A review” has been published [5]. The following research gaps were identified:

- Previous studies have investigated the suitability of a multi-blend of CC and RHA for the production of the SCC. Most researchers focused on the use of metakaolin as CC, which is an expensive material due to its frequent use in other competing industries and is less available compared to CC with low kaolinite content. There is a lack of knowledge when it comes to the use of low-kaolinitic CC as a sole SCM or in combination with RHA as a partial replacement to cement in SCC, which could be a very promising combination e.g., several countries in Africa.
- Also, previous studies have investigated the effects of blends of metakaolin and RHA on the SCC fresh properties, strength, and durability. However, the effects of these materials on the rheological properties of SCC in terms of yield stress, plastic viscosity, shear thickening behavior, flowability retention, plastic shrinkage, and drying shrinkage have not been reported [5].

In addition to the research gaps identified in the review paper, the following points are also relevant:

- Numerous investigations have established the pozzolanic potentials, hydration kinetics, interaction with superplasticizers, and the potential use of CC and RHA as partial replacements for cement in self-compacting mortar and concrete. The open question remains as, to what extent we can partially replace cement in SCC with CC and RHA to achieve higher CO_2 savings without compromising the mechanical and durability properties of SCC.
- Similarly, there are no previous studies in the literature on the potential use of low-kaolinitic CCs like those available in Nigeria in LC^3 cement.

3 Aim and objectives of the research

The overall objective of the study is to use the locally available SCMs (CC and RHA) in Nigeria and produce a SCC that has good resistance to chloride penetration. The study is mainly divided into two parts and answers the following questions.

i. Pozzolanic potentials of CC and RHA as partial replacement to OPC in general and the following open questions were considered.

- Are the physical, chemical, and mineralogical properties of the Nigerian-CCs (NCCs) comparable to the German-CC (CT7) used for the investigation? What are the physical and chemical properties of the RHA?
- How do the physical and mineralogical properties of the NCCs and CT7 affect their potentialities as partial replacements to cement in mortar?
- What is the influence of RHA on the workability and compressive strength of mortar?

ii. Influence of CC and RHA on mix design, rheology, hardened and durability properties of self-compacting paste, mortar, and concrete. The following open questions were considered.

- How do CC and RHA influence SCC mix design? How does the water demand of CC and RHA affect the rheological threshold of the self-compacting mortar? Is the same V_w/V_p value used for the deformation of the self-compacting paste without CC and RHA also suitable for the deformation of the CC- and RHA- self-compacting paste? What influence do CC and RHA have on the SP demand?
- What is the effect of binary and ternary blends of CC and RHA as partial replacement to cement (PLC) on the rheology, flowability retention, and flow resistance of SCC?
- How do the binary and ternary blends of CC and RHA affect the hydration process of self-compacting paste? What influence do they have on the microstructural densification of self-compacting paste?
- To what extent do the binary and ternary blends of CC and RHA influence the plastic shrinkage, drying shrinkage, and compressive strength of self-compacting mortar? To what extent can cement be replaced with CC and RHA in SCC to achieve a high level of CO_2 reduction?
- What is the effect of replacing 20 vol-% cement with CC and RHA on the mechanical behavior and durability of SCC? How do these materials affect the chloride resistance of the SCC?

4 Materials and summary of the methods used

4.1 Materials

4.1.1 Sourcing and processing of the calcined clays and rice husk ash

Four raw clay samples were collected from the areas of Nafada, Kwami and Billiri local government of Gombe state, Nigeria and denoted as Nigerian Raw Clay (NRC-1 to NRC-4). The NRCs were dried at 60 °C in the laboratory oven for 24 h and ground in the rotary disc mill (Retsch, RS 200) at 700 rpm for 5 min and calcined for 30 min using a laboratory muffle furnace at a temperature of 750 °C. After cooling to ambient temperature, they were subsequently ground in the rotary disc mill at 700 rpm for 5 min and labeled after calcination as NCC (Nigerian Calcined Clay)-1 to NCC-4. The raw material for the German calcined clay CT7 (RCT7) was an Amaltheen common clay originating from southern Germany, which was calcined at 750 °C on an industrial scale. For the RHA, rice husks from the vicinity of Zaria in Kaduna State, Nigeria, were calcined at 650 °C for 2 hours in an electric furnace and ground with a laboratory scale mill to obtain the RHA. It contained 96.8 % wt-% amorphous silica, measured using X-ray diffraction with an internal standard.

4.1.2 Properties of the research materials

To determine the pozzolanic potential of CC and RHA, OPC - CEM I 42.5 R - conforming to DIN EN 197-1 [98] was used as a reference material to compare the performance of CC and RHA. It contained (wt-%) 61.6 C_3S, 18.2 C_2S, 5.8 C_3A, 9.0 C_4AF, 3.2 sulfates and 0.6 calcite as mineralogical phases according to the supplier's information. To produce LC^3 blended cement and simulate a PLC, the cement was substituted by 15 vol.% of LP. The LP contained 99.8 wt-% calcite and 0.2 wt-% quartz, as determined by X-ray diffraction. Figure 1 shows the particle distribution of the research materials.

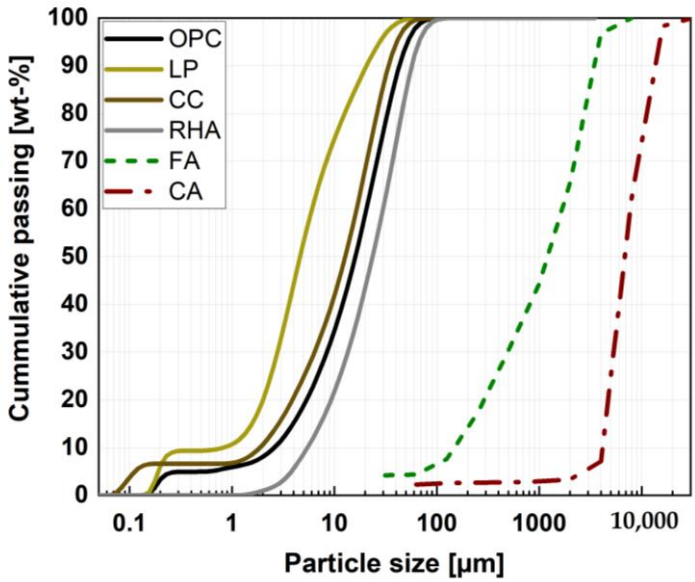

Figure 1 Particle size distribution of the research materials

An industrial isoprenyl oxy poly (ethylene glycol)-type polycarboxylatether-based SP with acrylic acid as anchor group and additional vinyloxybutyl poly (ethylene glycol) macromonomer was used in this study. It has a solid content of 38.6 wt-%, an anionic charge density of 1390 µmol/g, a molecular weight of 25,992 g/mol, and a side-chain length of n_{EO} = 31, according to

the supplier's information. The respective SP dosages were determined as wt-% of the binder. Sand with a grading 0/4 mm, bulk density of 2.87 g/cm^{3,} and having 7.6 wt-% passing of 125 µm sieve was used as FA. While round gravels with a grading 4/16 mm, a particle density of 2.68 g/cm^3 and 2.7 wt-% passing sieves 0.125 was used as CA.

4.2 Experimental methods

4.2.1 Characterization of the research binder

The thermal decomposition of the clay mineral phases was studied by thermogravimetric (TG) analysis conducted in Netzsch STA 449 F3 Jupiter equipment at a heating rate of 2 K/min. A similar test was also conducted for RHA to establish its calcination temperature. Further quantification of the mineralogical composition of the NRC was determined by X-ray diffraction (XRD) using a side loading preparation at a PANalytical Empyrean diffractometer, with Cu-Kα-radiation (1.54 Å) at 40 kV and 40 mA. Rietveld refinement was performed using Profex-BGMN. Inductively coupled plasma optical emission spectrometry (ICP-OES) was used to determine the oxide content of the research binder after melt fusion according to DIN EN ISO 11885 [99]. The Si- and Al- ion solubility of the CCs and RHA was evaluated by eluting the CC and RHA in NaOH solution (10 wt-%) for 24 h according to the method specified by [100]. The physical parameters of the binder determined include particle density (PD) measured with Helium Pycnometer according to DIN EN ISO 17892-3 [101], BET specific surface area (SSA) measured with HORIBA SA – 9600 series surface area analyzer, according to DIN ISO 9277 [102], particle size distribution (PSD), determined using laser light diffraction by Bettersizer, 3P instrument [103] and water demand (WD) according to the Puntke method [104].

4.2.2 Performance in mortar and early hydration behavior of CC and RHA

Two mortar series were investigated to evaluate the influence of the CC and RHA on the workability and strength activity index (SAI) of the binder. The first with binary blends containing CC and RHA only as a substitute for OPC at 20 vol-%. The second batch of the ternary blends contained a mortar produced with LP substituting OPC at 15 vol-% (forming PLC), and the remaining blends contained 55 vol-% OPC, 15 vol-% LP, and 30 vol-% of CC. The mortar constituents were mixed in a stainless steel 5 liters bowl mixer according to DIN EN 196-1 [105]. The flow diameter of the fresh mortar was determined according to DIN EN 1015-3 [106]. Table 1 shows the gravimetric mix designs of the different mortar systems.

Table 1 Materials mix designation

Mix designation	OPC [g]	LP [g]	CC [g]	Sand [g]	Water [g]	SP [wt-%]
M	450	-	-	1350	225	-
MCT7	360	-	73	1350	225	-
MN-1	360	-	76	1350	225	0.30
MN-2	360	-	80	1350	225	0.30
MN-3	360	-	79	1350	225	0.30
MN-4	360	-	81	1350	225	0.30
MRHA	360	-	66	1350	225	0.40
LC^3 mortar mix design						
ML	383	57	-	1350	225	-
MLN-1	248	57	113	1350	225	0.35
MLN-2	248	57	121	1350	225	0.35
MLN-3	248	57	118	1350	225	0.35
MLN-4	248	57	121	1350	225	0.35

For the SAI, the mortar was poured into sets of 40 mm x 40 mm x 160 mm steel molds and compacted on a vibrating table according to [105]. The specimens were covered and stored moist for 48 h and then cured under water. The compressive strength was tested at 7, 28, and 90 days using the Form + Test Prüfsysteme Alpha 1-3000 testing equipment at an increased uniform loading rate of 2400±200 N/s till failure. Early hydration behavior of the OPC, binary blends of OPC, and CC was monitored by isothermal calorimetric measurements using a TAM AIR 8-channel isothermal calorimeter. The test procedure is described in [36]. The heat flow was measured up to 48 hours and the result normalized to 1 g of cement.

4.2.3 Self-compacting paste, mortar and concrete mix design

From this point on, the research focuses on the use of CT7 as CC, the cement is PLC (OPC partially replaced by 15 vol-% LP). The amount of water confined by the binder was determined using the spread flow method. At a constant volume of the powder, V_w/V_p was varied in 0.1 increments between 1 and 2. Four points were used for each binder system, and the relative spread was determined using Equation (1). The V_w/V_p was plotted against the relative spread, and the amount of water confined by the individual binder system ($V_{w\Gamma o}$) was determined by extrapolating the points to the vertical axis as described by [6].

$$\Gamma_{RS} = [d/d_o]^2 - 1 \quad (1)$$

Where Γ_{RS} = relative spread area, $d = (d_1 + d_2)/2$, d_1 = largest flow diameter and d_2 = diameter perpendicular to d_1, and d_o = diameter of mini-slump cone, 100mm.

The influence of CC and RHA on the amount of water confined by the PLC was determined and was used as the basis for establishing the V_w/V_p of the SC-P using Equation (2).

$$V_w/V_p = [0.8 \text{ to } 0.9] \cdot V_{w\Gamma o} \quad (2)$$

Where $V_{w\Gamma o}$ = volume of water confined by binder in relation to its volume

Self-compacting mortar was designed considering the average V_w/V_p required to deform SC-P, and the volume of the fine aggregate (V_s) was set at 40 vol-% of the SC-M volume. The amount of SP is adjusted until for the individual SC-M systems self-compactability is achieved. The deformability of the SC-M systems was evaluated by measuring the slump flow with the mini-slump cone [36] and the range of Γ_m = 4.76 to 5.76 (equally to 24 cm to 26 cm) was used to assess the flowability and the viscosity (R_f) ranges from 0.91 to 1.43 s^{-1} (7 to 11 s) [36], while the segregation resistance of the SC-M was evaluated by visual inspection. To complete the SCC mix design, the volume of CA was adjusted along with the dosage of SP until it was maintained at 33 vol-% of the total volume of SCC. The air content was also set at 2 vol-% of the total SCC volume, according to [107].

Self-compacting paste mixes were produced according to DIN EN 196-1 [105]. The binder, mixing water, and the SP were added together and mixed for 4 minutes in a mortar mixer produced by Bluhm and Feuerherdt GmbH, Berlin, Germany. SC-M was produced by mixing the constituents for 8 minutes in the same mixer. The binder materials, FA, and two-thirds of the mixing water were mixed for 2 minutes, followed by a break of 1 minute to enable the addition of the remaining water and the SP. The entire mixture was then mixed for an additional 5 minutes.

The mixing sequence of SCC started with mixing the binder, FA, and CA for 1 minute in a UEZ ZM 50 concrete mixer (UEZ-MISCHTECHNIK), with a capacity of 60 liters and a mixing speed of 48 rpm. Two-thirds of the mixing water was then added while the mixer was running and

mixed for 2 minutes. The SP and the remaining mixing water were then added and the whole constituents were mixed for another 7 minutes.

4.2.4 Fresh properties of self-compacting concrete

The deformability of the SCC in the absence of obstacles was evaluated using the slump flow according to [108] while the J-ring test was employed to assess the passing ability of the SCC through an obstacle according to [109]. The viscosity of the SCC systems was assessed using both the T_{500} time and the V-funnel test according to [110]. The stability of the SCC was evaluated in two ways. First, using the sieve stability assessment method according to [111] and the washing test according to [112]. The uniform distribution of the CA in the SCC mixtures is monitored over time using a plunger method [113].

Rheology of the SCC in terms of the shear stress (τ), plastic viscosity (μ), and flow resistance were determined using a rotational rheometer, viskomat XL (Schleibinger Geräte) with a vane probe testing paddle at a constant temperature of 20 °C. The measurement started with the maximum rotational speed of 12 rpm for 80 s and decreased in 14 steps of 20 s each until the end of the measurement [114]. The recorded torque was used to estimate the yield stress (τ_0) and plastic viscosity (η) of the SCC according to the Bingham model [115, 116] using Equation (3). The flowability retention of the SCC is monitored by calculating the flow resistance of the SCC mixtures over time (area under the curve) obtained by plotting the torque against the velocity as described previously by [103].

$$\boldsymbol{T} = \boldsymbol{G} + \boldsymbol{N} \cdot \boldsymbol{H} \tag{3}$$

Where T = torque ≈ τ; G = y-intercept of the flow curve ≈ τ_0; N = velocity ≈ $\dot{\gamma}$; and H = the slope of the curve ≈ η.

4.2.5 Portlandite consumption and porosity of self-compacting paste

Portlandite consumption by the CC and RHA and the bound water in hydrate phases formed at 2, 7 and 28 days of curing were investigated by TG measurements in Netzsch STA 449 F3 Jupiter instrument. The constituents of the SC-P were mixed according to [105] and filled into 40 × 40 × 160 mm^3 steel molds and stored in humid conditions for 48 h and then cured under water until testing. At the time of testing, a representative portion of the sample is manually chipped out from the inner part of the prisms and crushed to < 1 mm size using the laboratory pestle and mortar. Hydration of the pulverized binder was stopped by solvent exchange as described in [117]. Approximately 300 mg of the pulverized binder was placed in alumina crucibles and heated to 1000 °C at a heating rate of 2 K/min under a nitrogen atmosphere. The bound water was determined as weight loss (wt-%) from the TG measurements between 25 °C and 400 °C, while the CH content was quantified from the weight loss between 400 °C and 490 °C using the tangent method according to March and Day [118].

Mercury intrusion porosimetry (MIP) was used to evaluate the effect of CC on the pore structure of the binder at 28 days of hydration according to DIN 66133 [119]. Approximately 1 cm^3 of the hardened binder paste was manually cut out from the inner part of the paste prisms. The samples were stored in isopropanol for at least three days and subsequently dried at 70 °C in a ventilated oven. After drying, they were cooled and stored in a desiccator and tested using ThermoFisher mercury intrusion porosimeter with the pressure range of 400 MPa to 400 kPa to measure pore radii from 2 nm to 2 μm. Mercury density of 13.54 g/cm^3, with a surface tension of 0.48 N/m and a contact angle of 140 ° were used as parameters for the MIP

experiments. The pore sizes of SC-P were classified into gel pores (2 – 30 nm), microcapillary pores (30 nm – 1 μm), capillary pores (1 μm – 50 μm) and air voids (> 50 μm).

4.2.6 Plastic, mechanical and durability of self-compacting mortar and concrete

Plastic shrinkage of SC-M at an early age was measured contactless using a shrinkage cone (Schleibinger Testing Systems, Buchbach, Germany) according to [120]. The measurement was started 15 minutes after water addition and lasted for up to 48 h [119]. Polypropylene foil was used to prevent the friction effect between the fresh SCC surface and the shrinkage cone. The SC-M drying shrinkage was measured on 40 × 40 × 160 mm^3 prisms according to [121]. SC-M compressive strength was determined according to DIN EN 196-1 [105]. For SCC compressive strength measurement, fresh SCC was cast into 150 × 150 × 150 mm^3 steel molds and stored moist for 48 h and then cured underwater until the test date. The measurement was performed according to [122] at 2, 7 and 28 days of curing on the Form + Test Prüfsysteme Alpha 1-3000 strength testing equipment with an increasing uniform loading rate of 2400±200 N/s until failure. The influence of CC and RHA on chloride resistance of SCC was investigated using a rapid chloride migration by applying an electric field axially to the test specimen to accelerate the chloride penetration, according to [123]. The depth of chloride penetration was determined on 100 x 50 mm^3 cores drilled and subsequently sliced from 150 × 150 × 150 mm^3 SCC specimens at the age of 28 days of curing.

4.2.7 Embodied energy and CO_2 equivalent quantification

The embodied energy (EE) and the CO_2 equivalent ($CO_{2\text{-eq}}$) of the different mix design used in the research work are estimated using equation (4), based on the EE and the global-warming potentials (GWP) of the individual concrete constituents obtained in the literature, as summarized in Table 2.

$$\mathbf{EE; CO_{2-eq}} = \sum_{i=1}^{n} g_i \times m_i \tag{4}$$

Where g_i = EE or GWP per unit mass of constituent and m_i = mass of concrete ingredient per m^3 of concrete.

Table 2 Embodied energy and CO_2 emission of raw materials [124, 125]

Constituents	Embodied energy (MJ/Kg)	Global-warming potentials ($KgCO_{2\text{-eq}}$)
OPC	4.727	0.83
LP	0.35	0.017
Calcined clay	3.48	0.4
RHA	2.07	0.157
FA	0.022	0.001
CA	0.113	0.007
water	0.006	0.0003
SP	18.3	0.72

Figure 2 shows the schematic representation of the laboratory experiment necessary to achieve the overall aim of the study.

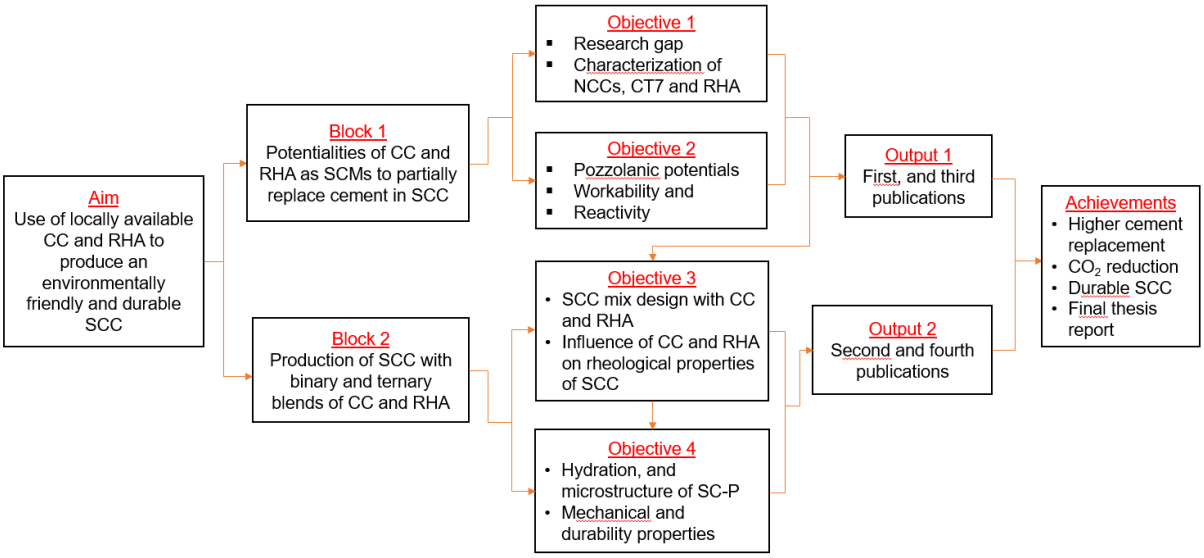

Figure 2 Schematic representation of the research objectives

5 Main results

The scope of the study is divided into two parts: First, the research gap related to the use of CC and RHA as partial replacement to cement in SCC is determined and published in [5]. Also, the pozzolanic potentials of CC and RHA as SCMs, partially replacing OPC at 20 vol-% in mortar were determined, and used as a basis to compare the performance of the Nigerian calcined clays (NCC) with the German calcined clay (CT7). In addition, the NCCs were also tested for their suitability as LC^3 blended cement. Details of the characterization, pozzolanic reactivity, and CO_2 savings that can be achieved by using NCC as a partial replacement to cement have been published in [16]. These two publications are the focus of the first and second objectives (block 1) of the research. The following results give a summary of the potentialities of NCCs, CT7, and RHA as pozzolanic materials in concrete.

5.1 Characterization of the research binder

5.1.1 Mineralogy of clays, chemical and physical properties of binders

Table 3 shows the quantification of the various mineralogical phases of the NRCs and RCT7. RCT7 is common clay with 37 wt-% mica/illite as the main clay mineral, 22 wt-% kaolinite as the second major mineral, and 20 wt-% quartz. NRC-1 and NRC-2 were smectite-rich clays containing about 70 wt-% smectite and about 13 and 22 wt-% kaolinite, respectively. NRC-3 and NRC-4 were kaolinite-rich clays (56 and 49 wt-%, respectively) and they contained more than 30 wt-% quartz as the second main phase.

Table 3 Mineralogical composition of raw clays (wt-%)

Phase [wt-%]	RCT7	NRC-1	NRC-2	NRC-3	NRC-4
Quartz	20	6	4	34	42
Kaolinite	22	13	22	56	49
Smectite	-	71	68	-	-
Mica/Illite	37	10	-	6	6
Rutile / Anatase	2	-	2	3	2
Chloride	6	-	-	-	-
Gypsum	-	< 1	4	-	-
Calcite	7	-	-	-	-
Feldspar	5	-	-	-	-

The mineralogical composition of the NRCs was further confirmed by differential thermal analysis as depicted in Figure 3. NRC-1 and 2 showed a typical differential thermal analysis (DTG) curve pattern of a smectitic clay, while NRC-3 and 4 showed a DTG curve pattern of a kaolinitic clay, confirming the XRD results shown in Table 3.

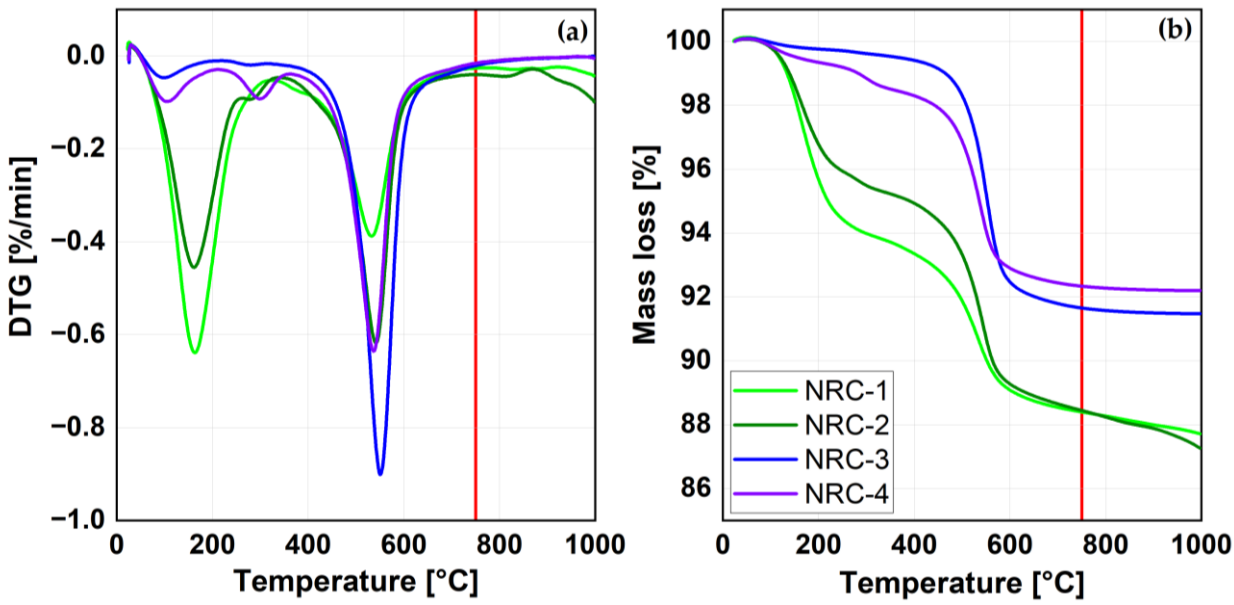

Figure 3 Differential thermal analysis (a) and mass loss (b) of the NRCs

The smectite-rich clays exhibited greater mass loss between 100 and 300 °C, which was related to the removal of water bound to the outer surfaces of the clay minerals. At an intermediate temperature (400 to 650 °C), the kaolinite-rich clays exhibited more dehydroxylation than the smectite-rich clays. Based on the TG results, the calcination temperature for all NRCs was set at 750 °C, i.e., between the dehydroxylation and recrystallization temperatures (red lines in Figure 3). While the calcination temperature of RHA was set at 650 °C based on the TG result presented in Figure 4.

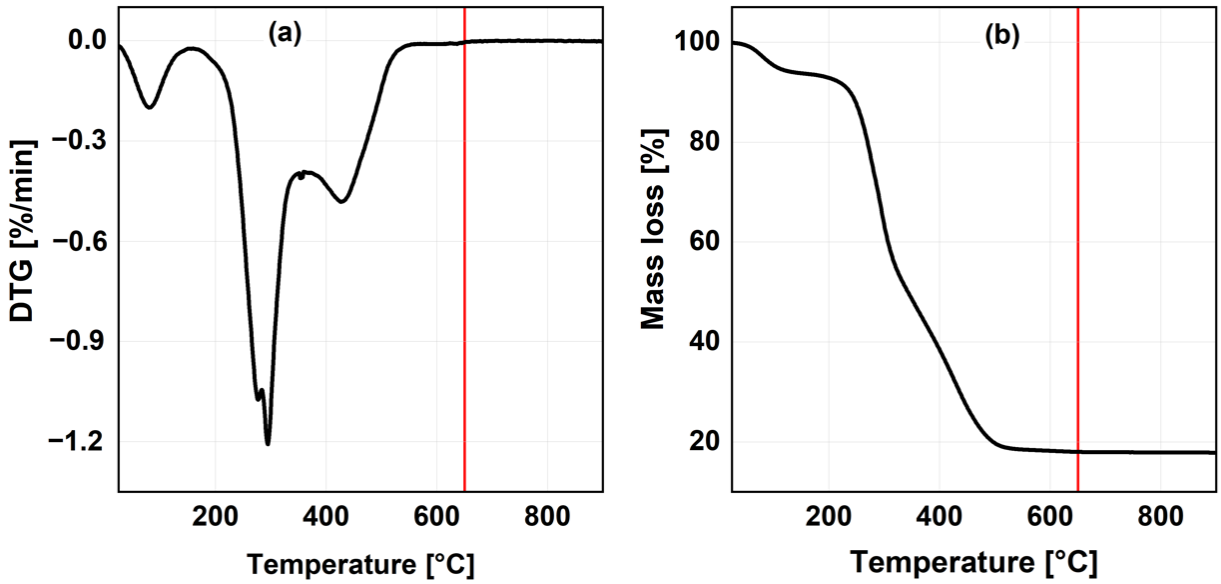

Figure 4 Differential thermal analysis (a) and mass loss (b) of the rice husk ash

The chemical compositions and physical properties of all research binders are summarized in Table 4.

Table 4 Chemical composition and physical properties of the research binders

Chemical composition (%)	OPC	LP	CT7	NCC-1	NCC-2	NCC-3	NCC-4	RHA
SiO_2	20.1	0.6	53.2	55.0	54.3	68.1	68.2	90.8
Al_2O_3	5.4	0.1	22.2	19.1	24.5	24.7	20.4	1.1
CaO	60.7	56.4	6.5	1.3	1.9	24.7	0.2	1.0
Fe_2O_3	2.9	0.1	8.0	7.7	9.5	2.5	8.2	0.8
K_2O	-	0.1	3.5	1.8	1.5	0.4	0.7	2.0
MgO	1.8	0.2	2.7	3.1	2.1	0.1	0.2	1.2
Na_2O	0.7	-	0.4	8.6	0.2	<0.1	<0.1	0.1
TiO_2	0.3	-	1.0	1.0	1.1	3.5	1.5	0.1
SO_3	3.4	-	2.0	0.8	1.9	<0.1	<0.1	0.2
LOI	1.8	42.6	0.02	1.6	3.0	0.5	0.6	2.7
Si/Al (ion solubility)	-	-	1.65	2.24	1.49	1.04	1.05	41.5
Physical properties								
SSA, m^2/g	1.0	1.6	3.9	95.9	75.4	16.7	32.0	160
WD, wt-%	29	20	38	37.3	35.1	31.6	32.5	96
PD, g/cm^3	3.3	2.8	2.7	2.7	2.8	2.78	2.9	2.4
d_{10}, µm	2.6	0.8	1.9	5.4	2.9	2.3	3.6	5.4
d_{50}, µm	16.0	4.6	12.7	34.5	21.7	13.8	28.2	23.7
d_{90}, µm	42.8	20.7	33.7	155.0	85.8	61.0	72.3	56.5

5.1.2 Influence of NCCs and CT7 on early hydration of OPC

The influence of CT7 and NCCs on the early age hydration behavior of OPC is shown in Figure 5. Three distinctive exothermic peaks could be identified. The first peak is related to the initial formation of the ettringite and is followed by a dormant period. The partial replacement of 20 wt-% OPC with CT7 and all the NCCs have no significant effect on the formation and duration of the dormant period. The formation of the second peak (silicate) is related to the dissolution of C_3S and precipitation of C-S-H and occurs after 12 h in the OPC system.

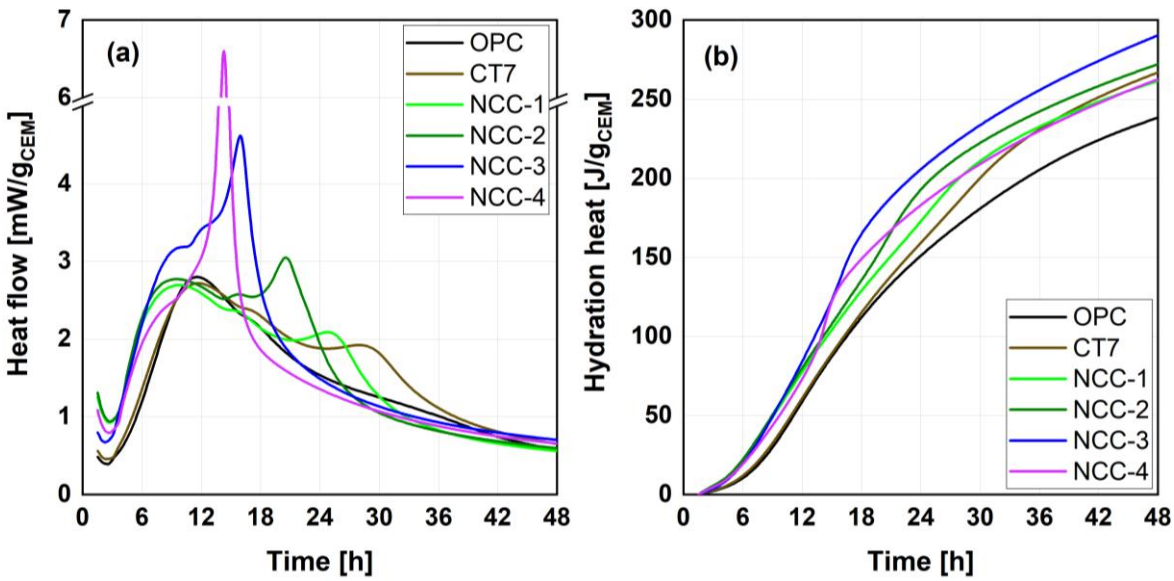

Figure 5 Heat flow (a) and hydration heat (b) of OPC and OPC + CC systems

Similarly, CT7 had no significant effect on the shape and occurrence of the second hydration peak. While the substitution by 20 wt-% NCCs resulted to a comparable acceleration of the silicate reaction for all four NCCs (occurrence after about 9 h). The third peak appeared after the silicate peak due to the depletion of sulfate leading to the dissolution of C_3A and further

precipitation of ettringite (aluminate peak). The aluminate peak occurred in the OPC and CT7 binder systems after about 28 hours of hydration. In contrast, a significant time shift in the aluminate reaction was observed for the NCC systems. The formation of the aluminate peak occurred after 25 h for NCC-1 and after 20 h for NCC-2 (mixtures with metasmectite-rich CC), while it occurred after 16 h for NCC-3 and after 14 h for NCC-4 (mixtures with metakaolin-rich CC) as shown in Figure 5a. Overall, a clear distinction could be made between silicate and aluminate reactions, and the onset of the aluminate reaction was evident in all NCC systems and CT7. Partial replacement of OPC with 20 wt-% NCCs and CT7 generally enhanced the heat of hydration of the OPC, partly due to the filler effect, which increased the nucleation sites and improved the hydration rate of the binder as previously reported by [126]. NCC-3 had the greatest effect, followed by NCC-2, while the other CCs showed similar trends, as depicted in Figure 5b.

5.1.3 Pozzolanic potentials of CC and RHA

The effect of partial replacement of 20 vol-% OPC with the NCCs, CT7, and RHA on workability (a) and compressive strength (b) of mortar is shown in Figure 6. Unlike the remaining CCs, the effect of CT7 on the workability of OPC mortar (M) is rather minor and requires no addition of the SP or adjustment of the w/p to attain a slump flow similar to the M system. All the NCCs require an adjustment of the w/p or addition of SP (0.3 wt-% SP was added to all of them) to achieve deformability similar to that of M, due to their higher SSA and water demand compared to OPC. Similarly, partial replacement of 20 vol-% RHA required adjustment of w/p or addition of SP to achieve deformability similar to M. In this case, 0.4 wt-% SP was added to deform the MRHA system. Both CC and RHA mortar systems achieved pozzolanic activity index (PAI) > 75 % at 28 days of hydration, as shown in Figure 6b. MN-3 achieved a PAI > 100, while MN-1 had the lowest value with a PAI = 80 %. MCT7, MN-2, MN-4, and MRHA have almost the same PAI of about 90 %.

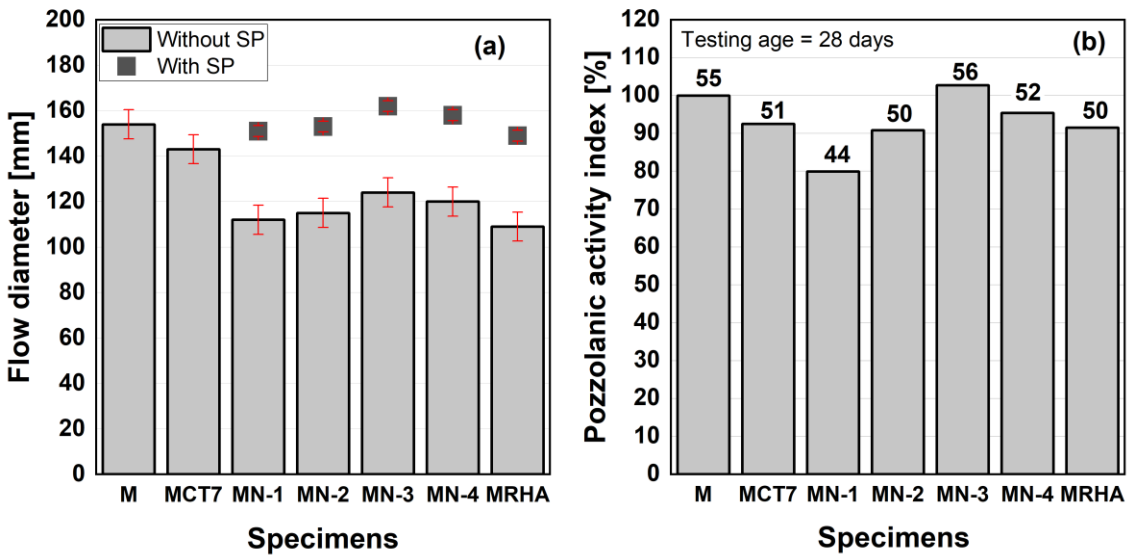

Figure 6 Influence of CC and RHA on workability (a) and PAI of mortar (b). The numbers placed above the bars in (b) denote the compressive strength values in MPa

5.1.4 Performance of the NCCs in the presence of LP

One of the objectives of the study is to achieve higher OPC partial replacement with CC (mix design = 55 vol-% OPC + 15 vol-% LP + 30 vol-% NCCs). It has been previously shown that CCs perform better in the presence of LP and when ternary blended have the potential to replace a high proportion of OPC [16, 36]. For comparison, the MLN-1 to 4 systems were presented together with the ML system as depicted in Figure 7. Similar to the binary blended systems with NCCs presented in Figure 6a, all the ternary blends of NCCs and LP mortar systems require an addition of 0.35 wt-% SP to achieve a slump flow of ± 5 cm of the ML system. Similar to what was previously observed for PAI of NCCs, MLN-3 achieved a compressive strength value = 48 MPa, which is greater than that of ML. MLN-1 and 2 have a compressive strength of 36 and 38 MPa, respectively. While MLN-4 reached a compressive strength of 41 MPa as shown in Figure 7b.

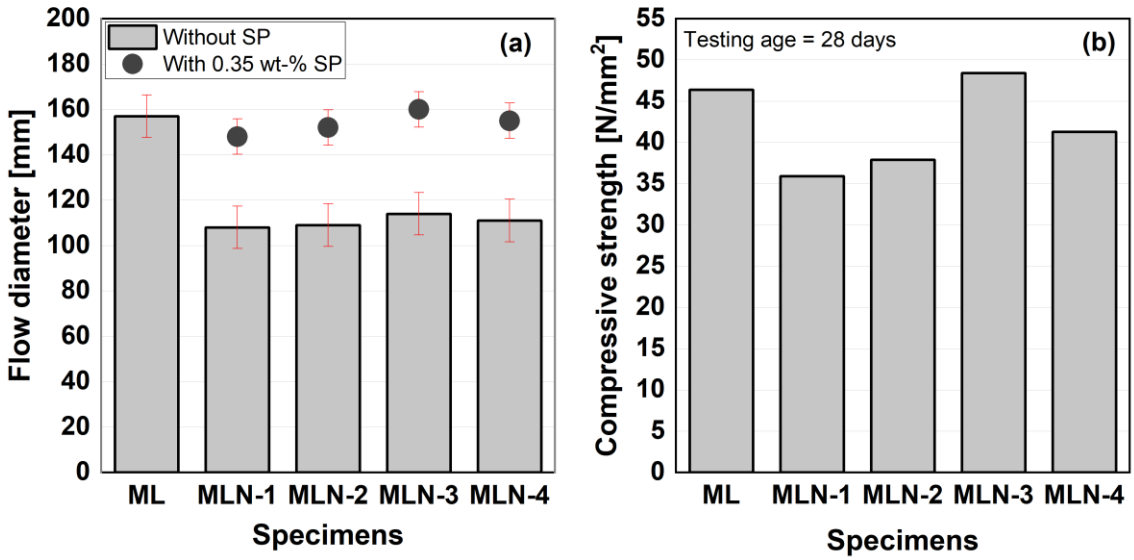

Figure 7 Performance of NCCs in the presence of LP

5.1.5 Discussion

In this chapter, all binders used for the research are characterized, the influence of CT7 and NCCs as partial replacements for OPC in mortars is compared, and the possibilities of higher partial replacement of OPC by NCCs in the presence of LP as a ternary blended binder are investigated. The NRCs can be broadly classified into two groups, namely the smectite-rich clays (NRC-1 and 2) and the kaolinite-rich clays (NRC-3 and 4). RCT7, on the other hand, is common clay with high mica/illite content. The reactivity of CT7 in terms of ion solubility (Si/Al) is intermediate between that of NCC-1 and NCC-2. In general, CT7, NCC-1, and 2 can be classified as 2:1-rich common CCs, while NCC-3 and 4 can be classified as 1:1-rich common CCs. The contents of SO_3 and LOI, as well as the summation of the SiO_2, Al_2O_3, and Fe_2O_3 contents in all the CCs and RHA, are within the limits recommended by ASTM C618 [127] for natural and calcined pozzolan to be used in concrete. Considering the effect of the NCCs and CT7 on the early hydration behavior of the OPC, a clear distinction existed between the silicate and aluminate hydration maxima in all CC blended systems, except NCC-4, which had a strong overlap of these maxima. Therefore, at 20 wt-% CC replacement, only NCC-4 requires a

sulfate adjustment to prevent flash setting and ensure the sequential occurrence of the hydration maxima as previously observed by [60, 128]. All the CCs enhanced the heat of hydration of OPC at 48 h of testing.

Considering the effect of CC and RHA on the workability of the mortar, the partial substitution of 20 vol-% CT7 had no significant effect on the slump flow of the OPC mortar and does not require w/p adjustment or SP addition to achieve similar workability to the OPC mortar system. Unlike CT7, all the NCCs and RHA require w/p adjustment and/or SP addition to achieve similar deformability to OPC. As for the CCs, although the NCCs have a water demand similar to that of CT7, they have a negative effect on the workability of the mortar by reducing the slump flow due to their high SSA compared to both OPC and CT7. More so, RHA affects the workability of the mortar due to its higher water demand and SSA as also previously observed by [80, 129]. Consequently, NCCs and RHA require an SP addition to achieve similar deformability performance to the OPC and PLC mortar reference systems. This would incur additional but negligible costs considering the ≥ 20 vol-% replacement of cement with a less costly material.

Moreover, considering the development of the compressive strength, similar to the CT7 mortar system, the NCCs achieve 28 days PAI > than the minimum specified by ASTM C618 [127] for natural and calcined pozzolan to be used in concrete. The performance of the RHA is comparable to that of CT7 in terms of the 28 days compressive strength. The minimum 28 days compressive strength achieved by the NCCs at 20 vol-% OPC partial replacement was 44 MPa, which is enough for general production of concrete up to grade C35/45. For the ternary composite cement with the NCCs and LP, the same application holds for the metakaolin-rich NCCs, whereas for the metasmectite-rich NCCs, the compressive strength values at 28 days of curing were 36 and 38 MPa for MLN-1 and 2, respectively. This limits their use to general construction work under normal environmental conditions and the production of concrete up to grade C25/30. In practice, this concrete grade is sufficient for general construction works to provide the required concrete infrastructure in the sub-Saharan Africa region.

The performance of the NCCs in terms of pozzolanic reactivity is comparable to that of CT7. The major difference identified so far in this research is the difference in physical properties such as SSA - which is due to the differences in mineralogical composition of the raw clays, and the PSD – which depends on the degree of grinding of the CCs, and additionally to the extent of treatment of the raw clays. For example, RCT7 was calcined and ground on an industrial scale, while the RNCs were calcined and pulverized in small quantities (≈1 kg) in the laboratory. The potentialities of the NCCs as SCMs partially replacing cement in mortar has been published in [16], and from this point, the research will consider the use of CT7 as CC for the production of self-compacting paste, mortar, and concrete, since such quantities needed for all samples will be difficult to be transported from Nigeria. OPC is partially replaced with 15 vol-% LP to form PLC blended cement. The essence of the LP addition is to reduce the friction between the particles of OPC and improve its deformability, in addition to the other benefits. This blended cement is used to produce the reference mixes for the research.

5.2 Optimization of SCC mix design with the blends of CC and RHA

The third objective of the thesis focuses on considering the challenging physical properties of CC and RHA to optimize SCC mix design and to measure its fresh properties. This was

achieved by designing and producing the paste phase of the SCC which was used as a medium to deform the fine aggregate, forming SC-M. The SC-M was used as a medium to deform the coarse aggregate, forming SCC. The outcome has been published in [36, 130]. The following summarizes the results obtained.

5.2.1 Self-compacting paste design

A stepwise rational mix design was adapted to optimize the final SCC proportioning of the constituents. First, the effect of CC and RHA on the ratio of confined water by the binder and the water demand of the respective binder systems was considered as shown in Figure 8a.

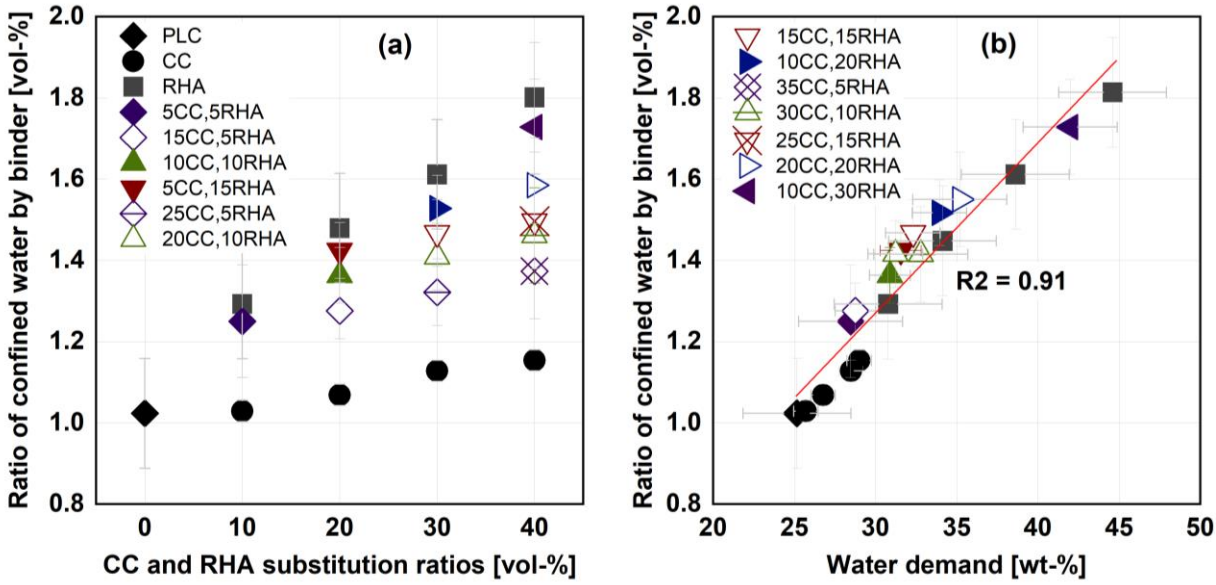

Figure 8 Influence of CC and RHA on the ratio of confined water by binder (a) and the relationship between the water demand and the water confined by binder (b). The legends hold for both parts of the graph.

At a constant volume of powder, PLC confined approximately a volume of water equal to the volume of solid - determined by extrapolating (on the vertical axis) the plot of V_w/V_p against the relative spread (as explained under section 4.2.3). PLC partial replacement with CC showed no significant effect on the volume of water confined and increased only by 12 vol-% of water at a substitution ratio of 40 vol-%. In contrast, partial replacement of PLC with RHA showed a significant effect on the volume of water confined by the binder, increasing to 76 vol-% at an RHA substitution ratio of 40 vol-%. However, the ternary blends of CC and RHA yielded no significant reduction in the ratio of water confined by binder due to the high-water demand of RHA, for instance, the ratio of water confined by 40 vol-% CC replacement is 1.15 and increased drastically to 1.37 when 5 vol-% of CC is replaced by RHA in the blend (35CC,5RHA). The ratio of confined water by the binder is related to its water demand, with an $R^2 = 0.91$ as depicted in Figure 8b. The PLC and the binary blends with CC and RHA appeared on and/or below the regression line, while the ternary blends of CC and RHA appeared above the regression line. This could be due to the dominant influence of RHA on the physical properties of the ternary blended binder. Another possible reason for this behavior could be improper mixing of the two materials due to the variation in their surface morphology, as explained in [130].

The V_w/V_p required to impart on paste self-compactability is calculated from the volume of water confined by the individual binder system, as shown in Table 5. PLC (0 CC + 0 RHA) requires an average of 0.87 V_w/V_p to achieve self-compactability. Partial substitution of CC showed no drastic effect on this value and therefore requires only a slight adjustment of this value or an increase of SP dosage to achieve similar deformability class as the PLC system. On the other hand, partial substitution of PLC with RHA requires a significant adjustment of V_w/V_p to achieve self-compactability. For instance, with partial substitution of 10 vol-% RHA, V_w/V_p already increased to 1.1, which is 21 % higher than the value required for PLC. In this case, SP adjustment is not sufficient to achieve the required degree of deformability because of the higher water demand and SSA of the RHA compared to PLC. Therefore, urgent adjustment of the V_w/V_p of the RHA and the ternary blended systems with CC and RHA is required to achieve a deformability characteristic similar to that of PLC. Consequently, the mix design will consider the individual effects of CC and RHA on the deformability of SC-M and establish what can be achieved by using these SCMs in terms of self-compactability requirement.

Table 5 Average Vw/Vp required by individual binder system to achieve self-compactability

CC / RHA	0	5	10	15	20	25	30	35	40
0	0.87		0.87		0.91		0.94		0.98
5		1.1		1.08		1.12		1.17	
10	1.10		1.16		1.2		1.24		
15		1.21		1.25		1.27			
20	1.26		1.3		1.35				
25		1.34		1.42					
30	1.37		1.47						
35		1.50							
40	1.51								

5.2.2 Self-compacting mortar design

The influence of adjusting the V_w/V_p, SP dosages, and V_s to achieve a workability threshold of both the relative flow Γ_m (4.76 to 5.76) and relative flow velocity R_f (0.91 to 1.43 s^{-1}) for the reference SC-M is presented in Figure 9 (red dot line). These attributes were accomplished at a V_s = 40 %, V_w/V_p = 0.875, and 0.45 wt-% SP and is denoted from here on as SC-M-1. It's possible to increase the V_s to 48 % but at the expense of increasing the SP dosage. Higher Γ_m values indicate higher deformability tendencies and smaller R_f values indicate higher viscosity [131]. Figure 10 shows the influence of PLC partial replacement with CC and RHA on the workability threshold (Γ_m and R_f) of SC-M-1. Increasing the PLC replacement level by CC resulted in a decrease of both the Γ_m and R_f of the SC-M. With the here used replacement levels beyond 20 vol-%, a higher dosage of SP is required to improve the deformability of the SC-M. The established R_f values were difficult to achieve with replacement levels beyond 10 vol-% CC. Nonetheless, the Γ_m were achieved with PLC partial replacement up to 40 vol-% CC. Therefore, the limits are adjusted to accommodate the effect of CC at higher replacement levels (blue dash line in Figure 10).

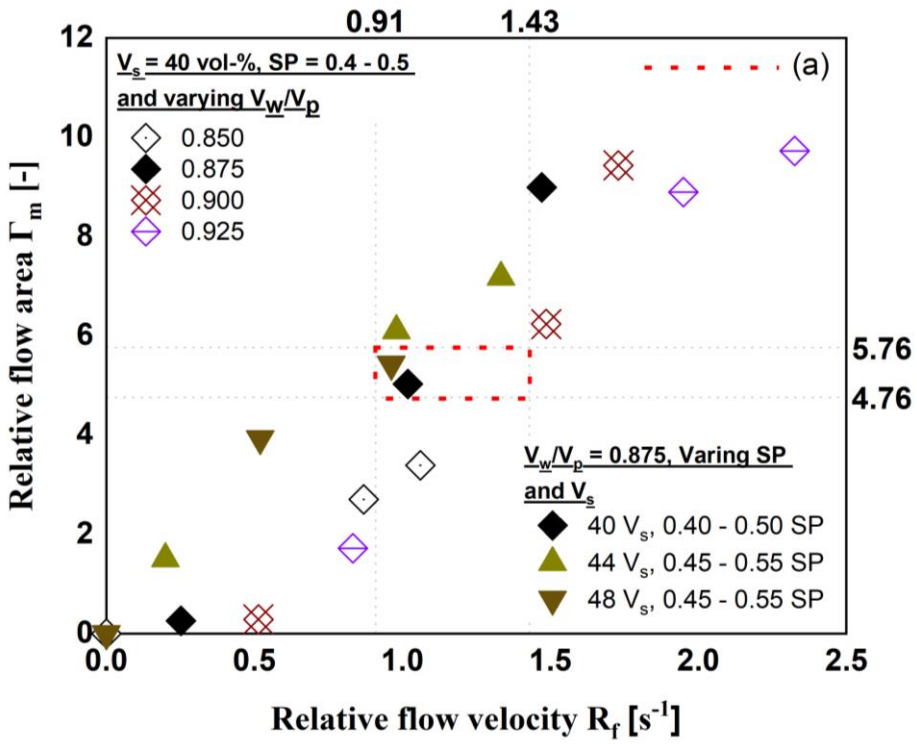

Figure 9 Influence of V_w/V_p, SP and V_s adjustment the Γ_m and R_f of SC-M, (a) = Γ_m and R_f thresholds recommended by [107]

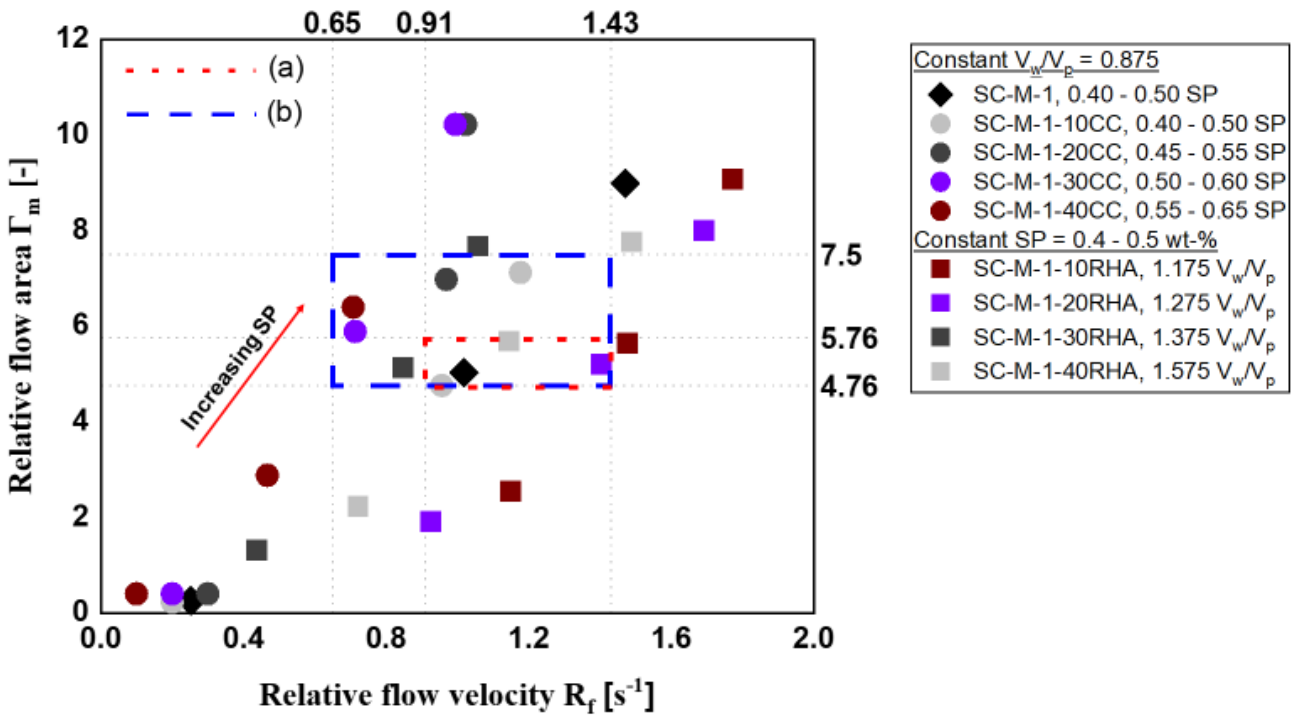

Figure 10 Influence of CC and RHA on the Γ_m and R_f of SC-M, (a) = Γ_m and R_f thresholds recommended by [107] and (b) = proposed Γ_m and R_f thresholds.

The use of CC as partial replacement to cement decreased the deformability rate of SC-M and, therefore, a new lower R_f limit of 0.65 s^{-1} is proposed based on the experimental results obtained to accommodate up to 40 vol-% PLC replacement by CC. The upper limit of R_f (1.43

s^{-1}) remains unchanged. Consequently, the established Γ_m upper limit has to be adjusted to accommodate SC-M with 20, 30, and 40 vol-% CC, as these mixes are still self-compacting. Therefore, a new SC-M workability window with R_f = 0.65 to 1.43 s^{-1} and Γ_m = 4.76 to 7.50 is proposed to accommodate cement replacement with up to 40 vol-% CC without an adjustment of the V_w/V_p as indicated by the blue dashes in Figure 10.

The partial replacement of PLC with RHA required a complete adjustment of V_w/V_p to achieve deformability comparable to SC-M-1, the adjustment of SP alone is not sufficient. Therefore, for each replacement level with RHA, an increase of the V_w/V_p is urgently required due to the higher water demand and SSA of RHA. The summary of V_w/V_p and SP required to deform the individual RHA system is also shown in Figure 10. These basic mixtures of CC as replacement to PLC with a V_w/V_p = 0.875, with varying SP dosages, and RHA as replacement to PLC with an SP dosage = 0.4 – 0.5 wt-%, with varying V_w/V_p were used to establish the grade of SCC and the level of CO_2 reduction that can be achieved with them.

5.2.3 Self-compacting concrete mix design

For SCC produced with the binary blends of CC as partial replacement to PLC, a V_w/V_p = 0.875 was used and PLC was partially substituted with CC up to 40 vol-% and the mix design has been published in [97]. For the binary and ternary blends with RHA, considering that RHA poses a challenge to deformability at higher PLC partial replacement due to its high water demand, PLC partial replacement with RHA was kept at 20 vol-%. For comparison, the binary blend with CC was also kept at 20 vol-%, and the ternary blend was achieved using 10 vol-% CC + 10 vol-% RHA. Therefore, V_w/V_p = 1.275 required to impart self-compactability to the 20 vol-% RHA binder system was considered to compare the influence of CC and RHA on the rheological and hardened properties of SCC. The V_s was adjusted to 44 vol-% of the total SC-M volume, while the SP and the volume of CA (finally fixed at 33 vol-% of the total SCC volume) were adjusted until acceptable deformability was achieved. The volume of air (V_a) was fixed at 2 vol-% of the total SCC volume according to [107]. Criteria for assessing the deformability of SCC in the absence of obstacles (filling ability) include the slump-flow and V-funnel time as an indication of viscosity, while the use of a J-ring gives an estimation of the deformability in the presence of obstacle (passing ability). By adjusting the SP dosages, SCC-1 achieved a deformability class SF2 and viscosity class VF1 according to [132] as shown in Figure 11a. With a slight increase in the SP dosage, SCC-1-20CC achieved similar deformability to the SCC-1, with viscosity class VF1. SCC-1-20RHA requires an increased SP dosage to attain deformability class SF2 and viscosity class VF1 compared to SCC-1-20CC. SCC-1-10CC+10RHA, exhibited a deformability and viscosity behavior somewhat in-between that of binary CC and RHA SCC. Similarly, by adjusting the SP dosages, the blocking tendency of the SCC decreases and it is possible to bring all the SCC mixtures to a passing ability class PJ2, classified according to [132] (Figure 11b).

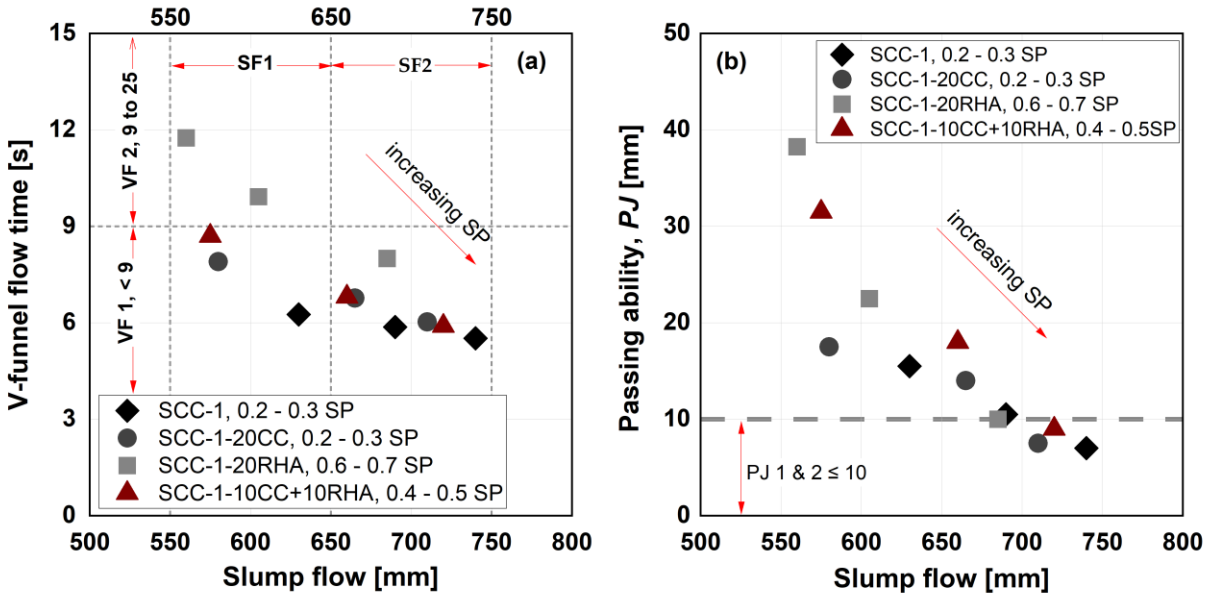

Figure 11 Influence of CC, RHA and varying SP dosages on the deformability characteristics of SCC, data already published in [130]

The final mix design of the research is divided into three areas: First, a mix design considering the effect of the binary blend of CC on the deformability of the SCC, in this case, a V_w/V_p = 0.875, corresponding to w/p = 0.29, similar to what has used previously by [133], was used for the production of the self-compacting paste, mortar and concrete. Details of the rheological and hardened properties of the self-compacting paste and mortar have already been published in [36, 97] as part of this research. For comparison purposes, only the SC-M mix design will be presented in this report as shown in Table 6. The compressive strength obtained will also be presented in section 5.7.7 of the report. Similarly, the mix design of individual RHA replacement levels is also presented and what can be achieved from each RHA-SC-M system is going to be presented in section 5.7.7.

Finally, to compare the blends of CC and RHA, a V_w/V_p = 1.275 (0.42 w/p equivalent) and varying SP dosages are used. This may particularly affect the stability of SCC-1 and SCC-1-20CC (binders with lower water demand), since the viscosity of SCC largely depends on the w/p: The higher the w/p, the higher the flow rate of SCC, as previous studies with a w/p ≥ 0.5 showed a VF time ≤ 6 s [134, 135]. When the w/p is < 0.4, SCC yields a VF time ≥ 6 s [97, 136]. SCC-1 with 0.25 SP dosages is at the limit for both the filling and passing ability values but is considered suitable for the final SCC mix design. The selection criterion for the final SCC mix design is therefore based on SF ≥ 650 mm, VF ≥ 6 s and PJ ≤ 10 mm, and the proportions of the final SCC mix designations are presented in Table 6, and are used to determine the influence of CC and RHA on the rheology, flowability retention, compressive strength and chloride migration resistance of SCC. The SC-P mixes, presented under the final mix design section in Table 6, are used to determine the influence of the binary and ternary blends of CC and RHA on the formation of hydrate phases of SC-P and its porosity. Similarly, the SC-M mixes are used to determine the influence of CC and RHA on plastic and drying shrinkage of the SC-M.

Table 6 Self-compacting paste, mortar and concrete mix designations

Mix designation	Constituent [dm³/m³]								
	V_w/V_p	OPC	LP	CC	RHA	Water	FA	CA	SP [wt-%]
Influence of CC on SC-M mix design, only SP is adjusted, V_w/V_p = 0.875									
SC-M-1	0.875	272	48	-	-	280	400	-	0.45
SC-M-1-10CC	0.875	245	43	32	-	280	400	-	0.45
SC-M-1-20CC	0.875	218	38	64	-	280	400	-	0.50
SC-M-1-30CC	0.875	190	34	96	-	280	400	-	0.55
SC-M-1-40CC	0.875	163	29	128	-	280	400	-	0.60
Influence of RHA on SC-M mix design, with adjusted V_w/V_p, SP = 0.45 wt-%									
SC-M-1	0.875	272	48	-	-	280	400	-	0.45
SC-M-1-10RHA	1.175	211	37	-	28	324	400	-	0.45
SC-M-1-20RHA	1.275	179	32	-	53	336	400	-	0.45
SC-M-1-30RHA	1.375	150	27	-	76	347	400	-	0.45
SC-M-1-40RHA	1.575	119	21	-	93	367	400	-	0.45
Final SCC mix design to compare the blend of CC and RHA, V_w/V_p = 1.275 and varying SP									
SC-P	1.275	374	66	-	-	560	-	-	0.05
SC-P-20CC	1.275	299	53	88	-	560	-	-	0.10
SC-P-20RHA	1.275	299	53	-	88	560	-	-	0.30
SC-P-10CC+10RHA	1.275	299	53	44	44	560	-	-	0.20
SC-M-1	1.275	224	40	-	-	336	400	-	0.15
SC-M-1-20CC	1.275	179	32	53	-	336	400	-	0.20
SC-M-1-20RHA	1.275	179	32	-	53	336	400	-	0.40
SC-M-1-10CC+10RHA	1.275	179	32	26	26	336	400	-	0.30
SCC-1	1.275	137	24	-	-	206	289	323	0.25
SCC-1-20CC	1.275	110	19	32	-	206	289	323	0.30
SCC-1-20RHA	1.275	110	19	-	32	206	289	323	0.70
SCC-1-10CC+10RHA	1.275	110	19	16	16	206	289	323	0.50

5.3 Rheological properties and flowability retention of SCC

5.3.1 Influence of CC and RHA on the segregation resistance of SCC

One important attribute that determines the acceptance of SCC is its ability to deform uniformly and fill all formwork corners and reinforcement gaps without segregation. Depending on the intended use of the fresh SCC, the self-compacting properties are expected to be maintained until the SCC is poured into the forms. For short-term segregation resistance, within 30 minutes of mixing, the sieve stability and aggregate washing test indicate the stability of SCC. Figure 12a shows the segregated portion of the SCC specimens determined by sieve stability. The segregated portion of all the SCC specimens is less than 11 wt-%, which is within the limit specified by [132]. The influence of CC and RHA on the uniform distribution of CA over the cross-section of fresh SCC evaluated by aggregate washing test is shown in Figure 12b. The mass deviation of the CA from the three segments of all four test specimens is less than 4 wt-%, well below the limit of 15 wt-% specified in [112].

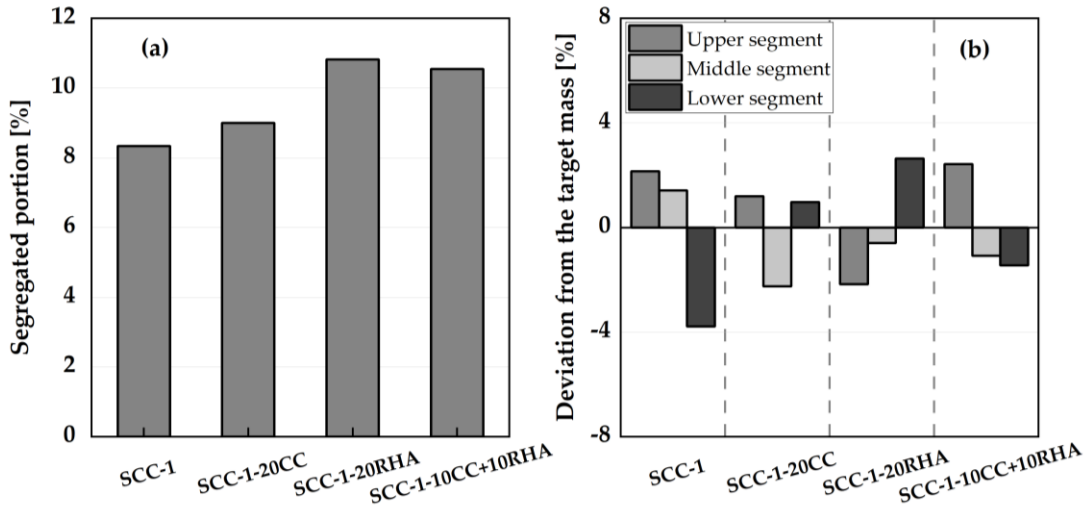

Figure 12 Sieve stability segregation resistance (a) and aggregate wash test (b) of SCC

For ready-mix SCC, extended flowability retention beyond 30 min may be required. The influence of CC and RHA on the flowability retention up to 90 min is monitored by sedimentation analysis using a plunger method as shown in Figure 13. SCC-1 and SCC-1-20CC remain stable until 75 minutes, the plunger almost reaching the bottom of the cylinder. At 90 minutes the immersion depths decrease indicating that setting has started. SCC-1-20RHA and the ternary blend SCC-10CC+10RHA also showed similar sedimentation tendencies. In this case, the stability retention lasts up to 30 minutes beyond which the plunger only sinks halfway down the cylinder, and at 60 minutes the penetration is virtually not possible due to the stiffening of the SCC surface.

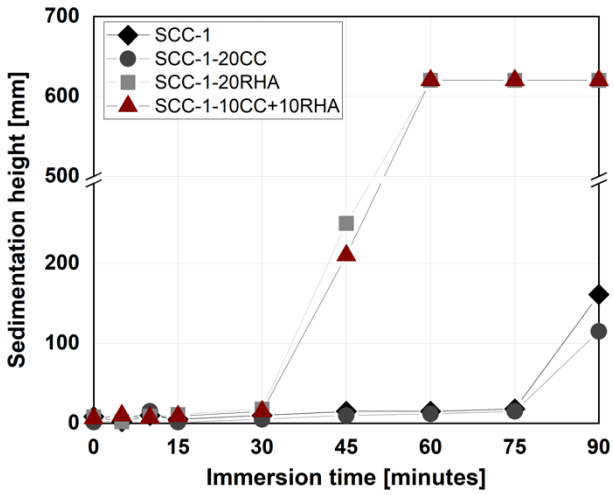

Figure 13 Flowability retention assessment of SCC

5.3.2 Rheological and time dependent flowability retention of SCC

The influence of CC and RHA on torque required to initiate and maintain displacement of SCC based on the applied shear rate measured with a viscometer is depicted in Figure 14. SCC-1 yielded a torque of 66 Nmm at a lower velocity of 1 rpm, and 109 Nmm at the maximum applied velocity of 12 rpm at 15 min of testing to initiate and maintain displacement. These values increased to 133 and 228 Nmm, respectively after 90 min of testing. Similar to what was observed on the flowability retention assessment of SCC in Figure 13, SCC-1-20CC required

lower torque to achieve and maintain displacement compared to SCC-1, both at lower and higher velocities and at all test times. For the RHA binder system, on the other hand, at 15 min of testing, a torque of 102 Nmm was measured at a lower velocity and 180 Nmm at a higher velocity. These values increased significantly after 30 min of testing due to the stiffening of the SCC-1-20RHA mixture as a result of the higher water demand of RHA. The ternary blend with CC and RHA behaved somewhat in between the SCC-1-20CC and SCC-1-20RHA, the presence of the CC in the blend decreased the torque required to achieve displacement at 90 min of testing by 53 and 59 % at lower and higher velocities, respectively, compared to RHA-SCC system.

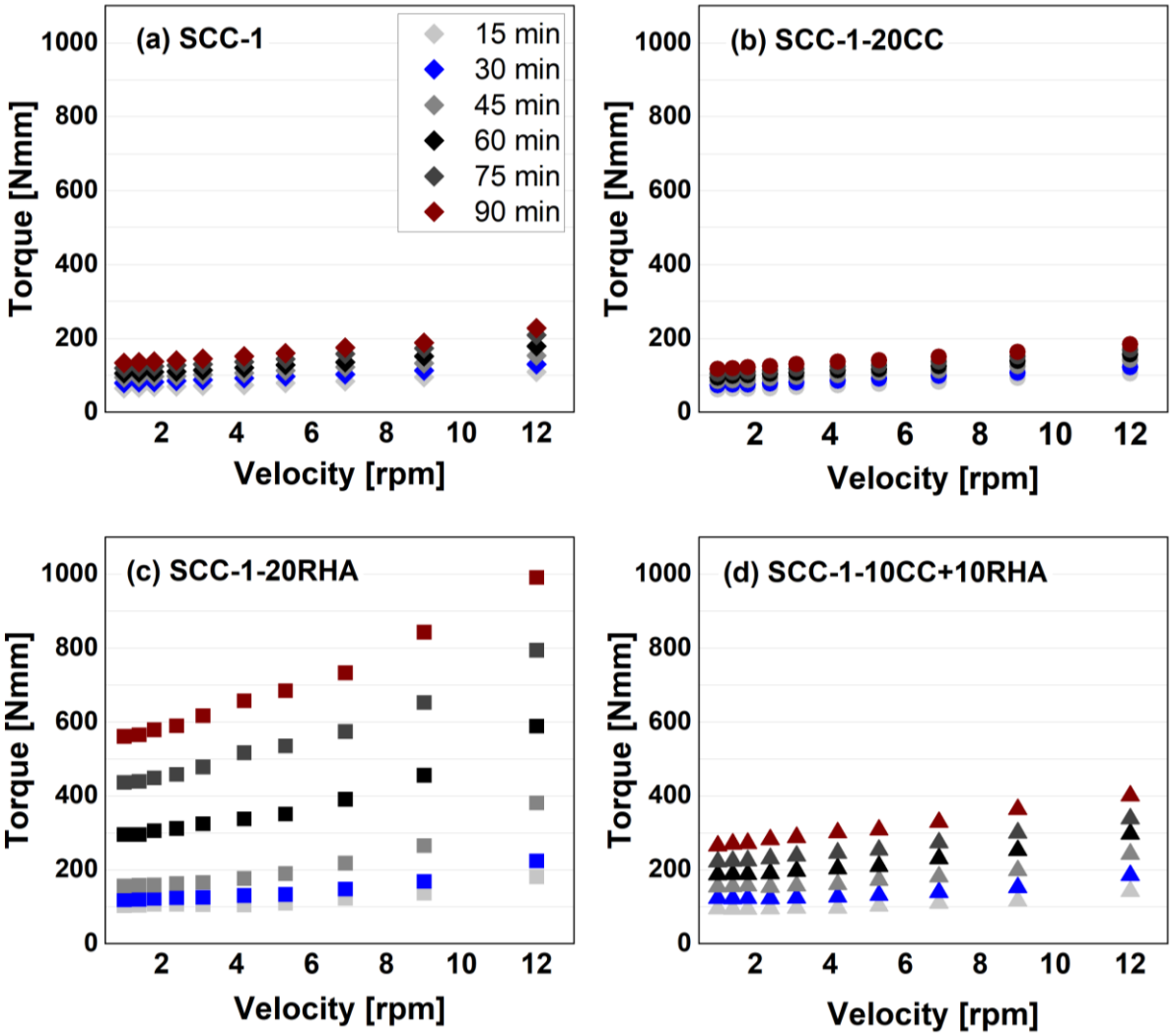

Figure 14 Influence CC and RHA on the time-dependent displacement of SCC

The yield stress and plastic viscosity of the SCC mixes were determined from the measured torque values induced by the applied velocity using a Bingham model as presented in Figure 15. The measured yield stress and plastic viscosity of SCC-1 at 15 min of testing were 60 Nmm and 3.9 Nmm*min, respectively, which gradually increased to 120 Nmm and 8.2 Nmm*min, after 90 min of testing. SCC-1-20CC showed a similar increasing trend in yield stress and viscosity values as SCC-1. SCC-1-20RHA had yield stress of 88.5 Nmm and a plastic viscosity of 6.2 at 15 min of testing, which are 47 and 59 % higher than SCC-1, respectively. This yield stress and plastic viscosity values increased rapidly up to 90 min of testing, unlike the SCC-1 and SCC-1-20CC systems. The ternary blend of CC and RHA on the other hand, had both,

lower dynamic yield, plastic viscosity values, and a smaller rate at which they increased compared to SCC-1-20RHA.

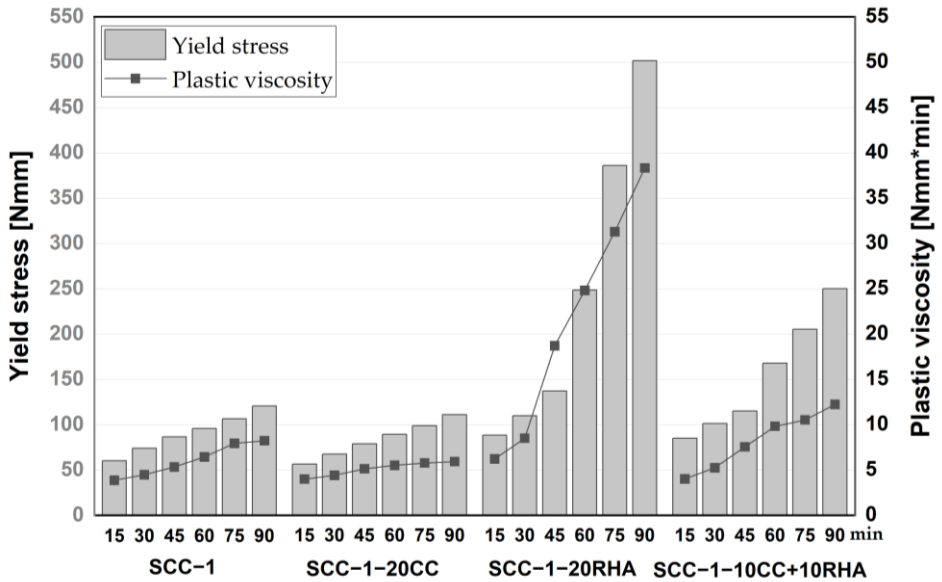

Figure 15 Time dependent dynamic yield stress and viscosity values of SCC measured up to 90 min after water addition

The effect of CC and RHA on the flowability retention of SCC was further assessed by determining the change in the flow resistance of SCC over time, as presented in Figure 16. SCC-1 had a flow resistance of 933 Nmm/min measured 15 min after water addition and increased to 1900 Nmm/min after 90 min. Partial replacement of PLC with 20 vol-% CC had no significant effect on the flow resistance of SCC-1, whereas partial replacement of PLC with 20 vol-% RHA had a great effect on the flow resistance of SCC especially after 30 min of testing. This is evident in SCC-1-20RHA, which already had a flow resistance value of 1388 Nmm/min at 15 min, which is 30 % higher than SCC-1 and increased to 8205 Nmm/min at 90 min of testing. SCC-1-10CC+10RHA showed similar flow resistance to SCC-1-20RHA up to 30 minutes of testing, after which it increased less compared to SCC-1-20RHA.

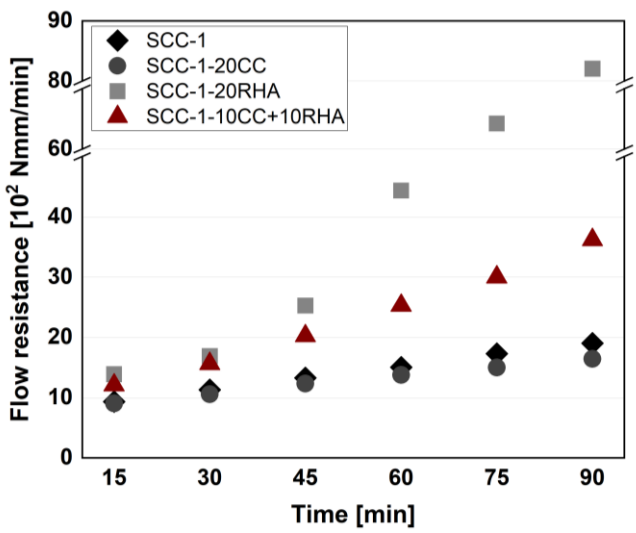

Figure 16 Effect of RHA and CC on the flow resistance of SCC

5.3.3 Discussion

Short-term stability in terms of segregation resistance is an important attribute that determines the acceptability of SCC. The segregation resistance of all SCC mixes is within the specified limits by [112, 132] and even SCC produced with 20 vol-% RHA as PLC partial replacement retained its stability up to 30 min after mixing. For flowability retention evaluation, the use of 20 vol-% RHA as a partial replacement to PLC is considered critical because the free water was absorbed after 30 min of mixing, making the SCC mix stiffer and rapidly losing its self-compactability. The use of 20 vol-% CC as a partial replacement to PLC in SCC resulted in a decrease in the torque required to initiate and maintain displacement of the SCC. Although CC has a higher water demand than PLC, the reduced torque could be due to the higher dosage of SP used to deform the SCC-1-20CC system, despite both binder systems required almost similar V_w/V_p to achieve self-compactability, as shown in Table 5.

Despite an increase in the SP dosages to deform the RHA-SCC systems, the use of RHA as a partial replacement for PLC resulted in an increase torque required to initiate and maintain displacement of the SCC due to higher water demand and SSA of RHA. All SCC mixes experienced an increase in the yield stress and plastic viscosity over time, which can be attributed to the loss of water from the SCC surfaces due to evaporation or the chemical reaction between the binder and mixing water leading to the initial formation of ettringite [137]. In all cases, SCC mixtures containing RHA exhibited higher values of yield stress and plastic viscosity due to their higher water demand. The rapid increase in yield stress and plastic viscosity is due to the increase in plastic stiffening caused by the continued absorption of the mixing water by the RHA particles.

Both SCC-1 and SCC-1-20CC showed similar flow resistance tendencies over time, but SCC-1-20RHA showed a significant increase in the flow resistance, especially after 30 min of testing. SCC-1-10CC+10RHA showed similar flow resistance to SCC-1-20RHA up to 30 min of testing, after which it increased less compared to SCC-1-20RHA. The decrease in the flow resistance of SCC-1-10CC+10RHA is due to the presence of CC in the blend, which reduces the water demand and SSA of the system. In general, by increasing the SP dosage, PLC partial replacement with 20 vol-% CC does not affect flowability retention of SCC up to 90 min and therefore, SCC-1-20CC can be used to produce both in-situ, precast, and ready-mix SCC. However, the use of 20 vol-% RHA and the ternary blend 10CC+10RHA developed high flow resistance and exhibited rapid loss of flowability after 30 min of mixing. Therefore, their flowability retention needs to be improved for applications beyond 30 minutes.

5.4 Plastic, hardened and durability properties

The fourth objective of the thesis deals with the study of the influence of CC and RHA on the formation of hydrate phases, portlandite consumption and porosity of self-compacting paste, plastic and total shrinkage of self-compacting mortar, compressive strength, and chloride migration resistance of self-compacting concrete. Results obtained have already been published in two journals [36, 130] and a conference paper [97]. In this section, the summary of the effect of binary and ternary blends of CC and RHA on the formation of hydrate phases of SCP and porosity up to 28 days of testing is presented. The plastic and drying shrinkage of SC-M and compressive strength are also presented. Finally, the compressive strength and chloride migration resistance of SCC are presented.

5.4.1 Formation of hydrate phases from the hardened SCP

The influence of partial replacement of PLC with CC up to 40 vol-% at a V_w/V_p = 0.875 on the formation of hydrate phases, CH consumption, and porosity of SCP had already been published in [36] as part of this thesis. For comparison with the influence of a binary blend with RHA and a ternary blend of CC and RHA, the following results at a V_w/V_p = 1.275 are presented and discussed. Figure 17 shows the differential thermal analysis of the SCP specimens at 2, 7 and 28 days of hydration. The first mass loss observed between 50 °C to 140 °C is due to dehydration of the ettringite (E) and calcium silicate hydrates (C-S-H), as previously reported by [138], and increases with hydration time for all the SCP specimens. The second mass loss, observed between 140 °C and 190 °C is attributed to the dehydration of the monophases (AFm) [139] and is more pronounced in the SCP with RHA partial replacement in all hydration stages. Calcium hydroxide (CH) decomposition occurs between 400 °C to 450 °C for all SCP specimens, while calcium carbonate ($CaCO_3$) decomposition takes place between 600 °C to 800 °C. The pattern of the formation of the hydrate phases is similar to what was observed previously by [36] when CC was used as a partial replacement for PLC in SCP.

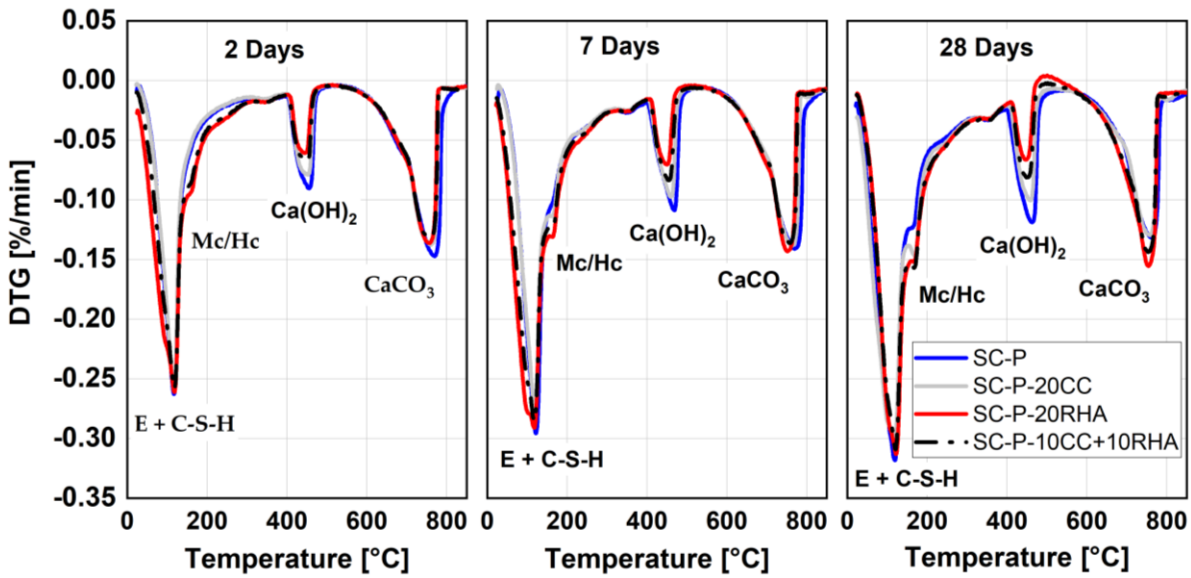

Figure 17 Differential thermal analysis of SCP specimens

The CH content in g/100g_{binder}, quantified by the tangent method from the weight loss between 400 °C and 450 °C of all SCP samples, is shown in Figure 18. SC-P has the highest CH content at each test age, while SC-P-20RHA exhibits the lowest CH content. The CH content of SC-P and SC-20CC increases with hydration age up to 28 days of testing. While the CH content of SC-P-20RHA and SC-P-10CC+10RHA increases up to 7 days and decreases at 28 days of testing. The CH content of SC-P-10CC+10RHA is halfway between that of SC-P-20CC and SC-P-20RHA at all test ages.

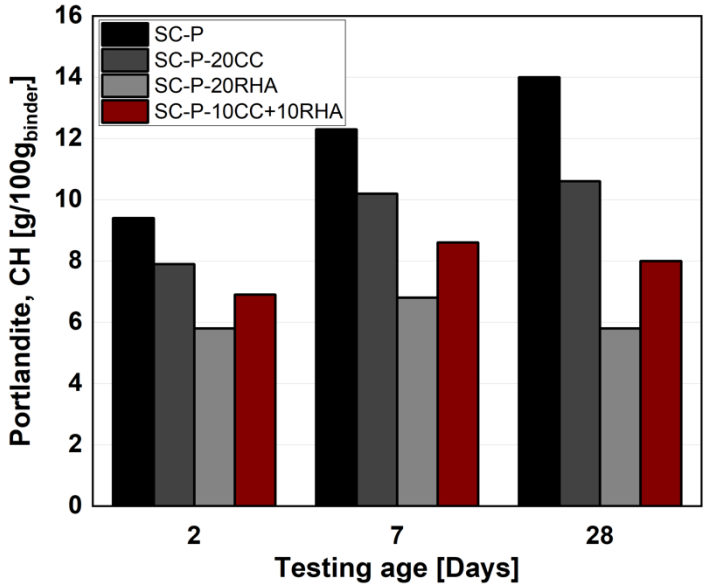

Figure 18 Influence of CC and RHA on the CH consumption

5.4.2 Formation of hydrate phases from the hardened SCP

Figure 19 shows the effect of CC and RHA on the specific pore volume (a) and average pore diameter of SC-P (b) measured by MIP at 28 days of hydration. PLC partial replacement with the binary blend of RHA and a ternary blend of CC and RHA decreased the average pore diameter of the SC-P, while PLC partial replacement with the binary blend with CC resulted in an increase in the pore diameter of SC-P due to its higher accessible porosity compared to the remaining SCP systems as explained in [36].

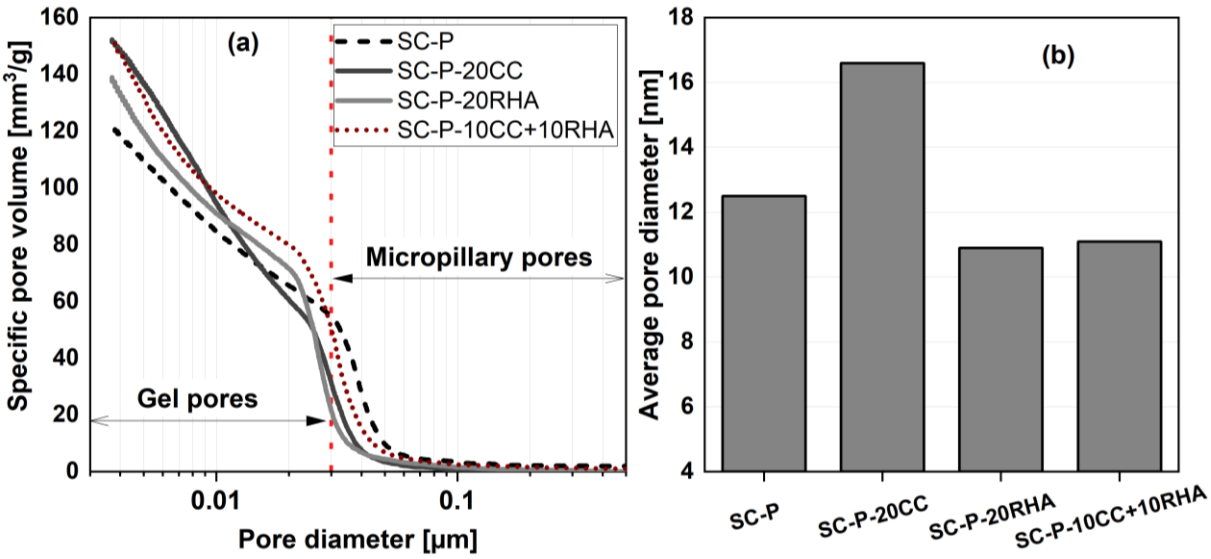

Figure 19 Influence of CC and RHA on porosity of SCP

5.4.3 Effect of CC and RHA on plastic and total shrinkage of SC-M

The plastic and drying shrinkage results of all the SC-M specimens are presented in Figure 20. SC-M-1 and SC-M-1-20CC exhibit high plastic shrinkage, reaching -7.0 mm/m from water addition to about 7 h of hydration, while the partial replacement of PLC by RHA lowers this value to -5.2 and -6.5 mm/m in SC-M-1-20RHA and SC-M-1-10CC+10RHA, respectively. From

7 to 16 h after water addition, the plastic shrinkage rate of SC-M-1 decreases and yields a shrinkage value of -7.3 mm/m, while SC-M-20CC exhibits no further plastic shrinkage. The plastic shrinkage of SC-M-20RHA further increases to -5.5 mm/m and -6.6 mm/m for SC-M-10CC+10RHA. Another phase of plastic shrinkage is from 16 to 48 hours of hydration. At this stage, the plastic shrinkage remains constant in all the SC-P specimens. For the total shrinkage, SC-M-1 and SC-M-1-20CC exhibited the same drying shrinkage tendencies for up to 14 days, after which SC-M-1-20CC shrank less than SC-M-1. SC-M-1-20RHA exhibited the highest initial drying shrinkage of all SC-M samples until it decreased after about 14 days and reached shrinkage values similar to SC-M-1 after 56 days. From 21 days and beyond, SC-M-1-10CC+10RHA shrank more than the other samples. A detailed explanation of the mechanism behind the shrinkage behavior of the SC-M specimens at all stages has been published in [36, 130].

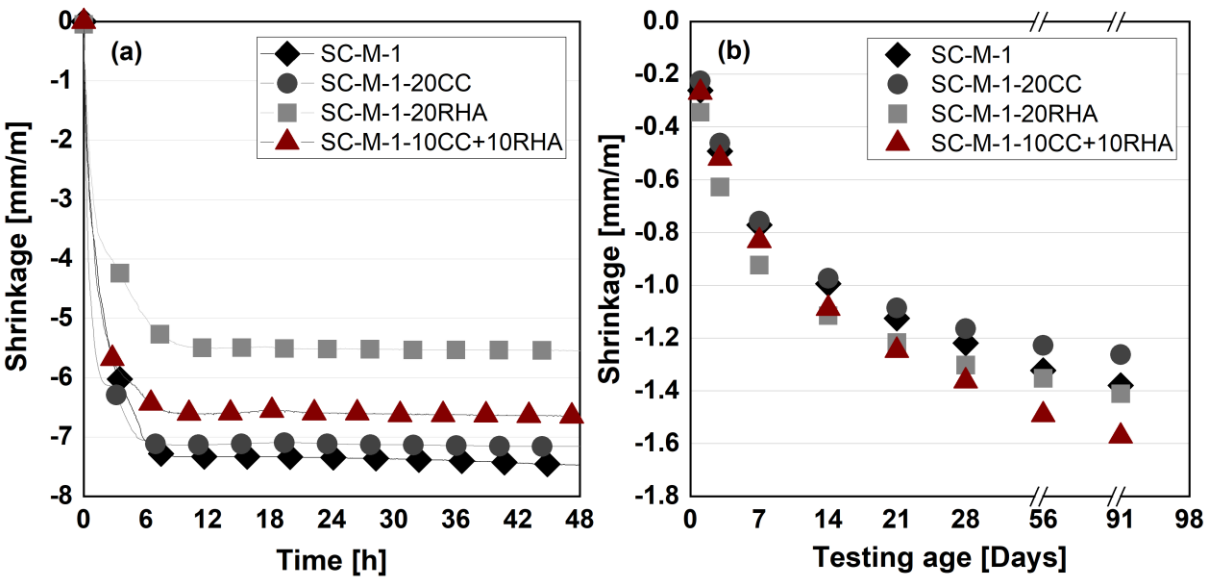

Figure 20 Effect CC and RHA on plastic (a) and total (b) shrinkage of SC-M

5.4.4 Compressive strength of self-compacting mortar and concrete

Calcined clay has a lower SSA and water demand compared to RHA and requires a lower V_w/V_p to achieve self-compactability. This has a major impact on the compressive strength values achievable with the two materials, making it difficult to compare their effects on compressive strength development. In this section, three different compressive strength values are presented, first, the self-compacting mortar compressive strength values that consider only the deformation properties of SC-M produced with binary blend of CC using a constant V_w/V_p = 0.875 and a partial replacement of PLC by CC up to 40 vol-%, as shown in Figure 21a. Another set of SC-M compressive strength values considers the effects of partial replacement of PLC by RHA up to 40 vol-% using varying V_w/V_p required to achieve self-compactability for each RHA replacement ratio. Finally, the compressive strength development considering the effects of binary and ternary blends of CC and RHA as partial replacement of PLC in SCC using a V_w/V_p = 1.275 as depicted in Figure 21b. Partial replacement of PLC with CC using a V_w/V_p = 0.875 improved the compressive strength of the self-compacting mortar, and even at 40 vol-%CC PLC partial replacement, the achieved compressive strength is comparable to SC-M-1. Partial replacement of PLC with RHA, on the other hand, requires an adjustment of V_w/V_p to achieve deformability comparable to SC-M-1. This resulted in a decrease in

compressive strength values, and each replacement level requires an adjustment of V_w/V_p, e.g., SC-M-1-10RHA requires a V_w/V_p = 1.175 to achieve self-compactability, resulting in a 40 % decrease in compressive strength. SC-M-1-20RHA had the highest compressive strength value of 57 N/mm^2 among SC-M made with RHA as a partial replacement for PLC. The V_w/V_p required for the deformability of each RHA-SC-M system and the corresponding compressive strength values are shown in Figure 21a. The comparison of the effect of CC and RHA as a partial replacement for PLC in SCC over the test period of 28 days was carried out using a V_w/V_p = 1.275 of each as a binary blend, and a ternary blend of 10CC+10RHA, as depicted in Figure 21b. SCC specimens produced with the binary and ternary blends of CC and RHA exhibited similar compressive strength values at 2 and 7 days, which are respectively, 8 % and 21 % lower than SCC-1, due to dilution effect and consequently a reduction in the compressive strength. At 28 days, SCC-1-20CC reached a compressive strength value comparable to that of SCC-1, while SCC-1-20RHA and SCC-1-10CC+10RHA showed a slight increase of 6 % compared to SCC-1 due to the pozzolanic reaction of CC and RHA.

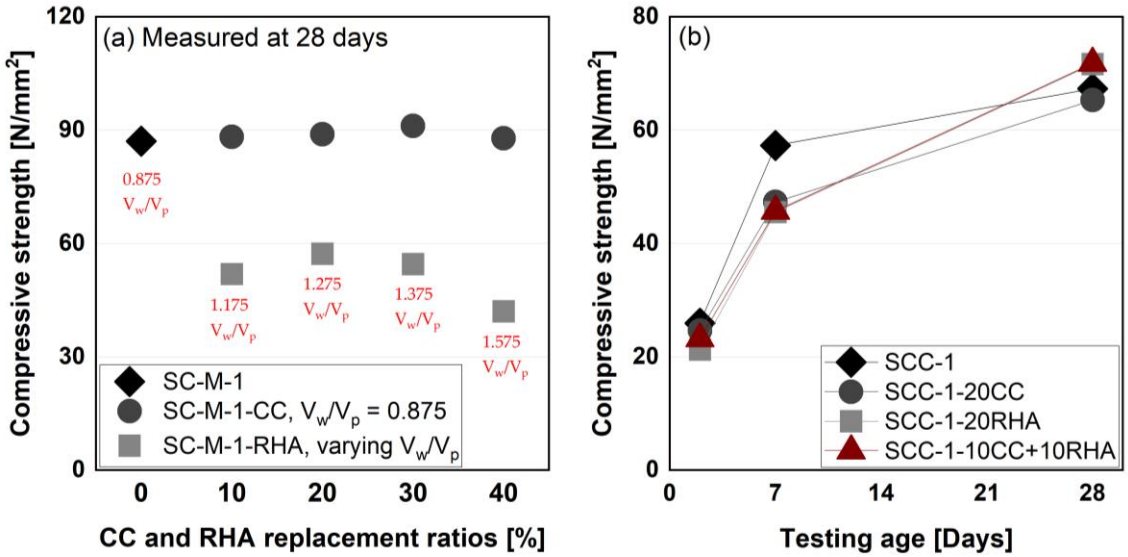

Figure 21 Effect of binary and ternary blends of CC and RHA on compressive strength of SC-M (a) and SCC (b)

5.4.5 Effect of CC and RHA on rapid chloride migration resistance of SCC

Figure 22 shows two sets of chloride migration resistance test results: (a) with V_w/V_p = 0.875 and only a binary blend of CC replacing PLC at 20 and 40 vol-% in SCC, and (b) with V_w/V_p = 1.275 and the binary and ternary blend of CC and RHA replacing PLC at 20 vol-% in SCC. At lower V_w/V_p (= 0.875), SCC-1 has a chloride migration coefficient (M_{RCM}) of 13.8 × 10^{-12}, which classifies it as having “Normal” SCC quality - 8 – 16 × 10^{-2} m^2/s - according to non-steady state chloride migration resistance concrete classification [140, 141]. Partial replacement of PLC with CC decreased the M_{RCM} of SCC-1 by 42 and 66 % at replacement ratios of 20 and 40 vol-%, respectively, resulting in an improvement of SCC quality to the "Good" classification - 2 - 8 × 10^{-2} m^2/s - in both cases.

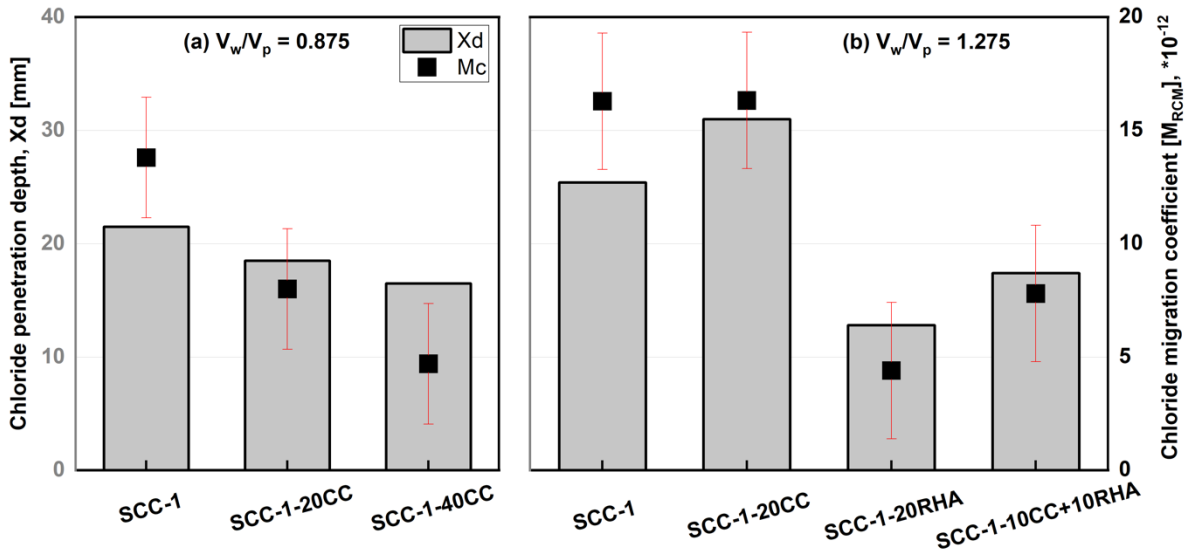

Figure 22 Influence of CC and RHA on chloride migration resistance of SCC

Increasing the V_w/V_p to 1.275 increases the M_{RCM} for SCC-1 and SCC-1-20CC to about 16 × 10^{-2} m^2/s, this changes the original classification of SCC-1-20CC from “good” SCC quality to “normal” quality, while SCC-1 retained its classification. The partial replacement of PLC by RHA and the ternary blend of CC and RHA decreases the M_{RCM} of SCC-1-20RHA and SCC-1-10CC+10RHA to 4.4 and 7.8 × 10^{-2} m^2/s, respectively, classifying them as "good" SCC quality in terms of chloride migration resistance.

5.4.6 Discussion

Increasing the V_w/V_p from 0.875 to 1.275 has a noticeable effect on the performance of CC as a partial replacement for PLC in SCC. At higher V_w/V_p (1.275), the DTA peak due to the dehydration of carbonate AFm phases is not evident in the SC-P and SC-P-20CC systems in TG measurements at 2 days of hydration due to the increase of the V_w/V_p, as was the case when V_w/V_p = 0.875, as published in [36]. This could decrease the volume of hydration products in the SCP-CC system and lead to less densification of its microstructure. In addition, a decrease in the compressive strength and chloride migration resistance of SCC-1 and SCC-1-20CC is observed when the V_w/V_p is increased from 0.875 to 1.275, which is due to the decrease in the volume of hydrate phases in the microstructure, leading to an increased average pore diameter and thus a decrease in chloride resistance of the SCC. In contrast, RHA and the ternary blends of CC and RHA enhanced the precipitated carbonate AFm phases at V_w/V_p = 1.275 even at 2 days of hydration and continued to increase up to 28 days of hydration. This increased the volume of the hydration products in the system, resulting in the densification of the SCC microstructure and refining its porosity, leading to an increase in both the 28-day compressive strength and the chloride migration resistance of the SCC. Using a V_w/V_p = 1.275, both CC and RHA reduced the CH content of SCP. The reduction of the CH content at 2 days of hydration is mainly due to the dilution effect. Simultaneously, CC and RHA provide more nucleation sites for the precipitation of hydration products at this stage of hydration, as previously observed by [36, 126]. The relative decrease in CH content at 7 days of hydration is due to the dilution effect and the initiation of the pozzolanic reaction of CC and RHA, which consumes CH. At 28 days of hydration, CH consumption is significant, especially in SC-Ps with RHA as a partial substitute for PLC, due to the pozzolanic reactivity of the CC and RHA.

The reduction in plastic shrinkage after 7 hours of hydration by the partial replacement of CC and RHA in SC-M could be attributed to the fact that both act as nuclei for the formation of hydration products at an early stage of hydration, thereby increasing the volume of the hydration product and densifying the SC-M microstructure as observed previously by [142]. In addition, RHA is expected to behave similarly to shrinkage-reducing admixtures in reducing the plastic shrinkage of SC-M, as it delays the setting time of the blended cement as observed by [87, 143] when shrinkage-reducing admixture was used to improve the plastic and long-term shrinkage behavior of concrete. Another possible explanation could be due to the release of the early absorbed water by the RHA particles, thereby increasing the internal relative humidity of the SC-M and reducing the autogenous shrinkage at an early age of the SC-M [144]. Beyond 28 days of testing, CC decreased the total shrinkage of SC-M, partly due to the increase in the volume of hydration product and or due to lower amount of evaporable water caused by the pozzolanic reaction of the CC, which consumes more water, as previously reported by [96] in the case of using metakaolin as partial replacement for cement. SC-M-1-20RHA shrank more than other specimens up to 7 days of testing, which was due to rapid evaporation of the absorbed water from the surfaces of the SC-M-1-20RHA specimens, because, according to [145], the absorbed water has a higher mobility than the water in the capillary pores and can evaporate easily, leading to an increase in drying shrinkage. After 7 days of testing, the total shrinkage of SC-M-1-20RHA decreased and was equal to that of SC-M-1 after 56 days and 91 days. The improvement in total shrinkage could be due to the further release of absorbed water by RHA to prevent the decrease in internal relative humidity of SC-M and thus a decrease in total shrinkage. This phenomenon was previously explained by [144] when RHA was used as an internal curing agent in cement paste. From 21 days of testing and beyond, SC-M-1-10CC+10RHA shrank more than any other specimen due to continues evaporation of the absorbed water from its surfaces.

In practice, the w/b and the strength of the binder determined the strength and durability class of the concrete and thus its application [132, 146]. Partial replacement of PLC by up to 40 vol-% CC is possible using a w/p = 0.3, although with an increase in SP dosage. For all partial replacements of PLC by CC in SC-M, compressive strength of about 90 N/mm^2 was achieved, which is sufficient for the production of high-strength SCC with wide applicability in different durability classes. A w/p = 0.36 is required for 10 vol-% RHA, which increases to 0.42, 0.45 and 0.50 for 20, 30 and 40 vol-% partial replacement, respectively. The SC-M compressive strength obtained with RHA as partial replacement for PLC, as shown in Figure 21a, can respectively produce SCC grades C50/60, C55/67, C40/50, and C30/37 for 10, 20, 30, and 40 vol% RHA PLC partial replacement ratios. Therefore, higher PLC partial replacement with RHA up to 40 vol% is also possible if a higher w/p of ≥ 0.5 is used. This concrete could also have a wide range of applications, e.g., in exposure classes XC, and some classes of XD and XS exposure according to [146].

5.4.7 CO_2 savings from the use of CC and RHA in mortar and SCC

Estimating the CO_2 savings that can be achieved by partially replacing cement with SCM is difficult due to the variability of their properties, extraction methods, and the extent of processing required. To obtain an approximate estimate of the CO_2 savings from the partial replacement of cement with CC and RHA, the embodied energy (EE) and $CO_{2\text{-eq}}$ of the binary and ternary binder blends with CC and RHA are compared with those of OPC and PLC binders in both mortar and SCC, based on the EE and global-warming potentials of the individual concrete constituents obtained in the literature [124, 125], as summarized in Table 2. Figure

23 shows the effect of partial replacement of OPC with 20 vol-% NCC and 15 vol-% LP + 30 vol-% NCC on the EE and $CO_{2\text{-eq}}$ of mortar. Compressive strength (CS) values were added as an indication of relative performance. The OPC mortar system (M) has an EE of 2593 MJ/m^3_{mortar} during its entire life cycle and is expected to release 451 kg/m^3 CO_2 to the environment.

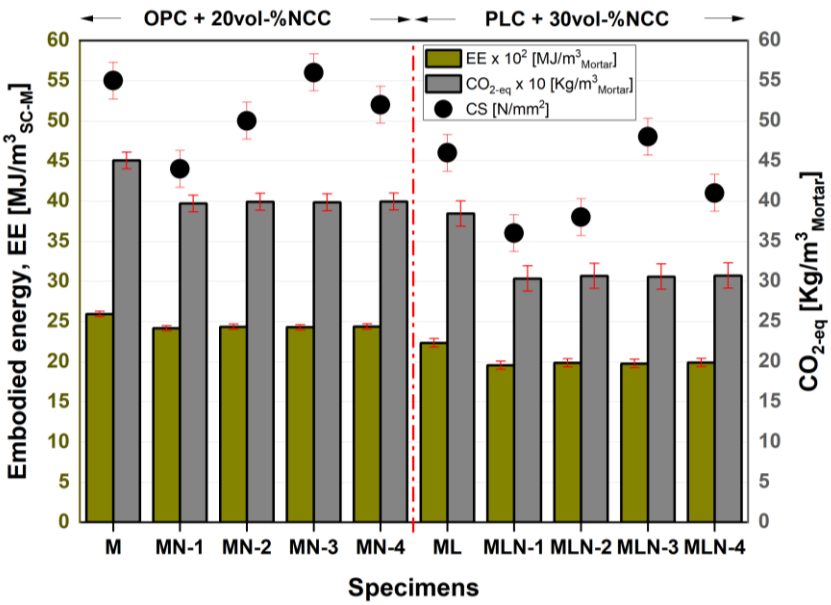

Figure 23 Influence of the NCC on the EE and GWP of OPC- and PLC-mortar

Partial replacement of OPC with 20 vol-% NCC resulted in an 8 % reduction in the total EE and an 11 % reduction in the $CO_{2\text{-eq}}$ of the mortar. Further partial replacement of OPC with ternary blends of 15 vol-% LP + 30 vol-% NCC resulted in a 23 % reduction in total EE and a 31 % reduction in the $CO_{2\text{-eq}}$ of the mortar. When considering the savings that can be achieved by directly replacing OPC with an SCM, the actual performance of the SCM in terms of pozzolanic reactivity must be considered. Considering the 28 days compressive strength values of the ternary blended binder (PLC + 15 LP + 30 NCC), only the MLN-3 and MLN-4 systems achieve the minimum PAI of 75 % of the reference OPC, so in this case it can be concluded that only the MLN-3 and MLN-4 mortar systems can save 23 % of the total EE of the reference OPC mortar system and achieve a CO_2 saving of 31 %. For the MLN-1 and MLN-2 mortar systems, the 28-day compressive strength corresponds to the 32.5 R cement grade. Therefore, the comparison can only be made with an OPC reference mortar produced with cement type 32.5 R.

Estimating the CO_2 savings from using CC as a partial replacement for PLC up to 40 vol-% in SC-M is straightforward because the SC-M-CC achieves a similar 28-day compressive strength class to the reference SC-M, as shown in Figure 24. The SC-M-1 system has an EE of 4058 $MJ/m^3_{SC\text{-}M}$ and is expected to release 703 kg/m^3 CO_2 to the environment. Partial replacement of PLC with CC at 10, 20, 30 and 40 vol-% reduced the EE by 2, 7, 10, and 12 %, and CO_2 by 4, 10, 16, and 20 %, respectively. The EE and CO_2 savings obtained by the partial replacement of PLC with up to 40 vol-% CC are lower than those previously obtained with the MLN-3 system, which is due to the fact that the comparison in this case is performed with a PLC-blended cement system that already contains 15 vol-% LP (LP has both low EE and global warming potential compared to OPC), while the comparison previously performed was with the OPC binder system.

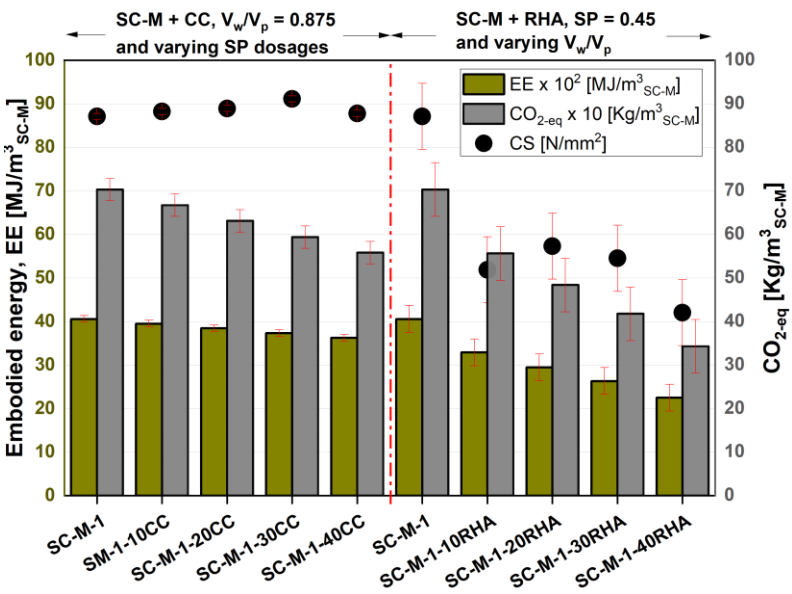

Figure 24 Influence of the CC and RHA on the EE and GWP of SC-M

Partial replacement of PLC with RHA in SC-M, on the other hand, requires an adjustment of the V_w/V_p to achieve self-compactability. This resulted in the reduction of the proportion of PLC in the systems, coupled with the low values of the EE and the global warming potential of RHA, leading to a reduction of the EE of the system by 20, 29, 37, and 44 % for the replacement ratios of 10, 20, 30 and 40 vol-%, and CO_2 savings of 20, 31, 40, and 51 %, for the replacement ratios of 10, 20, 30 and 40 vol-%, respectively. The EE reduction and CO_2 savings values achieved by the partial replacement of RHA are very high compared to their actual performance in terms of compressive strength values. Therefore, as already explained in the case of the MLN-1 and MLN-2 systems, the comparison should only be made considering the appropriate grade of cement.

The EE and $CO_{2\text{-eq}}$ of SCC are estimated in two stages, first considering V_w/V_p = 0.875 and CC replacing PLC at 20 and 40 vol%, and second using V_w/V_p = 1.275 and the binary and ternary mixtures of CC and RHA replacing PLC at 20 vol-%, as shown in Figure 25. The EE of SCC-1, using V_w/V_p = 0.875 is 2654 MJ/m^3_{scc} and 440 kg/m^3 CO_2 is expected to be released into the environment. Partial replacement of PLC with CC at 20 and 40 vol-% reduces EE by 7 and 11 %, and CO_2 savings of 9 and 20 %, respectively. When the V_w/V_p is increased to 1.275, the EE of SCC-1 decreases to 2361 MJ/m^3_{Scc} and 384 kg/m3 CO_2 is expected to be released to the environment. Partial replacement of PLC with binary and ternary blends of CC and RHA reduced EE by 6 %. CO_2 savings of 10, 16, and 13 are achieved by partial replacement of PLC with 20 vol-% CC, 20 vol-% RHA, and 10 vol-% CC + 10 vol-% RHA, respectively.

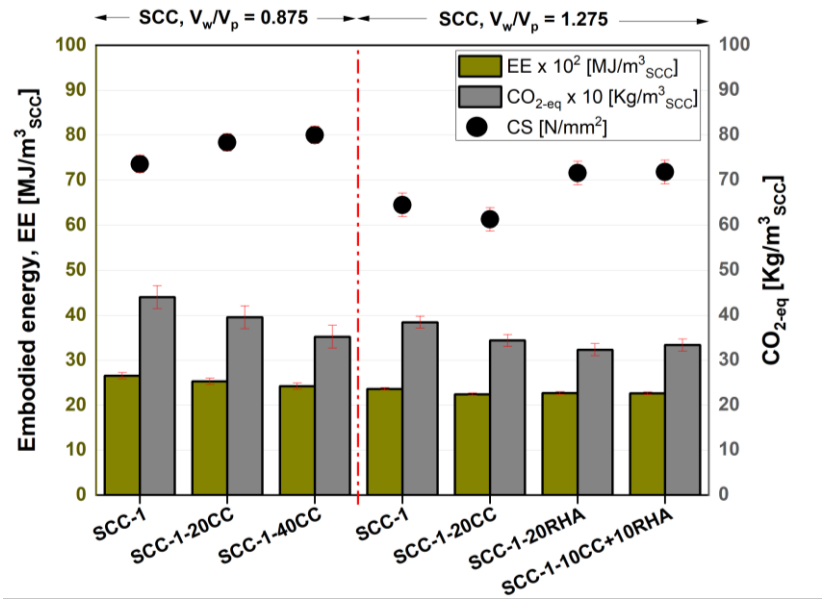

Figure 25 Influence of the CC and RHA on the EE and GWP of SCC

6 Summary and conclusions

The research focused on investigating the potential of high cement replacement by binary and ternary blends of calcined clays and rice husk ash to decarbonize self-compacting concrete. The pozzolanic reactivity of these supplementary cementitious materials was first established and their effect on mix design, fresh, rheological, and hardened properties of self-compacting paste, mortar and concrete produced with Portland limestone cement was assessed. The following can be summarized and concluded from the outcome of the study.

- The Nigerian calcined clays can be broadly classified into 2:1 common calcined clays (NCC-1 and 2), having similar characteristics with the German calcined clay (CT7), and 1:1 calcined clays (NCC-3 and 4). All the Nigerian calcined clays require w/p adjustment and/or SP addition to achieve similar deformability to OPC when used to replace OPC at 20 vol-% or in combination with limestone powder to replace OPC at 45 vol-%. The minimum 28 days compressive strength achieved by the Nigerian calcined clay mortar at 20 vol-% OPC partial replacement was 44 MPa, which is enough for general production of concrete up to grade C40/50. For the ternary composite cement with the Nigerian calcined clays and limestone powder, the same application holds for the 1:1 Nigerian calcined clays mortar systems, whereas for the 2:1 Nigerian calcined clays mortar systems, the compressive strength after 28 days of curing was 36 and 38 MPa for MLN-1 and 2, respectively. This limits their use to general construction work under normal environmental conditions and the production of concrete up to grade C30/37. In practice, this concrete grade is sufficient for general construction works to provide the required concrete infrastructure in the sub-Saharan African region. Therefore, the 1:1 Nigerian calcined clays can be used in combination with limestone powder to produce grade C40/50 concrete, whereas, the 2:1 Nigerian calcined clays can be used in combination with limestone powder to produce grade C30/37 concrete.
- The reference self-compacting concrete deformed at a V_w/V_p = 0.875. The use of CC as a partial replacement for PLC up to 40 vol-% achieved deformability comparable to the reference system at the same V_w/V_p = 0.875 with an increased SP dosage. The use of RHA as a partial replacement for PLC, on the other hand, requires urgent adjustment of the V_w/V_p even at a lower replacement level to achieve similar deformability to the PLC systems; SP adjustment alone cannot provide the required degree of deformability. The V_w/V_p must be increased to 1.175, 1.275, 1.375 and 1.575 at the partial replacement levels of 10, 20, 30 and 40 vol-%, respectively. Therefore, to achieve a strong and durable SCC with broad applicability, the partial replacement of PLC with RHA should be maintained at 20 vol-%. Although Higher PLC partial substitution with RHA up to 40 vol-% is also possible using a higher V_w/V_p of ≥ 1.575, this concrete could also have a wide range of applications, for instance in exposure classes XC, and some classes of XD and XS. Therefore, it's possible to produce SCC with fairly higher cement replacement with both RHA and CC leading to the reduction of the issues related to the use of higher volume of cement in SCC.
- The segregation resistance of all SCC mixes produced with binary or ternary blends of CC and RHA with 20 vol-% partial replacement of PLC is within the specified limits by [112, 132] and even SCC produced with 20 vol-% RHA as PLC partial replacement retained its flowability up to 30 min after mixing. For flowability retention evaluation, the

use of 20 vol-% RHA as a partial replacement to PLC is considered critical because the excess mixing water was absorbed after 30 min of mixing, making the SCC mix stiffer and rapidly losing its flowability. The use of 20 vol-% CC as a partial replacement to PLC in SCC resulted in a decrease in the torque required to initiate and maintain displacement of the SCC, while the 20 vol-% RHA has the opposite effect. Therefore, SCC-1-20CC can be used to produce both precast and ready-mix SCC. However, the binary blended mix SCC-1-20RHA and the ternary blend SCC-1-10CC+10RHA developed high flow resistance and showed rapid loss of flowability after 30 min of mixing. Therefore, their flowability retention needs to be improved for applications beyond 30 minutes. SCC with a high content of RHA, 20 vol-% and above, is recommended for the production of precast SCC elements only, due to the short flowability retention window required by precast SCC compared to ready-mix SCC. Although additional treatment may be required to improve early age strength development of RHA-SCC systems.

- SCC produced with RHA as PLC partial replacement showed higher flow resistance and viscosity and increased both the static and dynamic yield stress of SCC. This effect is reduced to some extent by ternary blending CC and RHA. Therefore, the proportion of RHA shall always be kept low, perhaps at 5 vol-%, in the binary and ternary blended SCC mixture, when flowability retention beyond 30 min is required, for example in the ready-mix concrete.
- At a lower V_w/V_p (= 0.875), partial replacement of PLC with 20 and 40 vol-% CC increased the compressive strength of SCC-1 and increased its chloride migration resistance, changing the SCC-1 quality in terms of chloride resistance from “Normal” to “Good”. The increase of the V_w/V_p to 1.275 increased the average pore diameter of SCC-1 and SCC-1-20CC, which changed the initial grade of SCC-1-20CC from “Good” classification to “Normal” classification. The SCC produced with RHA and the blend of CC and RHA with a V_w/V_p = 1.275 increased the 28 days compressive strength of SCC-1. The chloride migration resistance of 20 vol-% RHA is 3 times that of SCC produced with only PLC, while that of the ternary blend 10 vol-% CC + 10 vol-% RHA is 2 times that of SCC produced with only PLC. RHA is capable of improving the chloride migration resistance of SCC and should be used to improve the microstructural densification of SCC produced with only PLC.
- The ternary blend of kaolinite-rich Nigerian calcined clays and limestone powder replacing OPC at 45 vol-% resulted in the reduction in total embodied energy and CO_2 equivalent of the mortar. The same performance was recorded for the smectite-rich Nigerian calcined clays, but it should be noted here that the smectite-rich Nigerian calcined clays with the blend 55 OPC + 15 LP + 30 NCC did not reach the 75 % PAI of OPC even after 90 days of testing. Therefore, the savings in embodied energy and CO_2 can only be compared with the 32.5 R cement grade. When used as a partial replacement for PLC in SCC, both the binary and ternary blends of CC and RHA resulted in savings of the embodied energy and CO_2. However, RHA blended binders provide more CO_2 savings compared to CC blended binders. Therefore, up to 20 vol-% RHA can be used to decarbonize SCC.
- Calcined clays can replace PLC up to 40 vol-%, using a V_w/V_p = 0.875, and improve the compressive strength and durability of SCC. On the other hand, the selection of the

promising mix design for the binary and ternary blends with RHA depends on the intended use of the SCC. If maintaining flowability beyond 30 min is important, a V_w/V_p = 1.275 is recommended, while the proportion of RHA replacement should be kept minimal, perhaps as low as 5 vol-%. If improving the compressive strength and durability is important, V_w/V_p = 1.275 is recommended, and the proportion of RHA can be increased to 20 vol-%.

7 References

1. Tangtinthai, N., O. Heidrich, and D.A.C. Manning, *Role of policy in managing mined resources for construction in Europe and emerging economies.* Journal of Environmental Management, 2019. **236**: p. 613-621.
2. Schandl, H., et al., *Global material flows and resource productivity forty years of evidence.* Journal of Industrial Ecology, 2018. **22**(4): p. 827-838.
3. Schmidt, W., et al., *Sustainable circular value chains: From rural waste to feasible urban construction materials solutions.* Developments in the Built Environment, 2021. **6**: p. 100047.
4. Schneider, M., et al., *Sustainable cement production—present and future.* Cement and Concrete Research, 2011. **41**(7): p. 642-650.
5. Muhammad, A., K.-C. Thienel, and R. Sposito, *Suitability of Blending Rice Husk Ash and Calcined Clay for the Production of Self-Compacting Concrete: A Review.* Materials, 2021. **14**(21): p. 6252.
6. Okamura, H. and K. Ozawa, *Mix-design for self-compacting concrete.* Concrete Library of JSCE, 1995(25): p. 107-120.
7. Okamura, H., *Self-Compacting High-Performance Concrete.* Concrete International, 1997. **19**(7): p. 50-54.
8. Shi, C., et al., *A review on mixture design methods for self-compacting concrete.* Construction and Building Materials, 2015. **84**: p. 387-398.
9. Ramanathan, P., et al., *Performance of self-compacting concrete containing different mineral admixtures.* KSCE Journal of Civil Engineering, 2013. **17**(2): p. 465-472.
10. Van Der Vurst, F., et al., *Effect of the mix design on the robustness of fresh self-compacting concrete.* Cement and Concrete Composites, 2017. **82**: p. 190-201.
11. Rigueira, J.W., E. Garciá-Taengua, and P. Serna-Ros, *Self-consolidating concrete robustness in continuous production regarding fresh and hardened state properties.* ACI Materials Journal, 2009. **106**(3): p. 301-307.
12. Westerholm, M., et al., *Influence of fine aggregate characteristics on the rheological properties of mortars.* Cement and Concrete Composites, 2008. **30**(4): p. 274-282.
13. Nunes, S., et al., *Rheological characterization of SCC mortars and pastes with changes induced by cement delivery.* Cement and Concrete Composites, 2011. **33**(1): p. 103-115.
14. Feys, D., et al., *Changes in rheology of self-consolidating concrete induced by pumping.* Materials and Structures/Materiaux et Constructions, 2016. **49**(11): p. 4657-4677.
15. Schmidt, W., *SCC for Sub-Saharan Africa Based on Local Raw Materials – Material Development, Optimisation, and Application Concept*, in *Rheology and Processing of Construction Materials*, V. Mechtcherine, K. Khayat, and S. Secrieru, Editors. 2020, Springer International Publishing. p. 60-67.
16. Muhammad, A., K.-C. Thienel, and S. Scherb, *Calcined Clays from Nigeria - Properties and Performance of Supplementary Cementitious Materials Suitable for Producing Level 1 Concrete.* Materials, 2023. **16**(7): p. 2684.
17. Scrivener, K.L., V.M. John, and E.M. Gartner, *Eco-efficient cements: Potential economically viable solutions for a low-CO_2 cement-based materials industry.* Cement and Concrete Research, 2018. **114**: p. 2-26.
18. Schmidt, W., et al., *Innovation potentials for construction materials with specific focus on the challenges in Africa.* RILEM Technical Letters, 2020. **5**: p. 63-74.
19. Yetano Roche, M., *Built for net-zero: analysis of long-term greenhouse gas emission pathways for the Nigerian cement sector.* Journal of Cleaner Production, 2023. **383**: p. 135446.
20. Alsarhan, L.M., et al., *Circular carbon economy (CCE): A way to invest CO2 and protect the environment, a review.* Sustainability, 2021. **13**(21): p. 11625.
21. Messner, D., et al., *The budget approach: A framework for a global transformation toward a low-carbon economy.* Journal of Renewable and Sustainable Energy, 2010. **2**(3): p. 031003.

22. Bouzoubaâ, N. and M. Lachemi, *Self-compacting concrete incorporating high volumes of class F fly ash: Preliminary results.* Cement and Concrete Research, 2001. **31**(3): p. 413-420.
23. Yazici, H., *The effect of silica fume and high-volume Class C fly ash on mechanical properties, chloride penetration and freeze-thaw resistance of self-compacting concrete.* Construction and Building Materials, 2008. **22**(4): p. 456-462.
24. Saak, A.W., H.M. Jennings, and S.P. Shah, *New Methodology for Designing Self-Compacting Concrete.* ACI Materials Journal, 2001. **98**(6): p. 429-439.
25. Zhao, H., et al., *The properties of the self-compacting concrete with fly ash and ground granulated blast furnace slag mineral admixtures.* Journal of Cleaner Production, 2015. **95**: p. 66-74.
26. Uysal, M. and M. Sumer, *Performance of self-compacting concrete containing different mineral admixtures.* Construction and Building Materials, 2011. **25**(11): p. 4112-4120.
27. Chopra, D., R. Siddique, and Kunal, *Strength, permeability and microstructure of self-compacting concrete containing rice husk ash.* Biosystems Engineering, 2015. **130**: p. 72-80.
28. Memon, S.A., M.A. Shaikh, and H. Akbar, *Utilization of Rice Husk Ash as viscosity modifying agent in Self Compacting Concrete.* Construction and Building Materials, 2011. **25**(2): p. 1044-1048.
29. Siddique, R. and M.I. Khan, *Supplementary Cementing Materials*. Engineering Materials. 2011, Berlin Heidelberg: Springer. 287.
30. Madandoust, R. and S.Y. Mousavi, *Fresh and hardened properties of self-compacting concrete containing metakaolin.* Construction and Building Materials, 2012. **35**: p. 752-760.
31. Miller, S.A., et al., *Carbon dioxide reduction potential in the global cement industry by 2050.* Cement and Concrete Research, 2018. **114**: p. 115-124.
32. GEORGE, V. and J.M. DANDA, *URBANISATION AND THE HOUSING SECTOR IN SUB-SAHARAN AFRICA: CHALLENGES, OPPORTUNITIES.* Housing the Poor on the African Continent: Reconsidering Ubuntu Philosophy, 2022: p. 127.
33. MUBECUA, M.A., *HOUSING POVERTY: THE PRACTICE OF UBUNTU.* Housing the Poor on the African Continent: Reconsidering Ubuntu Philosophy, 2022: p. 1.
34. Godwill, I.T., O. Owei, and I. Brown, *An analysis of existing housing stock in selected neighbourhoods in port Harcourt municipality.* European Journal of Environment and Earth Sciences, 2021. **2**(3): p. 57-61.
35. Satterthwaite, D., *The impact of urban development on risk in sub-Saharan Africa's cities with a focus on small and intermediate urban centres.* International Journal of Disaster Risk Reduction, 2017. **26**: p. 16-23.
36. Muhammad, A., K.-C. Thienel, and R. Sposito, *Suitability of Clinker Replacement by a Calcined Common Clay in Self-Consolidating Mortar — Impact on Rheology and Early Age Properties.* Minerals, 2022. **12**(5): p. 625.
37. International Energy Agency (IEA), *Technology Roadmap - Low-Carbon Transition in the Cement Industry*. 2018: Paris, France. p. 66.
38. Lamb, W.F., et al., *A review of trends and drivers of greenhouse gas emissions by sector from 1990 to 2018.* Environmental Research Letters, 2021. **16**(7): p. 073005.
39. Behrouzi, D., et al., *Dekarbonisierung von Zement und Beton – Minderungspfade und Handlungsstrategien*, Verein Deutscher Zementwerke e.V. (VDZ), Editor. 2020, Verein Deutscher Zementwerke e.V. (VDZ),: Düsseldorf, Germany. p. 60.
40. Avet, F. and K. Scrivener, *Hydration Study of Limestone Calcined Clay Cement (LC3) Using Various Grades of Calcined Kaolinitic Clays*, in *Calcined Clays for Sustainable Concrete - Proceedings of the 2nd International Conference on Calcined Clays for Sustainable Concrete*, F. Martirena, A. Favier, and K. Scrivener, Editors. 2018, Springer Nature: La Havanna, Cuba. p. 35-40.
41. Scrivener, K., et al., *Calcined clay limestone cements (LC^3).* Cement and Concrete Research, 2018. **114**: p. 49-56.

42. Adelabu, O.S., *Documentation, Application and Utilisation of Clay Minerals in Kaduna State (Nigeria)*. Clay Minerals in Nature - Their Characterization, Modification and Application. 2012, London, UK: IntechOpen Limited. 18.
43. Aprianti, E., et al., *Supplementary cementitious materials origin from agricultural wastes – A review.* Construction and Building Materials, 2015. **74**: p. 176-187.
44. Tulashie, S.K., et al., *Production of Portland pozzolana cement from rice husk ash.* Materialia, 2021. **16**: p. 101048.
45. Patel, M.H. and N. Dawda, *Advancement in Self Compacting Concrete: A Review of Last Few Decades.* International Journal of Advance Engineering and Research Development, 2017: p. 50-54.
46. Sari, M., E. Prat, and J.F. Labastire, *High strength self-compacting concrete original solutions associating organic and inorganic admixtures.* Cement and Concrete Research, 1999. **29**(6): p. 813-818.
47. Zhu, W., M. Sonebi, and P.J.M. Bartos, *Bond and interfacial properties of reinforcement in self-compacting concrete.* Materials and Structures/Materiaux et Constructions, 2004. **37**(271): p. 442-448.
48. Su, N., K.C. Hsu, and H.W. Chai, *A simple mix design method for self-compacting concrete.* Cement and Concrete Research, 2001. **31**(12): p. 1799-1807.
49. Liu, M., *Wider application of additions in self-compacting concrete*, in *Department of Civil, Environmental and Geomatic Engineering*. 2009, University College London: London, UK. p. 392.
50. Ouchi, M., M. Hibino, and H. Okamura, *Effect of superplasticizer on self-compactability of fresh concrete.* Transportation Research Record, 1997. **1574**(1): p. 37-40.
51. Şahmaran, M., H.A. Christianto, and I.O. Yaman, *The effect of chemical admixtures and mineral additives on the properties of self-compacting mortars.* Cement and Concrete Composites, 2006. **28**(5): p. 432-440.
52. Leemann, A. and F. Winnefeld, *The effect of viscosity modifying agents on mortar and concrete.* Cement and Concrete Composites, 2007. **29**(5): p. 341-349.
53. Sedran, T., et al., *Mix Design of Self-Compacting Concrete (SCC)*, in *Production Methods and Workability of Concrete*, P.J.M. Bartos, D.J. Cleland, and D.L. Marrs, Editors. 1996, CRC Press: London. p. 12.
54. Petersson, O., P. Billberg, and B.K. Van, *A Model for Self-Compacting Concrete*, in *Production Methods and Workability of Concrete*, P.J.M. Bartos, D.J. Cleland, and D.L. Marrs, Editors. 1996, CRC Press: London. p. 10.
55. Barkat, A., et al., *Effects of local metakaolin addition on rheological and mechanical performance of self-compacting limestone cement concrete.* Journal of Adhesion Science and Technology, 2019. **33**(9): p. 963-985.
56. Rozière, E., et al., *Influence of paste volume on shrinkage cracking and fracture properties of self-compacting concrete.* Cement and Concrete Composites, 2007. **29**(8): p. 626-636.
57. Gesoğlu, M., E. Güneyisi, and E. Özbay, *Properties of self-compacting concretes made with binary, ternary, and quaternary cementitious blends of fly ash, blast furnace slag, and silica fume.* Construction and Building Materials, 2009. **23**(5): p. 1847-1854.
58. Kannan, V., *Relationship between ultrasonic pulse velocity and compressive strength of self compacting concrete incorporate rice husk ash and metakaolin.* Asian Journal of Civil Engineering, 2015. **16**(8): p. 1077-1088.
59. Zunino, F. and K. Scrivener, *Factors influencing the sulfate balance in pure phase C_3S/C_3A systems.* Cement and Concrete Research, 2020. **133**: p. 106085.
60. Zunino, F. and K. Scrivener, *Insights on the role of alumina content and the filler effect on the sulfate requirement of PC and blended cements.* Cement and Concrete Research, 2022. **160**: p. 106929.
61. Maier, M., et al., *Particle characteristics of calcined clays and limestone and their impact on the early hydration and sulfate demand of blended cement.* Cement and Concrete Research, 2022. **154**(106736): p. 15.

62. Scherb, S., et al., *Reaction kinetics during early hydration of calcined phyllosilicates in clinker-free model systems.* Cement and Concrete Research, 2021. **143**: p. 106382.
63. Beuntner, N. and K.-C. Thienel, *Pozzolanic efficiency of calcined clays in blended cements with focus on the early hydration.* Advances in Cement Research, 2022. **34**(8): p. 341-355.
64. Maier, M., et al., *Hydration of cubic tricalcium aluminate in the presence of calcined clays.* Journal of the American Ceramic Society, 2021. **104**(7): p. 3619-3631.
65. Zunino, F. and K. Scrivener, *Studying the Influence of the Filler Effect of SCMs on the Sulfate Requirement of Blended Cements*, in *ACI SP 349 11th International Conference on Cementitious Materials and Alternative Binders for Sustainable Concrete*, A. Tagnit-Hamou, Editor. 2021, American Concrete Institute: online. p. 117-124.
66. Salmang, H. and H. Scholze, *Keramik*. 7. ed. 2007: Springer-Verlag Berlin/Heidelberg, Germany. 1165.
67. Okrusch, M. and S. Matthes, *Mineralogie - Eine Einführung in die spezielle Mineralogie, Petrologie und Lagestättenkunde*. 8 ed. Springer-Lehrbuch. 2010, Berlin/Heidelberg, Germany: Springer Spektrum. XX, 728.
68. Parande, A.K., et al., *Study on strength and corrosion performance for steel embedded in metakaolin blended concrete/mortar.* Construction and Building Materials, 2008. **22**(3): p. 127-134.
69. Said-Mansour, M., et al., *Influence of calcined kaolin on mortar properties.* Construction and Building Materials, 2011. **25**(5): p. 2275-2282.
70. Lothenbach, B. and M. Zajac, *Application of thermodynamic modelling to hydrated cements.* Cement and Concrete Research, 2019. **123**: p. 105779.
71. Gholhaki, M., et al., *An investigation on the fresh and hardened properties of self-compacting concrete incorporating magnetic water with various pozzolanic materials.* Construction and Building Materials, 2018. **158**: p. 173-180.
72. Kannan, V. and K. Ganesan, *Chloride and chemical resistance of self compacting concrete containing rice husk ash and metakaolin.* Construction and Building Materials, 2014. **51**: p. 225-234.
73. Mirgozar Langaroudi, M.A. and Y. Mohammadi, *Effect of nano-clay on the freeze–thaw resistance of self-compacting concrete containing mineral admixtures.* European Journal of Environmental and Civil Engineering, 2019: p. 1-20.
74. Li, R., et al., *Effectiveness of PCE superplasticizers in calcined clay blended cements.* Cement and Concrete Research, 2021. **141**: p. 106334.
75. Sposito, R., et al., *Evaluation of zeta potential of calcined clays and time-dependent flowability of blended cement with customized polycarboxylate-based superplasticizers.* Construction and Building Materials, 2021. **308**: p. 125061.
76. Alujas, A., et al., *Pozzolanic Reactivity of Low Grade Kaolinitic Clays: Influence of Mineralogical Composition*, in *Calcined Clays for Sustainable Concrete*, K. Scrivener and A. Favier, Editors. 2015, Springer Netherlands. p. 339-345.
77. Maier, M., N. Beuntner, and K.-C. Thienel, *Mineralogical characterization and reactivity test of common clays suitable as supplementary cementitious material.* Applied Clay Science, 2021. **202**: p. 105990.
78. Dhandapani, Y., et al., *Mechanical properties and durability performance of concretes with Limestone Calcined Clay Cement (LC^3).* Cement and Concrete Research, 2018. **107**: p. 136-151.
79. Beuntner, N., A. Kustermann, and K.-C. Thienel, *Pozzolanic potential of calcined clay in high-performance concrete*, in *International Conference on Sustainable Materials, Systems and Structures – SMSS 2019 New Generation of Construction Materials*, M. Serdar, N. Štirmer, and J. Provis, Editors. 2019, RILEM Publications S.A.R.L.: Rovinj, Croatia. p. 470-477.
80. Singh, B., *Rice husk ash*, in *Waste and Supplementary Cementitious Materials in Concrete - Characterisation, Properties and Applications*, R. Siddique and P. Cachim, Editors. 2018, Woodhead Publishing. p. 417-460.

81. Le, H.T., et al., *Effect of macro-mesoporous rice husk ash on rheological properties of mortar formulated from self-compacting high performance concrete.* Construction and Building Materials, 2015. **80**: p. 225-235.
82. Xu, W., T.Y. Lo, and S.A. Memon, *Microstructure and reactivity of rich husk ash.* Construction and Building Materials, 2012. **29**: p. 541-547.
83. Zhang, M.H. and V.M. Malhotra, *High-Performance Concrete Incorporating Rice Husk Ash as a Supplementary Cementing Material.* ACI Materials Journal, 1996. **93**(6): p. 629-636.
84. He, J., et al., *Synthesis and characterization of red mud and rice husk ash-based geopolymer composites.* Cement and Concrete Composites, 2013. **37**(1): p. 108-118.
85. Van, V.T.A., et al., *Mesoporous structure and pozzolanic reactivity of rice husk ash in cementitious system.* Construction and Building Materials, 2013. **43**: p. 208-216.
86. Ganesan, K., K. Rajagopal, and K. Thangavel, *Rice husk ash blended cement: Assessment of optimal level of replacement for strength and permeability properties of concrete.* Construction and Building Materials, 2008. **22**(8): p. 1675-1683.
87. Gill, A.S. and R. Siddique, *Durability properties of self-compacting concrete incorporating metakaolin and rice husk ash.* Construction and Building Materials, 2018. **176**: p. 323-332.
88. Le, H.T., et al., *The mix design for self-compacting high performance concrete containing various mineral admixtures.* Materials and Design, 2015. **72**: p. 51-62.
89. Chao-Lung, H., B.L. Anh-Tuan, and C. Chun-Tsun, *Effect of rice husk ash on the strength and durability characteristics of concrete.* Construction and Building Materials, 2011. **25**(9): p. 3768-3772.
90. Rahman, M.E., et al., *Self compacting concrete from uncontrolled burning of rice husk and blended fine aggregate.* Materials and Design, 2014. **55**: p. 410-415.
91. Van, V.-T.-A., et al., *Rice husk ash as both pozzolanic admixture and internal curing agent in ultra-high performance concrete.* Cement and Concrete Composites, 2014. **53**: p. 270-278.
92. Kheder, G.F. and R.S. Al Jadiri, *New method for proportioning self-consolidating concrete based on compressive strength requirements.* ACI Materials Journal, 2010. **107**(5): p. 490-497.
93. Dinakar, P. and S.N. Manu, *Concrete mix design for high strength self-compacting concrete using metakaolin.* Materials & Design, 2014. **60**: p. 661-668.
94. Dinakar, P., *Design of self-compacting concrete with fly ash.* Magazine of Concrete Research, 2012. **64**(5): p. 401-409.
95. Xie, T., et al., *Modelling fresh and hardened properties of self-compacting concrete containing supplementary cementitious materials using reactive moduli.* Construction and Building Materials, 2021. **272**: p. 121954.
96. Güneyisi, E., M. Gesoğlu, and E. Özbay, *Strength and drying shrinkage properties of self-compacting concretes incorporating multi-system blended mineral admixtures.* Construction and Building Materials, 2010. **24**(10): p. 1878-1887.
97. Muhammad, A. and K.-C. Thienel, *Performance of Calcined Common Clay as Partial Replacement to Cement in Selfcompacting Concrete*, in *International Conference on Calcined Clays for Sustainable Concrete*, M. Sharma, et al., Editors. 2022: Lausanne, Switzerland. p. 102-103.
98. DIN EN 197-1, *Zement - Teil 1: Zusammensetzung, Anforderungen und Konformitätskriterien von Normalzement (Cement - Part 1: Composition, specifications and conformity criteria for common cements)*. 2011, Beuth-Verlag: Berlin, Germany. p. 8.
99. DIN EN ISO 11885, *Water quality - Determination of selected elements by inductively coupled plasma optical emission spectrometry (ICP-OES)*. 2009, Beuth-Verlag: Berlin, Germany. p. 37.
100. Kaps, C., et al. *Untersuchungen zur Binderoptimierung in alumosilikatischen Polymerbindern*. in *15. Internationale Baustofftagung ibausil*. 2003. Weimar, Germany: F.A. Finger-Institut für Baustoffkunde.

101. DIN EN ISO 17892-3, *Geotechnical investigation and testing - Laboratory testing of soil - Part 3: Determination of particle density*. 2015, Beuth-Verlag: Berlin, Germany. p. 21.
102. DIN ISO 9277, *Determination of the specific surface area of solids by gas adsorption - BET method*. 2003, Beuth-Verlag: Berlin, Germany. p. 19.
103. Sposito, R., et al., *Physical and mineralogical properties of calcined common clays as SCM and their impact on flow resistance and demand for superplasticizer.* Cement and Concrete Research, 2022. **154**(106743): p. 106743.
104. Puntke, W., *Wasseranspruch von feinen Kornhaufwerken.* Beton, 2002. **52**(5): p. 242-248.
105. DIN EN 196-1, *Prüfverfahren für Zement - Teil 1: Bestimmung der Festigkeit (Methods of testing cement - Part 1: Determination of strength)*. 2016, Beuth-Verlag: Berlin, Germany. p. 31.
106. DIN EN 1015-3, *Prüfverfahren für Mörtel für Mauerwerk-Teil 3: Bestimmung der Konsistenz von Frischmörtel (mit Ausbreittisch) (Methods of test for mortar for masonry - Part 3: Determination of consistence of fresh mortar (by flow table))*. 2007, Beuth-Verlag: Berlin, Germany. p. 12.
107. EFNARC, *Specification and Guidelines for Self-Compacting Concrete*, in *Specification and Guidelines*. 2002, EFNARC: Farnham, UK.
108. DIN EN 12350-8, *Prüfung von Frischbeton - Teil 8: Selbstverdichtender Beton – Setzfließversuch (Testing fresh concrete - Part 8: Self-compacting concrete – Slump-flow test)*. 2019, Beuth-Verlag: Berlin, Germany. p. 8.
109. DIN EN 12350-12, *Prüfung von Frischbeton - Teil 12: Selbstverdichtender Beton – Blockierring-Versuch (Testing fresh concrete - Part 12: Self-compacting concrete – J-ring test)*. 2010, Beuth-Verlag: Berlin, Germany. p. 11.
110. DIN EN 12350-9, *Prüfung von Frischbeton - Teil 9: Selbstverdichtender Beton – Auslauftrichterversuch (Testing fresh concrete - Part 9: Self-compacting concrete – V-funnel test)*. 2010, Beuth-Verlag: Berlin, Germany. p. 8.
111. DIN EN 12350-11, *Prüfung von Frischbeton - Teil 11: Selbstverdichtender Beton – Bestimmung der Sedimentationsstabilität im Siebversuch (Testing fresh concrete - Part 11: Self-compacting concrete – Sieve segregation test)*. 2010, Beuth-Verlag: Berlin, Germany. p. 11.
112. Brameshuber, W. and S. Uebachs, *Sedimentationsstabilität von Selbstverdichtenden Betonen (Sedimentation stability of self-compacting concretes)*, in *Rheologische Messungen an mineralischen Baustoffen - Workshop 2003*, W. Kusterle, Editor. 2003, Schleibinger: Regensburg, Germany. p. 10.
113. Kordts, S. and W. Breit, *Beurteilung der Frischbetoneigenschaften von Selbstverdichtendem Beton (Assessment of the fresh concrete properties of self compacting concrete).* Beton, 2003. **53**(11): p. 565-571.
114. Feys, D., R. Verhoeven, and G. De Schutter, *Fresh self compacting concrete, a shear thickening material.* Cement and Concrete Research, 2008. **38**(7): p. 920-929.
115. Barnes, H.A. and K. Walters, *The yield stress myth?* Rheologica Acta, 1985. **24**(4): p. 323-326.
116. Hackley, V.A. and C.F. Ferraris, *Guide to Rheological Nomenclature - Measurements in Ceramic Particulate Systems*. 2001, National Institute of Standards and Technology (NIST): Gaithersburg, Maryland, USA. p. III, 29.
117. Snellings, R., et al., *Report of TC 238-SCM: hydration stoppage methods for phase assemblage studies of blended cements—results of a round robin test.* Materials and Structures, 2018. **51**(4): p. 111.
118. Marsh, B.K. and R.L. Day, *Pozzolanic and cementitious reactions of fly ash in blended cement pastes.* Cement and Concrete Research, 1988. **18**(2): p. 301-310.
119. DIN 66133, *Bestimmung der Porenvolumenverteilung und der spezifischen Oberfläche von Feststoffen durch Quecksilberintrusion (Determination of pore volume distribution and specific surface area of solids by mercury intrusion)*. 1993, Beuth Verlag: Berlin, Germany. p. 3.

120. DIN EN 60825-1, *Sicherheit von Lasereinrichtungen - Teil 1: Klassifizierung von Anlagen und Anforderungen (Safety of laser products - Part 1: Equipment classification and requirements)*. 2015, Beuth-Verlag: Berlin, Germany. p. 115.
121. DIN EN 12617-4, *Produkte und Systeme für den Schutz und die Instandsetzung von Betontragwerken Prüfverfahren Teil 4: Bestimmung des Schwindens und Quellens (Products and systems for the protection and repair of concrete structures - Test methods - Part 4: Determination of shrinkage and expansion)*. 2002, Beuth-Verlag: Berlin, Germany. p. 14.
122. DIN EN 12390-3, *Prüfung von Festbeton - Teil 3: Druckfestigkeit von Probekörpern (Testing hardened concrete - Part 3: Compressive strength of test specimens)*. 2019, Beuth-Verlag: Berlin. p. 20.
123. DIN EN 12390-18, *Prüfung von Festbeton - Teil 18: Bestimmung des Chloridmigrationskoeffizienten (Testing hardened concrete Part 18: Determination of the chloride migration coefficient)*. 2021, Beuth-Verlag: Berlin, Germany. p. 20.
124. Selvaranjan, K., et al., *Development of sustainable mortar using waste rice husk ash from rice mill plant: Physical and thermal properties.* Journal of Building Engineering, 2021. **43**: p. 102614.
125. Long, G., Y. Gao, and Y. Xie, *Designing more sustainable and greener self-compacting concrete.* Construction and Building Materials, 2015. **84**: p. 301-306.
126. Berodier, E. and K. Scrivener, *Understanding the Filler Effect on the Nucleation and Growth of C-S-H.* Journal of the American Ceramic Society, 2014. **97**(12): p. 3764-3773.
127. ASTM C618 - 19, *Standard Specification for Coal Fly Ash and Raw or Calcined Natural Pozzolan for Use in Concrete*. 2019, ASTM International: West Conshohocken, PA.
128. Hay, R., L. Li, and K. Celik, *Shrinkage, hydration, and strength development of limestone calcined clay cement (LC3) with different sulfation levels.* Cement and Concrete Composites, 2022. **127**: p. 104403.
129. Singh, M. and M. Garg, *Cementitious binder from fly ash and other industrial wastes.* Cement and Concrete Research, 1999. **29**(3): p. 309-314.
130. Muhammad, A. and K.-C. Thienel, *Properties of Self-Compacting Concrete Produced with Optimized Volumes of Calcined Clay and Rice Husk Ash—Emphasis on Rheology, Flowability Retention and Durability.* Materials, 2023. **16**(16): p. 5513.
131. Okamura, H. and M. Ouchi, *Self-Compacting Concrete.* Journal of Advanced Concrete Technology, 2003. **1**(1): p. 5-15.
132. DIN EN 206, *Beton – Festlegung, Eigenschaften, Herstellung und Konformität (Concrete - Specification, performance, production and conformity)*. 2021, Beuth Verlag GmbH: Berlin, Germany. p. 105.
133. Sua-iam, G., P. Sokrai, and N. Makul, *Novel ternary blends of Type 1 Portland cement, residual rice husk ash, and limestone powder to improve the properties of self-compacting concrete.* Construction and Building Materials, 2016. **125**: p. 1028-1034.
134. Kannan, V., *Strength and durability performance of self compacting concrete containing self-combusted rice husk ash and metakaolin.* Construction and Building Materials, 2018. **160**: p. 169-179.
135. Diniz, H.A.A., et al., *Effects of the use of agricultural ashes, metakaolin and hydrated-lime on the behavior of self-compacting concretes.* Construction and Building Materials, 2022. **319**: p. 126087.
136. Gill, A.S. and R. Siddique, *Strength and micro-structural properties of self-compacting concrete containing metakaolin and rice husk ash.* Construction and Building Materials, 2017. **157**: p. 51-64.
137. Brooks, J.J. and M.A. Megat Johari, *Effect of metakaolin on creep and shrinkage of concrete.* Cement and Concrete Composites, 2001. **23**(6): p. 495-502.
138. Palou, M., et al., *Use of calorimetry and thermal analysis to assess the heat of supplementary cementitious materials during the hydration of composite cementitious binders.* Journal of Thermal Analysis and Calorimetry, 2020.

139. Boháč, M., et al., *Investigation on early hydration of ternary Portland cement-blast-furnace slag–metakaolin blends.* Construction and Building Materials, 2014. **64**: p. 333-341.
140. ASTM C1202 - 19, *Standard Test Method for Electrical Indication of Concrete's Ability to Resist Chloride Ion Penetration*. 2019, ASTM International: West Conshohocken, PA. p. 8.
141. Bjegović, D., et al., *Test methods for concrete durability indicators*, in *Performance-Based Specifications and Control of Concrete Durability: State-of-the-Art Report RILEM TC 230-PSC*, H. Beushausen and L. Fernandez Luco, Editors. 2016, Springer, Dordrecht. p. 51-105.
142. Shui, Z., et al., *Dominant factors on the early hydration of metakaolin-cement paste.* Journal of Wuhan University of Technology-Mater. Sci. Ed., 2010. **25**: p. 849-852.
143. Saliba, J., et al., *Influence of shrinkage-reducing admixtures on plastic and long-term shrinkage.* Cement and Concrete Composites, 2011. **33**(2): p. 209-217.
144. Huang, H., et al. *Use of rice husk ash for mitigating the autogenous shrinkage of cement pastes at low water cement ratio*. in *Proceedings of the HiPerMat 2016 4th international symposium on ultra-high performance concrete and high performance construction materials, Kassel, Germany*. 2016.
145. Mechtcherine, V., et al., *Effect of internal curing by using superabsorbent polymers (SAP) on autogenous shrinkage and other properties of a high-performance fine-grained concrete: results of a RILEM round-robin test.* Materials and Structures, 2014. **47**(3): p. 541-562.
146. DIN 1045-2, *Tragwerke aus Beton, Stahlbeton und Spannbeton – Teil 2: Beton – Festlegung, Eigenschaften, Herstellung und Konformität – Anwendungsregeln zu DIN EN 206-1 (Concrete, reinforced and prestressed concrete structures – Part 2: Concrete – Specification, properties, production and conformity – Application rules for DIN EN 206-1)*. 2008, Beuth-Verlag: Berlin, Germany. p. 62.

8 Publications

8.1 Suitability of Blending Rice Husk Ash and Calcined Clay for the Production of Self-Compacting Concrete: A Review

Reprint

Published in the Journal “MDPI/Materials” (Special Issue: Concrete Materials: Advancement in Materials Design, Manufacturing, and Applications)

Materials **2021**, *14*(21), 6252; https://doi.org/10.3390/ma14216252

Authors: Abubakar Muhammad, Karl-Christian Thienel and Ricarda Sposito

materials

MDPI

Review

Suitability of Blending Rice Husk Ash and Calcined Clay for the Production of Self-Compacting Concrete: A Review

Abubakar Muhammad *, Karl-Christian Thienel and Ricarda Sposito

Institute for Construction Materials, University of the Bundeswehr Munich, 85577 Neubiberg, Germany; christian.thienel@unibw.de (K.-C.T.); ricarda.sposito@unibw.de (R.S.)
* Correspondence: abubakar.muhammad@unibw.de

Abstract: One principal approach to achieve self-compacting properties is the increased amount of finer constituents of the mixture. This, in turn, increases cement consumption leading to higher greenhouse gas emissions. Pozzolanic materials, like rice husk ash or calcined highly kaolinitic clays, have gained increased attention as supplementary cementitious materials in self-compacting concrete production. These materials could be viable alternative supplementary cementitious materials for sub-Saharan Africa which already lacks fly ash, slag and silica fume. This current effort reviews the impact of rice husk ash and calcined clays for the production of self-compacting concrete. Special focus is on their impact on rheological, mechanical and durability properties of self-compacting concrete. Rice husk ash and, in particular, calcined highly kaolinitic clays are introduced as technical and cost-effective supplementary materials for use in self-compacting. The review disclosed a lack of knowledge when it comes to the use of low-kaolinitic calcined clays as sole SCM or together with rice husk ash, which could be a very promising combination for e.g., several countries in Africa. Further studies are needed on the rheological properties, shrinkage, creep, and durability of self-compacting concrete produced with other calcined common clays and their blend with rice husk ash.

Keywords: self-compacting concrete; metakaolin; calcined common clays; rice husk ash; rheology; compressive strength; durability; creep; shrinkage

check for updates

Citation: Muhammad, A.; Thienel, K.-C.; Sposito, R. Suitability of Blending Rice Husk Ash and Calcined Clay for the Production of Self-Compacting Concrete: A Review. *Materials* **2021**, *14*, 6252. https://doi.org/10.3390/ma14216252

Academic Editor: Jeong Gook Jang

Received: 20 September 2021
Accepted: 19 October 2021
Published: 20 October 2021

1. Introduction

The potential of various pozzolanic materials as partial replacements for cement in self-compacting concrete (SCC) production was established in previous studies. In order to continue with the trend of research on the use of rice husk ash (RHA) and metakaolin—one of the calcined clays—as a supplementary cementitious material (SCM) for SCC production, and to point out the missing gaps for further studies, the following review starts with introducing the concept of SCC and the SCM for its production, then a brief overview is given of the characteristics of rice husk ash and calcined clays as pozzolanic SCM. It is followed by a detailed literature study focusing on the fresh, mechanical, and durability properties of SCC with RHA, calcined clays, or a blend of both materials.

In reinforced concrete, a sufficient concrete cover usually serves to protect the reinforcement from adverse weather effects, harmful substances, and to improve durability. A dense microstructure can only be achieved if the concrete flows properly and embeds the reinforcement closely, fills all gaps and corners of formwork without any kind of obstruction. To achieve these attributes, concrete that requires very little compaction only was first produced and used in Europe in the early 1970s [1]. At that time, the concept of self-compacting concrete (SCC)—without the application of external vibration nor compaction—was still an imaginary vision. It was first proposed in 1986 and produced at the University of Tokyo, Japan, in 1988 [2–4].

The flow of SCC, measured as the total spread of the mixture particles purely under the influence of gravity, is normally achieved by controlling the water–powder ratio and

applying high range water-reducing admixtures (HRWR) [5]. Besides the water–powder ratio, the proportion of finer and coarser particles and the application of viscosity modifying agents (VMAs) in the mix design are decisive for the segregation resistance of SCC [3,6].

SCC can be classified into three types. The powder type: here, the fluidity of SCC is achieved by a reduction in coarser aggregate content and the addition of high-range water reducers. While the segregation resistance is achieved by increasing the percentage of fines [2,3,7]. This type is usually adopted for higher grades of SCC with a water-powder ratio of as low as 0.35. The VMA type: in this method, viscosity modifying agents are applied to provide the required segregation resistance of the SCC. Also, a small amount of HRWR is added to provide fluidity for the mixture [2,8,9]. This method is suitable for low grades of SCC with a water–powder ratio of 0.45. The combined type: this combines the use of VMA and increasing the percentage of powder, in controlling the segregation and fluidity of SCC. The combined type is usually employed for medium grades of SCC with the water–binder ratio of 0.4 [8,10].

The optimization of mix design towards self-compacting properties leads to superior qualities over conventional, vibrated concrete [4]. The modified flowing properties and segregation resistance both yields high homogeneity [10], a reduction of voids and higher early strength values [10–12], an improved interfacial transition zone, and hence to higher durability [13,14]. Also, the use of SCC improves the construction environment as the absence of concrete vibrators reduces noise pollution [1].

Despite its technological advantages, the market share of SCC is small due to some obstacles especially in developing countries [15,16]. First, SCC mixes are more sensitive even to a minor variation in constituent's proportions [16,17], change in materials properties [18,19], and the production method adopted [16,20]. Secondly, and eventually the most important concern of SCC, is the high cost of its production due to the use of high dosages of chemical admixtures and the higher binder content [21]. The cost of materials in SCC is exceeding approximately 20–50% those for conventional vibrated concrete (CVC) [15]. Although, this can be partially compensated by rapid and easy placing [22].

Mix design of SCC entails either a large reduction of coarse aggregate and an increased powder content [3,23] or a small reduction in the coarse aggregate content and the addition of VMAs [24]. From a technological point of view, a lower content of coarse aggregates in SCC might result in a lower modulus of elasticity, which may affect negatively time-dependent deformation (creep and shrinkage) of SCC [25]. Raising the binder content, furthermore, increases the environmental impact. The method to achieve SCC with small changes in the coarse aggregate and the use of VMA, instead, leads to altered mechanical properties of the concrete [25]. To provide solutions to these problems, researchers have focused on the potentials of supplementary cementitious materials (SCM) in SCC production.

The most commonly used SCM in SCC production include fly ash [24,26,27], silica fume [27–29], rice husk ash [10,30,31] and metakaolin [32–34]. These materials yielded positive results at optimal dosage levels [10,14,24,27,33]. Out of these four materials two will not be considered in this review. First, fly ash production decline with the reduction of coal-combustion which is enforced in order to limit the global CO_2 release. Right now, it is already hardly available in Africa or South America [35]. Second, the replacement-level of silica fume is limited due to its high water demand and portlandite consumption as well as for economic reasons.

Calcined clays and agro-waste materials could be an alternative source of SCM to sub-Saharan Africa [36]. This includes among others limestone powder [37,38], which is present in abundance across the region, clay minerals containing kaolinite and other mineral assemblage which can be calcined to a SCM [39–41]. The most widely used SCM from calcined clay in the region is metakaolin. However, the availability and potentialities of other clay minerals not rich in kaolinite have also been established [40,41]. Additionally, the fact that Agriculture is one of the leading economic sector of the sub-Saharan Africa, agricultural waste such as RHA, palm oil fuel ash, cassava ash, bagasse ash, bamboo leaf

ash, corn cob ash, are another viable source of SCM present in a significant amount to be used in concrete [21,36,42,43].

Rice husk ash contains about 90% reactive amorphous silica making it suitable to be used as a pozzolanic material. At cement replacement level of 15%, RHA was found to improve the microstructure of the interfacial transition zone between the cement and the coarse aggregate and, as a consequence, the strength and durability of SCC [31]. Further studies revealed improved mechanical properties of SCC with RHA as a substitute to VMA [10]. The use of RHA as both substitutes to VMA and partially to cement could cut the cost of SCC production by approximately 40% [10]. This may probably be true but it cannot be generalized due to variation in market forces, quality of the RHA itself, and the type of other binders used. However, the use of RHA in SCC requires an increased dosage of superplasticizers and causes a reduction in early strength [44].

Pozzolanic materials for SCC can also be obtained from common clays containing different phyllosilicates (kaolin, montmorillonite, illite, etc.) when thermally activated [30,45–49]. Similarly, it can also be obtained from clay wastes mostly obtain from dumps sludge, and water treatment plants [50], or further origin of burned clays such as clay bricks [51], ceramics, and tiles [52].

The use of metakaolin as cement replacement enhanced the precipitation of C-S-H leading to the refinement of specific pore size distribution of concrete, and densification of its microstructure [45,46,53,54]. These attributes make it the most commonly used calcined clay in SCC. On the other hand, the use of metakaolin increases the water demand of cement paste and the heat of hydration due to its chemo-physical properties and high pozzolanic reactivity [55,56]. Higher cement replacement with metakaolin is often hardly attractive from the economical point of view, as it is a high-price material due to its common application in other competing industries. For this reason, the suitability of other common calcined clays—not rich in kaolinite- has been investigated within the last years [57–60] and should be extended to their application in SCC as well.

Researches have investigated the behavior of binary blends of cement with RHA or calcined clays in SCC, for instance, Memon et al. [10] and Chopra et al. [31] studied the potential of RHA as VMA substitute in SCC production, and reported the possibility of a significant SCC cost reduction due to VMA elimination. Madandoust and Mousavi [34] and Ling et al. [46] explored the benefit of using metakaolin in SCC production and recommended respectively 10 and 6 wt.% cement replacement with metakaolin due to its effect on fresh properties. However, Gill and Siddique [61], and Kannan [30] have focused on ternary blends of cement with both RHA and metakaolin regarding their rheological behavior, their impact on deformation characteristics, and durability.

2. Research Gap

There has been a lot of research done on the influence of RHA [10,30,31] and calcined clay [32–34] on the fresh and mechanical characteristics of SCC. However, research on the effect of these materials on the rheology, deformation characteristics, and durability of SCC is limited especially with calcined common clays.

3. Properties of Rice Husk Ash (RHA) and Calcined Clays

Supplementary cementitious materials in the form of pozzolanic materials are used to replace some proportions of cement, for instance in the production of SCC. These include among others: RHA and calcined clays, both materials that obtain their pozzolanic reactivity by thermal activation (calcination).

RHA is produced by calcination of rice husk at temperatures between 600 and 700 °C to keep the ash in the amorphous phase [31,62,63]. It contains a high amount of amorphous silica, designating it as pozzolanic material according to [64,65]. RHA consists mainly of microporous, regular, and angular particles, having large specific surface area particle micromorphology [66–68]. It was also characterized as having irregular, mesoporous, and rough-textured particle surfaces [31,62,69].

Furthermore, RHA was described as a three-layer material, containing inner and outer strata of dense structure. The interfacial strata, however, consist of a cross mesh of chips-like structure arranged in a loose honeycombed fashion containing a large number of holes (Figure 1) [63]. Transmission electron microscopy (TEM) analysis conducted on RHA calcined at 600 °C showed a very large amount of fine cooked rice-like particles as shown in Figure 1 [63]. This structure is responsible for its high specific surface area and reactivity.

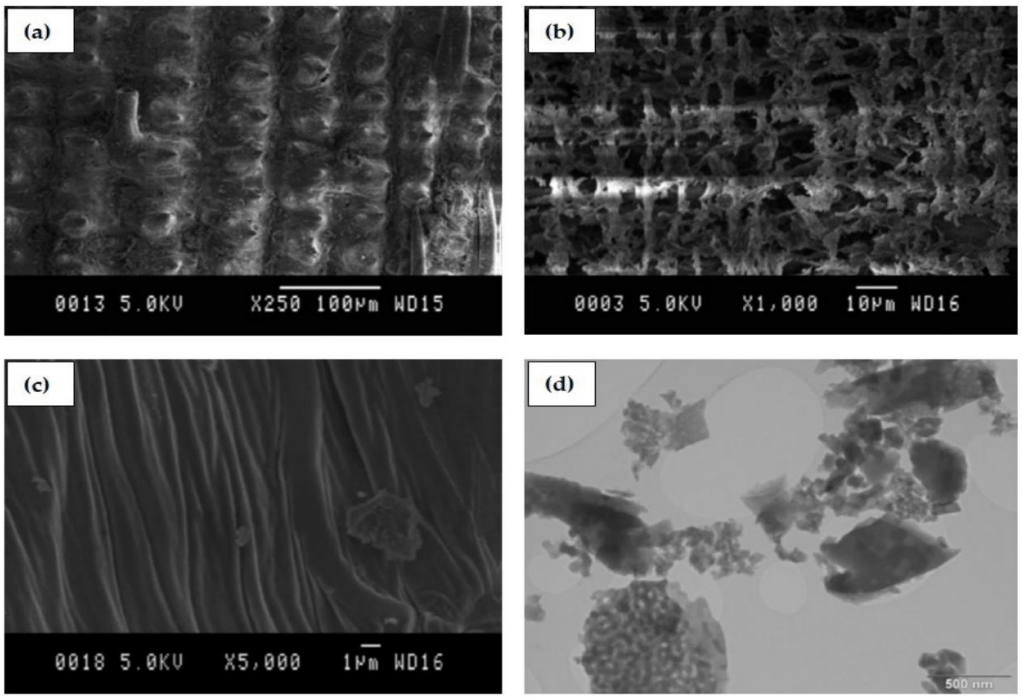

Figure 1. Micromorphology of rice husk ash (RHA) showing (**a**) outer surface (**b**) inter layer (**c**) Inner surface (**d**) transmission electron microscopy (TEM) image of RHA [63].

Although, when obtained from an uncontrolled burning, the formation of crystalline silica is possible leading to poor pozzolanic properties and high water and superplasticizer (SP) demand [66,70].

Ganesanet et al. [64] observed an increase in standard consistency when RHA is added to the cement. This could be due to a higher specific surface area and or higher carbon content leading to high water demand [71]. A reduction in both the initial and final setting time of the mixture was achieved, especially at a higher replacement level of cement with RHA [64]. Le et al. [70] recorded about 79 wt.% water demand of RHA with a particle mean size of 22.6 µm which was reduced to 57 wt.% when grinding to 5.7µm mean particle size. Increasing RHA fineness has a slight effect only on its specific surface area [62].

Metakaolin (MK), as the most famous representative of calcined clays, is the metaphase of the phyllosilicate kaolinite after calcination. The calcination temperature (500–650 °C) is chosen based on the dehydroxylation temperature of kaolinite. Kaolinite is a 1:1 phyllosilicate consisting of (SiO_4) tetrahedral and (AlO_6) octahedral sheets that are connected via OH-groups and aluminum cations [72,73]. By dehydroxylation, the structure of metakaolin becomes highly disordered and amorphous. MK is rich in aluminum and can differ significantly in the physical properties. Besides metakaolin, the suitability of calcined common clays—with various types of 2:1 phyllosilicates and further inert components—as SCM has been investigated within the last few years [60,74,75].

The addition of up to 15 wt.% MK improved the strength of SCC [53]. At the same time Mk has a high specific surface area and high water demand. Consequently, the fluidity of self-compacting concrete decreases gradually with the increase of metakaolin content [46].

Table 1 shows some relevant physical and chemical properties of cement, RHA, and metakaolin reported by scholars. The cements used were ordinary Portland cement (OPC) having almost a similar range of silicon oxide of between 19.4% to 20.25%. The aluminum oxide ranges from 5.04% to 5.3%. The percentage of calcium oxide ranges between 61.2% to 63.61%. All the cements have a lost on ignition (LOI) of < 5.0. The RHA used is rich in silica ranging from 82.05% to 87.32%, with minor traces of aluminum oxide and other chemical oxides as shown in Table 1. RHA used by Zhang et al. [76] exhibits the highest LOI compared to the remaining RHAs, this could be perhaps due to the high content of unburnt carbon in the material. Metakaolin is both rich in both silica and alumina. The silicon/aluminum ratio of the metakaolin used by Kennan [77] is less than the remainder, which is an indication of purity of the metakaolin and can significantly affects its reactivity. RHA has the highest specific surface area due to its porous nature, followed by bthe metakaolin and then cement. Both RHA and metakaolin are pozzolanic in terms of chemical properties and can be used as partial substitutes to cement.

Table 1. Properties of cement, RHA, and metakaolin.

Materials	Reference	SiO_2 (%)	Al_2O_3 (%)	Fe_2O_3 (%)	CaO (%)	MgO (%)	Na_2O (%)	K_2O (%)	LOI (%)	Specific Surface Area (m^2/g)	Mean Particles Size (μm)
Cement	[77]	20.21	5.06	3.18	63.30	4.20	0.09	0.52	3.07	316 [Bl]	23.40
	[64]	20.25	5.04	3.16	63.61	4.56	0.08	0.51	3.12	326 [Bl]	22.50
	[62]	19.4	5.3	2.5	61.2	1.2	0.07	0.61	4.9	2.07 [B]	7.07
RHA	[77]	82.05	0.45	2.21	0.62	0.62	0.95	4.43	4.97	916 [Bl]	6.57
	[64]	87.32	0.22	0.28	0.48	0.28	1.02	3.14	2.10	36.47 [B]	3.80
	[77]	87.20	0.15	0.16	0.55	0.35	1.12	3.68	8.55	38.90 [B]	7.00
Metakaolin	[77]	49.50	44.23	0.92	0.17	0.08	0.10	0.02	0.32	2342 [Bl]	3.71
	[78]	54.3	38.3	4.28	0.39	0.08	0.12	0.50	0.68	15.00 [B]	NR
	[79]	56.20	37.20	1.40	1.20	0.20	NR	1.20	2.10	18.70 [B]	11.50

NR = Not Reported; Bl = Blain's (m^2/kg); B = BET (m^2/kg).

4. Mix Design of Self-Compacting Concrete (SCC) with Rice Husk Ash and/or Calcined Clays

Different methods have been developed for designing SCC mixes since, unlike CVC, SCC is susceptible to nuances in material properties and other environmental factors. Initially, Okamura and Ozawa [2] used an empirical design method to achieve self-compactability, which later was adopted and modified by [80–82] and concrete production regulatory bodies. Both coarse and fine aggregate are kept constant using this method. The water to powder ratio and SP amount are adjusted to achieve the required degree of self-compactability. This method eliminates repeatability during SCC production. However, it is considered too complicated for practical application [5] and the water to powder ratio cannot be fixed based on strength, but rather on the self-compactability requirement.

Subsequently, methods based on rheometer tests were developed to characterize the yield stress and plastic viscosity of SCC. Sedran et al. [83] used a torsional rheometer to obtain values of yield stress and plastic viscosity to characterize SCC. RENE-LCPC™ software developed based on solid suspension was used to determine the optimal packing density using less water to achieve the same or improved workability. Petersson et al. [84] developed an SCC mix design similar to the work of [83]. In their experiment, the tendency of blocking was determined using an equation to obtain the minimum paste volume while a rheometer was used to determine the suitable water to powder proportion and SP dosages. This method was adopted and modified to check the robustness of SCC produced [70,85–88]. Just like the previous method, this method does not take compressive strength as a determinant factor in designing SCC mixes and required more sophisticated tools to measure the rheology.

Su et al. [5] used the aggregate packing method to achieve self-compactability. In this method, the least void between the loosely piled aggregate framework is determined and a liquid phase (paste) is used to fill the void and provide a lubricating layer around each particle. Although this method simplifies the SCC grades, it yields the required mix proportion for only medium to high strength concrete. This method was adopted and simplified by [70,89].

Kheder and Jadiri [90] factored in compressive strength as a determinant in designing self-compacting mixes. Their method, determines water to binder ratio based on maximum aggregate size and compressive strength requirement. Similarly, Dinakar [78,91] achieved self-compactability by considering the efficiency of pozzolanic materials added to SCC. With this method, even low-grade SCC can be achieved, although it requires adjustment to all concrete constituents in case of a minute change. Xie et al. [92] further considered even the fraction of the key oxides of a particular SCM to model both fresh and hardened properties of SCC. Their method permits achieving, both self-compactability and strength by knowing the exact characteristics of the SCC binder.

The same mix design methods were adopted when the clinker phase is replaced with RHA and or calcined clays. Usually, a high dosage of SP is required for SCC produced with the addition of RHA and or metakaolin [10,53,55,93] due to their high surface area and water demand. The optimal replacement level for both RHA and metakaolin in SCC is usually 15 wt.% of cement [10,94,95]. Also, Dinkar and Manu [78] developed a new SCC mix design method by considering the efficiency factor of the metakaolin. Here, the replacement level is based on the efficiency factor of the metakaolin, not by simple substitution. Both RHA and MK were found to provide sufficient segregation resistance required in SCC mixes and therefore, eliminate the use of VMAs [10,34].

5. Fresh Properties of SCC

5.1. Rheological Properties of SCC

One difference between CVC and SCC is the behavior of the fresh concrete. SCC is characterized by high deformability, passing ability, and segregation resistance [2,6,96]. Various limits to these attributes are well established [97–99]. Commonly measured characteristic includes the flowability, viscosity, passing ability, and the segregation resistance. The flowability is divided into three classes and is determined using the slump flow diameter measured in millimeters: SF1 from 550 to 650; SF2 660 to 750; SF3 760 to 850. The viscosity is determined using V-funnel time measured in seconds and is divided into two classes: VF1, <9 and VF 2, 9 to 25. T_{500} measured in seconds can also be used to assess the viscosity of SCC and is divided into three classes: VS1, $\leq$2; vs. 2, 3 to 6 and VS3, >6. The passing ability is usually determined as a blocking ratio of SCC and is divided into two: PL1, $\geq$0.8 with two rebars; PL2, $\geq$0.8 with three rebars. Sieve stability is used to assess the segregation resistance of SCC. The limiting values are $\leq$20 for SR1 and $\leq$15 for SR2 [97–99].

Viscometers are also used to quantify SCC parameters in relation to plastic viscosity and yield values. SCC exhibits low yield stress of about 0 to 60 Pa compare to CVC and plastic viscosity of about 20 Pa·s to almost over 100 Pa·s. Various limits of SCC yield stress (τ) and plastic viscosity (μ) across the globe have been summarized in the form of rheographs and a workability box by [100]. The use of rheometers, as discussed under the mix design section, provide an alternative way to design and test the rheological properties of SCC in a more accurate and advanced way, and to provide the best assessment of bleeding tendency and or segregation resistance [101–103].

Benaicha et al. [104] proposed another simple method—V-funnel coupled to a horizontal Plexiglas channel—to assess the yield stress and plastic viscosity of SCC, especially at the construction site. A positive correlation was obtained between the theoretical yield stress and plastic viscosity obtained from the V-funnel, calculated using the equations provided by [102,105], and the actual yield stress and plastic viscosity values obtained using a R/S+ rheometer.

5.2. Rheological Properties of SCC with RHA or Metakaolin (MK)

Figures 2–4 display the influence of binary and ternary blends of cement, RHA, and calcined clays on fresh properties of SCC. The use of a binary blends using RHA or MK to replace cement up to 15 wt.% was found to improve the slump flow and viscosity of SCC [33,34,61,106]. The improvement in slump flow could perhaps be due to the high dosage of superplasticizer used to achieve the required properties of the fresh SCC. Consequently, a decrease in slump flow of SCC was reported [30,31] when the blends of RHA or MK were used to replaced cement. This is because both RHA and MK have high water demand compared to cement [53], leading to a decrease in the flow of SCC produced with them. At replacement levels above 25 wt.% in the case of RHA and 40 wt.% for blends of RHA and MK, the slump flow is below the limits for SCC (Figure 2). The viscosity of the SCC increased with increasing cement replacement level as shown in Figure 3. This could be because the high cohesive forces between the MK and/or RHA particles increased the friction between the mortar constituents, slowing the rate of deformation. A replacement level of 15 wt.% can be regarded more or less as threshold between VF1 and VF2. The passing ability of SCC keeps decreasing with an increase in cement replacement by RHA and MK. Any cement replacement beyond 15 wt.% with RHA and MK resulted in a poor passing ability of the SCC produced [30,34,61] (Figure 4). On the other hand, a good passing ability was obtained, at 30 wt.% cement replacement with a ternary blend of RHA and MK [30,61].

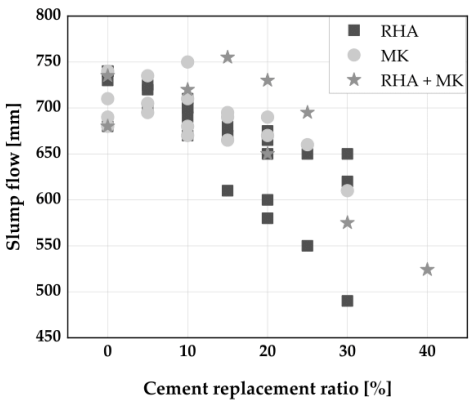

Figure 2. Slump flow of self-compacting concrete (SCC): Kannan [30], Chopra et al. [31], Rahman et al. [106], Madandoust [34], Gill [61].

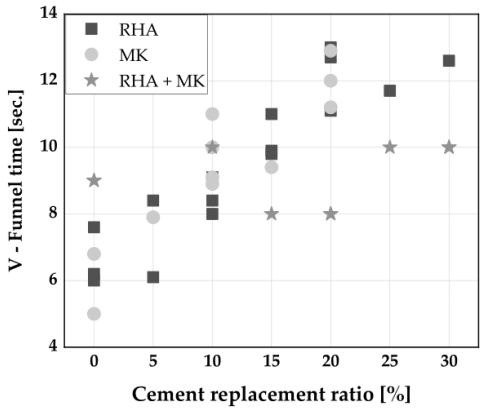

Figure 3. Viscosity of SCC: Chopra et al. [31], Kannan [30], Gill [61], and Madandoust [34].

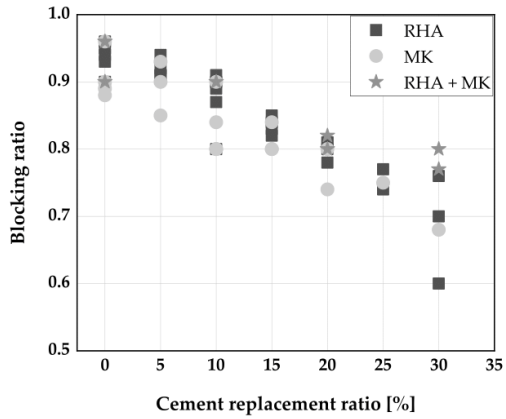

Figure 4. Blocking ratio of SCC: Chopra et al. [31], Kannan [30], Gill [61], Madandoust [34].

Rheological measurements on self-compacting mortar produced with RHA as clinker replacement revealed increased yield stress and viscosity due to an increase in water demand [62]. Ling et al. [46] reported similar findings related to the use of metakaolin as SCM.

Although both RHA and MK have good potential to be used as SCM in concrete production due to their superior pozzolanic reactivity, their use as clinker substitute in SCC production results in a significant decrease in slump flow and an increase in viscosity. Consequently, when both materials are to be added to SCC higher dosage of SP is required.

6. Hardened Properties of SCC

6.1. Compressive Strength

RHA addition up to 10 wt.% of binder was found to increase the compressive strength of SCC [10]. The authors used RHA as a substitute to VMA and not as SCM. The increase in strength is due to a reduction in water to binder ratio, because of RHA addition resulting in denser particle packing, pore, and grain size refinement [10]. When used as a SCM, RHA improves the microstructure of the paste matrix and transition zone, due to its high reactivity leading to the formation of more C–S–H, thereby improving the strength development of SCC [30,31,106]. Similarly, a compact formation of hydration product leading to a reduction in porosity of the concrete was observed [69] when RHA replaced up to 15 wt.% of cement. Figure 5 shows the compressive strength of SCC produced with RHA and MK and in combination as cement replacement.

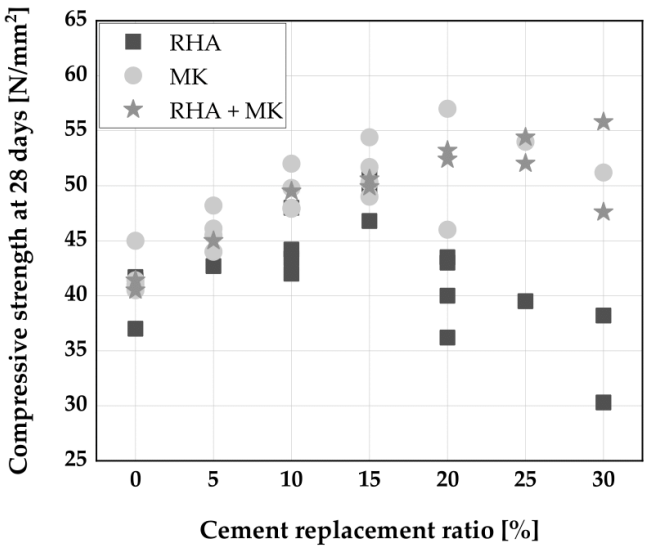

Figure 5. Compressive strength of SCC: Chopra et al. [31], Kannan [30], Kavitha [53], Madandoust [34], Vivek [107], and Gill [61].

It becomes clear from Figure 5 that cement replacement with RHA up to 15 wt.% can improve compressive strength of SCC [30,31]. Also, a decrease in compressive strength was reported by [106] for all the replacement levels with RHA, which could perhaps be due to the extent of treatment (calcination and grinding) performed on the RHA which largely determines its reactivity [76,108]. Le et al. [70] reported a decrease in compressive strength at the early age of curing for a higher percentage of cement replacement with RHA. It was followed by an increase in compressive strength at 56 days of curing and above. Furthermore, RHA is considerably more effective than fly ash in improving compressive strength, mainly due to its high content of reactive amorphous silica and higher specific surface area [70].

Metakaolin can lead to an acceleration of cement hydration and strength development when properly treated and added to cement [109]. An increase in compressive strength was reported by [34,107] when up to 15 wt.% cement is replaced with MK as depicted in Figure 5. A higher replacement level just maintains compressive strength but yield no further gain.

Ternary blends of RHA and MK were found to improve both early and later compressive strength development in SCC as reported by [61,110]. A higher percentage replacement level of 20 wt.% of cement and above was possible for optimum performance when the two pozzolanic materials were blended.

6.2. Ultrasonic Pulse Velocity

Ultrasonic pulse velocity (UPV) is a proper parameter for testing the homogeneity and integrity of concrete non-destructively. Increased UPV values correspond to the densification in the internal structure of the SCC [111]. Higher UPV values were achieved at all ages of SCC when replacing 20 wt.% of cement with RHA [111].

Özcan and Kaymak [109], observed a strong positive relationship between compressive strength and UPV values of SCC produced with a binary blend of cement and metakaolin. This is an indication that whenever metakaolin is replacing cement up to an optimal level, the homogeneity, and integrity of the SCC increases. Similarly, Kannan [30] reported a "good" concrete quality for SCC produced without the addition of pozzolanic materials, while an "excellent" concrete quality was reported for SCC with cement replaced with up to 25 wt.% RHA; "excellent" concrete quality was achieved for all levels of cement

replacement with MK and a ternary blend of RHA and MK as shown in Figure 6. The concrete integrity classification was based on IAEA, 2002 [112] classification as "excellent", above 4.5 km/s; "good", 3.5 to 4.5 km/s; "doubtful", 3.0 to 3.5 km/s; "poor", 2.0 to 3.0 km/s and "very poor", below 2.0 km/s.

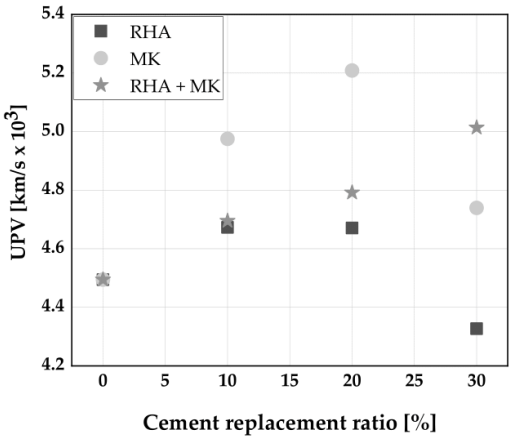

Figure 6. Ultrasonic pulse velocity of SCC [30].

6.3. Modulus of Elasticity

The mechanism of achieving SCC entails a reduction in size and quantity of coarser aggregate content of the mixture, this raised concern that SCC may have lower values of modulus of elasticity, which in turn will affect the deformation characteristics of the concrete [25]. Several publications investigated the influence of RHA and metakaolin addition on the modulus of elasticity properties of SCC [30,46,113,114]. Metakaolin had no significant impact SCC [22,56,93,115] as displayed in Figure 7. A slight increase in modulus of elasticity was observed when RHA was used as SCM [116–118]. A further increase in the replacement level with RHA beyond 10 wt.% of cement caused rather a slight reduction in the modulus of elasticity values of SCC [116] (Figure 7).

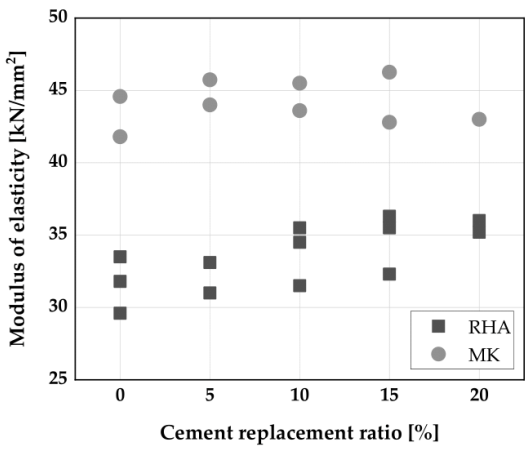

Figure 7. Modulus of elasticity: Molaeiraisi [116], He [117], Ramezanianpour et al. [118], Barkat et al. [22], Johari [119].

6.4. Shrinkage and Creep

Shrinkage and creep behavior are important attributes to be studied when introducing any pozzolanic material as SCM. This is related to high water evaporation rates, especially in dry conditions, due to slow hydration kinetics resulting in high free plastic shrinkage compared to SCC without SCMs [120]. So far, there has been no literature on shrinkage and creep behavior of SCC with RHA and metakaolin in ternary blends.

Few papers deal with the impact of RHA on shrinkage behavior of SCC [121,122]. Both reported no significant effect due to the addition of RHA on the shrinkage behavior of SCC. However, when finely ground, RHA increased the drying shrinkage of concrete due to its microfine particles [123]. However, when used as a substitute to the clinker phase in CVC, RHA was found to reduce the drying shrinkage of concrete [66,124]. This might be due to the ability of RHA to behave like an internal curing agent, whereby continuously releasing the absorbed free water in its mesoporous cellular structure for hydration, and thus controlling concrete internal relative humidity, delaying self-desiccation and preventing autogenous shrinkage of concrete [68,118,125,126]. Similarly, creep and drying shrinkage strains were found to exhibit a similar tendency. Concrete specimens with a high RHA to binder ratio yield a smaller strain and creep coefficient compared to the control specimens as shown in Figure 8 [117].

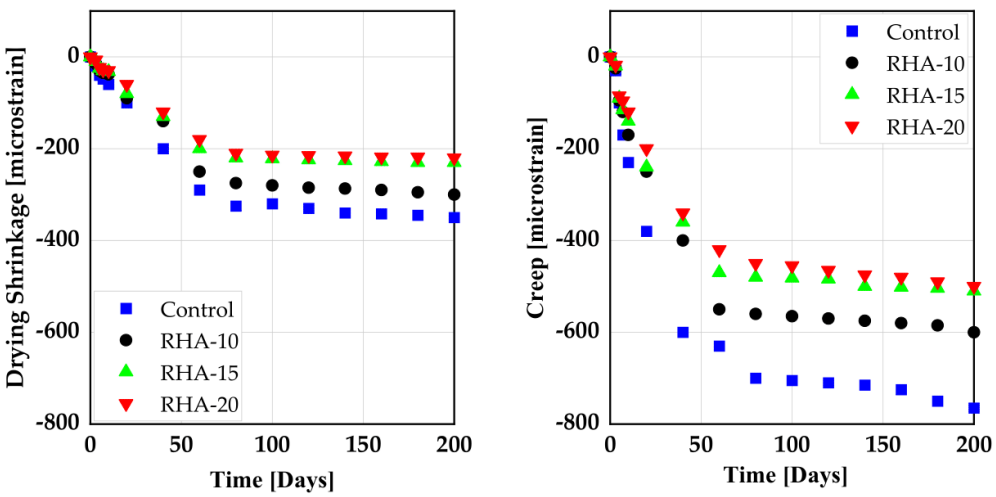

Figure 8. Drying shrinkage and creep of concrete produced with RHA: He [117].

With the addition of MK at 15 wt.%, the drying plastic shrinkage value of SCC increased by about 20 % since MK contributes to the high water evaporation rate of the system and consequently the tendency of higher sensitivity to drying [120,127]. SCC specimens with 15 wt.% MK as cement substitute experienced high values of autogenous shrinkage up to 10 days of curing, beyond which the shrinkage values decline and become less than the control specimens as depicted in Figure 9 [120]. This effect of MK is due the formation of finer pores leading to more self-desiccation and consequently high autogenous shrinkage [120,128,129]. On the other hand, SCC produced with MK as SCM exhibited lower drying and autogenous shrinkage values than the control specimens [120,130]. This was attributed to low evaporation of the free water and the pozzolanic reactivity of MK leading to the formation of denser microstructure and hence higher resistance to deformation [33,131]. The autogenous and drying shrinkage remains less than the SCC specimens without MK [120].

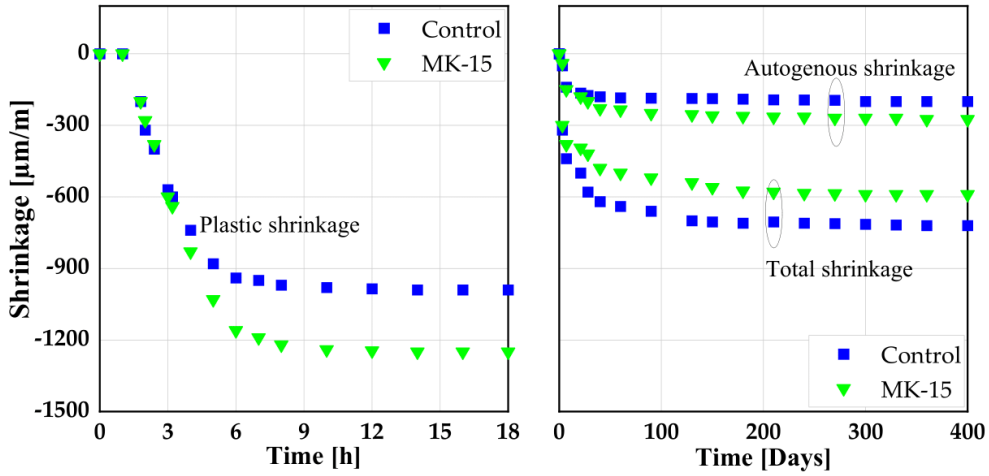

Figure 9. Plastic, autogenous and total shrinkage of concrete produced with metakaolin (MK) [120].

Nesvetaev et al. [132], studied the effect of metakaolin on the creep properties of SCC. On control specimens, they observed an increased final creep coefficient (Δ 1.3 to 1.8) of SCC compared to NVC. However, when MK and silica fume were both added to the mixture of SCC, the creep coefficient dropped by 0.5 to 0.6 compared to CVC. From this point of view, it is important to study the effect of RHA with and without MK on shrinkage and creep behavior of SCC. Figure 10 shows the shrinkage and creep of CVC produced with MK as cement substitute. Autogenous as well as drying shrinkage of CVC is significantly smaller than observed for SCC.

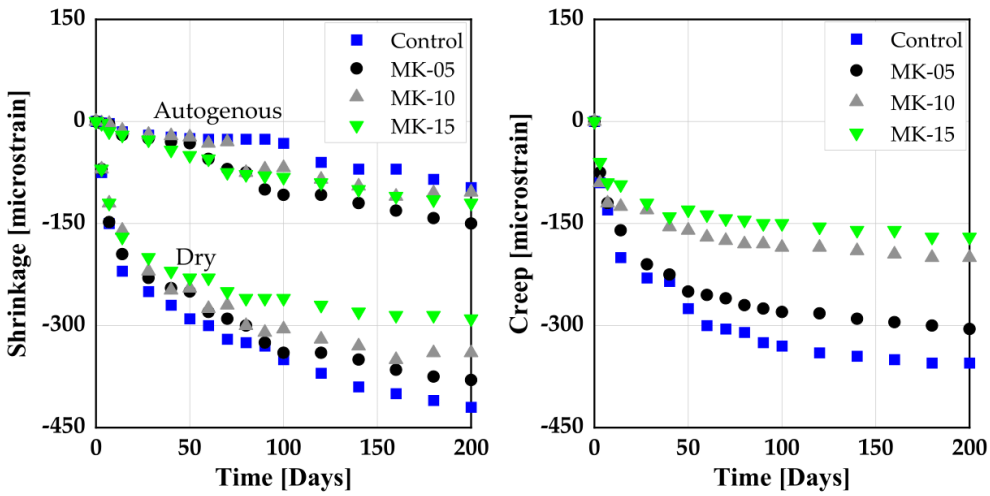

Figure 10. Shrinkage and creep of conventional vibrated concrete (CVC) produced with MK [120].

7. Durability Properties

7.1. Water Absorption and Sorptivity

Figure 11 shows the water absorption of SCC produced with a binary blend of RHA, MK, and a ternary blend of RHA and MK. A good concrete quality [133] having low water absorption capacity was reported when RHA, MK, and blends of RHA and MK were added to SCC. A decrease in water absorption for RHA replacement up to 20 wt.% was

reported by [110,134]. This decrease is due to additional C-S-H formation caused by the pozzolanic reaction of RHA and a micro filler effect leading to refinement of the grading of the concrete [110]. However, Rahman et al. [106] reported an increase in water absorption of SCC at all replacement levels when uncontrolled burnt RHA was used to replace cement.

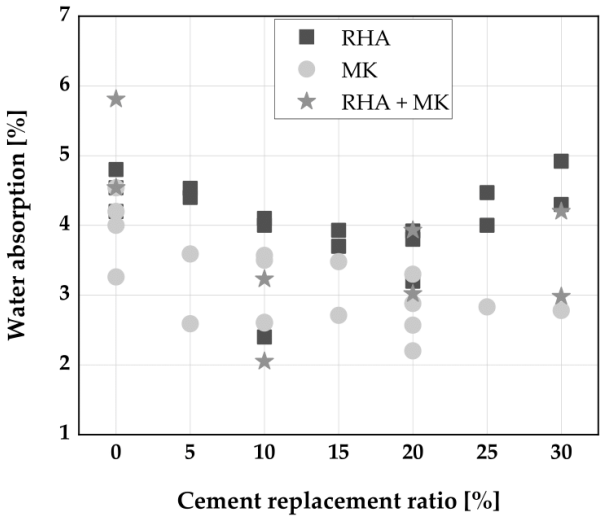

Figure 11. Water absorption of SCC produced with RHA and MK: Kannan [110], Rahman [106], Madandoust [34], Gill [135].

Similarly, a reduction in water absorption of SCC was noticed for all replacement levels (5, 10, 15, and 20 wt.%) of MK as shown in Figure 11. This is due to a reduced porosity and finer pore size distribution [32,34,110,134]. Gill/Siddique [135] reported a sharp decrease in water absorption when a ternary blend of RHA and MK was used to replace cement at 15 wt.%, while a further increase in replacement level leads to an increase in water absorption. However, Kannan/Ganesan [110] and Gill/Siddique [135] reported a continuous decrease in water absorption up to 30 wt.% cement replacement level with a ternary blend incorporating RHA and MK. Generally, water absorption values of SCC made with these ternary blends are significantly reduced compared to the binary systems with RHA only.

Sorptivity of SCC produced without the addition of SCMs was found to be very high compared to CVC and was attributed to the higher binder content of SCC [107]. However, the addition of MK up to 30 wt.% reduced sorptivity and lower capillary suction [107]. Kannan and Ganesan [110], reported a reduction by 7% when 15 wt.% of RHA was used as cement substitute, while a further increase in the replacement level resulted in a rise of the sorptivity values. Similar to the water absorption, a higher reduction in sorptivity (26%) was observed when the ternary blend (15 wt.% RHA and 15 wt.% MK) was used to replace cement compared to the binary blends only [110].

7.2. Porosity

The use of RHA (up to a replacement level of 25 wt.% of cement) was found to decrease the porosity of SCC and, thereby, to lower its permeability [31,136]. This decrease becomes more pronounced with an increase in curing age as shown in Figure 12. Similarly, metakaolin, up to 25 wt.% cement replacement slightly decreased the porosity of SCC [22,137]. However, these findings hold only up to 28 days age of concrete. A minimum porosity was achieved for RHA and MK at a replacement level of. At a later age, Gill [135] reported an increase in porosity especially with higher percentages of cement replacement

exceeding 15 wt.% with RHA and MK, and attributed this to the higher surface area of RHA, and its subsequent water demand.

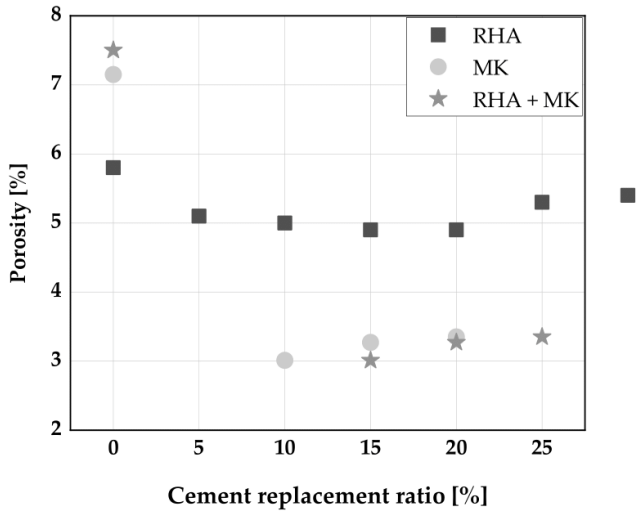

Figure 12. Porosity of SCC produced with RHA and MK: Chopra et al. [31], Barkat et al. [22], Gill [135].

7.3. Chloride Penetration Resistance

The rapid chloride permeability test (RCP), by passing an electric charge through concrete specimens, is used to assess the chloride penetration resistance of concrete according to (ASTM C1202 [138], DIN EN 12390-11 [139], etc.). Figure 13 depicts the results of RCP of SCC with RHA, MK, and a blend of RHA and MK as SCM. A reduction in total electrical charge passed through SCC was observed by [31,110,140] when RHA was used as a cement substitute. This reduction is due to the densification of the SCC microstructure, because of the pozzolanic reaction of RHA leading to the formation of more C-S-H in the system and consequently a reduction of micropores and cracking tendency [31].

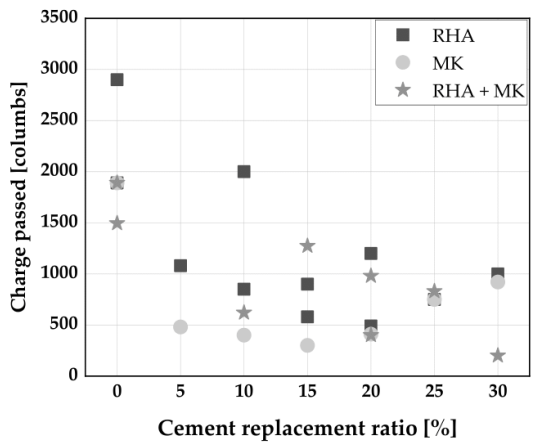

Figure 13. Rapid chloride penetration of SCC produced with RHA and/or MK [110].

Similarly, for all cement replacement with MK up to 15 wt.%, a reduction in chloride permeability was reported by [53]. Badogiannis [141] expressed chloride permeability in

terms of chloride migration coefficient and observed about a 70% decrease in permeability when MK was used to replace cement. This is perhaps due to the densification of the pore structure, from the pozzolanic reactivity of MK, leading to the reduction in the width of the interfacial transition zone by creating more C–A–H, thereby decreasing the diffusion rate of SCC [53]. Also, the least total charge passed by RCP was recorded by [110] and [135] with a ternary blend of RHA and MK at up to 40 wt.% cement replacement. This indicates that a ternary blend of RHA and MK provides a better chloride penetration resistance than the individual binary blend with RHA and MK, due to further densification of the pore structure and the formation of more C-S-H gel [135,142].

7.4. Resistance to Magnesium Sulfate

Sulfate resistance of SCC with RHA and MK is also an aspect of durability that only a few researchers [53,135,142] have paid attention to. Kavitha and Shanthi [53] studied the weight loss, compressive strength, and micro-structure of SCC with MK, up to 12 weeks of curing in 5 wt.% $MgSO_4$ solution and reported a greater resistance at all replacement levels with MK compared to control SCC. This was attributed to the pozzolanic reaction between CH and MK, leading to pore size refinement, and increased resistance to diffusion of harmful ions [53]. SCC with MK replacing cement up to 20 wt.% lost less weight in a $MgSO_4$ solution than the remaining specimens [53].

In addition, Gill and Siddique [135] have reported a reduction in compressive strength of SCC produced with a ternary blend of RHA and MK even at 28 days of curing in the sulfate environment. SCC produced with the addition of ternary blend (10 wt.% MK + 10 wt.% RHA) showed better resistance to the magnesium sulfate attack compared to the remaining specimens as shown in Figure 14. The mechanism behind the resistance to $MgSO_4$ is perhaps because of the ternary blend of RHA and MK leading to more C-S-H in the mixture, thereby leading to pore size refinement, and increase resistance to diffusion of harmful ions [135].

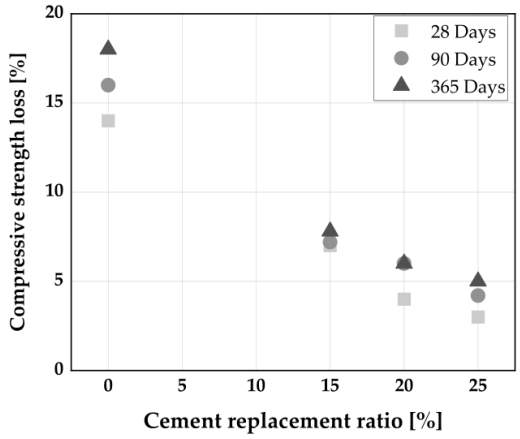

Figure 14. Compressive strength loss of SCC [135].

7.5. Carbonation

Carbonation occurs due to the reaction between carbon dioxide and the alkaline components of cement hydration, mainly CH. This causes a reduction in the pH-value of the paste pore solution [143]. The addition of RHA as a substitute to the clinker phase in concrete decreased the amount of CH on the one hand but provided better resistance to carbonation at the same time [144–147]. Lower carbonation coefficients were reported when RHA was used to replace cement at 20 wt.% and, a further decrease was obtained when 1 wt.% K_2SO_4 was added to the mixture as a chemical activator [144]. Consequently, the use of RHA increases the depth of carbonation in concrete [148,149]. This was attributed

to lower cement content in the system and higher porosity [118] allowing more CO_2 to penetrate into the concrete. This could perhaps be due to the treatment given to the RHA or because the pore solution under the carbonation process is yet to be consolidated, as the result of the accelerated method adopted [146]. The authors were not aware of literature on the effect of RHA on the carbonation resistance of SCC.

Metakaolin as partial replacement of cement was found to be more effective in reducing the carbonation resistance of SCC, than observed for CVC [150]. In both cases, the use of MK led to a reduced carbonation depth and improved the permeability resistance. This was due to the consumption of CH and pore size refinement from the pozzolanic reactivity of MK. Similar results were reported by [151,152]. On the other hand, a slight decrease of pH values compared to the control specimens was observed when MK was used to substitute cement at 10 wt.% and subjected to 14 years of natural carbonation [146].

7.6. Freeze-Thaw

The use of RHA to replace cement decreases the internal damage caused by freeze-thaw (F-T) and as well, limits its impact on the dynamic modulus of elasticity of SCC subjected to F-T cycles. The durability factor, determined based on ASTM C 666-15 method of SCC without RHA subjected to up to 300 F-T (+4 to −18 °C and subsequently −18 to +4 °C for 5 h) cycles was found to be 56%. When RHA was used as cement replacement at 15 wt.%, the durability factor increased to 80% [153]. SCC with cement replacement suffered less weight and compressive strength losses, its electrical resistivity increased, and exhibited higher values of dynamic modulus of elasticity when subjected to F-T cycles compared to their companion control specimens [153]. This was explained by the consumption of CH by the reactive silica in RHA and producing more C-S-H in the cement matrix, leading to the formation of dense microstructure and thereby decreases porosity and permeability of the SCC [147]. Similar observations hold for CVC [154,155]. Figure 15 shows the relative compressive strength of SCC subjected to 100, 200, and 300 F-T cycles and at +4 to −18 °C and, subsequently, −18 to +4 °C for 5 h.

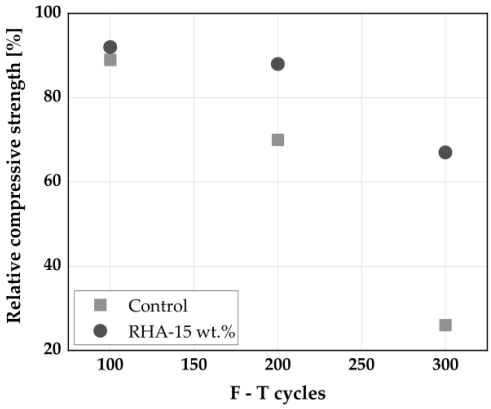

Figure 15. Relative compressive strength of SCC subjected to F-T [153].

Duan et al. [156] observed a reduction of the interconnected pores in the concrete structure when MK was used as cement replacement. This prevented osmotic pressure resulting from the migration of supercooled water and thereby improved the F-T resistance of the concrete. The reduction of the interconnected pores is attributed to better particle packing and pore size refinement in the course of the pozzolanic reaction of MK [156,157]. An improvement in the residual UPV values, compressive strength, and weight loss was observed when MK was used as cement replacement in concrete subjected to F-T cycles by [157–159]. The authors found no data on the combined effect of RHA and MK on the impact of F-T.

8. Discussion

Both RHA and metakaolin are pozzolanic and are used as a SCM for SCC production [10,30–34]. RHA derives its pozzolanicity from optimization of proper calcination and grinding [31,62,63]. The hydration mechanism of RHA in concrete is related to the consumption of portlandite and enhancement of precipitation of C-S-H, which reduces the specific pore size of the binder matrix and densified its microstructure [70,71,76]. These attributes make it possible to partially substitute cement with RHA up to 20 wt.% without an adverse effect on its strength and or durability [30,31,106]. Another possible reason for this could be caused by the ability of RHA to behave like an internal curing agent, whereby it is continuously releasing the absorbed free water from its mesoporous cellular structure for hydration, which facilitates the precipitation of more C-S-H in the system [68,118,126]. Metakaolin, on the other hand, behaves similarly to RHA in binder matrix densification but the mechanism of its pozzolanic reactivity is more complex. Metakaolin reacts faster than RHA and promotes in addition to the silicate the aluminate reaction especially in the presence of $CaCO_3$, thereby promoting the precipitation of hemi/monocarboaluminate AFm phases of binder hydrates [22,30,115]. Cement can be partially replaced with up to 45 wt.% of a blend of metakaolin and limestone (LC^3, cement) without an adverse effect on its strength and durability. The use of both RHA and metakaolin as a partial replacement for cement increases the water demand of the blended system [21,46,123] and, therefore, care has to be taken in selecting the degree of viscosity of the self-compactability required especially at higher levels of cement replacement. Pure metakaolin has other industrial attraction and is more costly compared to cement. Although the suitability of other common clays not rich in kaolinite has been established as discussed in [60,74,75], research on their use as binary blend with cement, or as multi-blend in addition to RHA, is deficient especially in the aspects of rheological measurements, shrinkage, creep and the durability of SCC. Therefore, the need to expand the frontier of research on studying the rheology, mechanical and durability of SCC produced with calcined common clays and its multi-blend with RHA is paramount.

9. Conclusions

The following conclusions were drawn from the findings of the study:

- Metakaolin was found to be the most commonly used calcined clay for the production of SCC thus far. The suitability of other clayey materials such as calcined clay waste, calcined red mud, and calcined common clays with low kaolinite content for the production of SCC was not yet explored.
- Rice husk ash and metakaolin are pozzolanic materials and have the potentials to be used as supplementary cementitious materials in self-compacting concrete production. The potentials of rice husk ash as a viscosity-modifying agent in concrete production is also established.
- Both rice husk ash and metakaolin have high water demand compared to cement. Therefore, their use as a supplementary cementitious material in SCC entails the application of a high dosage of superplasticizers.
- Rice husk ash was found to be very effective in increasing self-compacting concrete strength due to its high content of reactive amorphous silica and higher specific surface area. Metakaolin, on the other hand, was also found to improve early strength development due to its fast pozzolanic reaction.
- The optimal replacement level for both the binary blend with RHA and MK is usually between 15 and 20 wt.%. However, with a ternary blend with RHA and MK, larger cement replacements of between 20 to 40 wt.% are possible.
- Studies on the effect of ternary blends of rice husk ash and metakaolin on shrinkage and creep behavior of SCC were not found by the authors.
- Although researchers have presented results of the durability of SCC produced with a blend of rice husk ash and metakaolin, there is a need to further study the effect of these materials on porosity, carbonation and freeze-thaw resistance of SCC.

- The review disclosed a lack of knowledge when it comes to the use of low-kaolinitic calcined clays as sole SCM or together with rice husk ash which could be a very promising combination for e.g., several countries in Africa.
- Greenhouse gas emissions and environmental problems could be reduced by partially replacing cement with RHA and metakaolin.

10. Proposal for Further Investigation

The effect of RHA on the rheological properties of SCC in terms of yield stress, plastic viscosity, shear-thickening behavior, and workability retention was reported in the literature. However, such detailed studies were not found on a binary blend with calcined common clays nor a ternary blend of RHA and calcined common clay. The fracture mechanism and durability (in terms of freeze-thaw, carbonation, chemical resistance etc.) of SCC produced with RHA and calcined common clays as a partial replacement for cement needs to be further investigated as well.

Author Contributions: Conceptualization, A.M.; writing—original draft preparation, A.M.; writing—review and editing, A.M., K.-C.T. and R.S.; supervision, K.-C.T. All authors have read and agreed to the published version of the manuscript.

Funding: The first author was funded by the German Academic Exchange Service (DAAD) and the Nigerian Petroleum Technology Development Fund (PTDF): P3140941509075699. We acknowledge financial support by Universität der Bundeswehr München.

Institutional Review Board Statement: Not applicable.

Informed Consent Statement: Not applicable.

Data Availability Statement: Data Sharing is not applicable.

Conflicts of Interest: The authors declare no conflict of interest.

References

1. Patel, M.H.; Dawda, N. Advancement in Self Compacting Concrete: A Review of Last Few Decades. *Int. J. Adv. Eng. Res. Dev.* **2017**, *50–54*, 50–54.
2. Okamura, H. Self-Compacting High-Performance Concrete. *Concr. Int.* **1997**, *19*, 50–54.
3. Okamura, H.; Ozawa, K. Mix-design for self-compacting concrete. *Concr. Libr. JSCE* **1995**, *19*, 107–120.
4. Shi, C.; Wu, Z.; Lv, K.; Wu, L. A review on mixture design methods for self-compacting concrete. *Constr Build. Mater.* **2015**, *84*, 387–398. [CrossRef]
5. Su, N.; Hsu, K.C.; Chai, H.W. A simple mix design method for self-compacting concrete. *Cem. Concr. Res.* **2001**, *31*, 1799–1807. [CrossRef]
6. Liu, M. Wider Application of Additions in Self-Compacting Concrete. Ph.D. Thesis, University College London, London, UK, 2009; p. 392.
7. Ouchi, M.; Hibino, M.; Okamura, H. Effect of superplasticizer on self-compactability of fresh concrete. *Transp Res. Rec* **1997**, *1574*, 37–40. [CrossRef]
8. Şahmaran, M.; Christianto, H.A.; Yaman, I.O. The effect of chemical admixtures and mineral additives on the properties of self-compacting mortars. *Cem. Concr. Compos.* **2006**, *28*, 432–440. [CrossRef]
9. Leemann, A.; Winnefeld, F. The effect of viscosity modifying agents on mortar and concrete. *Cem. Concr. Compos.* **2007**, *29*, 341–349. [CrossRef]
10. Memon, S.A.; Shaikh, M.A.; Akbar, H. Utilization of Rice Husk Ash as viscosity modifying agent in Self Compacting Concrete. *Constr Build. Mater.* **2011**, *25*, 1044–1048. [CrossRef]
11. Sari, M.; Prat, E.; Labastire, J.F. High strength self-compacting concrete original solutions associating organic and inorganic admixtures. *Cem. Concr. Res.* **1999**, *29*, 813–818. [CrossRef]
12. Leung, H.Y.; Kim, J.; Nadeem, A.; Jaganathan, J.; Anwar, M.P. Sorptivity of self-compacting concrete containing fly ash and silica fume. *Constr Build. Mater.* **2016**, *113*, 369–375. [CrossRef]
13. Zhu, W.; Sonebi, M.; Bartos, P.J.M. Bond and interfacial properties of reinforcement in self-compacting concrete. *Mater. Struct. /Mater. Et Constr.* **2004**, *37*, 442–448. [CrossRef]
14. Uysal, M.; Sumer, M. Performance of self-compacting concrete containing different mineral admixtures. *Constr Build. Mater.* **2011**, *25*, 4112–4120. [CrossRef]
15. Ramanathan, P.; Baskar, I.; Muthupriya, P.; Venkatasubramani, R. Performance of self-compacting concrete containing different mineral admixtures. *KSCE J. Civ. Eng.* **2013**, *17*, 465–472. [CrossRef]

16. Van Der Vurst, F.; Grünewald, S.; Feys, D.; Lesage, K.; Vandewalle, L.; Vantomme, J.; De Schutter, G. Effect of the mix design on the robustness of fresh self-compacting concrete. *Cem. Concr. Compos.* **2017**, *82*, 190–201. [CrossRef]
17. Rigueira, J.W.; Garciá-Taengua, E.; Serna-Ros, P. Self-consolidating concrete robustness in continuous production regarding fresh and hardened state properties. *ACI Mater. J.* **2009**, *106*, 301–307. [CrossRef]
18. Westerholm, M.; Lagerblad, B.; Silfwerbrand, J.; Forssberg, E. Influence of fine aggregate characteristics on the rheological properties of mortars. *Cem. Concr. Compos.* **2008**, *30*, 274–282. [CrossRef]
19. Nunes, S.; Oliveira, P.M.; Coutinho, J.S.; Figueiras, J. Rheological characterization of SCC mortars and pastes with changes induced by cement delivery. *Cem. Concr. Compos.* **2011**, *33*, 103–115. [CrossRef]
20. Feys, D.; De Schutter, G.; Khayat, K.H.; Verhoeven, R. Changes in rheology of self-consolidating concrete induced by pumping. *Mater. Struct./Mater. Constr.* **2016**, *49*, 4657–4677. [CrossRef]
21. Schmidt, W. SCC for Sub-Saharan Africa Based on Local Raw Materials–Material Development, Optimisation, and Application Concept. In Proceedings of the International Conference on Rheology and Processing of Construction Materials—International Symposium on Self-Compacting Concrete, Dresden, Germany, 8–11 September 2019; pp. 60–67. [CrossRef]
22. Barkat, A.; Kenai, S.; Menadi, B.; Kadri, E.; Soualhi, H. Effects of local metakaolin addition on rheological and mechanical performance of self-compacting limestone cement concrete. *J. Adhes. Sci. Technol.* **2019**, *33*, 963–985. [CrossRef]
23. Ozawa, K.; Maekawa, K.; Okamura, H. Development of High Performance Concrete. *J. Fac. Eng. Univ. Tokyo B* **1992**, *41*, 381–439.
24. Brouwers, H.J.H.; Radix, H.J. Self-compacting concrete: Theoretical and experimental study. *Cem. Concr. Res.* **2005**, *35*, 2116–2136. [CrossRef]
25. Rozière, E.; Granger, S.; Turcry, P.; Loukili, A. Influence of paste volume on shrinkage cracking and fracture properties of self-compacting concrete. *Cem. Concr. Compos.* **2007**, *29*, 626–636. [CrossRef]
26. Bouzoubaâ, N.; Lachemi, M. Self-compacting concrete incorporating high volumes of class F fly ash: Preliminary results. *Cem. Concr. Res.* **2001**, *31*, 413–420. [CrossRef]
27. Yazici, H. The effect of silica fume and high-volume Class C fly ash on mechanical properties, chloride penetration and freeze-thaw resistance of self-compacting concrete. *Constr Build. Mater.* **2008**, *22*, 456–462. [CrossRef]
28. Gesoğlu, M. Influence of steam curing on the properties of concretes incorporating metakaolin and silica fume. *Mater. Struct* **2009**, *43*, 1123–1134. [CrossRef]
29. Saak, A.W.; Jennings, H.M.; Shah, S.P. New Methodology for Designing Self-Compacting Concrete. *ACI Mater. J.* **2001**, *98*, 429–439. [CrossRef]
30. Kannan, V. Relationship between ultrasonic pulse velocity and compressive strength of self compacting concrete incorporate rice husk ash and metakaolin. *Asian J. Civ. Eng.* **2015**, *16*, 1077–1088.
31. Chopra, D.; Siddique, R.; Kunal. Strength, permeability and microstructure of self-compacting concrete containing rice husk ash. *Biosyst. Eng.* **2015**, *130*, 72–80. [CrossRef]
32. Siddique, R.; Khan, M.I. *Supplementary Cementing Materials*; Springer: Berlin/Heidelberg, Germany, 2011; p. 287, ISBN 978-3-642-17865-8. [CrossRef]
33. Güneyisi, E.; Gesoğlu, M.; Özbay, E. Strength and drying shrinkage properties of self-compacting concretes incorporating multi-system blended mineral admixtures. *Constr Build. Mater.* **2010**, *24*, 1878–1887. [CrossRef]
34. Madandoust, R.; Mousavi, S.Y. Fresh and hardened properties of self-compacting concrete containing metakaolin. *Constr Build. Mater.* **2012**, *35*, 752–760. [CrossRef]
35. Miller, S.A.; John, V.M.; Pacca, S.A.; Horvath, A. Carbon dioxide reduction potential in the global cement industry by 2050. *Cem. Concr. Res.* **2018**, *114*, 115–124. [CrossRef]
36. Schmidt, W.; Commeh, M.; Olonade, K.; Schiewer, G.L.; Dodoo-Arhin, D.; Dauda, R.; Fataei, S.; Tawiah, A.T.; Mohamed, F.; Thiedeitz, M.; et al. Sustainable circular value chains: From rural waste to feasible urban construction materials solutions. *Dev. Built Environ.* **2021**, *6*, 100047. [CrossRef]
37. Msinjili, N.S.; Schmidt, W.; Rogge, A.; Kühne, H.-C. Optimising available resources for production of good concrete prop. In Proceedings of the 2nd International Conference on Advances in Cement and Concrete Technology in Africa, Dar es Salaam, Tanzania, 27–29 January 2016; pp. 323–331.
38. Ede, A.N.; Olofinnade, O.M.; Joshua, O.; Nduka, D.O.; Oshogbunu, O.A. Influence of bamboo fiber and limestone powder on the properties of self-compacting concrete. *Cogent Eng.* **2020**, *7*, 1721410. [CrossRef]
39. Adeniyi, F.I.; Ogundiran, M.B.; Hemalatha, T.; Hanumantrai, B.B. Characterization of raw and thermally treated Nigerian kaolinite-containing clays using instrumental techniques. *SN Appl. Sci.* **2020**, *2*, 821. [CrossRef]
40. Akindahunsi, A.A.; Avet, F.; Scrivener, K. The Influence of some calcined clays from Nigeria as clinker substitute in cementitious systems. *Case Stud. Constr. Mater.* **2020**, *13*, e00443. [CrossRef]
41. Bediako, M.; Purohit, S.S.; Kevern, J.T. Investigation into Ghanaian Calcined Clay as Supplementary Cementitious Material. *ACI Mater. J.* **2017**, *114*, 889–896. [CrossRef]
42. Aprianti, E.; Shafigh, P.; Bahri, S.; Farahani, J.N. Supplementary cementitious materials origin from agricultural wastes–A review. *Constr Build. Mater.* **2015**, *74*, 176–187. [CrossRef]
43. Tulashie, S.K.; Ebo, P.; Ansah, J.K.; Mensah, D. Production of Portland pozzolana cement from rice husk ash. *Materialia* **2021**, *16*, 101048. [CrossRef]

44. Nuruddin, M.F.; Chang, K.Y.; Azmee, N.M. Workability and compressive strength of ductile self compacting concrete (DSCC) with various cement replacement materials. *Constr Build. Mater.* **2014**, *55*, 153–157. [CrossRef]
45. Fernandez, R.; Martirena, F.; Scrivener, K.L. The origin of the pozzolanic activity of calcined clay minerals: A comparison between kaolinite, illite and montmorillonite. *Cem. Concr. Res.* **2011**, *41*, 113–122. [CrossRef]
46. Ling, G.; Shui, Z.; Sun, T.; Gao, X.; Wang, Y.; Sun, Y.; Wang, G.; Li, Z. Rheological behavior and microstructure characteristics of SCC incorporating metakaolin and silica fume. *Materials* **2018**, *11*, 2576. [CrossRef]
47. Garg, N.; Skibsted, J. Pozzolanic reactivity of a calcined interstratified illite/smectite (70/30) clay. *Cem. Concr. Res.* **2016**, *79*, 101–111. [CrossRef]
48. Taylor-Lange, S.C.; Lamon, E.L.; Riding, K.A.; Juenger, M.C.G. Calcined kaolinite–bentonite clay blends as supplementary cementitious materials. *Appl Clay Sci* **2015**, *108*, 84–93. [CrossRef]
49. Taylor-Lange, S.C.; Rajabali, F.; Holsomback, N.A.; Riding, K.; Juenger, M.C.G. The effect of zinc oxide additions on the performance of calcined sodium montmorillonite and illite shale supplementary cementitious materials. *Cem. Concr. Compos.* **2014**, *53*, 127–135. [CrossRef]
50. Zhou, D.; Wang, R.; Tyrer, M.; Wong, H.; Cheeseman, C. Sustainable infrastructure development through use of calcined excavated waste clay as a supplementary cementitious material. *J. Clean. Prod.* **2017**, *168*, 1180–1192. [CrossRef]
51. Toledo Filho, R.D.; Gonçalves, J.P.; Americano, B.B.; Fairbairn, E.M.R. Potential for use of crushed waste calcined-clay brick as a supplementary cementitious material in Brazil. *Cem. Concr. Res.* **2007**, *37*, 1357–1365. [CrossRef]
52. Mohammed, S. Processing, effect and reactivity assessment of artificial pozzolans obtained from clays and clay wastes: A review. *Constr Build. Mater.* **2017**, *140*, 10–19. [CrossRef]
53. Kavitha, O.R.; Shanthi, V.M. Effect of metakaolin on the properties of self compacting concrete. *Intl. J. Earth Sci. Eng.* **2015**, *8*, 1454–1459.
54. Badogiannis, E.; Tsivilis, S. Exploitation of poor Greek kaolins: Durability of metakaolin concrete. *Cem. Concr. Compos.* **2009**, *31*, 128–133. [CrossRef]
55. Güneyisi, E.; Gesoğlu, M. Properties of self-compacting mortars with binary and ternary cementitious blends of fly ash and metakaolin. *Mater. Struct. Mater. Constr.* **2008**, *41*, 1519–1531. [CrossRef]
56. Dadsetan, S.; Bai, J. Mechanical and microstructural properties of self-compacting concrete blended with metakaolin, ground granulated blast-furnace slag and fly ash. *Constr Build. Mater.* **2017**, *146*, 658–667. [CrossRef]
57. Beuntner, N.; Kustermann, A.; Thienel, K.-C. Pozzolanic potential of calcined clay in high-performance concrete. In Proceedings of the International Conference on Sustainable Materials, Systems and Structures–SMSS 2019 New Generation of Construction Materials, Rovinj, Croatia, 20–22 March 2019; pp. 470–477.
58. Neißer-Deiters, A.; Scherb, S.; Beuntner, N.; Thienel, K.-C. Influence of the calcination temperature on the properties of a mica mineral as a suitability study for the use as SCM. *Appl. Clay Sci.* **2019**, *179*, 105168. [CrossRef]
59. Sposito, R.; Schmid, M.; Beuntner, N.; Scherb, S.; Plank, J.; Thienel, K.-C. Early hydration behavior of blended cementitious systems containing calcined clays and superplasticizer. In Proceedings of the 15th International Congress on the Chemistry of Cement, Prague, Czech Republic, 16–20 September 2019; p. 10.
60. Maier, M.; Beuntner, N.; Thienel, K.-C. An approach for the evaluation of local raw material potential for calcined clay as SCM, based on geological and mineralogical data: Examples from German clay deposits. In *Calcined Clays for Sustainable Concrete–Proceedings of the 3rd International Conference on Calcined Clays for Sustainable Concrete, New Dehli, India*; Bishnoi, S., Ed.; Springer: Singapore, 2020; pp. 37–47, ISBN 978-981-15-2806-4. [CrossRef]
61. Gill, A.S.; Siddique, R. Strength and micro-structural properties of self-compacting concrete containing metakaolin and rice husk ash. *Constr. Build. Mater.* **2017**, *157*, 51–64. [CrossRef]
62. Le, H.T.; Kraus, M.; Siewert, K.; Ludwig, H.M. Effect of macro-mesoporous rice husk ash on rheological properties of mortar formulated from self-compacting high performance concrete. *Constr. Build. Mater.* **2015**, *80*, 225–235. [CrossRef]
63. Xu, W.; Lo, T.Y.; Memon, S.A. Microstructure and reactivity of rich husk ash. *Constr. Build. Mater.* **2012**, *29*, 541–547. [CrossRef]
64. Ganesan, K.; Rajagopal, K.; Thangavel, K. Rice husk ash blended cement: Assessment of optimal level of replacement for strength and permeability properties of concrete. *Constr. Build. Mater.* **2008**, *22*, 1675–1683. [CrossRef]
65. *Tragwerke aus Beton, Stahlbeton und Spannbeton–Teil 2: Beton–Festlegung, Eigenschaften, Herstellung und Konformität–Anwendungsregeln zu DIN EN 206-1 (Concrete, Reinforced and Prestressed Concrete Structures–Part 2: Concrete–Specification, Properties, Production and Conformity–Application Rules for DIN EN 206-1)*; DIN 1045-2; Beuth-Verlag: Berlin, Germany, 2008; p. 62.
66. Zhang, M.H.; Malhotra, V.M. High-Performance Concrete Incorporating Rice Husk Ash as a Supplementary Cementing Material. *ACI Mater. J.* **1996**, *93*, 629–636. [CrossRef]
67. He, J.; Jie, Y.; Zhang, J.; Yu, Y.; Zhang, G. Synthesis and characterization of red mud and rice husk ash-based geopolymer composites. *Cem. Concr. Compos.* **2013**, *37*, 108–118. [CrossRef]
68. Van, V.T.A.; Rößler, C.; Bui, D.D.; Ludwig, H.M. Mesoporous structure and pozzolanic reactivity of rice husk ash in cementitious system. *Constr. Build. Mater.* **2013**, *43*, 208–216. [CrossRef]
69. Mohseni, E.; Naseri, F.; Amjadi, R.; Khotbehsara, M.M.; Ranjbar, M.M. Microstructure and durability properties of cement mortars containing nano-TiO2 and rice husk ash. *Constr Build. Mater.* **2016**, *114*, 656–664. [CrossRef]
70. Le, H.T.; Müller, M.; Siewert, K.; Ludwig, H.M. The mix design for self-compacting high performance concrete containing various mineral admixtures. *Mater. Des.* **2015**, *72*, 51–62. [CrossRef]

71. Chao-Lung, H.; Anh-Tuan, B.L.; Chun-Tsun, C. Effect of rice husk ash on the strength and durability characteristics of concrete. *Constr. Build. Mater.* **2011**, *25*, 3768–3772. [CrossRef]
72. Salmang, H.; Scholze, H. *Keramik*, 7th ed.; Telle, R., Ed.; Springer: Berlin/Heidelberg, Germany, 2007; p. 1165, ISBN 978-3-540-63273-3.
73. Okrusch, M.; Matthes, S. *Mineralogie—Eine Einführung in die Spezielle Mineralogie, Petrologie und Lagestättenkunde*, 8th ed.; Springer Spektrum: Berlin/Heidelberg, Germany, 2010; Volume 728, ISBN 978-3-642-34659-0. [CrossRef]
74. Danner, T. Reactivity of Calcined Clays. Ph.D. Thesis, Norwegian University of Science and Technology (NTNU), Trondheim, Norway, 2013; p. 229.
75. Beuntner, N. Zur Eignung und Wirkungsweise calcinierter Tone als reaktive Bindemittelkomponente in Zement (On the suitability And Mode of Action of Calcined Clays as Reactive Binder Components in Cement). Doctoral Thesis, Universität der Bundeswehr München, Neubiberg, Germany, 2017; p. 207. Available online: https://athene-forschung.unibw.de/121217 (accessed on 19 October 2021).
76. Kannan, V. Strength and durability performance of self compacting concrete containing self-combusted rice husk ash and metakaolin. *Constr. Build. Mater.* **2018**, *160*, 169–179. [CrossRef]
77. Zhang, M.H.; Lastra, R.; Malhotra, V.M. Rice-husk ash paste and concrete: Some aspects of hydration and the microstructure of the interfacial zone between the aggregate and paste. *Cem. Concr. Res.* **1996**, *26*, 963–977. [CrossRef]
78. Dinakar, P.; Manu, S.N. Concrete mix design for high strength self-compacting concrete using metakaolin. *Mater. Des.* **2014**, *60*, 661–668. [CrossRef]
79. Cassagnabère, F.; Diederich, P.; Mouret, M.; Escadeillas, G.; Lachemi, M. Impact of metakaolin characteristics on the rheological properties of mortar in the fresh state. *Cem. Concr. Compos.* **2013**, *37*, 95–107. [CrossRef]
80. Aggarwal, P.; Siddique, R.; Aggarwal, Y.; Gupta, S.M. Self-compacting concrete—Procedure for mix design. *Leonardo J. Pract. Technol.* **2008**, *7*, 15–24.
81. Nepomuceno, M.C.S.; Pereira-De-Oliveira, L.A.; Lopes, S.M.R. Methodology for the mix design of self-compacting concrete using different mineral additions in binary blends of powders. *Constr. Build. Mater.* **2014**, *64*, 82–94. [CrossRef]
82. Khaleel, O.R.; Al-Mishhadani, S.A.; Abdul Razak, H. The Effect of Coarse Aggregate on Fresh and Hardened Properties of Self-Compacting Concrete (SCC). *Procedia Eng.* **2011**, *14*, 805–813. [CrossRef]
83. Sedran, T.; de Larrard, F.; Hourst, F.; Contamines, C. Mix Design of Self-Compacting Concrete (SCC). In *Production Methods and Workability of Concrete*, 1st ed.; Bartos, P.J.M., Cleland, D.J., Marrs, D.L., Eds.; CRC Press: London, UK, 1996; p. 12, ISBN 9780429077623. [CrossRef]
84. Petersson, O.; Billberg, P.; Van, B.K. A Model for Self-Compacting Concrete. In *Production Methods and Workability of Concrete*, 1st ed.; Bartos, P.J.M., Cleland, D.J., Marrs, D.L., Eds.; CRC Press: London, UK, 1996; p. 10, ISBN 9780429077623. [CrossRef]
85. Feys, D.; Verhoeven, R.; De Schutter, G. Fresh self compacting concrete, a shear thickening material. *Cem. Concr. Res.* **2008**, *38*, 920–929. [CrossRef]
86. Wu, Q.; An, X. Development of a mix design method for SCC based on the rheological characteristics of paste. *Constr Build. Mater.* **2014**, *53*, 642–651. [CrossRef]
87. Abo Dhaheer, M.S.; Al-Rubaye, M.M.; Alyhya, W.S.; Karihaloo, B.L.; Kulasegaram, S. Proportioning of self–compacting concrete mixes based on target plastic viscosity and compressive strength: Part I—mix design procedure. *J. Sustain. Cem. Based Mater.* **2016**, *5*, 199–216. [CrossRef]
88. Li, P.; Ran, J.; Nie, D.; Zhang, W. Improvement of mix design method based on paste rheological threshold theory for self-compacting concrete using different mineral additions in ternary blends of powders. *Constr. Build. Mater.* **2021**, *276*. [CrossRef]
89. Zuo, W.; Liu, J.; Tian, Q.; Xu, W.; She, W.; Feng, P.; Miao, C. Optimum design of low-binder Self-Compacting Concrete based on particle packing theories. *Constr. Build. Mater.* **2018**, *163*, 938–948. [CrossRef]
90. Kheder, G.F.; Al Jadiri, R.S. New method for proportioning self-consolidating concrete based on compressive strength requirements. *ACI Mater. J.* **2010**, *107*, 490–497. [CrossRef]
91. Dinakar, P. Design of self-compacting concrete with fly ash. *Mag. Concr. Res.* **2012**, *64*, 401–409. [CrossRef]
92. Xie, T.; Mohamad Ali, M.S.; Elchalakani, M.; Visintin, P. Modelling fresh and hardened properties of self-compacting concrete containing supplementary cementitious materials using reactive moduli. *Constr. Build. Mater.* **2021**, *272*, 121954. [CrossRef]
93. Kannan, V.; Ganesan, K. Synergic Effect of Pozzolanic Materials on the Structural Properties of Self-Compacting Concrete. *Arab. J. Sci. Eng.* **2014**, *39*, 2601–2609. [CrossRef]
94. Safiuddin, M.; West, J.S.; Soudki, K.A. Flowing ability of the binder pastes formulated from self-compacting concretes incorporating rice husk ash. *Kuwait J. Sci. Eng.* **2011**, *38*, 19–36. [CrossRef]
95. Sfikas, I.P.; Badogiannis, E.G.; Trezos, K.G. Rheology and mechanical characteristics of self-compacting concrete mixtures containing metakaolin. *Constr Build. Mater.* **2014**, *64*, 121–129. [CrossRef]
96. Okamura, H.; Ouchi, M. Self-Compacting Concrete. *J. Adv. Concr. Technol.* **2003**, *1*, 5–15. [CrossRef]
97. EFNARC. In *The European Guidelines for Self Compacting Concrete*; European Federation of Specialist Construction Chemicals and Concrete Systems: Farnham, UK, 2005.
98. *Beton—Festlegung, Eigenschaften, Herstellung und Konformität (Concrete—Specification, Performance, Production and Conformity)*; DIN-EN-206.; Beuth Verlag GmbH: Berlin, Germany, 2017; p. 98.

99. *Standard Test Method for Rapid Assessment of Static Segregation Resistance of Self-Consolidating Concrete Using Penetration Test*; ASTM C1712—20; ASTM International: West Conshohocken, PA, USA, 2020.
100. Wallevik, O.H.; Wallevik, J.E. Rheology as a tool in concrete science: The use of rheographs and workability boxes. *Cem. Concr. Res.* **2011**, *41*, 1279–1288. [CrossRef]
101. Diamantonis, N.; Marinos, I.; Katsiotis, M.S.; Sakellariou, A.; Papathanasiou, A.; Kaloidas, V.; Katsioti, M. Investigations about the influence of fine additives on the viscosity of cement paste for self-compacting concrete. *Constr Build. Mater.* **2010**, *24*, 1518–1522. [CrossRef]
102. Ben Aicha, M.; Burtschell, Y.; Alaoui, A.H.; El Harrouni, K.; Jalbaud, O. Correlation between bleeding and rheological characteristics of self-compacting concrete. *J. Mater. Civ. Eng.* **2017**, *29*. [CrossRef]
103. Saleh Ahari, R.; Kemal Erdem, T.; Ramyar, K. Effect of various supplementary cementitious materials on rheological properties of self-consolidating concrete. *Constr Build. Mater.* **2015**, *75*, 89–98. [CrossRef]
104. Benaicha, M.; Hafidi Alaoui, A.; Jalbaud, O.; Burtschell, Y. Dosage effect of superplasticizer on self-compacting concrete: Correlation between rheology and strength. *J. Mater. Res. Technol.* **2019**, *8*, 2063–2069. [CrossRef]
105. Roussel, N. The LCPC BOX: A cheap and simple technique for yield stress measurements of SCC. *Mater. Struct. /Mater. Et Constr.* **2007**, *40*, 889–896. [CrossRef]
106. Rahman, M.E.; Muntohar, A.S.; Pakrashi, V.; Nagaratnam, B.H.; Sujan, D. Self compacting concrete from uncontrolled burning of rice husk and blended fine aggregate. *Mater. Des.* **2014**, *55*, 410–415. [CrossRef]
107. Vivek, S.S.; Dhinakaran, G. Durability characteristics of binary blend high strength SCC. *Constr Build. Mater.* **2017**, *146*, 1–8. [CrossRef]
108. Le, H.T.; Ludwig, H.M. Effect of rice husk ash and other mineral admixtures on properties of self-compacting high performance concrete. *Mater. Des.* **2016**, *89*, 156–166. [CrossRef]
109. Özcan, F.; Kaymak, H. Utilization of Metakaolin and Calcite: Working Reversely in Workability Aspect—As Mineral Admixture in Self-Compacting Concrete. *Adv. Civ. Eng.* **2018**, *2018*, 12. [CrossRef]
110. Kannan, V.; Ganesan, K. Chloride and chemical resistance of self compacting concrete containing rice husk ash and metakaolin. *Constr. Build. Mater.* **2014**, *51*, 225–234. [CrossRef]
111. Sua-iam, G.; Sokrai, P.; Makul, N. Novel ternary blends of Type 1 Portland cement, residual rice husk ash, and limestone powder to improve the properties of self-compacting concrete. *Constr. Build. Mater.* **2016**, *125*, 1028–1034. [CrossRef]
112. International Atomic Energy Agency. *Guidebook on Non-Destructive Testing of Concrete Structures—Training Course Series No. 17*; IAEA–TCS–17; International Atomic Energy Agency: Vienna, Austria, 2002; p. 242.
113. Molaei Raisi, E.; Vaseghi Amiri, J.; Davoodi, M.R. Influence of rice husk ash on the fracture characteristics and brittleness of self-compacting concrete. *Eng. Fract. Mech.* **2018**, *199*, 595–608. [CrossRef]
114. Barluenga, G.; Puentes, J.; Palomar, I. Early age monitoring of self-compacting concrete with mineral additions. *Constr. Build. Mater.* **2015**, *77*, 66–73. [CrossRef]
115. Ahmad, S.; Adekunle, S.K. Utilization of Limestone Powder and Metakaolin as Mineral Fillers in High-Performance Self-Compacting Concrete. In *Calcined Clays for Sustainable Concrete—Proceedings of the 3rd International Conference on Calcined Clays for Sustainable Concrete*; Bishnoi, S., Ed.; Springer: Cham, Germany, 2020; Volume 25, pp. 701–712, ISBN 2211-0844. [CrossRef]
116. Molaei Raisi, E.; Vaseghi Amiri, J.; Davoodi, M.R. Mechanical performance of self-compacting concrete incorporating rice husk ash. *Constr. Build. Mater.* **2018**, *177*, 148–157. [CrossRef]
117. He, Z.H.; Li, L.Y.; Du, S.G. Creep analysis of concrete containing rice husk ash. *Cem. Concr. Compos.* **2017**, *80*, 190–199. [CrossRef]
118. Ramezanianpour, A.A.; Mahdikhani, M.; Ahmadibeni, G. The effect of rice husk ash on mechanical properties and durability of sustainable concretes. *Int. J. Civ. Eng.* **2009**, *7*, 83–91.
119. Megat Johari, M.A.; Brooks, J.J.; Kabir, S.; Rivard, P. Influence of supplementary cementitious materials on engineering properties of high strength concrete. *Constr. Build. Mater.* **2011**, *25*, 2639–2648. [CrossRef]
120. Niknezhad, D.; Kamali-Bernard, S.; Mesbah, H.-A. Self-Compacting Concretes with Supplementary Cementitious Materials: Shrinkage and Cracking Tendency. *J. Mater. Civ. Eng.* **2017**, *29*. [CrossRef]
121. Momtazi, A.S.; Ranjbar, M.M.; Balalaei, F.; Nemati, R. The effect of Iran's metakaolin in enhancing the concrete compressive strength. In Proceedings of the International Conference on Sustainable Construction Materials and Technologies, Coventry, UK, 11–13 June 2007; pp. 116–122.
122. Sadrmomtazi, A.; Barzegar, A. Assessment of the effect of nano-SiO_2 on physical and mechanical properties of self-compacting concrete containing rice husk ash. In Proceedings of the Second International Conference on Sustainable Construction Materials and Technologies, Università Politecnica delle Marche, Ancona, Italy, 28—30 June 2010.
123. Habeeb, G.A.; Mahmud, H.B. Study on Properties of Rice Husk Ash and Its Use as Cement Replacement Material. *Mater. Res.* **2010**, *13*, 185–190. [CrossRef]
124. Shaaban, M. Properties of concrete with binary binder system of calcined dolomite powder and rice husk ash. *Heliyon* **2021**, *7*, e06311. [CrossRef] [PubMed]
125. de Sensale, G.R.; Ribeiro, A.B.; Gonçalves, A. Effects of RHA on autogenous shrinkage of Portland cement pastes. *Cem. Concr. Compos.* **2008**, *30*, 892–897. [CrossRef]
126. Amin, M.; Abdelsalam, B.A. Efficiency of rice husk ash and fly ash as reactivity materials in sustainable concrete. *Sustain. Envir. Res.* **2019**, *1*, 1–10. [CrossRef]

127. Wild, S.; Khatib, J.M.; Roose, L.J. Chemical shrinkage and autogenous shrinkage of Portland cement—metakaolin pastes. *Adv. Cem Res.* **1998**, *10*, 109–119. [CrossRef]
128. Brooks, J.J.; Megat Johari, M.A. Effect of metakaolin on creep and shrinkage of concrete. *Cem. Concr. Compos.* **2001**, *23*, 495–502. [CrossRef]
129. Gleize, P.J.P.; Cyr, M.; Escadeillas, G. Effects of metakaolin on autogenous shrinkage of cement pastes. *Cem. Concr. Compos.* **2007**, *29*, 80–87. [CrossRef]
130. Güneyisi, E.; Gesoğlu, M.; Mermerdaş, K. Improving strength, drying shrinkage, and pore structure of concrete using metakaolin. *Mater. Struct.* **2008**, *41*, 937–949. [CrossRef]
131. Poon, C.S.; Lam, L.; Kou, S.C.; Wong, Y.L.; Wong, R. Rate of pozzolanic reaction of metakaolin in high-performance cement pastes. *Cem. Concr. Res.* **2001**, *31*, 1301–1306. [CrossRef]
132. Nesvetaev, G.V.; Koryanova, Y.I.; Kolleganov, A.V. E-Modulus and Creep Coefficient of Self-Compacting Concretes and Concretes with some Mineral Additives. *Solid State Phenom.* **2018**, *284*, 963–969. [CrossRef]
133. CEB-FIP. *Model. Code 90*; ICE Publishing, Thomas Telford Services Ltd.: London, UK, 1991; ISBN 978-0-7277-1696-5. [CrossRef]
134. Gholhaki, M.; Kheyroddin, A.; Hajforoush, M.; Kazemi, M. An investigation on the fresh and hardened properties of self-compacting concrete incorporating magnetic water with various pozzolanic materials. *Constr Build. Mater.* **2018**, *158*, 173–180. [CrossRef]
135. Gill, A.S.; Siddique, R. Durability properties of self-compacting concrete incorporating metakaolin and rice husk ash. *Constr Build. Mater.* **2018**, *176*, 323–332. [CrossRef]
136. Fediuk, R.S.; Lesovik, V.S.; Svintsov, A.P.; Mochalov, A.V.; Kulichkov, S.V.; Stoyushko, N.Y.; Gladkova, N.A.; Timokhin, R.A. Self-compacting concrete using pretreatmented rice husk ash. *Mag. Civ. Eng.* **2018**, *79*, 66–76. [CrossRef]
137. Badogiannis, E.G.; Sfikas, I.P.; Voukia, D.V.; Trezos, K.G.; Tsivilis, S.G. Durability of Metakaolin Self-Compacting Concrete. *Constr Build. Mater.* **2015**, *82*, 133–141. [CrossRef]
138. *Standard Test Method for Electrical Indication of Concrete's Ability to Resist Chloride Ion Penetration*; ASTM C1202-19; ASTM International: West Conshohocken, PA, USA, 2019; p. 8.
139. *Prüfung von Festbeton—Teil 18: Bestimmung des Chloridmigrationskoeffizienten (Testing Hardened Concrete Part 18: Determination of the Chloride Migration Coefficient)*; DIN EN 12390-18; Beuth-Verlag: Berlin, Germany, 2021; p. 20.
140. Rukzon, S.; Chindaprasirt, P. Strength, chloride penetration and corrosion resistance of ternary blends of *portland cement* self-compacting concrete containing bagasse ash and rice husk-bark ash. *Chiang Mai J. Sci.* **2018**, *45*, 1863–1874.
141. Badogiannis, E.; Kakali, G.; Dimopoulou, G.; Chaniotakis, E.; Tsivilis, S. Metakaolin as a main cement constituent. Exploitation of poor Greek kaolins. *Cem. Concr. Compos.* **2005**, *27*, 197–203. [CrossRef]
142. Kannan, V.; Ganesan, K. Effect of tricalcium aluminate on durability properties of self-compacting concrete incorporating rice husk ash and metakaolin. *J. Mater. Civ. Eng.* **2016**, *28*. [CrossRef]
143. Thomas, R.J.; Lezama, D.; Peethamparan, S. On drying shrinkage in alkali-activated concrete: Improving dimensional stability by aging or heat-curing. *Cem. Concr. Res.* **2017**, *91*, 13–23. [CrossRef]
144. Gastaldini, A.L.G.; Isaia, G.C.; Gomes, N.S.; Sperb, J.E.K. Chloride penetration and carbonation in concrete with rice husk ash and chemical activators. *Cem. Concr. Compos.* **2007**, *29*, 176–180. [CrossRef]
145. Praveenkumar, T.R.; Vijayalakshmi, M.M. Microstructural properties of nano-rice husk ash concrete. *Nanotechnol. Environ. Eng.* **2019**, *4*. [CrossRef]
146. Cascudo, O.; Pires, P.; Carasek, H.; de Castro, A.; Lopes, A. Evaluation of the pore solution of concretes with mineral additions subjected to 14 years of natural carbonation. *Cem. Concr. Compos.* **2021**, *115*, 103858. [CrossRef]
147. Sugita, S.; Yu, Q.; Shoya, M.; Tsukinaga, Y.; Isojima, Y. The Resistance of Rice Husk Ash Concrete to Carbonation, Acid Attack and Chloride Ion Penetration. In Proceedings of the ACI SP 172-3rd ACI International Conference: High-Performance Design and Materials and Recent Advances in Concrete Technology", Kuala Lumpur, Malaysia, 12 January 1999; pp. 29–44. [CrossRef]
148. Chatveera, B.; Lertwattanaruk, P. Durability of conventional concretes containing black rice husk ash. *J. Env. Manag.* **2011**, *92*, 59–66. [CrossRef]
149. Antiohos, S.K.; Tapali, J.G.; Zervaki, M.; Sousa-Coutinho, J.; Tsimas, S.; Papadakis, V.G. Low embodied energy cement containing untreated RHA: A strength development and durability study. *Constr. Build. Mater.* **2013**, *49*, 455–463. [CrossRef]
150. Lenka, S.; Panda, K.C. Effect of metakaolin on the properties of conventional and self compacting concrete. *Adv. Concr. Constr.* **2017**, *5*, 31–48. [CrossRef]
151. Bai, J.; Wild, S.; Sabir, B.B. Sorptivity and strength of air-cured and water-cured PC–PFA–MK concrete and the influence of binder composition on carbonation depth. *Cem. Concr. Res.* **2002**, *32*, 1813–1821. [CrossRef]
152. Vejmelková, E.; Pavlíková, M.; Keppert, M.; Keršner, Z.; Rovnaníková, P.; Ondráček, M.; Sedlmajer, M.; Černý, R. High performance concrete with Czech metakaolin: Experimental analysis of strength, toughness and durability characteristics. *Constr. Build. Mater.* **2010**, *24*, 1404–1411. [CrossRef]
153. Mirgozar Langaroudi, M.A.; Mohammadi, Y. Effect of nano-clay on the freeze–thaw resistance of self-compacting concrete containing mineral admixtures. *Eur. J. Environ. Civ. Eng.* **2019**, *1–20*. [CrossRef]
154. Park, C.; Salas, A.; Chung, C.W.; Lee, C.J. Freeze-thaw resistance of concrete using acid-leached rice husk ash. *KSCE J. Civ. Eng.* **2014**, *18*, 1133–1139. [CrossRef]

155. Dhinakaran, G.; Sreekanth, B. Physical, mechanical, and durability properties of ternary blend concrete. *Sci. Iran.* **2018**, *25*, 2440–2450. [CrossRef]
156. Duan, P.; Shui, Z.; Chen, W.; Shen, C. Enhancing microstructure and durability of concrete from ground granulated blast furnace slag and metakaolin as cement replacement materials. *J. Mater. Res. Technol.* **2013**, *2*, 52–59. [CrossRef]
157. Nas, M.; Kurbetci, S. Durability properties of concrete containing metakaolin. *Adv. Concr. Constr.* **2018**, *6*, 159–175. [CrossRef]
158. Shi, X.; Yang, Z.; Liu, Y.; Cross, D. Strength and corrosion properties of Portland cement mortar and concrete with mineral admixtures. *Constr Build. Mater.* **2011**, *25*, 3245–3256. [CrossRef]
159. Bumanis, G.; Bajare, D.; Locs, J.; Korjakins, A. Alkali-silica reactivity of foam glass granules in structure of lightweight concrete. *Constr Build. Mater.* **2013**, *47*, 274–281. [CrossRef]

8.2 Suitability of Clinker Replacement by a Calcined Common Clay in Self-Consolidating Mortar—Impact on Rheology and Early Age Properties

Reprint

Published in the Journal “MDPI/Minerals” (Special Issue: Blended Cements Incorporating Calcined Clay and Limestone)

Minerals **2022**, *12*(5), 625; https://doi.org/10.3390/min12050625

Authors: Abubakar Muhammad, Karl-Christian Thienel and Ricarda Sposito

minerals

MDPI

Article

Suitability of Clinker Replacement by a Calcined Common Clay in Self-Consolidating Mortar—Impact on Rheology and Early Age Properties

Abubakar Muhammad *, Karl-Christian Thienel and Ricarda Sposito

Institute for Construction Materials, University of the Bundeswehr Munich, 85577 Neubiberg, Germany; christian.thienel@unibw.de (K.-C.T.); ricarda.sposito@unibw.de (R.S.)
* Correspondence: abubakar.muhammad@unibw.de

Abstract: The use of a high amount of calcined clays as cement replacement presents a great challenge in designing self-consolidating concrete. This current attempt evaluates the influence of cement replacement with up to 40 vol.% by a calcined common clay (CC), dominated by 2:1 phyllosilicates in combination with a fixed limestone powder (LP) content on fresh and hardened properties of self-consolidating mortar (SC-M). The fresh properties of SC-M were investigated by mini-slump flow, V-funnel and rotational viscometer measurements. Setting and hardening behavior were observed via dynamic modulus of elasticity and plastic shrinkage. Hydration mechanisms were determined by isothermal calorimetry and thermal analysis. Hardened properties of SC-M were evaluated using compressive strength tests and mercury intrusion porosimetry (MIP). The results revealed a decreased rate of deformability in SC-M when cement is substituted increasingly by CC and a rising superplasticizer (SP) demand, but indicated an improved stability of SC-M even at a higher dosage of SP and hardly any impact on the setting behavior. CC enhanced the precipitation of monocarboaluminate phases and thereby refined the pore size distribution of the binder matrix. SC-M can be produced with up to 40 vol.% CC as cement replacement without having effect on its 28 days mechanical properties.

Keywords: self-consolidating mortar; calcined common clay; mix design; rheology; hydration; setting; hardening; shrinkage; microstructure; porosity; compressive strength

check for updates

Citation: Muhammad, A.; Thienel, K.-C.; Sposito, R. Suitability of Clinker Replacement by a Calcined Common Clay in Self-Consolidating Mortar—Impact on Rheology and Early Age Properties. *Minerals* **2022**, *12*, 625. https://doi.org/10.3390/min12050625

Academic Editor: Franco Zunino

Received: 7 April 2022
Accepted: 11 May 2022
Published: 14 May 2022

1. Introduction

Rapid urbanization and a higher annual population growth rate increases the demand for housing and other concrete-based infrastructures, especially in emerging economies worldwide [1,2]. Concrete remains the most widely used construction material to provide the needed infrastructures [3]. The integrity and ease of handling concrete determines its lifespan and application. Self-consolidating concrete (SCC) is one of the concreting techniques developed to provide durable and self-deformable concrete without the need for external compaction [4,5]. In this concreting technique, the proportion of the coarse aggregate is reduced while the fine aggregate (FA) is increased to ease the rate of deformability of the concrete. Increasing the proportion of fines (powder) or the use of viscosity modifying admixtures can improve segregation resistance in the SCC [4–6]. Consequently, higher amounts of cement in SCC lead to more cement consumption and hence increase the greenhouse gas emissions related to cement production.

Cement production worldwide accounted for about 8% of the world's greenhouse gas emissions [7]. The research trend in the cement industry is currently geared towards establishing the potential of blended cements produced with the use of supplementary cementitious materials (SCMs) as a substitute to cement. Fly ash, ground-granulated blast furnace slag (GGBFS), silica fume, natural pozzolans and heat-treated agro-waste are the most commonly used SCMs as partial substitutes to cement [8–10]. However, there is a

drawback in the use of some of these SCMs as, for instance, fly ash production declined with the reduction in coal combustion. GGBFS is not readily available especially in countries with less industrial development. The use of silica fume in concrete is also limited due to some technical and economic reasons [11].

Limestone powder (LP) is one of the natural SCMs that can be used as a partial replacement to cement, especially for the production of SCC. LP is capable of substituting up to 35 wt.% of clinker without an adverse effect on the 28 days performance of SCC. It is less expensive than cement and its use in SCC was found to reduce the cement interparticle friction, thereby providing some more free mixing water and decreasing the flow resistance [12–14].

LP performs better in the presence of aluminum-rich SCMs, and promotes the reaction of C_3S and the formation of AFm phases (hemi/monocarboaluminate) [15,16]. An effort has recently been directed towards establishing the potentials of blending LP and calcined (mostly kaolinite-rich) clays as partial clinker replacement for the production of concrete in the proportions of 50 wt.% ground clinker, 30 wt.% calcined clay, 15 wt.% LP and 5 wt.% gypsum (LC3-50) [15,16]. The use of calcined kaolinite-rich clays, however, is expensive, as in many countries the price of pure metakaolin is almost two to three times the cost of cement [16]. The suitability of using common clays instead that contain other phyllosilicates and further components has been established recently [17–21] and should be extended to their application in SCC as well.

Unlike the conventional vibrated concrete, SCC has no standardized method for its mix design due to its susceptibility to nuances in material characteristics and other environmental factors. The empirical method was initially adopted in order to produce SCC [4,5]. In this method, the water to powder ratio as well as the dosage of SP are both adjusted to achieve the required degree of deformability, followed by the determination of the volume of FA required to produce self-consolidating mortar (SC-M). Finally, the required volume of coarse aggregate (CA) is determined. Other methods used to achieve self-consolidation include the yield stress and plastic viscosity method (rheometer method) and aggregate packing method [22–24]. Various limits have been set in order to achieve the desired deformability, viscosity, and segregation resistance of SCC based on the empirical design method [4,5].

The use of metakaolin as partial replacement to cement for concrete production decreases the deformability of concrete and increases its viscosity [25,26]. This is due to its higher water demand and higher specific surface area compared to cement [20,27,28] and leads to the use of high dosages of superplasticizer (SP) to liquify the system and to keep the viscosity within the specified limit. Furthermore, unlike cement particles, calcined clay particles have, overall, a negatively charged surface, which can cause flocculation when added to the heterogeneously charged cement, and therefore require more SP to deflocculate the cementitious system [28,29]. SCC is a very fragile mixture, which requires a perfectly optimized mix design to obtain a sufficient deformability but also to achieve an excellent stability.

Therefore, the current effort is directed towards determining the influence of a higher percentage of cement replacement with both LP and a CC dominated by 2:1 phyllosilicates on self-consolidation and early age properties of SC-M, also under the consideration of increased demand for SP. Numerous studies have already been carried out in this field, especially with calcined kaolinite-rich clays and mainly for the production of vibrated concrete [15,16,25,26]. In this study, the potential of a calcined low-grade kaolinite clay (CC) in combination with LP as a substitute for up to 55 vol.% of cement for the production of SC-M was determined. The limits for the self-compactability of mortar specified in [4,30,31] were reviewed and modified to cover the use of CC in the production of SCC.

2. Materials and Methods

2.1. Materials and Mix Design

2.1.1. Materials

Ordinary Portland cement (OPC) CEM I 42.5 R conforming to DIN EN 197-1 [32] was used. It contained (wt.%) 61.6 C_3S, 18.2 C_2S, 5.8 C_3A, 9.0 C_4AF, 3.2 sulfates and 0.6 calcite as mineralogical phases according to supplier's information. The cement was substituted by 15 vol.% of LP in order to simulate a Portland limestone cement (PLC). The LP contained 99.8 wt.% calcite and 0.2 wt.% quartz, as determined by X-ray diffraction. This basic mixture of OPC and LP (forming, PLC) was partly substituted with 10 to 40 vol.% of a calcined common clay (CC). The raw material for CC was an Amaltheen common clay originating from southern Germany, which was calcined on industrial scale at 750 °C. It contained (wt.%) 60.8 amorphous phase, 16.2 quartz, 2.2 muscovite, 0.6 calcite, 4.6 illite and 1.6 sulfates. The characterization of the CC was described thoroughly in [33–35]. Tables 1 and 2 show the chemical and physical characteristics of the powder materials, respectively. The oxide composition of LP and CC was determined by using inductively coupled plasma optical emission spectrometry (ICP-OES) according to DIN EN ISO 11885 [36]. An industrial isoprenyl oxy poly (ethylene glycol)-type polycarboxylatether-based superplasticizer (SP) with acrylic acid as anchor group and additional vinyloxybutyl poly(ethylene glycol) macromonomer was used in this study as it showed excellent performance in a previous study [37]. It has a solid content of 38.6 wt.%, an anionic charge density of 1390 µmol/g, a molecular weight of 25,992 g/mol and a side-chain length of n_{EO} = 31, according to the supplier's information. The respective SP dosages were determined as wt.% of binder. The results on rheological and early ageing properties presented in this report are specific to this SP, and other SPs may produce different results, e.g., in terms of dosage increase, influence on rheology and early ageing properties. Sand with bulk density of 2.87 g/cm^3 and having 7.6 wt.% passing of 125 µm sieve was used as an FA. Figure 1 shows the particle size distribution of the FA.

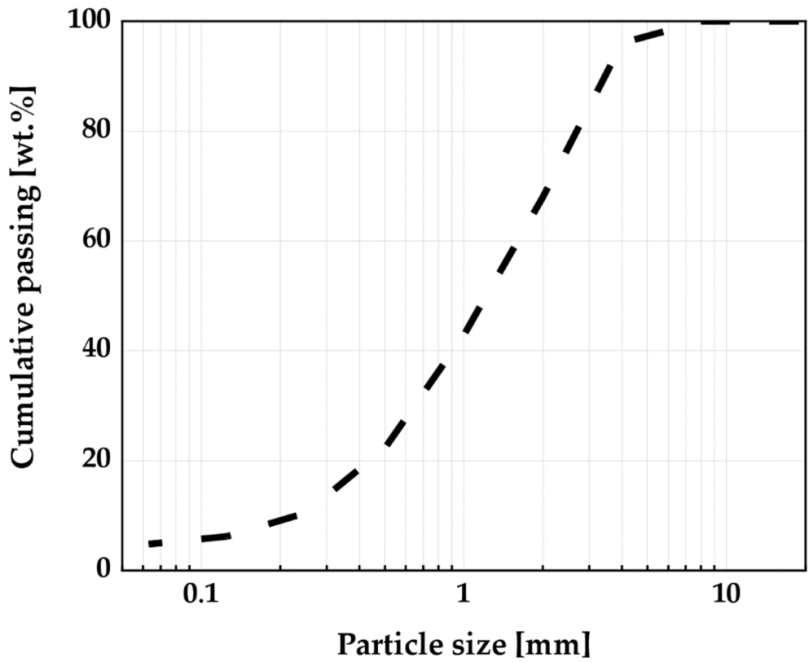

Figure 1. Particle size distribution of fine aggregate determined according to DIN EN 933-1 [44].

Table 1. Oxide compositions of OPC, LP and CC (wt.%).

Binder Materials	SiO_2	Al_2O_3	CaO	Fe_2O_3	MgO	SO_3	TiO_2	Na_2O	LOI
OPC	20.1	5.4	60.7	2.9	1.8	3.4	0.3	0.65	1.80
LP	0.6	0.1	56.4	0.1	0.2	0.0	0.0	0.0	42.60
CC	53.2	22.2	6.5	8.0	2.7	2.0	1.0	0.4	0.02

Table 2. Physical properties of OPC, LP and CC.

Properties	Methodology	OPC	LP	CC
Specific surface area, m^2/g	DIN ISO 9277 [38]	1.0	1.6	3.9
Water demand, wt.%	DIN EN ISO 196-3 [39] for OPC and Puntke method for LP and CC [40]	28.9 *	20	38
Particle density, g/cm^3	DIN EN ISO 17892-3 [41]	3.17	2.71	2.63
d_{10}, µm		4.1	1.7	4.0
d_{50}, µm	ISO 13320 [42]	15.8	5.1	13.2
d_{90}, µm		46.0	13.0	37.0

* data taken from Sposito et al. [43].

2.1.2. Mix Design

SC-M was designed by using the empirical method developed by Okamura and Ozawa [4]. The paste phase of the mortar was first designed by determining the volumetric water-to-powder ratio (V_w/V_p) at which the paste systems cease to deform. A range of V_w/V_p was established by using Equation (1) to determine the most suitable V_w/V_p for the different SC-M systems that satisfied both the deformability and segregation resistance requirements. Effect of cement replacement with CC on the relative flow area (Γ_m) of the SC-P was determined using a constant V_w/V_p of 0.850 and varying the SP dosage. Γ_m was calculated by using Equation (2):

$$V_w/V_p = [0.8 \text{ to } 0.9]\ \Gamma_{m0} \tag{1}$$

where Γ_{m0} is the zero relative flow area:

$$\Gamma_m = (d/d_0)^2 - 1 \tag{2}$$

Here, $d = (d_1 + d_2)/2$ with d_1 = largest diameter of the flow and d_2 = diameter perpendicular to d_1 and d_0 = the initial diameter (= diameter of the cone).

The volume of FA (V_s) was fixed at 40 vol.% of the total SC-M volume (V_m) to achieve the final SC-M control mix design. Self-consolidating paste (SC-P) was mixed according to DIN EN 196-1 using a mortar mixer produced by Testing Bluhm and Feuerherdt GmbH, Berlin, Germany. The binder materials, mixing water and the SP were added together and mixed for 4 min. These mixtures at different SP dosages were used for the determination of SP saturation dosage, thermogravimetric measurements, and MIP. The SC-P was mixed manually for isothermal calorimetric measurements.

The same mixer was used to produce SC-M with a total mixing time of 8 min. In the first stage, the binder, FA and two-thirds of the mixing water were mixed for 2 min, followed by a break of 1 min to enable the addition of the remaining mixing water and SP. The whole mixture was then mixed for 5 more minutes. SC-M mixtures were used to determine the effect of varying V_w/V_p and different SP dosages on the deformability and viscosity of SC-M, its dynamic modulus of elasticity, plastic shrinkage and compressive strength.

2.2. Experimental Program

2.2.1. Paste and Mortar Tests

Flowability of the SC-M was determined by using a mini slump cone, and the mini V-funnel [4,45] was used to assess the segregation resistance of the SC-M. The Γ_m of the

SC-M and the relative flow velocity (R_f) were calculated by using Equations (2) and (3), respectively. A range of Γ_m = 4.76 to 5.76 (equally to 24 cm to 26 cm) was used to assess the flowability and the viscosity (R_f) ranges from 0.91 to 1.43 s^{-1} (7 to 11 s) [4,30]. The measurements were performed 15 min after the addition of water. Effects of cement replacement with CC on Γ_m and R_f were determined to serve as a basis for the SCC mix design later on:

$$R_f = 10/t \tag{3}$$

where t = mini V-funnel time measured in sec.

Shear stress (τ) and plastic viscosity (μ) of the SC-M were determined via rotational rheometer Viskomat NT (Schleibinger Testing Systems) at a constant temperature of 20 °C. The measurement started 15 min after water addition with a maximum rotational speed of 12 rpm for 80 s and decreased in 14 steps of 20 s each to eliminate the effect due to thixotropy [46]. Shear stress (τ) and shear rate ($\dot{\gamma}$) were derived from the measured torque (T) and rotational speed (N), respectively, as presented in Equations (4) and (5). The dynamic yield stress (τ_0) and plastic viscosity (η) were calculated according to the Bingham model [47,48] as presented in Equation (6):

$$\text{Shear stress } (\tau) = 0.95 \times T \tag{4}$$

$$\text{Shear rate } (\dot{\gamma}) = 0.584 \times N \tag{5}$$

$$T = g + N \times h \tag{6}$$

where T = torque $\approx \tau$; g = y-intercept of the flow curve $\approx \tau_0$; N = velocity $\approx \dot{\gamma}$; and h = the slope of the curve $\approx \eta$.

2.2.2. Early Age Paste and Mortar Tests

The early hydration behavior of selected binder systems was monitored by isothermal calorimetric measurements. The tests were conducted with a TAM AIR eight-channel isothermal calorimeter (TA instruments, New Castle, DE, USA). The materials required for this test were stored in a closed chamber at a temperature of 25 °C for at least 24 h before the test. For the reference system (SC-P), 4.25 g OPC and 0.75 g LP were manually homogenized for 60 s and mixed with distilled water (w/cm = 0.29) for a further 60 s. For SC-P-20CC and SC-P-40CC, the OPC and LP was equally reduced and 1.0 g and 2.0 g, respectively, of CC were added to the cement. About 2 g of the paste were filled in plastic ampoules and subsequently inserted into the calorimeter. The heat flow was measured up to 48 h, and the result was normalized to g of cement.

The setting and hardening behavior of the SC-M was monitored according to EN 12504-4:2004 [49], using a Vikasonic apparatus integrated with a datalogger (Schleibinger Testing Systems, Buchbach, Germany). The tests were conducted in a climate chamber at 20 °C/65% relative humidity. Fresh SC-M was placed to set between two ultrasonic transducers, which are supplied with 0.25 s pulse per s at a frequency of 54 kHz. The ultrasound speed was monitored for 48 h starting 15 min after water addition. The dynamic modulus of elasticity (E_{dyn}) was determined based on the density (ρ) of the SC-M and the recorded ultrasonic velocity (v), as presented in Equation (7). This is used to delineate points of a complete crystalline structural change in the system [43,50]:

$$E_{dyn} = \rho \times v^2 \tag{7}$$

The plastic shrinkage of SC-M was assessed contactless via a shrinkage cone (Schleibinger Testing Systems, Buchbach, Germany) with a volume/height sample container of 682 cm^3/125 mm and equipped with a Class 2 laser having a power of <1 mW at 670 nm according to DIN EN 60825-1:2015-07 [51]. The measurement was also conducted in a climate chamber (20 °C/65% relative humidity) for 48 h to eliminate external influences.

A wall fraction effect was avoided by using a polypropylene foil between the shrinkage cone, and the SC-M. Thermocouples were attached to measure the specimen temperature.

2.2.3. Hardened Paste and Mortar Tests

For thermogravimetric measurements (TG) and MIP, the paste phase of the SC-M designed in Section 3.2 were produced and filled into 40 × 40 × 160 mm^3 steel molds and stored in a moist condition for 48 h. After demolding, the prisms were cured under water until testing. The proportioning of the paste constituents is provided in Table 3.

Table 3. Proportioning of the paste constituents for TG and MIP.

Mix Designation	V_w/V_p	Constituent (Measured in dm^3/m^3)				Constituent (Measured in kg/m^3)				
		OPC	LP	CC	Water	OPC	LP	CC	Water	SP [wt.%]
SC-P	0.875	453	80	-	467	1405	218	-	467	0.2
SC-P-20CC	0.875	363	64	107	467	1124	175	283	467	0.3
SC-P-40CC	0.875	272	48	213	467	843	131	565	467	0.4

Thermogravimetric measurements were conducted with Netzsch STA 449 F3 Jupiter equipment at the hydration ages of 2 and 28 days. A representative of the sample was manually chipped out from the inner part of the paste prisms and crushed to <1 mm size using laboratory mortar and pestle. Binder hydration was stopped by solvent exchange method [52] and dried in a ventilated oven at 60 °C for 12 h. About 300 mg of the pulverized hardened binder paste was loaded into alumina crucibles and heated from 25 to 1000 °C at a heating rate of 2 K/min under nitrogen atmosphere. Tangent method according to Marsh and Day [53] was used to quantify the portlandite in the hydration phase from the mass loss between the temperatures of 400 °C and 490 °C.

MIP was employed to assess the effect of CC on the pore structure of the binder at 28 days of hydration according to DIN 66133 [54]. Approximately 1 cm^3 of the hardened binder paste was manually chipped from the inner part of the paste prisms. The samples were stored in isopropanol for at least three days and subsequently dried at 70 °C in a ventilated oven. After drying, they were cooled and stored in a desiccator and tested by using ThermoFisher mercury intrusion porosimeter with a high pressure unit (400 MPa) to measure up to 2 nm pore radii and a low pressure unit (400 kPa) for up to 2 µm radii. Mercury density of 13.54 g/cm^3 with a surface tension of 0.48 N/m and a contact angle of 140° were used as parameters for the MIP experiments. The SC-P pore sizes were classified as gel pores (0–30 nm), microcapillary pores (30 nm–1 µm), capillary pores (1 µm–50 µm) and air voids (>50 µm).

The compressive strength of the SC-M specimens was determined according to DIN EN 196–1 [55] at 2, 7 and 28 days of curing. 40 × 40 × 160 mm^3 specimens were cast into steel molds. They were covered and stored in a moist condition for 48 h and subsequently cured underwater until the date of testing. The compressive strength test was conducted on the Form + Test Prüfsysteme Alpha 1-3000 with an increased uniform loading rate of 2400 ± 200 N/s until failure.

3. Results and Discussion

3.1. Flow Behavior of the Studied Binders

Figure 2 shows the V_w/V_p at which the different binder systems cease to deform (zero relative flow area: Γ_{m0}). These points are denoted as the amount of water confined by the binder particles [4]. The V_w/V_p confined by the cement was 1.03. This value increased to 1.19 at 40 vol.% cement replacement with CC. Here, it is worth mentioning that an increasing cement substitution with CC increased the water confined by the system in a non-linear manner. This non-linearity is more pronounced with CC substitution beyond 20 vol.%. The combined effect of high water demand of CC compared to cement and its

particle shape led to the increased interparticle friction, and hence more water is entrapped in the system with large volume of CC. On average, V_w/V_p between 0.850 and 0.925 was selected as a basis for SC-M design. These values were calculated from the V_w/V_p for Γ_{m0} using Equation (1).

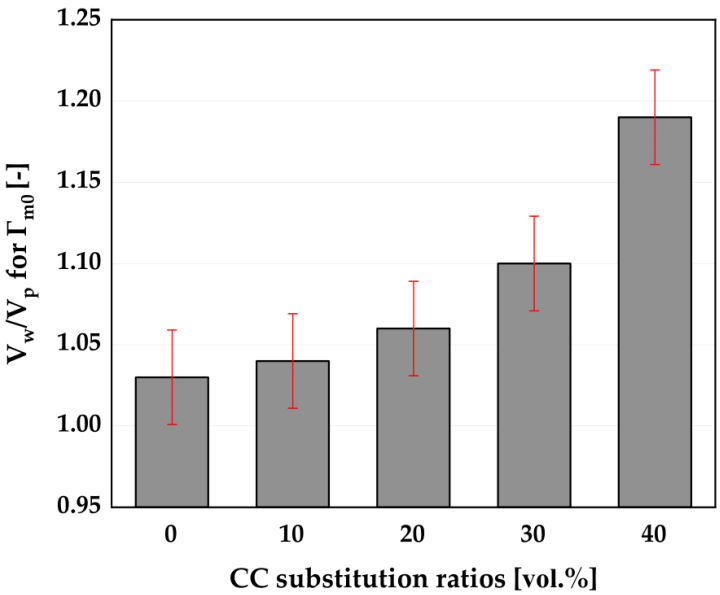

Figure 2. Volumetric water to powder ratio for zero relative flow area depending on the CC substitution rate.

Figure 3 shows the effect of CC on the Γ_m of SC-P at a constant V_w/V_p of 0.850 and varying SP dosages. More SP was required to deform a binder system with CC, especially at cement replacement beyond 20 vol.%. This was attributed to the higher specific surface area and water demand of CC compared to cement (Table 2). Furthermore, it is known that the negatively charged CC particles cause flocculation when added to cement [20,28,56]. The required dosage of SP to achieve the same deformability of the cement matrix with 40 vol.% CC was almost 65% greater than the SP required for cement without CC replacement. At 0.3 wt.% SP, 7.5 Γ_m was achieved for PLC only. This declined already to 4.0 Γ_m with the replacement of 10 vol.% CC. Further replacement of cement with CC reduced Γ_m to almost zero, meaning no flowablity at all. By increasing the percentage of SP to 0.4 wt.% influenced less significantly the Γ_m of PLC substituted with up to 30 vol.% CC. With 40 vol.% CC, at least 0.5 wt.% SP dosage was required to achieve the required deformability of the system. At this SP dosage, cement replacement with CC beyond 20 vol.% had no significant impact on the relative flow area of the system, as shown in Figure 3.

3.2. Design of Self-Consolidating Mortar

Figure 4 shows the effect of varying the V_w/V_p and SP dosages on the relative flow area (Γ_m) and the relative flow velocity (R_f) of SC-M produced with 40 vol.% FA (V_s = 0.4). The Γ_m and R_f increased both with increasing V_w/V_p and SP dosage. At 0.4 wt.% SP dosage, the variation in V_w/V_p up to 0.90 had less impact on the Γ_m but affected the R_f values significantly. Increasing the SP dosage to 0.45 wt.% and beyond caused a significant increase in both the Γ_m and R_f.

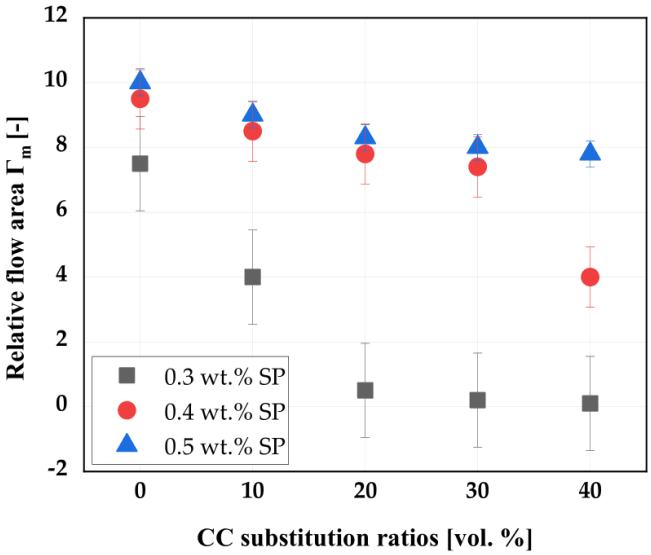

Figure 3. Influence of CC on the Γ_m of SC-P.

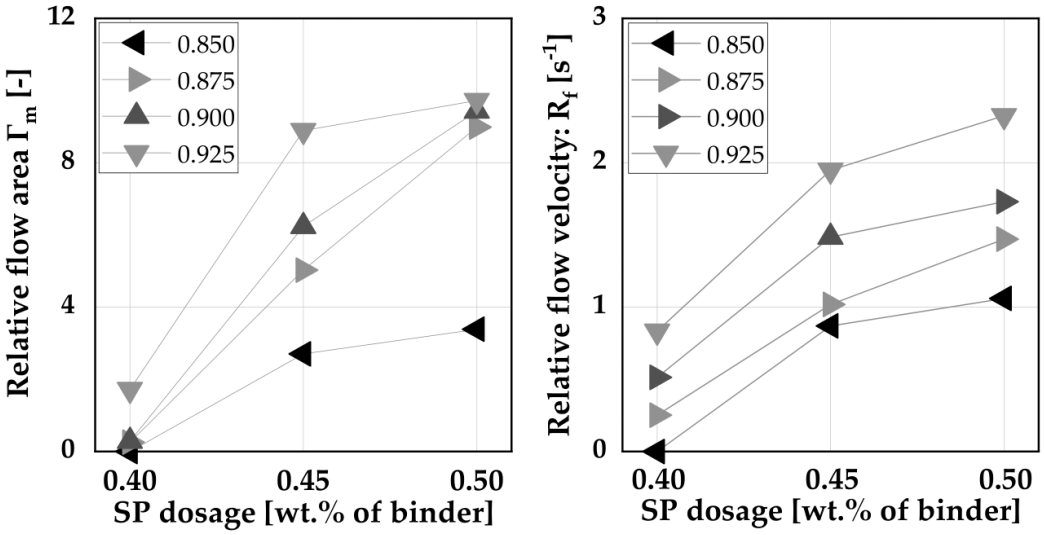

Figure 4. Γ_m and R_f of SC-M with varying V_w/V_p ratios of 0.850 to 0.925 and constant V_s = 0.4.

The combination V_w/V_p and SP dosage that satisfied the thresholds of both the Γ_m (4.76 to 5.76) and R_f (0.91 to 1.43 s^{-1}) [4,30] was selected as a start for the subsequent increasing replacement of cement by CC. For constant V_s = 0.4, this was accomplished with V_w/V_p = 0.875 and 0.45 wt.% SP and is denoted from here on as SC-M-1. When cement is substituted with CC, the volumetric proportion of the CC used will be added in front of this designation. By increasing the volume of the CC as cement replacement, the fluidity of the mixture decreased, and the viscosity increased. This necessitated the addition of higher dosages of SP (0.5 and 0.6 wt.%, respectively) to maintain the deformability of SC-M. Figure 5 shows the influence of varying the V_w/V_p and the replacement of cement with CC on Γ_m and R_f of the SC-M. The aforementioned thresholds of Γ_m and R_f were used to classify the SC-M into different viscosities. Increasing the V_w/V_p led to a decrease in viscosity with a high tendency of segregation. On the other hand, increasing the cement replacement level

by CC resulted in a decreased Γ_m and increased R_f of the SC-M. With replacement levels beyond 20 vol.%, a higher dosage of SP is required to improve the deformability of the SC-M. The established R_f values were difficult to achieve with replacement levels beyond 10 vol.%. Nonetheless, the Γ_m were achieved with cement replacement up to 40 vol.% CC as depicted in Figure 5. Therefore, these limits need to be adjusted to accommodate the effect of CC at higher replacement levels. The major concern is an even lower limit of R_f, which is at 0.91 s^{-1} for cement and other SCMs that have a similar deformability rate compared to cement [4,30]. The CC used in this context behaved differently from cement due to its slow deformability rate and, therefore, a new lower R_f limit of 0.65 s^{-1} is proposed based on the experimental results obtained to accommodate up to 40 vol.% cement replacement by CC. The upper limit of R_f (1.43 s^{-1}) remains unchanged. Consequently, the established Γ_m upper limit has to be adjusted to achieve the proposed R_f limits. A window with R_f = 0.65 to 1.43 s^{-1} and Γ_m = 4.76 to 7.50 is proposed to accommodate cement replacement with up to 40 vol.% CC as shown in Figure 5.

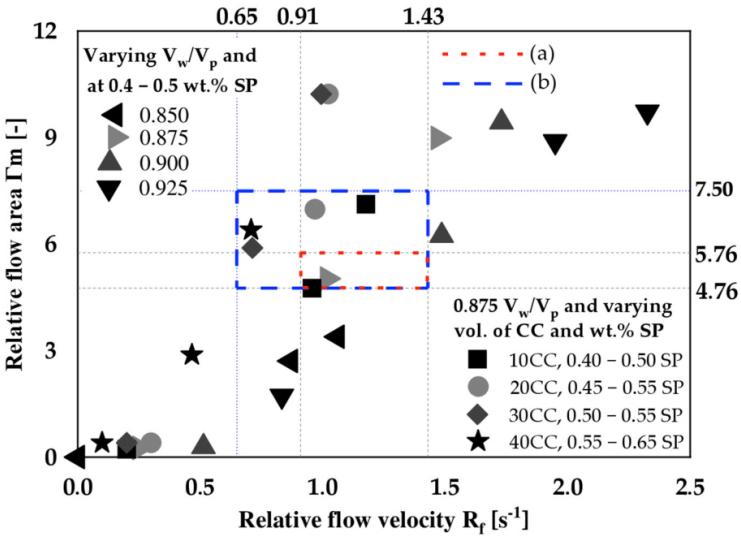

Figure 5. Γ_m and R_f of SC-M, (a) = Γ_m and R_f thresholds recommended by Okamura and (b) = proposed Γ_m and R_f thresholds.

SC-M was designed using an empirical method and the influence of cement replacement with CC was determined. The rate of deformability of the SC-M decreased with increased CC content. As consequence, a new window for R_f and Γ_m was derived to accommodate cement replacement with up to 40 vol.% CC. For ease of identification of the mix designs, Table 4 summarizes the proportioning of the SC-M constituents.

Table 4. SC-M mix designation.

Mix Designation	V_w/V_p	Constituent (Measured in dm^3/m^3)					Constituent (Measured in kg/m^3)					
		OPC	LP	CC	FA	Water	OPC	LP	CC	FA	Water	SP [wt.%]
SC-M-1	0.875	272	48	-	400	280	843	131	-	111	280	0.40–0.55
SC-M-1-10CC	0.875	245	43	32	400	280	759	118	85	111	280	0.40–0.55
SC-M-1-20CC	0.875	218	38	64	400	280	675	105	170	111	280	0.45–0.60
SC-M-1-30CC	0.875	190	34	96	400	280	590	92	254	111	280	0.45–0.60
SC-M-1-40CC	0.875	163	29	128	400	280	506	79	339	111	280	0.45–0.65

3.3. Rheological Properties of SC-M Blended with CC

To further characterize the behavior of the SC-M produced, the rheological behavior was closely monitored by using a rotational viscometer. At a constant V_w/V_p of 0.875 and SP dosage of 0.5, a higher volume of cement replacement with CC significantly increased the shear stress at both low and high shear rate values, as depicted in Figure 6. At low shear rate values, for instance, the addition of CC increased the shear stress of the system in a non-linear way by 26% and 171% at the 20 and 40 vol.% replacement levels, respectively. Similarly, by increasing the shear rate, the shear stress increased. Hence, an increased content in CC resulted in higher plastic viscosity and reduced the deformation rate.

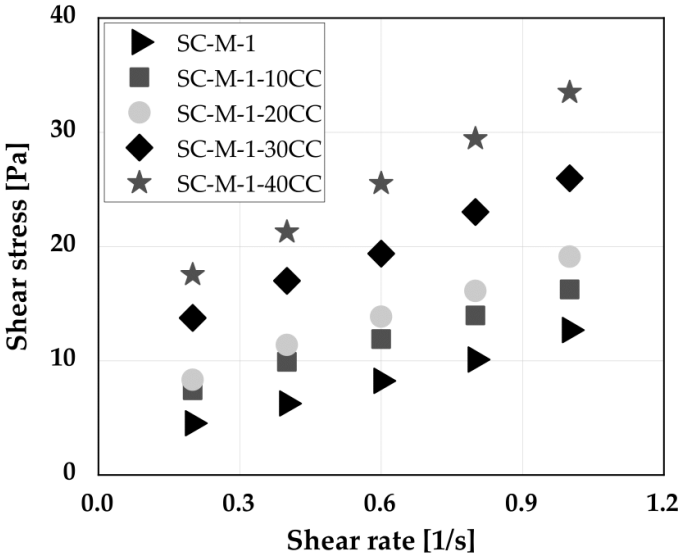

Figure 6. Shear stress of SC-M with varying V_{cc}, at constant V_w/V_p = 0.875 and SP dosage of 0.50.

The adjustment of SP dosage is urgently required to control the degree of deformity of SC-M with increasing the volume of CC as cement replacement. Figure 7 shows the influence of increasing SP dosage on dynamic yield stress and plastic viscosity of SC-M produced with a varying volume of CC. A higher SP dosage decreased both the yield stress and plastic viscosity of the mortar with and without CC. This decrease was more pronounced in the control mixture, resulting in a higher tendency of segregation, as observed also in Figure 5. For instance, about 0.5 wt.% SP dosage was required to deform the control mixture and to reduce the dynamic yield stress from 10.6 Pa to 3.1 Pa, while the corresponding plastic viscosity dropped from 20 Pa·s to 12 Pa·s. For the SC-M with CC replacement at 20 and 40 vol.%, the required dosage of SP increased to 0.55 and 0.60 wt.% SP in order to achieve the same degree of deformability, respectively. The corresponding plastic viscosities, however, remained at 19 and 22 Pa·s, respectively. At 40 vol.% CC, the viscosity of the SC-M increased relatively to the other mixes, whereas the yield stress values remained in a similar range. This was related to a higher SP dosage used to deform the system with CC. Furthermore, it clearly indicated that the stability of the CC blended systems is less affected despite the adjustment of SP dosage and that the deformability rate of SC-M with CC is very slow compared to the control mixture due to their lower relative flow velocity.

The rheological measurements of SC-M showed that a sufficient reduction in yield stress and plastic viscosity values is possible by adjusting the SP dosages. Once similar fresh properties are achieved with up to 40 vol.% cement replacement with CC as for mixtures without CC, the question arises how it affects the properties of SC-P and SC-M within the first 48 h after water addition.

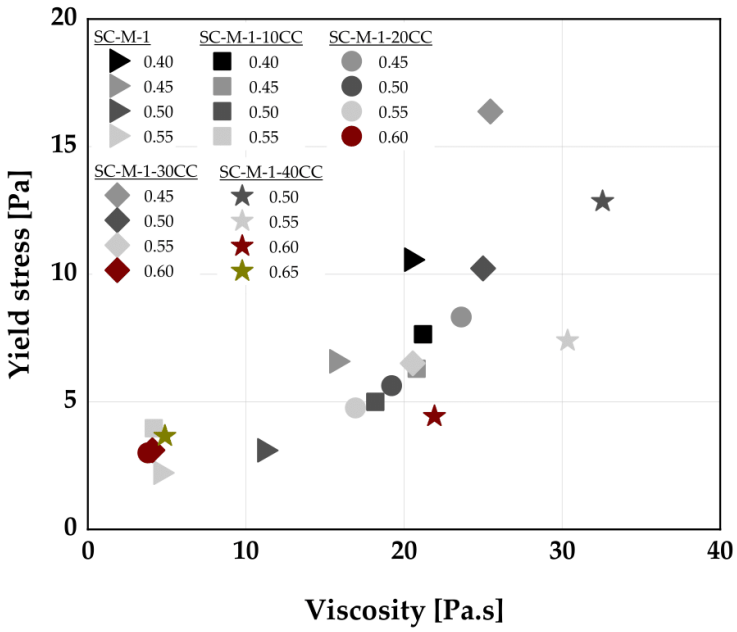

Figure 7. Comparison of yield stress and plastic viscosity of SC-M-1 with varying V_{cc} and SP dosages.

3.4. Early Age Characteristics of Self-Consolidating Paste and Mortar

Early age properties of SC-P and SC-M were closely monitored using isothermal calorimetry, ultrasonic pulse velocity (UPV) and plastic shrinkage measurements. Figure 8a,b show the heat flow and hydration heat curves of cement with 0, 20 and 40 wt.% CC. The heat flow curves exhibited four exothermic peaks. The first peak occurred due to the mixing reaction between the binder and water leading to the initial formation of ettringite and the release of a considerable amount of energy. This was followed by the dormant period and subsequent formation of the second peak after 7 h of hydration. The use of CC as cement replacement at both 20 and 40 vol.% had no significant impact on the formation and duration of the dormant period. The formation of the second peak (alite peak) is commonly related to the dissolution of C_3S and precipitation of C-S-H [57,58]. Again, the cement replacement by CC had no significant effect on the shape and occurrence of this peak, although it was slightly higher for SC-P-40CC. The third peak appeared shortly after the alite peak due to the depletion of sulfate in the system leading to the fast dissolution of C_3A and precipitation of ettringite. At about 23 h of hydration, it was assumed that ettringite converted with carbonate ions from LP to hemicarboaluminate (AFm-Hc). The presence of CC in these systems enhanced the formation of this fourth peak and increased its intensity significantly from 2.2 mW/g_{cement} to 3.6 mW/g_{cement}. This was due to the presence of more aluminum ions in the systems with CC, which further reacted with the carbonate ions to form more AFm-Hc [18]. As shown in Figure 8b, the addition of CC enhanced the hydration heat. This effect can be explained in two stages. First, from 0 to about 24 h of hydration, the CC increased the nucleation sites and improved the hydration rate by acting as filler [59,60]. Second, from 24 to 48 h of hydration, the reaction between the aluminum ions and the carbonate ions was enhanced due to the presence of more aluminate in the system with CC, which promoted the formation of ettringite and conversion to AFm-Hc and consequently lead to a higher hydration heat [18,61].

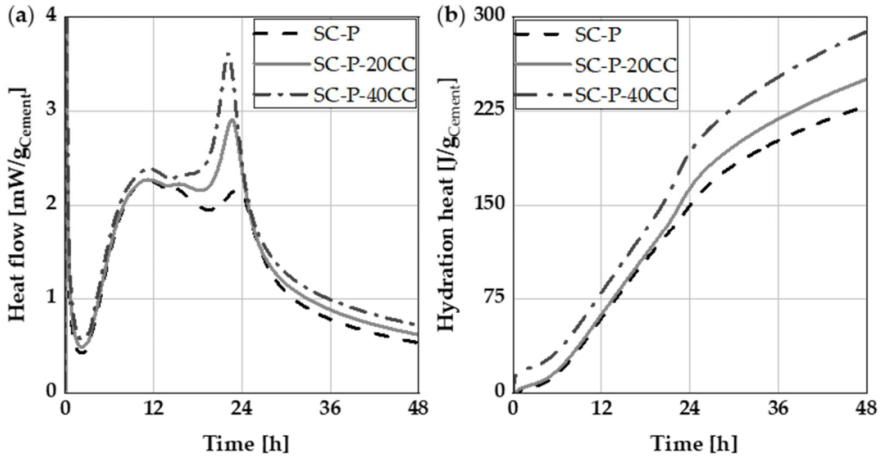

Figure 8. Heat flow (**a**) and Hydration heat (**b**) of SC-P with and without CC.

Figure 9 shows the dynamic modulus of elasticity of SC-M as deduced from UPV. A constant value of dynamic modulus of <1.5 kN/mm^2 was recorded for up to 7 h. At this stage, the SC-M experienced a transition from fluid to solid state and the addition of 20 wt.% CC had only minor influence on the setting behavior of the cement. The addition of 40 wt.% CC, however, prolonged the period of constant dynamic modulus by an hour. The measured UPV value corresponded to the velocity passed through the aggregate grains [62] during the dormant period of the mixtures, as observed in Figure 8a. Consequently, the formation of densifying hydration products was yet to begin. It was characterized by gradual loss of slump and described the time of initial setting according ASTM 1679-13 [63], as also observed by Sposito et al. [43]. From 7 to almost 24 h, the dynamic modulus of elasticity increased rapidly in all the SC-M specimens. The SC-M at this stage experienced a transition from semi-rigid to a rigid state due to the formation of C-S-H, leading to the densification of its microstructure. Once the setting process of SC-M was completed, the growth of dynamic modulus of elasticity slowed down in all specimens beyond 24 h. The use of CC reduced the dynamic modulus of elasticity at 48 h of hydration by 18 and 26% at replacement levels of 20 and 40 wt.%, respectively.

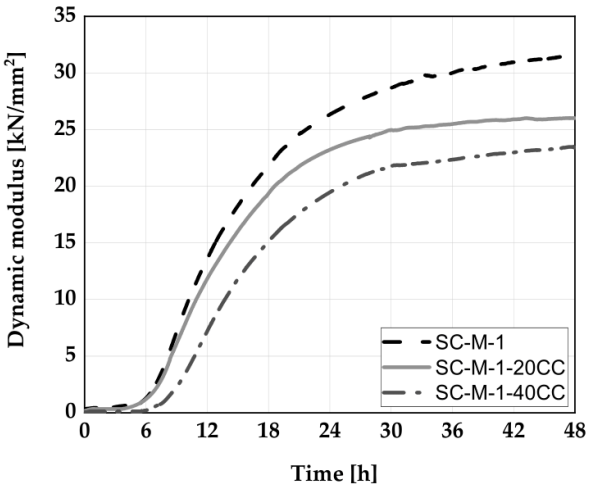

Figure 9. Dynamic modulus of elasticity of SC-M specimens.

The mechanism of plastic shrinkage could also be divided in three stages. During the first stage, which was from water addition to about 7 h of hydration, the SC-M experienced a rapid increase in plastic shrinkage (up to −6 mm/m as shown in Figure 10). This was attributed to the settlement of the SC-M solid particles and the evaporation of water from the surface of the SC-M. A further yet significantly slowed down course of plastic shrinkage was observed between 7 h and 16 h of hydration. Here, the effect of CC became more obvious, as its addition decreased plastic shrinkage by up to 15%. This corresponded to the combined effect of SC-M particles settlement, evaporation, and the continuous water consumption by hydration products and the calcined clay itself. This confirmed findings of Beuntner and Thienel [17] who explained a lower plastic shrinkage with a lower effective water-to-cement ratio and a better particle packing in the mortar. Beyond 16 h of hydration, the plastic shrinkage was almost constant up to the end of the measurement at 48 h. A slight expansion was observed after 24 h of hydration, which was related to the formation of voluminous AFm-Hc and an along-going reduction in plastic shrinkage.

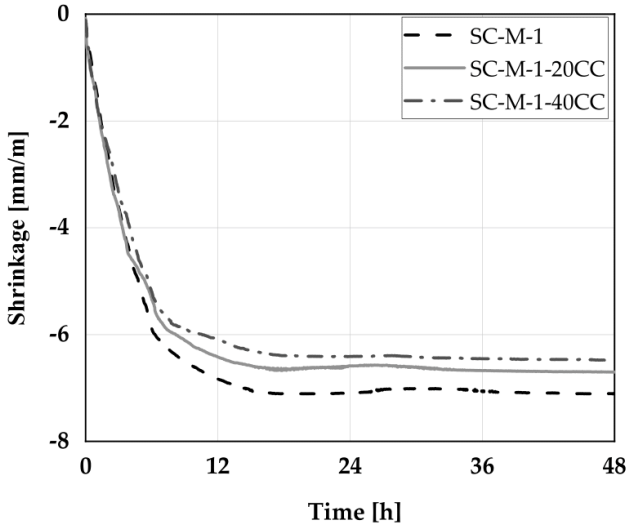

Figure 10. Plastic shrinkage of SC-M specimens.

Based on the early age investigations, the addition of CC to SC-M enhanced the formation of AFm-Hc, reduced the dynamic modulus of elasticity but also the plastic shrinkage of the SC-M.

3.5. Hardened Properties of Self-Consolidating Paste and Mortar

The hardened properties of SC-M were studied by using thermogravimetric analysis, mercury intrusion porosity and compressive strength tests. Figure 11a,b depict the differential thermal analysis (DTA) curves of SC-P conducted at 2 and 28 days of hydration, respectively.

Four distinct stages were identified from the DTG curves. A reduced mass loss was observed at all four stages at 2 days of hydration when CC was used as a cement replacement. This reduction was due to the effect of cement replacement by the CC thereby reducing the rate of precipitation of the hydrate phases in the system. The first peak occurred between T = 50 °C and 140 °C and was mainly related to the dehydration of ettringite (E) and C-S-H [64–67]. The second mass loss between 140 °C and 190 °C was associated with the dehydration of carboaluminates, both AFm-Mc (short: Mc) and AFm-Hc (Hc), which were formed from the reaction of aluminate and carbonate ions in the PLC systems [64,65]. This peak was more pronounced at 28 days and increased with higher replacement by CC. Another mass loss was observed between T = 450 °C and 550 °C due

to the decomposition of $Ca(OH)_2$ [64–67]. Cement replacement with CC led at both ages to a reduction in the quantity of portlandite in the system as depicted in Figure 12. At 2 days of hydration, the reduced amount of portlandite in the systems with CC was due to there being less cement to produce hydrate phases compared to the reference. The physical presence of CC at this stage acted as a filler, thereby providing more nucleation sites for C-S-H to precipitate [59,60]. At 28 days of hydration, the pozzolanic reaction of the CC led to the further reduction (here: consumption) in portlandite in the system. Between T = 600 °C and 800 °C, the decomposition of calcium carbonate ($CaCO_3$) occurred due to the presence of unreacted calcite in the system stemming from LP [64–67]. The peak decreased with the increasing replacement level, as more carboaluminates were formed from LP and CC.

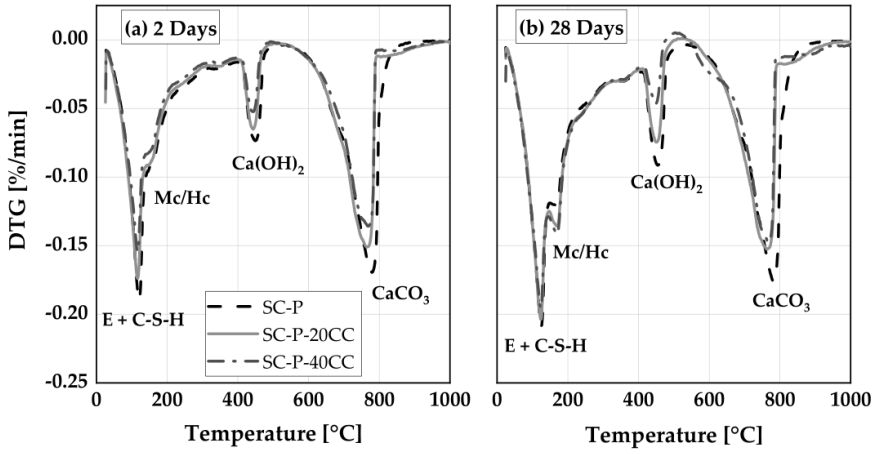

Figure 11. DTA curves of SC-P at 2 days (**a**) and 28 days (**b**) of hydration (E = ettringite, Mc = monocarboaluminat, Hc = hemicarboaluminate).

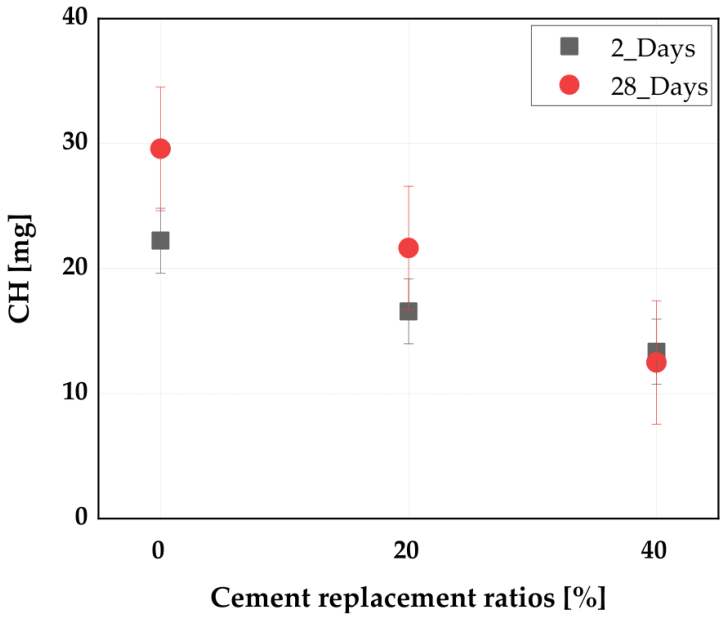

Figure 12. Portlandite (CH) in [mg] at 2 and 28 days of hydration.

Figure 13 shows the specific pore volume of SC-P produced with and without CC as measured by MIP at 28 days of hydration. At 20 vol.% cement replacement by CC, the cumulative intruded volume of the mercury decreased by 4%, which is assumed to be within the deviation range of measurements, while at 40 vol.% cement replacement, the total intruded volume of the mercury increased by 18%. This is due to the higher accessible porosity of the 40 vol.% CC compared to both the 0 and 20 vol.% CC. The volume fraction of the gel pores in the systems with CC was greater than the reference, whereas the fraction of capillary pores was smaller. This pore size refinement was related to the pozzolanic reaction and the formation of more AFm phases in the binder systems with CC, as observed, e.g., by [17,68–71].

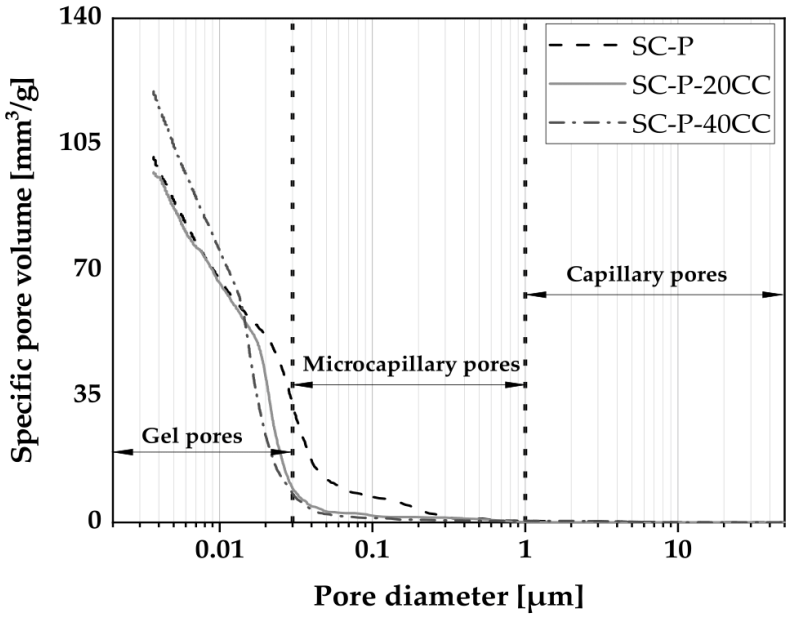

Figure 13. Pore size distribution of SC-P at 28 days of hydration.

The compressive strength of SC-M was measured at ages of 2, 7 and 28 days (Figure 14a). Good correlations were observed between the 2 days compressive strength of the SC-M and its dynamic modulus of elasticity and hydration heat of the respective SC-P at 48 h, as shown in Figure 14b. At 2 and 7 days, the compressive strength values of the SC-M with CC were lower than that of the SC-M without CC due to the dilution effect by the CC. Nonetheless, the strength activity index of the SC-M with 20 and 40 vol.% CC at 7 days were 0.91 and 0.74, respectively, which was enough to consider the latter as SCM in concrete according to ASTM C311-18 [72]. At 28 days of curing, the pozzolanic reactivity of the CC led to the formation of more AFm phases and densification of the SC-M microstructure, as presented by thermal analysis and MIP. Consequently, higher values of compressive strength were achieved as depicted in Figure 14a. The strength activity index of the SC-M with 20 and 40 vol.% CC at this age were 1.08 and 1.07, respectively.

The influence of CC on hardened properties of SC-M was studied. The use of CC as a cement replacement at an early age of hydration (2 days) led to the reduction of the compressive strength, and limited the precipitation of hydrate phases. At later age of hydration, namely 28 days, the pozzolanic reactivity of CC led to specific pore volume refinement and improved the compressive strength of the SC-M.

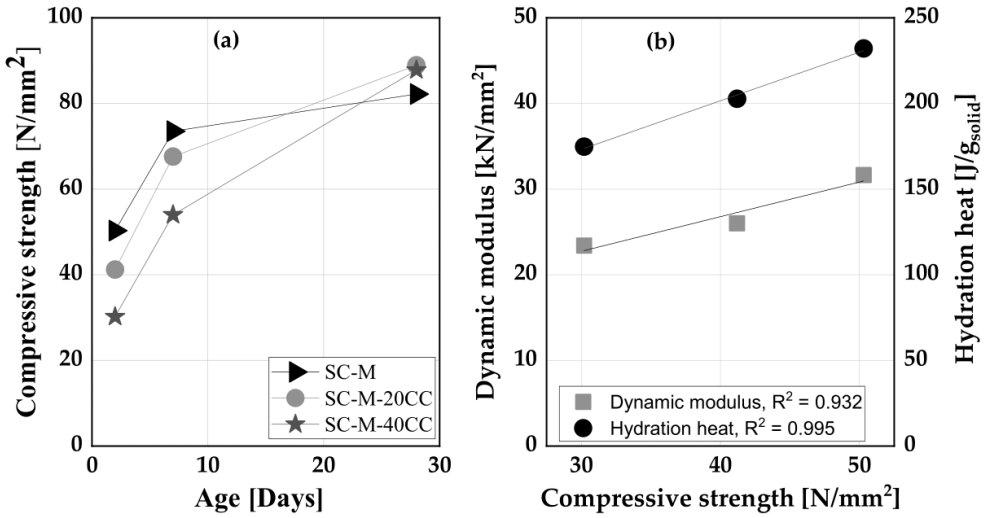

Figure 14. (**a**) Compressive strength development of SC-M specimens, (**b**) Correlation between the compressive strength at 2 days with dynamic modulus and hydration heat at 2 days of hydration.

4. Summary and Conclusions

The current study evaluated the potential of a calcined low-grade kaolinite clay as an alternative for metakaolin and for the production of SC-M and its future application in SCC. Although the calcined clay used in this experiment had a lower water demand than metakaolin, its specific surface area and water demand still surpassed that of cement. As a consequence, the calcined clay increased the viscosity of cementitious systems, and increased dosages of SP were necessary to deform the system and to achieve the targeted SC-M viscosity with up to 40 vol.% calcined clay as cement replacement. Based on the well-established SCC mix design method by Okamura, it was found that new thresholds are required for calcined clay blended SC-M. During the first two days of hydration, the calcined clay mainly acts as filler, leading to lower dynamic modulus of elasticity and compressive strength values. On the other hand, plastic shrinkage is reduced due to the higher water demand of calcined clay. Later on, the enhanced formation of carboaluminates and the consumption of portlandite to form C-S-H, AFt and AFm phases leads to both pore size refinement and higher compressive strength values. Based on the results obtained, these calcined common clays represent an attractive alternative for metakaolin in regions where kaolin is scarce and for high replacement levels. SC-M can be produced with up to 40 vol.% binder replacement with calcined common clay when adjusting the rheological properties by adding higher amounts of suitable superplasticizers. Further investigations will concentrate on determining the influence of these calcined clays on the rheology and durability of SCC. Therefore, the following new knowledge will be considered:

Replacing cement with calcined clay (CC) by up to 40 vol.% increased the water demand of SC-M by up to 16%. Thus, the required amount of superplasticizer increased by up to 65% to maintain the deformability of the cement matrix. High dosages of superplasticizer enabled a significant reduction in yield stress, while the plastic viscosity remained constant.

Higher values of relative flow area up to 10.2 (-) were achieved with up to 40 vol.% CC. The established lower value for relative flow velocity (R_f = 0.91 s^{-1}), as obtained from the Okamura method, is not feasible with cement replacement beyond 10 vol.% of CC. The common thresholds for Γ_m (4.76 to 5.76), however, were conveniently achieved with replacement levels up to 40 vol.% of CC. An adjustment of the lower R_f thresholds could require shifting the upper limits of the Γ_m as well. The lower limit of the R_f requires an adjustment from 0.91 s^{-1} to 0.65 s^{-1} and the upper limit of the Γ_m from 5.76 to 7.50 to accommodate up to 40 vol.% cement replacement with CC.

The addition of CC had no significant effect on the time of initial setting and hardening of the cement. At 48 h of cement hydration, it reduced the dynamic modulus of elasticity by 14 and 24% at replacement levels of 20 and 40 vol.%, respectively.

The presence of CC in the cement system led to lower early strength values due to filler and dilution effects but also reduced plastic shrinkage tendency. This is of special interest for SCCs, as they commonly contain a higher amount of binder compared to conventional concrete and tend therefore to increased shrinkage and cracks.

At later ages, the pozzolanic activity was evident, shown in terms of portlandite consumption and an increased amount in AFm and C-S-H phases. The formation of AFm phases in the presence of CC was responsible for specific pore size reduction. Especially the microcapillary pore fraction of SC-P with 20 and 40 vol.% replacement levels was 71.4 and 77.8% lower, respectively, than for the reference. The gel pore fractions of SC-P with 20 and 40 vol.% cement replacement, instead, were 23.8 and 53.2% greater, respectively. The accessible porosity of the SC-P decreased by 6.8% at 20 vol.% CC, while at 40 vol.% CC, it increased by 11.4%. At 28 days, the addition of CC at 20 and 40 vol.% could improve the compressive strength values by up to 8.1 and 6.8%, respectively.

Author Contributions: Conceptualization, A.M.; writing—original draft preparation, A.M.; writing—review and editing, A.M., K.-C.T. and R.S.; supervision, K.-C.T. All authors have read and agreed to the published version of the manuscript.

Funding: The first author was funded by the German Academic Exchange Service (DAAD) and the Nigerian Petroleum Technology Development Fund (PTDF). We acknowledge financial support by University of the Bundeswehr Munich.

Data Availability Statement: Not applicable.

Conflicts of Interest: The authors declare no conflict of interest.

References

1. Tangtinthai, N.; Heidrich, O.; Manning, D.A.C. Role of policy in managing mined resources for construction in Europe and emerging economies. *J. Environ. Manag.* **2019**, *236*, 613–621. [CrossRef] [PubMed]
2. Schandl, H.; Fischer-Kowalski, M.; West, J.; Giljum, S.; Dittrich, M.; Eisenmenger, N.; Geschke, A.; Lieber, M.; Wieland, H.; Schaffartzik, A.; et al. Global material flows and resource productivity forty years of evidence. *J. Ind. Ecol.* **2018**, *22*, 827–838. [CrossRef]
3. Schneider, M.; Romer, M.; Tschudin, M.; Bolio, H. Sustainable cement production—present and future. *Cem. Concr. Res.* **2011**, *41*, 642–650. [CrossRef]
4. Okamura, H.; Ozawa, K. Mix-design for self-compacting concrete. *Proc. JSCE* **1995**, *25*, 107–120.
5. Okamura, H. Self-Compacting High-Performance Concrete. *Concr. Int.* **1997**, *19*, 50–54.
6. Shi, C.; Wu, Z.; Lv, K.; Wu, L. A review on mixture design methods for self-compacting concrete. *Constr. Build. Mater.* **2015**, *84*, 387–398. [CrossRef]
7. Lamb, W.F.; Wiedmann, T.; Pongratz, J.; Andrew, R.; Crippa, M.; Olivier, J.G.J.; Wiedenhofer, D.; Mattioli, G.; Khourdajie, A.A.; House, J.; et al. A review of trends and drivers of greenhouse gas emissions by sector from 1990 to 2018. *Environ. Res. Lett.* **2021**, *16*, 073005. [CrossRef]
8. Memon, S.A.; Shaikh, M.A.; Akbar, H. Utilization of Rice Husk Ash as viscosity modifying agent in Self Compacting Concrete. *Constr. Build. Mater.* **2011**, *25*, 1044–1048. [CrossRef]
9. Yazici, H. The effect of silica fume and high-volume Class C fly ash on mechanical properties, chloride penetration and freeze-thaw resistance of self-compacting concrete. *Constr. Build. Mater.* **2008**, *22*, 456–462. [CrossRef]
10. Bouzoubaâ, N.; Lachemi, M. Self-compacting concrete incorporating high volumes of class F fly ash: Preliminary results. *Cem. Concr. Res.* **2001**, *31*, 413–420. [CrossRef]
11. Miller, S.A.; John, V.M.; Pacca, S.A.; Horvath, A. Carbon dioxide reduction potential in the global cement industry by 2050. *Cem. Concr. Res.* **2018**, *114*, 115–124. [CrossRef]
12. Yahia, A.; Tanimura, M.; Shimoyama, Y. Rheological properties of highly flowable mortar containing limestone filler-effect of powder content and W/C ratio. *Cem. Concr. Res.* **2005**, *35*, 532–539. [CrossRef]
13. Uysal, M.; Sumer, M. Performance of self-compacting concrete containing different mineral admixtures. *Constr. Build. Mater.* **2011**, *25*, 4112–4120. [CrossRef]
14. Ghezal, A.; Khayat, K.H. Optimizing self-consolidating concrete with limestone filler by using statistical factorial design methods. *ACI Mater. J.* **2002**, *99*, 264–272. [CrossRef]

15. Avet, F.; Scrivener, K. Hydration Study of Limestone Calcined Clay Cement (LC3) Using Various Grades of Calcined Kaolinitic Clays. In *Calcined Clays for Sustainable Concrete—Proceedings of the 2nd International Conference on Calcined Clays for Sustainable Concrete*; Martirena, F., Favier, A., Scrivener, K., Eds.; Springer Nature: La Havanna, Cuba, 2018; pp. 35–40.
16. Scrivener, K.; Martirena, F.; Bishnoi, S.; Maity, S. Calcined clay limestone cements (LC^3). *Cem. Concr. Res.* **2018**, *114*, 49–56. [CrossRef]
17. Beuntner, N.; Thienel, K.-C. Performance and properties of concrete made with calcined clays. In Proceedings of the ACI SP 320-10th ACI/RILEM International Conference on Cementitious Materials and Alternative Binders for Sustainabe Concrete, Montreal, QC, Canada, 2–4 October 2017; pp. 7.1–7.12. [CrossRef]
18. Scherb, S.; Beuntner, N.; Köberl, M.; Thienel, K.-C. The early hydration of cement with the addition of calcined clay—From single phyllosilicate to clay mixture. In Proceedings of the 20. Internationale Baustofftagung ibausil, Weimar, Germany, 12–14 September 2018; pp. 658–666.
19. Maier, M.; Beuntner, N.; Thienel, K.-C. An approach for the evaluation of local raw material potential for calcined clay as SCM, based on geological and mineralogical data: Examples from German clay deposits. In *Calcined Clays for Sustainable Concrete—Proceedings of the 3rd International Conference on Calcined Clays for Sustainable Concrete*; Bishnoi, S., Ed.; RILEM Bookseries; Springer: Singapore, 2020; Volume 25, pp. 37–47. [CrossRef]
20. Schmid, M.; Plank, J. Dispersing Performance of Different Kinds of Polycarboxylate (PCE) Superplasticizers in Cement Blended With a Calcined Clay. *Constr. Build. Mater.* **2020**, *258*, 119576. [CrossRef]
21. Cardinaud, G.; Rozière, E.; Martinage, O.; Loukili, A.; Barnes-Davin, L.; Paris, M.; Deneele, D. Calcined clay—Limestone cements: Hydration processes with high and low-grade kaolinite clays. *Constr. Build. Mater.* **2021**, *277*, 122271. [CrossRef]
22. Su, N.; Hsu, K.C.; Chai, H.W. A simple mix design method for self-compacting concrete. *Cem. Concr. Res.* **2001**, *31*, 1799–1807. [CrossRef]
23. Sedran, T.; de Larrard, F.; Hourst, F.; Contamines, C. Mix Design of Self-Compacting Concrete (SCC). In *Production Methods and Workability of Concrete*, 1st ed.; Bartos, P.J.M., Cleland, D.J., Marrs, D.L., Eds.; CRC Press: London, UK, 1996; p. 12.
24. Petersson, O.; Billberg, P.; Van, B.K. A Model for Self-Compacting Concrete. In *Production Methods and Workability of Concrete*, 1st ed.; Bartos, P.J.M., Cleland, D.J., Marrs, D.L., Eds.; CRC Press: London, UK, 1996; p. 10.
25. Kannan, V. Relationship between ultrasonic pulse velocity and compressive strength of self compacting concrete incorporate rice husk ash and metakaolin. *Asian J. Civ. Eng.* **2015**, *16*, 1077–1088.
26. Madandoust, R.; Mousavi, S.Y. Fresh and hardened properties of self-compacting concrete containing metakaolin. *Constr. Build. Mater.* **2012**, *35*, 752–760. [CrossRef]
27. Pierkes, R.; Schulze, S.E.; Rickert, J. Durability of Concretes Made with Calcined Clay Composite Cements. In Proceedings of the Calcined Clays for Sustainable Concrete—Proceedings of the 2nd International Conference on Calcined Clays for Sustainable Concrete, La Havanna, Cuba, 5–7 December 2017; pp. 366–371. [CrossRef]
28. Li, R.; Lei, L.; Sui, T.; Plank, J. Effectiveness of PCE superplasticizers in calcined clay blended cements. *Cem. Concr. Res.* **2021**, *141*, 106334. [CrossRef]
29. Sposito, R.; Maier, M.; Beuntner, N.; Thienel, K.-C. Evaluation of zeta potential of calcined clays and time-dependent flowability of blended cement with customized polycarboxylate-based superplasticizers. *Constr. Build. Mater.* **2021**, *308*, 125061. [CrossRef]
30. EFNARC. The European Guidelines for Self Compacting Concrete. *Specif. Prod. Use* **2005**, *22*, 563.
31. EFNARC. *Europäische Richtlinie für Spritzbeton/European Specification for Sprayed Concrete*; EFNARC: Farnham, UK, 1997; p. 32.
32. *DIN EN 197-1*; Zement—Teil 1: Zusammensetzung, Anforderungen und Konformitätskriterien von Normalzement (Cement—Part 1: Composition, Specifications and Conformity Criteria for Common Cements). DIN: Berlin, Germany, 2011; p. 8. [CrossRef]
33. Beuntner, N.; Thienel, K.-C. Properties of Calcined Lias Delta Clay—Technological Effects, Physical Characteristics and Reactivity in Cement. In *Calcined Clays for Sustainable Concrete—Proceedings of the 1st International Conference on Calcined Clays for Sustainable Concrete*; Scrivener, K., Favier, A., Eds.; RILEM Bookseries; Springer: Dordrecht, The Netherlands, 2015; Volume 10, pp. 43–50. [CrossRef]
34. Gmür, R.; Thienel, K.-C.; Beuntner, N. Influence of aging conditions upon the properties of calcined clay and its performance as supplementary cementitious material. *Cem. Concr. Compos.* **2016**, *72*, 114–124. [CrossRef]
35. Sposito, R.; Schmid, M.; Beuntner, N.; Scherb, S.; Plank, J.; Thienel, K.-C. Early hydration behavior of blended cementitious systems containing calcined clays and superplasticizer. In Proceedings of the 15th International Congress on the Chemistry of Cement, Prague, Czech Republic, 16–20 September 2019; p. 10.
36. *DIN EN ISO 11885*; Water Quality—Determination of Selected Elements by Inductively Coupled Plasma Optical Emission Spectrometry (ICP-OES). DIN: Berlin, Germany, 2009; p. 37.
37. Sposito, R.; Maier, M.; Beuntner, N.; Thienel, K.-C. Physical and mineralogical properties of calcined common clays as SCM and their impact on flow resistance and demand for superplasticizer. *Cem. Concr. Res.* **2022**, *154*, 106743. [CrossRef]
38. *DIN ISO 9277*; Determination of the Specific Surface Area of Solids by Gas Adsorption—BET Method. DIN: Berlin, Germany, 2003; p. 19.
39. *DIN EN 196-3*; Prüfverfahren für Zement—Teil 3: Bestimmung der Erstarrungszeiten und der Raumbeständigkeit (Methods of Testing Cement—Part 3: Determination of Setting Times and Soundness). DIN: Berlin, Germany, 2009; p. 17.
40. Puntke, W. Wasseranspruch von feinen Kornhaufwerken. *Beton* **2002**, *52*, 242–248.

41. *DIN EN ISO 17892-3*; Geotechnical Investigation and Testing—Laboratory Testing of Soil—Part 3: Determination of Particle Density. DIN: Berlin, Germany, 2015; p. 21.
42. *ISO 13320*; Particle Size Analysis—Laser Diffraction Methods. ISO: Geneva, Switzerland, 2020; p. 59.
43. Sposito, R.; Beuntner, N.; Thienel, K.-C. Rheology, setting and hydration of calcined clay blended cements in interaction with PCE-based superplasticisers. *Mag. Concr. Res.* **2021**, *73*, 785–797. [CrossRef]
44. *DIN EN 933-1*; Pru"fverfahren fu"r Geometrische Eigenschaften von Gesteinskörnungen—Teil 1: Bestimmung der Korngrößenverteilung—Siebverfahren (Tests for Geometrical Properties of Aggregate—Part 1: Determination of Particle size Distribution—Sieving Method). DIN: Berlin, Germany, 2012; p. 19.
45. Okamura, H.; Ouchi, M. Self-Compacting Concrete. *J. Adv. Concr. Technol.* **2003**, *1*, 5–15. [CrossRef]
46. Le, H.T.; Kraus, M.; Siewert, K.; Ludwig, H.M. Effect of macro-mesoporous rice husk ash on rheological properties of mortar formulated from self-compacting high performance concrete. *Constr. Build. Mater.* **2015**, *80*, 225–235. [CrossRef]
47. Barnes, H.A.; Walters, K. The yield stress myth? *Rheologica Acta* **1985**, *24*, 323–326. [CrossRef]
48. Hackley, V.A.; Ferraris, C.F. *Guide to Rheological Nomenclature—Measurements in Ceramic Particulate Systems*; National Institute of Standards and Technology: Gaithersburg, MD, USA, 2001; Volume 3, p. 29.
49. *DIN EN 12504-4*; Prüfung von Beton in Bauwerken—Teil 4: Bestimmung der Ultraschallgeschwindigkeit (Testing concrete in structures—Part 4: Determination of ultrasonic pulse velocity). DIN: Berlin, Germany, 2004; p. 15.
50. Lootens, D.; Bentz, D.P. On the relation of setting and early-age strength development to porosity and hydration in cement-based materials. *Cem. Concr. Compos.* **2016**, *68*, 9–14. [CrossRef] [PubMed]
51. *DIN EN 60825-1*; Sicherheit von Lasereinrichtungen—Teil 1: Klassifizierung von Anlagen und Anforderungen (Safety of Laser Products—Part 1: Equipment Classification and Requirements). DIN: Berlin, Germany, 2015; p. 15.
52. Snellings, R.; Chwast, J.; Cizer, Ö.; Belie, N.; Dhandapani, Y.; Durdziński, P.; Elsen, J.; Haufe, J.; Hooton, D.; Patapy, C.; et al. RILEM TC-238 SCM recommendation on hydration stoppage by solvent exchange for the study of hydrate assemblages. *Mater. Struct.* **2018**, *51*, 1–4. [CrossRef]
53. Marsh, B.K.; Day, R.L. Pozzolanic and cementitious reactions of fly ash in blended cement pastes. *Cem. Concr. Res.* **1988**, *18*, 301–310. [CrossRef]
54. *DIN 66133*; Bestimmung der Porenvolumenverteilung und der spezifischen Oberfläche von Feststoffen durch Quecksilberintrusion (Determination of Pore Volume Distribution and Specific Surface Area of Solids by Mercury Intrusion). DIN: Berlin, Germany, 1993; p. 3.
55. *DIN EN 196-1*; Prüfverfahren für Zement—Teil 1: Bestimmung der Festigkeit (Methods of Testing Cement—Part 1: Determination of Strength). DIN: Berlin, Germany, 2016; p. 31.
56. Sposito, R.; Schmid, M.; Plank, J.; Thienel, K.-C. An approach to the rheological behavior of cementitious systems blended with calcined clays and superplasticizers. In Proceedings of the ACI SP 349 11th International Conference on Cementitious Materials and Alternative Binders for Sustainable Concrete, Online, 28 April 2021; pp. 659–685.
57. Zunino, F.; Scrivener, K. Studying the Influence of the Filler Effect of SCMs on the Sulfate Requirement of Blended Cements. In Proceedings of the ACI SP 349 11th International Conference on Cementitious Materials and Alternative Binders for Sustainable Concrete, Online, 22 April 2021; pp. 117–124.
58. Andrade Neto, J.D.S.; De la Torre, A.G.; Kirchheim, A.P. Effects of sulfates on the hydration of Portland cement—A review. *Constr. Build. Mater.* **2021**, *279*, 122428. [CrossRef]
59. Berodier, E.; Scrivener, K. Understanding the Filler Effect on the Nucleation and Growth of C-S-H. *J. Am. Ceram. Soc.* **2014**, *97*, 3764–3773. [CrossRef]
60. Thomas, J.J.; Jennings, H.M.; Chen, J.J. Influence of nucleation seeding on the hydration mechanisms of tricalcium silicate and cement. *J. Phys. Chem. C* **2009**, *113*, 4327–4334. [CrossRef]
61. Hesse, C.; Goetz-Neunhoeffer, F.; Neubauer, J. A new approach in quantitative in-situ XRD of cement pastes: Correlation of heat flow curves with early hydration reactions. *Cem. Concr. Res.* **2011**, *41*, 123–128. [CrossRef]
62. Barluenga, G.; Puentes, J.; Palomar, I. Early age monitoring of self-compacting concrete with mineral additions. *Constr. Build. Mater.* **2015**, *77*, 66–73. [CrossRef]
63. *ASTM C1679-17*; Standard Practice for Measuring Hydration Kinetics of Hydraulic Cementitious Mixtures Using Isothermal Calorimetry. ASTM International: West Conshehoken, PA, USA, 2018; p. 13.
64. Palou, M.; Boháč, M.; Kuzielová, E.; Novotný, R.; Žemlička, M.; Dragomirová, J. Use of calorimetry and thermal analysis to assess the heat of supplementary cementitious materials during the hydration of composite cementitious binders. *J. Therm. Anal. Calorim.* **2020**, *142*, 97–117. [CrossRef]
65. Ma, J.; Yu, Z.; Shi, H.; Zhang, Y.; Shen, X. Long-term hydration behavior and pore structure development of cement–limestone binary system. *J. Therm. Anal. Calorim.* **2021**, *143*, 843–852. [CrossRef]
66. Qin, L.; Gao, X.; Zhang, A. Potential application of Portland cement-calcium sulfoaluminate cement blends to avoid early age frost damage. *Constr. Build. Mater.* **2018**, *190*, 363–372. [CrossRef]
67. Ye, G.; Liu, X.; De Schutter, G.; Poppe, A.M.; Taerwe, L. Influence of limestone powder used as filler in SCC on hydration and microstructure of cement pastes. *Cem. Concr. Compos.* **2007**, *29*, 94–102. [CrossRef]

68. Laidani, Z.E.-A.; Benabed, B.; Abousnina, R.; Gueddouda, M.K.; Kadri, E.-H. Experimental investigation on effects of calcined bentonite on fresh, strength and durability properties of sustainable self-compacting concrete. *Constr. Build. Mater.* **2020**, *230*, 117062. [CrossRef]
69. San Nicolas, R.; Cyr, M.; Escadeillas, G. Performance-based approach to durability of concrete containing flash-calcined metakaolin as cement replacement. *Const.r Build. Mater.* **2014**, *55*, 313–322. [CrossRef]
70. Vejmelková, E.; Koňáková, D.; Doleželová, M.; Scheinherrová, L.; Svora, P.; Keppert, M.; Reiterman, P.; Černý, R. Effect of calcined Czech claystone on the properties of high performance concrete: Microstructure, strength and durability. *Constr. Build. Mater.* **2018**, *168*, 966–974. [CrossRef]
71. Tironi, A.; Sposito, R.; Cordoba, G.P.; Zito, S.V.; Rahhal, V.; Thienel, K.-C.; Irassar, E.F. Influence of different calcined clays to the water transport performance of concretes. *Mag. Concr. Res.* **2022**, *12*, 1–13. [CrossRef]
72. *ASTM C311-22*; Standard Test Method for Sampling and Testing Fly Ash or Natural Pozzolans for Use in Portland-Cement Concrete. ASTM International: West Conshehoken, PA, USA, 2022; p. 11.

8.3 Calcined Clays from Nigeria—Properties and Performance of Supplementary Cementitious Materials Suitable for Producing Level 1 Concrete

Reprint

Published in the Journal “MDPI/Materials” (Section: Construction and Building Materials)

Materials **2023**, *16*(7), 2684; https://doi.org/10.3390/ma16072684

Authors: Abubakar Muhammad, Karl-Christian Thienel and Sebastian Scherb

materials

MDPI

Article

Calcined Clays from Nigeria—Properties and Performance of Supplementary Cementitious Materials Suitable for Producing Level 1 Concrete

Abubakar Muhammad *, Karl-Christian Thienel and Sebastian Scherb

Institut für Werkstoffe des Bauwesens, Universität der Bundeswehr München, 85577 Neubiberg, Germany
* Correspondence: abubakar.muhammad@unibw.de

Abstract: In this work, four naturally occurring (two kaolinite-rich and two smectite-rich) clay samples were collected from different areas around the Ashaka cement production plant, located in Gombe State, Nigeria and calcined in a laboratory. The mineralogical characterization of the clays was carried out by XRD. The hydration kinetics of the calcined clay–cement systems were monitored by isothermal calorimetry. Workability was determined using the flow table method. The reactivity of the calcined clays was determined from the solubility of Si and Al ions and the strength activity index. All calcined clays studied met the requirements of ASTM C618 for the use of natural pozzolans as a partial replacement for hydraulic cement. The metasmectite clays yielded a higher specific surface area, increased water demand, and less reactive Si and Al ions compared to the metakaolin clays. The two calcined clay groups require the addition of superplasticizer to achieve a workability class similar to the Portland cement mortar system. They can be used to replace Portland cement at replacement levels of up to 45%, in combination with limestone powder to form an LC^3 cement, thereby achieving at least a "Level 1" reduction in greenhouse gas emissions.

Keywords: clay mineralogy; calcined clay; hydration mechanism; ion solubility; workability; strength activity index; metakaolin; metasmectite

check for updates

Citation: Muhammad, A.; Thienel, K.-C.; Scherb, S. Calcined Clays from Nigeria—Properties and Performance of Supplementary Cementitious Materials Suitable for Producing Level 1 Concrete. *Materials* **2023**, *16*, 2684. https://doi.org/10.3390/ma16072684

Received: 23 February 2023
Revised: 23 March 2023
Accepted: 26 March 2023
Published: 28 March 2023

1. Introduction

Demand for shelters and other civil engineering infrastructure has recently increased in Nigeria and other African countries due to rapid urbanization and a high annual population growth rate [1,2]. To meet the country's infrastructural requirements, the Federal Government of Nigeria in partnership with private investors embarked on massive infrastructural development, such as construction of the Abuja world trade center, Eko Atlantic, and Lekki free trade zone. These projects and others ongoing in the country consume a large quantity of cement annually. The production of cement, an essential component of concrete, presents two major challenges. First, a large amount of energy is needed for its production and grinding. This is a problem especially in developing countries, making cement more expensive. Second, cement production accounts for about 6% to 10% of the global carbon emissions [2]. Although the total per capita carbon emissions of sub-Saharan Africa in 2018 were only 0.81 kt, below the 2.7 kt threshold for limiting global warming to below 2 °C by 2050 [3], the rate of urbanization in the region is increasing rapidly compared to the rest of the world, leading to an increase in demand for shelter and other concrete infrastructure, with a consequently higher demand for cement [1]. For example, the cement production capacity of Nigeria—the most populous country in the sub-Saharan region—was only 21 Mt in 2015, but increased to 28 Mt by 2020, and it is expected to reach 53 Mt in 2040 [4]. Although total carbon emissions from cement production were estimated at 11 $MtCO_2e$ in 2015, they increased to 15 $MtCO_2e$ in 2020 and are expected to reach 28 $MtCO_2e$ in 2040 [4].

In order to continue to benefit from the use of concrete as the main construction material and to limit its environmental impact, the use of concrete with lower embodied

carbon is necessary. One of the potential steps in the route map to achieve this is reducing the amount of clinker used per m^3 of concrete, as this is the main factor of embodied carbon in concrete [5]. Therefore, partial replacement of cement with supplementary cementitious materials (SCMs) that require less energy for production and release less CO_2 is essential to help limit global warming [6]. One of these SCMs that has the potential to replace a high percentage of cement is calcined clay (CC) [2]. This material is particularly suitable for Nigeria with a lower supply of conventional SCMs such as fly ash, slag, and silica fume [7].

Common clays can be used as reactive SCMs after thermal activation [8–10]. The mineralogical diversity consisting of activatable phyllosilicates (e.g., kaolinite, illite, and smectite) and accompanying minerals (e.g., quartz and feldspars) inevitably requires an individual characterization (e.g., mineralogical and chemical composition) of each clay deposit to verify its suitability as SCM [11]. The R^3 test [12,13] or the determination of the solubility of silicon and aluminum in alkaline solution [14,15] has been shown to be reliable for assessing the reactivity of CC [11,16]. As an indirect method, determining the strength activity index (SAI) has been shown to be accurate for evaluating the pozzolanic potential of CC as a partial replacement for cement [9]. In addition to mineralogical and chemical composition and the reactivity of the CC, physical properties such as water demand are important factors that significantly influence the possibilities of high replacement levels [17]. The higher water demand and higher specific surface area of CC in comparison to cement negatively affect the workability of the system [18], which is an important attribute, especially when considering the ease of compactability, which in turn affects strength and durability of mortar and concrete [19].

The pozzolanic potential of a CC for its intended use in concrete and mortar can be evaluated according to the provisions of ASTM C618 [20]. To obtain the relative performance of the CC blended cement, 20 wt.% ordinary Portland cement (OPC) is substituted with CC, and the w/p is adjusted to achieve a flow diameter similar to OPC system. In this study, a constant volumetric proportioning system was used as previously described in [21]. OPC was replaced on a volumetric basis while maintaining the same amounts of limestone powder (LP), sand, and water. SP was added to the CC mortar system to achieve a workability class similar to that of the OPC mortar system.

The great potential of CC is based on physical effects such as the filler effect [22,23] and the adsorption of ions from the pore solution [24], as well as on the release of silicon and aluminum ions at an early time of hydration [15,25]. This is evidenced by a strong influence of the early clinker hydration in CC blended systems [26–28]. The released aluminum exploits its full potential, especially in the presence of LP [18,29,30]. When CC and LP are blended and used as a substitute for clinker, they promote the formation of monocarboaluminate/hemicarboaluminate AFm phases and densify the concrete microstructure, which in turn have positive effects on the mechanical and durability properties of mortar and concrete [18,31–33].

Using the technology of LC^3 cement [34,35] (50 wt.% ground clinker, 30 wt.% CC, 15 wt.% LP, and 5 wt.% gypsum), which is currently gaining more attention in the global construction market, reactive kaolinite-rich CC (40 wt.% kaolinite and above) achieves a 28 day compressive strength similar to the OPC reference system [36]. However, clays with low kaolinite content should also come into focus due to their economic and ecological advantages and lower competition with other industries. For many simple applications that can solve the housing shortage in the sub-Saharan African region, these clays could be of great interest.

2. Research Gap

Numerous investigations have been carried out on the suitability of replacing up to 45 wt.% OPC with a blend of CC and LP forming LC^3 cement (e.g., [34,36,37]). Some criteria have been established as a basis for the selection of the appropriate CC, which include the mineralogical composition of the raw clay, the oxide composition, its reactivity, and its pozzolanic potentials. There are no previous studies in the literature on the potential use of

the CCs presented in this manuscript in LC^3 cements. Therefore, this work investigates the suitability of four common clays from Gombe State, Nigeria, for use as SCMs to achieve at least a "Level 1" reduction in greenhouse gas emissions. The focus is on determining the mineralogical composition, physical and chemical properties, and effects of CC on the hydration mechanism, workability, and SAI of the OPC.

3. Materials and Methods

3.1. Selection of the Nigerian Raw Clays

Nigeria has different cement manufacturers across its regions. Figure 1 shows some of the cement plants, most of which are located near limestone deposits [38], as well as the location of the sampling sites. The potential of clay deposits in the vicinity of some of the cement plants has already been established. For instance, clay from Ogun State has already been studied by [39–41]. The current research, therefore, focuses on studying the clay deposits around the Ashaka cement plant. Four raw clay samples were collected from the areas of the Nafada, Kwami, and Billiri local governments of Gombe state and denoted as NRC (Nigerian raw clay)-1 to NRC-4.

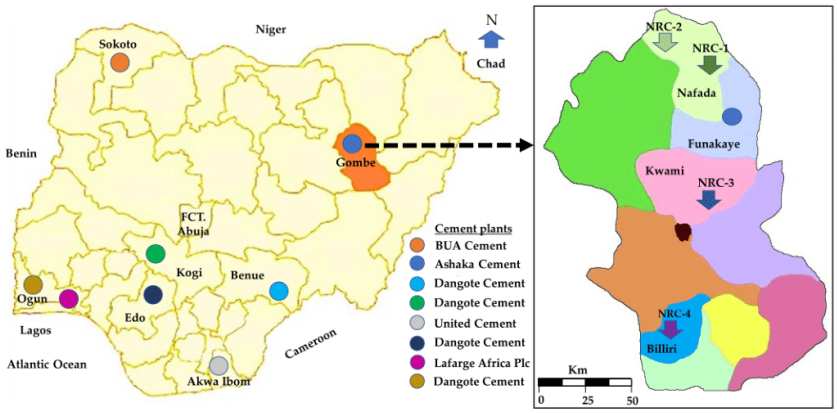

Figure 1. Map of Nigeria obtained from [42]. The location of different cement plants and of the sampling sites are added.

3.2. Methods

3.2.1. Calcination and Grinding of NRC

After delivery, the NRCs were dried at 60 °C in the laboratory oven for 24 h and ground in a rotary disc mill (Retsch, RS 200) at 700 rpm for 5 min for further investigation. On the basis of the development of the thermal decomposition presented in Figure 2, the NRCs were calcined for 30 min using a laboratory muffle furnace at a temperature of 750 °C (red lines in Figure 2); after cooling to ambient temperature, they were subsequently ground in a rotary disc mill at 700 rpm for 5 min and labeled after calcination as NCC (Nigerian calcined clay)-1 to NCC-4. From this point on, the term "meta" refers to the calcined material.

3.2.2. Characterization of the Cement, Limestone Powder, and Superplasticizer

The cement used (CEM I 42.5 R) complied with DIN EN 197-1 [43]. It contained (wt.%) 61.6 C_3S, 18.2 C_2S, 5.8 C_3A, 9.0 C_4AF, 3.2 sulfate, and 0.6 calcite as the mineralogical phases (according to manufacturer's information). The limestone contained 99.8 wt.% calcite and 0.2 wt.% quartz. SP with a solid content of 38.6 wt.%, anionic charge density of 1390 µmol/g, molecular weight of 25,992 g/mol, and side-chain length of n_{EO} = 31 as specified by the supplier was used. Standard sand according to EN 196-1 [44] was used as fine aggregate for mortar tests.

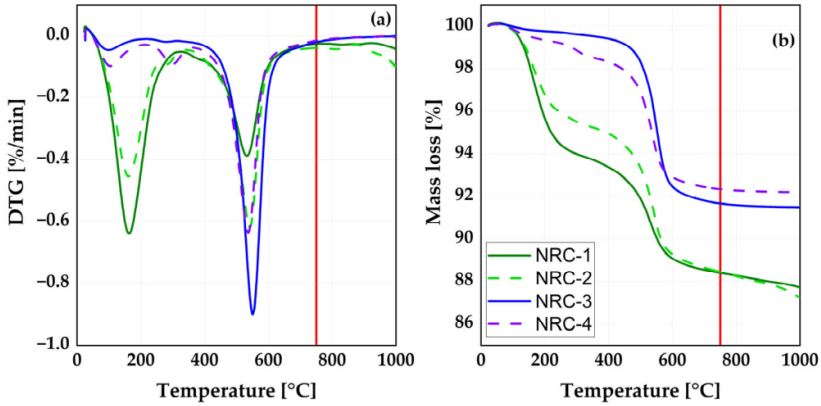

Figure 2. Differential thermal analysis (**a**) and mass loss (**b**) of the raw clays.

3.2.3. Characterization of the Raw and Calcined Nigerian Clays

Thermal decomposition of the clay mineral phases was investigated using thermogravimetric (TG) analysis conducted in Netzsch STA 449 F3 Jupiter equipment with a heating rate of 2 °C/min. Further quantification of the mineralogical composition of the NRC was determined by X-ray diffraction using a side-loading preparation in a PANalytical Empyrean diffractometer, with CuKα radiation (1.54 Å) at 40 kV and 40 mA; Rietveld refinement was performed using Profex-BGMN [45]. Since there was no significant amount of amorphous phase in the NRC, the values were normalized to 100%. Inductively coupled plasma optical emission spectrometry (ICP-OES) was used to determine the oxide content of the NCCs after melt fusion as described in [46] in accordance with DIN EN ISO 11885 [47]. The reactivity of the NCCs was evaluated by eluting the NCCs in NaOH solution (10%) for 24 h to determine the solubility of silicon (Si) and aluminum (Al) ions according to the method specified by [48] and described in [46,49].

The determined physical parameters of the NCCs included the particle density measured using a helium pycnometer, according to DIN EN ISO 17892-3 [50], the BET specific surface area measured using a HORIBA SA-9600 series surface area analyzer, according to DIN ISO 9277 [51], particle size distribution (PSD) determined using laser light diffraction (Bettersizer, 3P instrument) [30], and water demand based on the Puntke method [52].

3.2.4. Performance in Mortar and Early Hydration Behavior of the NCC

To evaluate the influence of NCCs on the workability and SAI of blends with OPC, two mortar series were investigated. The first with binary blends containing CC only as a substitute for OPC at 20 vol.%, designated as M—the reference system, with OPC only as a binder, and MN-1 to 4 (mortar produced with NCC-1 to 4 substituting OPC at 20 vol.%). The second batch of the ternary blends, labeled ML, constituted mortars produced with LP substituting OPC at 15 vol.% (later on referred to as Portland limestone cement (PLC)), and MLN-1 to 4 (containing 55 vol.% OPC, 15 vol.% LP, and 30 vol.% of NCC-1 to 4). Table 1 shows the gravimetric mix designs of the different mortar systems. The constituents were mixed in a stainless-steel 5 L bowl mixer according to DIN EN 196-1 [44]. The flow diameter of the fresh mortar was determined according to DIN EN 1015-3 [53]. For the SAI, the mortar was poured into sets of 40 mm × 40 mm × 160 mm steel molds and compacted on a vibrating table according to [44]. The specimens were covered and stored moist for 48 h, and then cured under water. The compressive strength was tested at 7, 28, and 90 days using the Form + Test Prüfsysteme Alpha 1-3000 testing equipment at an increased uniform loading rate of 2400 ± 200 N/s till failure. The SAI for each test age was calculated as the ratio of the compressive strength of the specimens with cement replacement to those without replacement, multiplied by 100 [54].

Table 1. Mortar mix designation.

Mix Designation	OPC [g]	LP [g]	CC [g]	Sand [g]	Water [g]	SP [%]
M	450	-	-	1350	225	-
MN-1	360	-	76	1350	225	0.30
MN-2	360	-	80	1350	225	0.30
MN-3	360	-	79	1350	225	0.30
MN-4	360		81	1350	225	0.30
ML	383	57	-	1350	225	-
MLN-1	248	57	113	1350	225	0.35
MLN-2	248	57	121	1350	225	0.35
MLN-3	248	57	118	1350	225	0.35
MLN-4	248	57	121	1350	225	0.35

Early hydration behavior of the OPC, binary blends of OPC and NCC, and ternary blends of OPC, LP, and NCC were monitored through isothermal calorimetric measurements using a TAM AIR eight-channel isothermal calorimeter. Two series of measurements were carried out: the first with 20 wt.% NCC replacing OPC (OPC-20NCC); the second with 55 wt.% OPC, 15 wt.% LP, and 30 wt.% NCC (OPC-15LP-30NCC). Both series were performed with a water-to-binder ratio (w/b) of 0.5. The test procedure is given in [55]. The heat flow was measured up to 48 h, and the result was normalized to 1 g of cement. According to the LC^3 (CEM II/C-M (Q-LL) [56]) system recipe, the calorimetry was also performed on sulfated systems with an increased content of 5 wt.%.

4. Results

4.1. Characterization of the Clays

4.1.1. Nigerian Raw Clay Characterization

Figure 2a depicts the differential thermal decomposition of the NRC mineral phases and their accompanied mass loss due to decomposition (Figure 2b). Some similarities and distinctions among the clays could easily be identified. NRC-1 and 2 showed a typical differential thermal analysis (DTG) curve pattern of a smectitic clay, whereas NRC-3 and 4 showed a DTG curve pattern of a kaolinitic clay. All NRCs exhibited mass loss at lower temperatures (100 °C) due to the release of free water. The smectite-rich clays had a greater mass loss between the temperatures of 100 and 300 °C, associated with the removal of water bound to the outer surfaces of the clay minerals. At an intermediate temperature (400 to 650 °C), the kaolinite-rich clays exhibited more dehydroxylation than the smectite-rich clays. On the basis of the results, the calcination temperature for all NRCs was set at 750 °C, between the dehydroxylation and recrystallization temperatures.

Figure 3 displays the diffraction pattern of all four NRCs. The y-axes are shifted in the cases of NRC-1, 2, and 4 (the maximum shift for NRC-1 was 1000 counts). The large smectite peak was clearly visible for NRC-1 and 2. Kaolinite and quartz were visible for all four clays. Quantification of the various mineralogical phases is provided in Table 2. NRC-1 and NRC-2 were smectite-rich clays containing about 70 wt.% smectite and about 13 and 22 wt.% kaolinite, respectively. NRC-3 and NRC-4 were kaolinite-rich clays (56 and 49 wt.%, respectively) and they contained more than 30 wt.% quartz as the second main phase.

Table 2. Mineralogical composition of the raw clays (wt.%).

Materials	Kaolinite	Smectite	Quartz	Mica/Illite	Rutile/Anatase	Hematite	Gypsum
NRC-1	13	71	6	10	-	-	<1
NRC-2	22	68	4	-	2	-	4
NRC-3	56	-	34	6	3	-	-
NRC-4	49	-	42	6	2	1	-

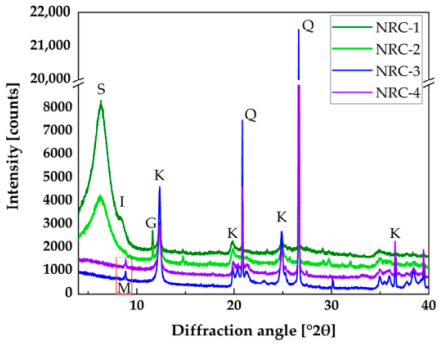

Figure 3. XRD patterns of the NRC: K—kaolinite, S—smectite, Q—quartz, M—mica, I—illite, and G—gypsum. The y-axes are shifted in the cases of NRC-1, 2, and 4 (the maximum shift for NRC-1 was 1000 counts).

Table 3 provides the oxide composition of the four NCCs. The content of sulfur trioxide (SO_3) and the loss on ignition (LOI) of all clays were within the thresholds specified by ASTM C618 [20]. Furthermore, the summation of the SiO_2, Al_2O_3, and Fe_2O_3 contents of all clays was greater than 70 wt.% (the minimum recommended by ASTM C618). Therefore, from the oxide composition point of view, all four NCCs satisfied the minimum requirements specified by [20] for the use of natural pozzolans as cement replacement.

Table 3. Oxide composition of the CC (wt.%).

Materials	SiO_2	Al_2O_3	CaO	MgO	Fe_2O_3	TiO_2	K_2O	Na_2O	SO_3	LOI
NCC-1	55.0	19.1	1.3	3.1	7.7	1.0	1.8	8.6	0.8	1.6
NCC-2	54.3	24.5	1.9	2.1	9.5	1.1	1.5	0.2	1.9	3.0
NCC-3	68.1	24.7	0.1	0.1	2.5	3.5	0.4	<0.1	<0.1	0.5
NCC-4	68.2	20.4	0.2	0.2	8.2	1.5	0.7	<0.1	<0.1	0.6

The metakaolin-rich CC had a lower specific surface area than the metasmectite-rich ones. The order of increasing surface area was NCC-3 < NCC-4 < NCC-2 < NCC-1. The variation of the specific surface area had a less significant effect on the water demand and density of the NCC, as shown in Table 4. Similar to the surface area, the same sequence of increasing water demand was observed, with smaller differences between samples. All four NCCs had almost similar density values ranging from 2.66 to 2.85 g/cm^3. NCC-3 had the finest particle size distribution among the four NCCs with a d_{50} of 13.8 µm, followed by NCC-2 (d_{50} = 21.7 µm) and NCC-4 (d_{50} = 28.2 µm), while NCC-1 (d_{50} = 34.5 µm) had the coarsest particle size distribution.

Table 4. Physical properties of the OPC, LP, and CC.

Materials	Specific Surface Area [m^2/g]	Water Demand [wt.%]	Density [g/cm^3]	d_{10} [µm]	d_{50} [µm]	d_{90} [µm]
OPC	1.0	28.9	3.17	2.6	16.0	42.8
LP	1.6	20	2.71	0.8	4.6	20.7
NCC-1	95.9	37.3	2.66	5.4	34.5	155.0
NCC-2	75.4	35.1	2.83	2.9	21.7	85.8
NCC-3	16.7	31.6	2.78	2.3	13.8	61.0
NCC-4	32.0	32.5	2.85	3.6	28.2	72.3

4.1.2. Reactivity Assessment of the NCC

Figure 4 provides the Si and Al ion solubilities of the NCCs, where the numbers placed above the bars denote the Si/Al ratio. NCC-3 released the most Si and Al ions, followed by

NCC-4, NCC-2, and NCC-1. NCC-3 and NCC-4 were metakaolin-rich clays with a Si/Al ratio approximately equal to 1.0. NCC-2 had a Si/Al ratio of 1.49, while NCC-1 had the highest Si/Al ratio of 2.24.

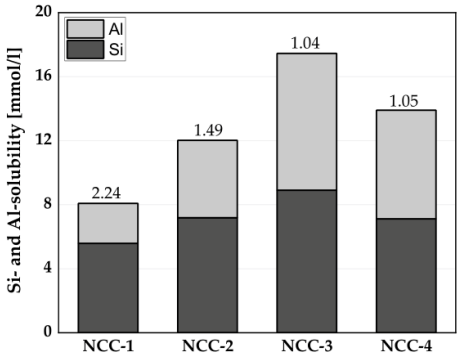

Figure 4. Si and Al ion solubilities of the CC.

4.2. Influence of NCCs and LP on Mortar Proparties

When substituting part of the cement with NCCs, the water demand of the system increased, which affected the workability of the mortar. Figure 5 shows the influence of the CC with and without LP on the flow spread of the mortar. All CC mortar systems demanded an increased amount of water to attain a slump flow similar to OPC and PLC (the reference systems), due to their higher water demand compared to OPC and PLC. Consequently, the w/b ratio must be adjusted or an SP dosage must be added when CC is used as a partial replacement for OPC and PLC, until a slump flow of ±5 cm is achieved compared to the reference mortar mix. In this study, a constant SP dosage of 0.3 and 0.35 wt.% of binder was used to bring both the M and ML systems to a slump flow approximately ±5 cm of the reference mortar. In both systems, the effect of the NCC on the flow diameter of the mortar was in the following order: NCC-1 > NCC-2 > NCC-4 > NCC-3. However, this effect across the NCCs is rather narrow, as there were no significant differences in slump flow values. Therefore, both the metakaolin and the metasmectite systems had a similar effect on the mortar workability.

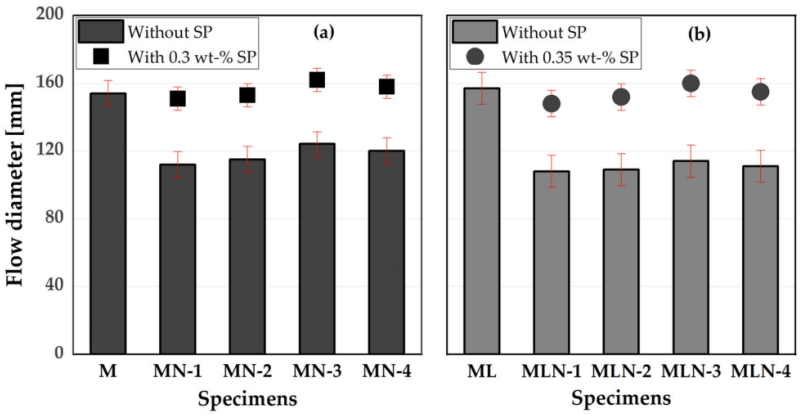

Figure 5. Influence of CC and LP on the flow spread of the mortar: (**a**) 20 vol.% CC + 80 vol.% OPC; (**b**) 30 vol.% CC + PLC.

The pozzolanic activity of all four NCCs at 20 vol.% cement replacement was quite similar at 7 days and exceeded the minimum of 75% SAI of the OPC as recommended by

ASTM C618 [20]. After 28 days of curing, the SAI improved with a clear distinction across the four NCCs, which could be attributed to the differences in the solubility of the Si and Al ions, as depicted in Figure 4. At 28 and 90 days, the MN-3 mixture attained a SAI of more than 100% as a binary blended system. This is due to the higher solubility of Si and Al ions in NCC-3 compared to other NCCs (Figure 3). With the ternary blend of 30 vol.% NCC and 15 vol.% LP in the MLN mortars, lower compressive strength values were achieved, and the SAI fell below the recommended 75% SAI value, as shown in Figure 6b. After 28 and 90 days of curing, only the metakaolin-rich NCC mortar systems achieved the minimum SAI of 75%, while the SAI of the metasmectite-rich NCCs fell below the recommended value of 75%.

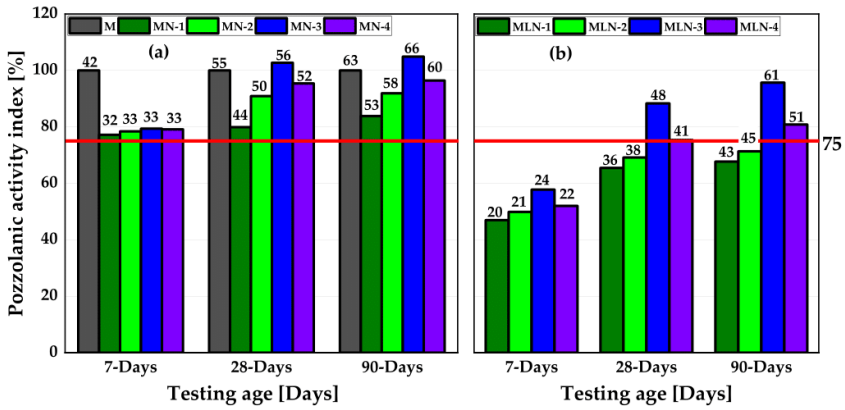

Figure 6. SAI of the mortars: (**a**) 20 vol.% CC + 80 vol.% OPC; (**b**) 30 vol.% CC + 15 vol.% LP and 55 vol.% OPC. The numbers placed above the bars denote the compressive strength value in MPa, approximated to the nearest whole number.

The actual performance of the NCC blended cement mixes compared to PLC is shown in Figure 7. Here, all NCC blended cements achieved a pozzolanic activity index >75% after 28 days of curing, making them suitable as substitutes for PLC in concrete and mortar. Again, the mortar made with NCC-3 exceeded the reference at 28 and 90 days resulting, in a SAI greater than 100%.

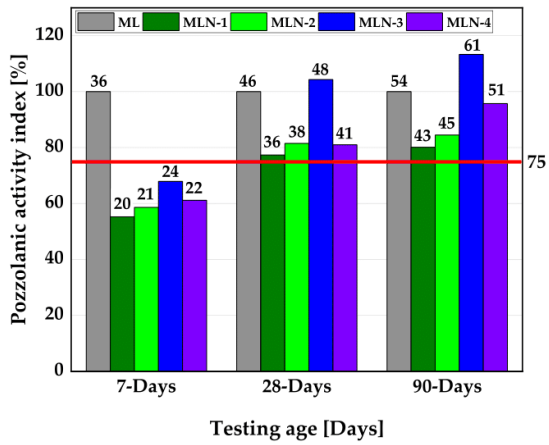

Figure 7. SAI of the NCC mortars compared to PLC mortar mixes. The numbers placed above the bars denote the compressive strength value in MPa, approximated to the nearest whole number.

4.3. Influence of NCC on Early Hydration

Heat flow curves obtained for OPC-20NCC and OPC-15LP-30NCC are presented in Figure 8a and b, respectively. While the addition of 20 wt.% NCC led to a comparable acceleration of the silicate reaction for all four NCCs (occurrence after about 9 h), a significant time shift could be observed for the aluminate reaction. Comparing the physical parameters of the NCCs, no correlation could be drawn between the PSD or BET surface area and the acceleration of the silicate and aluminate reaction. Despite considerable differences, the physical filler effect seemed to be comparable for all NCCs. Maier et al. [24] assumed the agglomeration effects of CC particles as one of the reasons for the different behavior of CC compared to limestone powders. Such agglomerations could also be a reason for the small differences in silicate reaction among the NCCs. The formation of the aluminate peak occurred after 25 h (NCC-1) and 20 h (NCC-2) in the mixtures with metasmectite-rich CC and after 16 h (NCC-3) and 14 h (NCC-4) in the mixtures with metakaolin-rich CC. Overall, a clear distinction could be made between silicate and aluminate reactions, and the onset of the aluminate reaction [57] was clearly visible for all 20NCC systems.

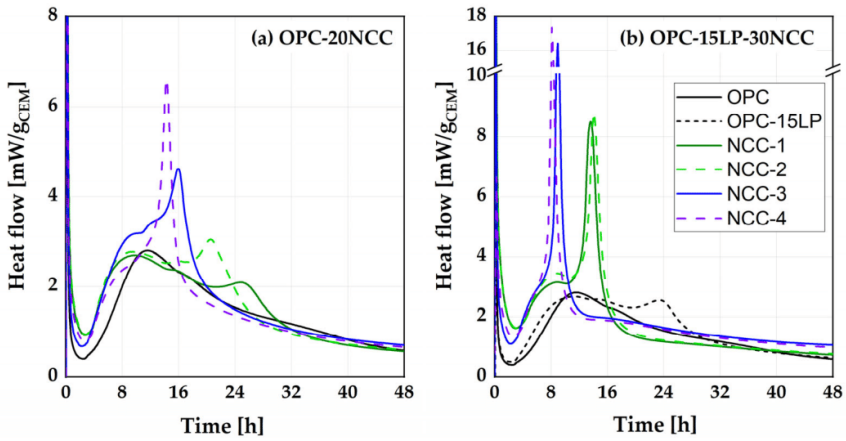

Figure 8. Heat flow of OPC-20NCC (**a**) and of OPC-15LP-30NCC (**b**) systems.

The addition of 15LP30NCC led to a pairwise similar curve shape of the metasmectite- and metakaolin-rich samples (Figure 8b). While the end of the dormant period was comparable for all four NCCs, the aluminate reaction was strongly accelerated to such an extent that it overlapped with the silicate reaction between 8 and 9 h, and no onset of the aluminate reaction was detectable for the metakaolin-rich NCCs, indicating an undersulfated system, as previously observed by [23,24,28]. For the metasmectite-rich CC, the differentiation between the silicate reaction (between 8–9 h) and the aluminate reaction after 14 h was still possible.

The current study considered, in addition to the adsorption of SO_3 on CSH phases [22,57], the adsorption of ions from the pore solution onto the negatively charged surface of the CC particles [58] as a major reason for the different shift in aluminate reaction [24,59]. In this context, various metaclay minerals exhibit markedly different surface properties (e.g., zeta potential), as shown by Schmid and Plank through interactions with superplasticizers [58].

Figure 9 displays the influence of further substituting the OPC with 5 wt.% G (G = gypsum) on the hydration behavior of OPC-15LP-30NCC systems. The authors are aware that 5 wt.% gypsum is the maximum allowable amount. Nevertheless, an additional 5 wt.% was added to the 1.6 wt.% already present in the OPC to monitor the degree of sulfation required by different OPC-15LP-30NCC binder systems. The additional gypsum led to a shift in the aluminate reaction toward 23–24 h for the metakaolinite-rich systems. This was very well balanced compared to OPC-15LP. In comparison, no clear aluminate peak could be identified in the metasmectite-rich samples due to the further addition

of gypsum, already indicating a too high sulfate dosage for these systems. The lower sulfate requirement for 2:1 compared to 1:1 meta-phyllosilicates is in line with previous studies [26].

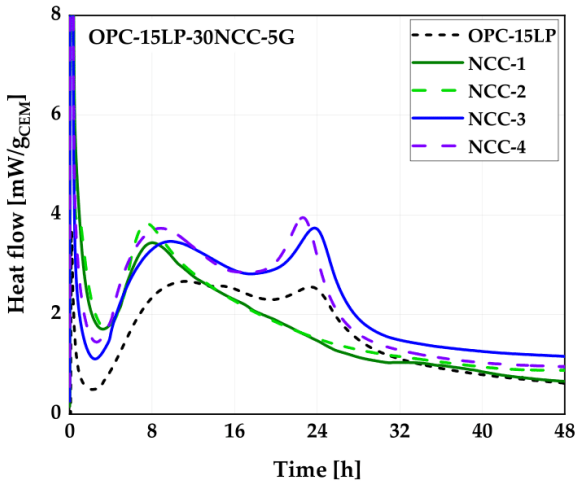

Figure 9. Heat flow of the OPC-15LP-30NCC systems with 5 wt.% G.

The heat of hydration values per gram of cement after 48 h (Table 5) revealed a significant increase with the addition of both 20NCC and 15LP-30NCC compared to the respective reference mixture. Within the series of measurements, however, the different NCCs exhibited hardly any differences. Clear differences could only be detected between the metakaolin- and smectite-rich systems when gypsum was added (OPC-15LP-30NCC-5G). The metakaolin-rich samples had about 20% higher heat of hydration compared to the metasmectite-rich samples. This could have been due to the strong overlapping of the silicate and aluminate reaction in the undersulfated systems and, thus, a higher reaction rate of the clinker phases for the balanced system. Since metakaolin is able to independently form a high content of hydrate phases at early times of hydration [15], the higher heat of hydration could also be explained by a chemical contribution of metakaolin and, thus, additional hydrate phase formation. Hence, the additional gypsum provided an improvement in performance only for the metakaolin-rich samples, while no improvement could be derived for metasmectite-rich samples in terms of the heat of hydration.

Table 5. Hydration heat [J/g_{CEM}] of OPC-20NCC and OPC-15LP-30NCC(+5G) systems after 48 h.

Specimens	OPC-20NCC	OPC-15LP-30NCC	OPC-15LP-30NCC-5G
OPC	254	-	-
PLC	-	270	-
NCC-1	300	349	346
NCC-2	307	332	349
NCC-3	320	361	426
NCC-4	293	340	426

5. Discussion

Among the four clays studied in detail, two were kaolinite-rich, while the other two were smectite-rich clays. Previous studies [29,36] revealed the possibility of substituting up to 45 wt.% cement with a blend of 15 wt.% LP and 30 wt.% reactive metakaolin. Reactive metakaolin is considered particularly suitable in this context due to its early age reactivity potential. The two metakaolin-rich CCs (NCC-3 and NCC-4) released the most reactive silicon and aluminum ions compared to the metasmectite ones, obviously indicating good

pozzolanic potential [60,61]. Both groups of CCs could be used as partial replacement of cement in order to obtain decarbonized concrete.

Partial replacement of cement with CC is one of the potential pathways to achieve a clinker-efficient cement [4]. Although clinker is the most important component of cement and contributes greatly to the strength formation of concrete, its production is the main driver of the embodied carbon in concrete [62]. The current challenge is how to further decarbonize concrete without compromising its engineering properties such as workability, strength, and durability. In this context, the performance of NCC mortar compared to OPC can be explained in two aspects.

First, the actual performance of the NCCs in relation to the compressive strength development and their effect on the workability of the mortar qualify them for use as SCMs in concrete. Both the binary and the ternary blends of NCCs and LP reduced the workability of the mortar, requiring the addition of up to 0.35% SP to achieve similar performance to the OPC and PLC mortar reference system (Figure 5). This would incur additional but negligible costs considering the ≥20 vol.% and replacement of cement with a less costly material. Moreover, considering development of the compressive strength, the binary mix with CC (20 vol.% cement replacement) had less impact on the compressive strength development after 28 days of curing. The minimum strength achieved was 44 MPa for the OPC-NCC composite cement, which is enough for use in plastering and general production of concrete up to grade C40/50, except for the production of precast elements which require a higher early strength [63,64] than achievable with these blends without further measures [65]. For the ternary composite cements, the same application holds for the metakaolin-rich NCCs, whereas for the metasmectite-rich NCCs, the compressive strength after 28 days of curing was 36 and 38 MPa for MLN-1 and 2, respectively. This limits their use to general construction work under normal environmental conditions and the production of concrete up to grade C35/45. In practice, this concrete grade is sufficient for general construction works to provide the required concrete infrastructure in the sub-Saharan African region. Thus, it can significantly reduce the cost of cement and increase the affordability of houses.

Second, the performance of CC and LP can be used as a lever for the decarbonization of cement, which can help to reduce the cement industry's contribution to CO_2 emissions. The cement industry contributes about 6–7% of global CO_2 emissions, of which two-thirds are process-related (CO_2 released during calcination of limestone) and one-third are fuel-related [62]. The average greenhouse gas emissions from the use of CEM I for the production of C25/30 grade concrete are estimated at 237 kg CO_2 equivalent/m^3 of concrete [66]. Substituting this cement with CC at 20 vol.%, which releases only about 40% of the CO_2 released by OPC [67–69], results in a CO_2 reduction of 12%. For a ternary blend of 30% cement with 15% LP, a CO_2 reduction of about 30% is achieved. Therefore, from an environmental view point, the ternary blend of NCC, LP, and OPC achieved at least a "Level 1" reduction in the greenhouse gas emissions, according to the concrete sustainability council classification [66]. This makes it a suitable material for general concreting works in the sub-Saharan African region, where a high volume of construction work is expected in the near future.

As previously reported [18,70], the use of CC as a partial replacement for cement favors the precipitation of hemicarboaluminate phases from the aluminate and ettringite reaction, which occurred earlier and more broadly in the CC studied here in the following order: NCC-4 > NCC-3 > NCC-2 > NCC-1. A clear distinction also existed between the silicate and aluminate hydration maxima in all CC blended systems, except NCC-4, which had a strong overlap of these maxima. Therefore, at 20 wt.% CC replacement, only NCC-4 requires a sulfate adjustment to prevent flash setting and ensure sequential occurrence of the hydration maxima. For the ternary mixtures, the hydration kinetics of the blended cement changed. Here, the silicate and the aluminate peaks were merged together due to the rapid dissolution of sulfate in all ternary binders and occurred earlier in the metakaolin

systems than in the metasmectite systems [24]. Similar to NCC-4 binary binder systems, proper sulfation is urgently required in the ternary blend CC systems.

6. Conclusions

The contents of SO_3 and LOI, as well as the summation of the SiO_2, Al_2O_3, and Fe_2O_3 contents in all clays, were within the limits recommended by ASTM C618 for natural pozzolan to be used in concrete.

Although the metakaolin-rich CC released more reactive Si and Al ions compared to the metasmectite-rich CC, the metasmectite-rich CC also yielded relatively good reactivity both in a 20 vol.% binary mixture with cement and in a ternary mixture in the presence of LP with a combined 45% OPC substitution, as measured by isothermal calorimetry.

The metasmectite-rich CC had a larger specific surface and a higher water demand than metakaolin-rich CC. This would affect the workability of the mortars and necessitate the use of SP to achieve the same flow diameter as the OPC system.

In binary binders using 20 vol.% cement replacement, all CC mortar systems achieved a SAI greater than 75% at 7 days of hydration onward, the minimum value recommended by ASTM C618 for a natural pozzolan to be used as a pozzolanic cement replacement.

For the ternary mix containing 15 vol.% LP and 30 vol.% CC, in addition to OPC, the metasmectite-rich CC mortar systems did not reach the minimum SAI of 75% within 90 days when compared with OPC. The metakaolin-rich CC mortar systems, on the other hand, achieved the minimum requirement after only 28 days of curing.

Sulfate adjustment was not required for the binary CC binder systems except for NCC-4 and all ternary blended CC and LP systems, which require urgent sulfate adjustment to avoid flash setting and maintain the sequential formation of hydration peaks.

The Nigerian calcined clays NCC-1, NCC-2 and NCC-3 can be used as direct replacements for 20 vol.% of OPC without sulfate adjustment. For the production of LC^3 (CEM II/C-M (Q-LL) [56], NCC-3 and NCC-4 require sulfate adjustment to control the hydration properties of the blended LC^3 system.

The ternary blends of NCC, LP, and OPC achieved at least a "Level 1" reduction in greenhouse gas emissions.

Author Contributions: Conceptualization, A.M.; writing—original draft preparation, A.M.; writing—review and editing, A.M., S.S. and K.-C.T.; supervision, K.-C.T. All authors have read and agreed to the published version of the manuscript.

Funding: The first author was funded by the German Academic Exchange Service (DAAD) and the Nigerian Petroleum Technology Development Fund (PTDF): P3140941509075699. We acknowledge financial support by Universität der Bundeswehr München.

Institutional Review Board Statement: Not applicable.

Informed Consent Statement: Not applicable.

Data Availability Statement: Not applicable.

Conflicts of Interest: The authors declare no conflict of interest.

References

1. Schmidt, W.; Commeh, M.; Olonade, K.; Schiewer, G.L.; Dodoo-Arhin, D.; Dauda, R.; Fataei, S.; Tawiah, A.T.; Mohamed, F.; Thiedeitz, M.; et al. Sustainable circular value chains: From rural waste to feasible urban construction materials solutions. *Dev. Built Environ.* **2021**, *6*, 100047. [CrossRef]
2. Scrivener, K.L.; John, V.M.; Gartner, E.M. Eco-efficient cements: Potential economically viable solutions for a low-CO_2 cement-based materials industry. *Cem. Concr. Res.* **2018**, *114*, 2–26. [CrossRef]
3. Schmidt, W.; Otieno, M.; Olonade, K.; Radebe, N.; Van-Damme, H.; Tunji-Olayeni, P.; Kenai, S.; Tawiah, A.T.; Manful, K.; Akinwale, A.; et al. Innovation potentials for construction materials with specific focus on the challenges in Africa. *RILEM Tech. Lett.* **2020**, *5*, 63–74. [CrossRef]
4. Yetano Roche, M. Built for net-zero: Analysis of long-term greenhouse gas emission pathways for the Nigerian cement sector. *J. Clean. Prod.* **2023**, *383*, 135446. [CrossRef]

5. Mullholland, A.; Achkerman, C.; Astle, P.; Drewnlok, M.; Dunster, A.; Hibbert, A.; Imman, R.; Kershaw, R.; Martin, B.; McCague, C.; et al. *Low Carbon Concrete Routemap*; Institution of Civil Engineers: London, UK, 2022; p. 80.
6. Messner, D.; Schellnhuber, J.; Rahmstorf, S.; Klingenfeld, D. The budget approach: A framework for a global transformation toward a low-carbon economy. *J. Renew. Sustain. Energy* **2010**, *2*, 031003. [CrossRef]
7. Muhammad, A.; Thienel, K.-C.; Sposito, R. Suitability of Blending Rice Husk Ash and Calcined Clay for the Production of Self-Compacting Concrete: A Review. *Materials* **2021**, *14*, 6252. [CrossRef]
8. Fernandez, R.; Martirena, F.; Scrivener, K.L. The origin of the pozzolanic activity of calcined clay minerals: A comparison between kaolinite, illite and montmorillonite. *Cem. Concr. Res.* **2011**, *41*, 113–122. [CrossRef]
9. Tironi, A.; Trezza, M.A.; Scian, A.N.; Irassar, E.F. Assessment of pozzolanic activity of different calcined clays. *Cem. Concr. Compos.* **2013**, *37*, 319–327. [CrossRef]
10. Baronio, G.; Binda, L. Study of the pozzolanicity of some bricks and clays. *Constr. Build. Mater.* **1997**, *11*, 41–46. [CrossRef]
11. Maier, M.; Beuntner, N.; Thienel, K.-C. Mineralogical characterization and reactivity test of common clays suitable as supplementary cementitious material. *Appl. Clay Sci.* **2021**, *202*, 105990. [CrossRef]
12. Avet, F.; Snellings, R.; Alujas Diaz, A.; Ben Haha, M.; Scrivener, K. Development of a new rapid, relevant and reliable (R^3) test method to evaluate the pozzolanic reactivity of calcined kaolinitic clays. *Cem. Concr. Res.* **2016**, *85*, 1–11. [CrossRef]
13. Snellings, R.; Li, X.; Avet, F.; Scrivener, K. Rapid, Robust, and Relevant (R^3) Reactivity Test for Supplementary Cementitious Materials. *ACI Mater. J.* **2019**, *116*, 155–162. [CrossRef]
14. Buchwald, A.; Kriegel, R.; Kaps, C.; Zellmann, H.-D. Untersuchung zur Reaktivität von Metakaolinen für die Verwendung in Bindemittelsystemen. In Proceedings of the Gesellschaft Deutscher Chemiker e.V-Jahrestagung, Munich, Germany, 9–10 October 2003.
15. Scherb, S.; Maier, M.; Beuntner, N.; Thienel, K.-C.; Neubauer, J. Reaction kinetics during early hydration of calcined phyllosilicates in clinker-free model systems. *Cem. Concr. Res.* **2021**, *143*, 106382. [CrossRef]
16. Londono-Zuluaga, D.; Gholizadeh-Vayghan, A.; Winnefeld, F.; Avet, F.; Ben Haha, M.; Bernal, S.A.; Cizer, Ö.; Cyr, M.; Dolenec, S.; Durdzinski, P.; et al. Report of RILEM TC 267-TRM phase 3: Validation of the R3 reactivity test across a wide range of materials. *Mater. Struct.* **2022**, *55*, 142. [CrossRef]
17. Neißer-Deiters, A.; Scherb, S.; Beuntner, N.; Thienel, K.-C. Influence of the calcination temperature on the properties of a mica mineral as a suitability study for the use as SCM. *Appl. Clay Sci.* **2019**, *179*, 105168. [CrossRef]
18. Muhammad, A.; Thienel, K.-C.; Sposito, R. Suitability of Clinker Replacement by a Calcined Common Clay in Self-Consolidating Mortar—Impact on Rheology and Early Age Properties. *Minerals* **2022**, *12*, 625. [CrossRef]
19. Bhogayata, A.C.; Arora, N.K. Workability, strength, and durability of concrete containing recycled plastic fibers and styrene-butadiene rubber latex. *Constr. Build. Mater.* **2018**, *180*, 382–395. [CrossRef]
20. *ASTM C618-19*; Standard Specification for Coal Fly Ash and Raw or Calcined Natural Pozzolan for Use in Concrete. ASTM International: West Conshohocken, PA, USA, 2019.
21. Bentz, D.P.; Durán-Herrera, A.; Galvez-Moreno, D. Comparison of ASTM C311 strength activity index testing versus testing based on constant volumetric proportions. *J. ASTM Int.* **2012**, *9*, 1–7. [CrossRef]
22. Zunino, F.; Scrivener, K. Factors influencing the sulfate balance in pure phase C_3S/C_3A systems. *Cem. Concr. Res.* **2020**, *133*, 106085. [CrossRef]
23. Zunino, F.; Scrivener, K. Insights on the role of alumina content and the filler effect on the sulfate requirement of PC and blended cements. *Cem. Concr. Res.* **2022**, *160*, 106929. [CrossRef]
24. Maier, M.; Sposito, R.; Beuntner, N.; Thienel, K.-C. Particle characteristics of calcined clays and limestone and their impact on the early hydration and sulfate demand of blended cement. *Cem. Concr. Res.* **2022**, *154*, 15. [CrossRef]
25. Beuntner, N.; Thienel, K.-C. Pozzolanic efficiency of calcined clays in blended cements with focus on the early hydration. *Adv. Cem. Res.* **2022**, *34*, 341–355. [CrossRef]
26. Maier, M.; Scherb, S.; Neißer-Deiters, A.; Beuntner, N.; Thienel, K.-C. Hydration of cubic tricalcium aluminate in the presence of calcined clays. *J. Am. Ceram. Soc.* **2021**, *104*, 3619–3631. [CrossRef]
27. Maier, M.; Scherb, S.; Sposito, R.; Beuntner, N.; Thienel, K.-C. Parameters Influencing the Aluminate Clinker Reaction in Presence of Calcined Clay: Implications from Model Systems and Blended Cements. In Proceedings of the International Conference on Calcined Clays for Sustainable Concrete, Lausanne, Switzerland, 5–7 July 2022; pp. 112–113.
28. Zunino, F.; Scrivener, K. Studying the Influence of the Filler Effect of SCMs on the Sulfate Requirement of Blended Cements. In Proceedings of the ACI SP 349 11th International Conference on Cementitious Materials and Alternative Binders for Sustainable Concrete, Online, 22 April 2021; pp. 117–124. [CrossRef]
29. Scrivener, K.; Martirena, F.; Bishnoi, S.; Maity, S. Calcined clay limestone cements (LC^3). *Cem. Concr. Res.* **2018**, *114*, 49–56. [CrossRef]
30. Sposito, R.; Maier, M.; Beuntner, N.; Thienel, K.-C. Physical and mineralogical properties of calcined common clays as SCM and their impact on flow resistance and demand for superplasticizer. *Cem. Concr. Res.* **2022**, *154*, 106743. [CrossRef]
31. Beuntner, N.; Thienel, K.-C. Performance and properties of concrete made with calcined clays. In Proceedings of the ACI SP 320-10th ACI/RILEM International Conference on Cementitious Materials and Alternative Binders for Sustainabe Concrete, Montreal, QC, Canada, 2–4 October 2017; pp. 7.1–7.12. [CrossRef]
32. Tironi, A.; Sposito, R.; Cordoba, G.P.; Zito, S.V.; Rahhal, V.; Thienel, K.-C.; Irassar, E.F. Influence of different calcined clays to the water transport performance of concretes. *Mag. Concr. Res.* **2022**, *74*, 702–714. [CrossRef]

33. Zunino, F.; Scrivener, K. The reaction between metakaolin and limestone and its effect in porosity refinement and mechanical properties. *Cem. Concr. Res.* **2021**, *140*, 106307. [CrossRef]
34. Dhandapani, Y.; Sakthivel, T.; Santhanam, M.; Gettu, R.; Pillai, R.G. Mechanical properties and durability performance of concretes with Limestone Calcined Clay Cement (LC^3). *Cem. Concr. Res.* **2018**, *107*, 136–151. [CrossRef]
35. Dhandapani, Y.; Santhanam, M.; Kaladharan, G.; Ramanathan, S. Towards ternary binders involving limestone additions—A review. *Cem. Concr. Res.* **2021**, *143*, 106396. [CrossRef]
36. Avet, F.; Scrivener, K. Hydration Study of Limestone Calcined Clay Cement (LC3) Using Various Grades of Calcined Kaolinitic Clays. In *Calcined Clays for Sustainable Concrete—Proceedings of the 2nd International Conference on Calcined Clays for Sustainable Concrete*; Martirena, F., Favier, A., Scrivener, K., Eds.; Springer Nature: La Havanna, Cuba, 2018; pp. 35–40. ISBN 978-94-024-1207-9. [CrossRef]
37. Muzenda, T.R.; Hou, P.; Kawashima, S.; Sui, T.; Cheng, X. The role of limestone and calcined clay on the rheological properties of LC3. *Cem. Concr. Compos.* **2020**, *107*, 103516. [CrossRef]
38. Adelabu, O.S. *Documentation, Application and Utilisation of Clay Minerals in Kaduna State (Nigeria)*; Valaškova, M., Martynkova, G.S., Eds.; IntechOpen Limited: London, UK, 2012; pp. 3–20. ISBN 978-953-51-0738-5. [CrossRef]
39. Olofinnade, O.; Ogara, J. Workability, strength, and microstructure of high strength sustainable concrete incorporating recycled clay brick aggregate and calcined clay. *Clean. Eng. Technol.* **2021**, *3*, 100123. [CrossRef]
40. Akindahunsi, A.A.; Avet, F.; Scrivener, K. The Influence of some calcined clays from Nigeria as clinker substitute in cementitious systems. *Case Stud. Constr. Mater.* **2020**, *13*, e00443. [CrossRef]
41. Badmus, B.S.; Olatinsu, O.B. Geophysical evaluation and chemical analysis of kaolin clay deposit of Lakiri village, Southwestern Nigeria. *Int. J. Phys. Sci.* **2009**, *4*, 592–606.
42. Al-Mujtaba, M.; Shobo, O.; Oyebola, B.C.; Ohemu, B.O.; Omale, I.; Shuaibu, A.; Anyanti, J. Assessing the acceptability of village health workers' roles in improving maternal health care in Gombe State, Nigeria a qualitative exploration from women beneficiaries. *PLoS ONE* **2020**, *15*, e0240798. [CrossRef] [PubMed]
43. *DIN EN 197-1*; Zement—Teil 1: Zusammensetzung, Anforderungen und Konformitätskriterien von Normalzement (Cement—Part 1: Composition, Specifications and Conformity Criteria for Common Cements). Beuth-Verlag: Berlin, Germany, 2011; p. 8. [CrossRef]
44. *DIN EN 196-1*; Prüfverfahren für Zement—Teil 1: Bestimmung der Festigkeit (Methods of Testing Cement—Part 1: Determination of Strength). Beuth-Verlag: Berlin, Germany, 2016; p. 31.
45. Doebelin, N.; Kleeberg, R. Profex: A graphical user interface for the Rietveld refinement program BGMN. *J. Appl. Crystallogr.* **2015**, *48*, 1573–1580. [CrossRef] [PubMed]
46. Scherb, S.; Köberl, M.; Beuntner, N.; Thienel, K.-C.; Neubauer, J. Reactivity of Metakaolin in Alkaline Environment: Correlation of Results from Dissolution Experiments with XRD Quantifications. *Materials* **2020**, *13*, 2214. [CrossRef] [PubMed]
47. *DIN EN ISO 11885*; Water Quality—Determination of Selected Elements by Inductively Coupled Plasma Optical Emission Spectrometry (ICP-OES). Beuth-Verlag: Berlin, Germany, 2009; p. 37.
48. Kaps, C.; Buchwald, A.; Hohmann, M.; Zellmann, H.-D. Untersuchungen zur Binderoptimierung in alumosilikatischen Polymerbindern. In Proceedings of the 15 Internationale Baustofftagung Ibausil, Weimar, Germany, 24–27 September 2003.
49. Maier, M.; Beuntner, N.; Thienel, K.-C. An approach for the evaluation of local raw material potential for calcined clay as SCM, based on geological and mineralogical data: Examples from German clay deposits. In *Calcined Clays for Sustainable Concrete—Proceedings of the 3rd International Conference on Calcined Clays for Sustainable Concrete*; Bishnoi, S., Ed.; Springer: Singapore, 2020; RILEM Bookseries Volume 25, pp. 37–47. ISBN 978-981-15-2806-4. [CrossRef]
50. *DIN EN ISO 17892-3*; Geotechnical Investigation and Testing—Laboratory Testing of Soil—Part 3: Determination of Particle Density. Beuth-Verlag: Berlin, Germany, 2015; p. 21.
51. *DIN ISO 9277*; Determination of the Specific Surface Area of Solids by Gas Adsorption—BET Method. Beuth-Verlag: Berlin, Germany, 2003; p. 19.
52. Puntke, W. Wasseranspruch von feinen Kornhaufwerken. *Beton* **2002**, *52*, 242–248.
53. *DIN EN 1015-3*; Prüfverfahren für Mörtel für Mauerwerk-Teil 3: Bestimmung der Konsistenz von Frischmörtel (mit Ausbreittisch) (Methods of Test for Mortar for Masonry—Part 3: Determination of Consistence of Fresh Mortar (by Flow Table)). Beuth-Verlag: Berlin, Germany, 2007; p. 12.
54. *ASTM C311-22*; Standard Test Method for Sampling and Testing Fly Ash or Natural Pozzolans for Use in Portland-Cement Concrete. ASTM International: West Conshohocken, PA, USA, 2022; p. 11. [CrossRef]
55. Scherb, S.; Beuntner, N.; Thienel, K.-C.; Neubauer, J. Quantitative X-ray diffraction of free, not chemically bound water with the PONKCS method. *J. Appl. Crystallogr.* **2018**, *51*, 1535–1543. [CrossRef]
56. *DIN EN 197-5*; Zement—Teil 5: Portlandkompositzement CEM II/C-M und Kompositzement CEM VI (Cement—Part 5: Portland-Composite Cement CEM II/C-M and Composite Cement CEM VI). Beuth-Verlag: Berlin, Germany, 2021; p. 12.
57. Zunino, F.; Scrivener, K. The influence of the filler effect on the sulfate requirement of blended cements. *Cem. Concr. Res.* **2019**, *126*, 105918. [CrossRef]
58. Schmid, M.; Plank, J. Interaction of individual meta clays with polycarboxylate (PCE) superplasticizers in cement investigated via dispersion, zeta potential and sorption measurements. *Appl. Clay. Sci.* **2021**, *207*, 106092. [CrossRef]

59. Sposito, R.; Maier, M.; Beuntner, N.; Thienel, K.-C. Evaluation of zeta potential of calcined clays and time-dependent flowability of blended cement with customized polycarboxylate-based superplasticizers. *Constr. Build. Mater.* **2021**, *308*, 125061. [CrossRef]
60. Maier, M.; Forster, B.; Beuntner, N.; Thienel, K.-C. Potential of calcined recycling kaolin from silica sand processing as supplementary cementitious material. In *Calcined Clays for Sustainable Concrete—Proceedings of the 3rd International Conference on Calcined Clays for Sustainable Concrete*; Bishnoi, S., Ed.; Springer: Singapore, 2020; RILEM Bookseries Volume 25, pp. 75–83. ISBN 978-981-15-2806-4. [CrossRef]
61. Beuntner, N.; Sposito, R.; Thienel, K.-C. Potential of Calcined Mixed-Layer Clays as Pozzolans in Concrete. *ACI Mater. J.* **2019**, *116*, 19–29. [CrossRef]
62. Behrouzi, D.; Fleiger, K.; Hoenig, V.; Hoppe, H.; Mohr, M.; Müller, C.; Palm, S.; Reiners, J.; Richter, T.; Rickert, J.; et al. *Dekarbonisierung von Zement und Beton—Minderungspfade und Handlungsstrategien*; Verein Deutscher Zementwerke e.V. (VDZ): Düsseldorf, Germany, 2020; p. 60.
63. *DIN 1045-2*; Tragwerke aus Beton, Stahlbeton und Spannbeton—Teil 2: Beton—Festlegung, Eigenschaften, Herstellung und Konformität—Anwendungsregeln zu DIN EN 206-1. Beuth-Verlag: Berlin, Germany, 2001; p. 48.
64. *DIN EN 206*; Beton—Festlegung, Eigenschaften, Herstellung und Konformität (Concrete—Specification, Performance, Production and Conformity). Beuth Verlag GmbH: Berlin, Germany, 2017; p. 98.
65. Ouellet-Plamondon, C.; Scherb, S.; Köberl, M.; Thienel, K.-C. Acceleration of cement blended with calcined clays. *Constr. Build. Mater.* **2020**, *245*, 118439. [CrossRef]
66. Deutscher Ausschuss für Stahlbeton. *Nachhaltig bauen mit Beton—Planungshilfe des Deutschen Ausschusses für Stahlbeton (DAfStb)*; Deutscher Ausschuss für Stahlbeton, Ed.; Deutscher Ausschuss für Stahlbeton: Berlin, Germany, 2021; p. 15.
67. Van Oss, H.G.; Padovani, A.C. Cement manufacture and the environment, Part II: Environmental challenges and opportunities. *J. Ind. Ecol.* **2003**, *7*, 93–126. [CrossRef]
68. Ali, M.B.; Saidur, R.; Hossain, M.S. A review on emission analysis in cement industries. *Renew. Sustain. Energy Rev.* **2011**, *15*, 2252–2261. [CrossRef]
69. Cancio Díaz, Y.; Sánchez Berriel, S.; Heierli, U.; Favier, A.R.; Sánchez Machado, I.R.; Scrivener, K.L.; Martirena Hernández, J.F.; Habert, G. Limestone calcined clay cement as a low-carbon solution to meet expanding cement demand in emerging economies. *Dev. Eng.* **2017**, *2*, 82–91. [CrossRef]
70. Scherb, S.; Beuntner, N.; Köberl, M.; Thienel, K.-C. The early hydration of cement with the addition of calcined clay—From single phyllosilicate to clay mixture. In Proceedings of the 20 Internationale Baustofftagung ibausil, Weimar, Germany, 12–14 September 2018; pp. 658–666.

8.4 Properties of Self-Compacting Concrete Produced with Optimized Volumes of Calcined Clay and Rice Husk Ash—Emphasis on Rheology, Flowability Retention and Durability

Reprint

Published in the Journal “MDPI/Materials” (Special Issue: The 15th Anniversary of *Materials*—Recent Advances in Construction and Building Materials)

Materials **2023**, *16*(16), 5513; https://doi.org/10.3390/ma16165513

Authors: Abubakar Muhammad and Karl-Christian Thienel

materials

MDPI

Article

Properties of Self-Compacting Concrete Produced with Optimized Volumes of Calcined Clay and Rice Husk Ash—Emphasis on Rheology, Flowability Retention and Durability

Abubakar Muhammad * and Karl-Christian Thienel

Institut für Werkstoffe des Bauwesens, Universität der Bundeswehr München, 85577 Neubiberg, Germany; christian.thienel@unibw.de
* Correspondence: abubakar.muhammad@unibw.de

Abstract: The durability of concrete requires a dense microstructure which can be achieved by using self-compacting concrete (SCC). Both calcined clay (CC) and rice husk ash (RHA) are promising supplementary cementitious materials (SCMs) that can partially replace cement, but their use in SCC is critical due to their higher water demand (WD) and specific surface area (SSA) compared to cement. The effect of partial substitution of cement at 20 vol-% with binary and ternary blends of CC and RHA on flowability retention and durability of SCC was investigated. The empirical method of SCC design was adopted considering the physical properties of both CC and RHA. The deformability of the SCC was evaluated using the slump flow and J-ring tests. The T_{500} time and the V-funnel test were used to assess the viscosity of the SCC. The flowability retention was monitored by the plunger method, and flow resistance was determined based on the rheological measurements of SCC. The evolution of the hydrate phases of the binder in SCC was determined by thermogravimetric analysis, while the durability was evaluated by a rapid chloride migration test. Cement partial replacement with 20 vol-% CC has no significant effect on fresh SCC, flowability retention, compressive strength and durability properties. On the other hand, 20 vol-% RHA requires a higher dosage of SP to achieve self-compactability and increase the viscosity of SCC. Its flowability retention is only up to 30 min after mixing and exhibited higher flow resistance. It consumes more calcium hydroxide (CH) and improves the compressive strength and chloride resistance of SCC. The ternary blending with CC and RHA yielded better fresh SCC properties compared to the binary blend with RHA, while an improved chloride penetration resistance could be achieved compared to the binary CC blend.

Keywords: self-compacting concrete; calcined clay; rice husk ash; reactivity; flowability retention; rheology; flow resistance; durability

check for updates

Citation: Muhammad, A.; Thienel, K.-C. Properties of Self-Compacting Concrete Produced with Optimized Volumes of Calcined Clay and Rice Husk Ash—Emphasis on Rheology, Flowability Retention and Durability. *Materials* **2023**, *16*, 5513. https://doi.org/10.3390/ma16165513

Academic Editor: Eddie Koenders

Received: 29 June 2023
Revised: 2 August 2023
Accepted: 4 August 2023
Published: 8 August 2023

1. Introduction

For decades, concrete has provided the infrastructure that was synonymous with economic growth and development, partly because of its peculiar mechanical and durability characteristics, ease of production and placement, and the wide availability of its constituents [1]. After hardening, concrete becomes a robust stone-like material capable of withstanding the effects of deteriorative mechanisms such as the ingress of harmful chemicals, freeze–thaw cycle, rain storms or other harsh environmental conditions [2,3]. Therefore, concrete requires a dense microstructure that can provide adequate cover to the embedded reinforcement bars and resist the ingress of harmful substances, which could jeopardize the concrete itself. One possible way to ensure better compaction of the concrete and for filling all the corners of formwork and embedding the steel reinforcements is to adopt a self-compacting method of concrete production [4,5].

A self-compacting placement method ensures homogeneous deformation of the fresh concrete, under the influence of gravity, to fill all the gaps and corners of the formwork and embed the reinforcement bars without the need for external vibration or compaction, thereby ensuring a homogeneous and dense hardened concrete microstructure with excellent strength and durability [6]. The flowability of the SCC is achieved by proper optimization of the volumetric water-to-powder ratio (V_w/V_p) and the use high range water-reducing admixtures [7], while the homogeneity of the powder type of SCC is achieved by an optimal proportioning of fine and coarse particles of the concrete constituents [6]. In this regard, the proportion of coarse aggregate (CA) is reduced while the volume of mortar in the system is increased. Consequently, the quantity of the powder required to achieve optimized fresh SCC properties (powder-type) is greater than that of the conventional vibrated concrete [8], making the concrete more expensive and less environmentally friendly.

One potential way to make SCC cost-effective and reduce the effects of excessive use of cement per m^3 of SCC—such as shrinkage and high CO_2 emission—is to reduce the amount of cement per m^3 of SCC. This can be achieved by partially replacing cement with filler and/or supplementary cementitious materials (SCMs). The most commonly used natural filler in SCC is limestone powder (LP), which can replace up to 35 wt.% of cement clinker [9], thereby reducing cement interparticle friction and decreasing the flow resistance of the SCC [10,11] and promoting the reaction of C_3S and the formation of AFm phases (hemi/monocarboaluminate) [12,13]. SCMs such as fly ash, silica fume, metakaolin, rice husk ash (RHA) and others can also be used as partial cement substitutes in SCC. Binary and ternary cement partial replacement with fly ash up to 30 wt.% improves the durability of SCC and reduces its drying shrinkage [14,15]. Higher cement partial replacement by fly ash will soon no longer be possible due to the decline in coal combustion enforced to limit global CO_2 release. Similarly, silica fume at 10 wt.% cement partial substitute improves the compressive strength and durability of SCC [16,17], but its use at higher dosage is also limited due to its cost, high water demand and portlandite consumption.

CC are anhydrous aluminosilicate pozzolanic materials that can partially replace cement at high proportions and improve the strength and durability of concrete. Metakaolin is the most reactive CC in concrete and mortar due to its higher early strength compared to other CCs [18–20]. However, due to its frequent use in other competing industries, metakaolin is an expensive material and less available compared to the other 2:1 CCs. Although the relevance of other common CCs for conventional vibrated concrete has been investigated in recent years [21,22], their application should also be extended to SCC. RHA, on the other hand, is a silica-rich SCM that can be used as a viscosity modifying agent or as a partial replacement to cement in SCC [20,23–25]. Its specific SSA and WD exceed those of cement and metakaolin [20,23]. Therefore, similar to silica fume, its use in SCC is limited due to its effect on the deformability characteristics of SCC. It is obvious that both metakaolin and RHA at a certain cement replacement ratio densified the concrete microstructure, improving its chloride penetration resistance, increasing compressive strength and decreasing drying shrinkage tendency, but both are known for their high SSA and high WD, both significantly exceeding those of cement [20]. Consequently, the flow resistance of SCC is increased when cement is replaced with metakaolin and RHA, as the flow resistance of the blended cement increases due to the increase in the WD of the system [26].

SCC usually differs from conventional vibrated concrete only in its fresh properties. Its deformability characteristics and flowability retention are important attributes that determine its application. Previous investigations have established the potential use of binary and ternary blends of CC and RHA as partial replacements to cement up to 30 wt.% [27–31]; most of these investigations assessed the influence of these materials on the deformability of SCC only up to 30 min after production. Flowability retention of SCC is important, especially when considering applications requiring extended fresh properties retention. For instance, in the precast concrete plant, SCC can be cast into forms about 10 to

30 min after mixing, and the flowability retention is not as important as in the ready-mix concrete, which often requires 30 to 120 min after mixing [32]. The major concern at this point is the peculiar physical properties of CC and RHA, both of which have higher WD and SSA greater than cement, although RHA is more critical in this context because it can absorb the mixing water, causing the SCC to lose its stability quickly. Although maintaining the flowability of the SCC over an extended period of time is not readily achievable, it is important that the ready-mixed SCC still exhibit the required fresh SCC properties at the time of placement. None of the previous studies have reported the effects of CC and RHA on the flowability retention of SCC.

The deformability characteristics of SCC after mixing can be assessed by measuring the yield value (slump flow), which defines the flowability of the SCC, and by checking the deformation rate by V-funnel measurement as an indication of viscosity [33,34]. The SCC can then be finally analyzed for its blocking and segregation tendency [35]. These properties are usually measured within 30 min of mixing and are not indicative of the flowability retention of the SCC. The flowability retention of SCC can be assessed by determining the immersion depth of the plunger in SCC in a cylindrical mould, as developed by FIZ (Research Institute of the Cement Industry) Düsseldorf [36], or by comparing the flow resistance of the SCC over time, calculated from the curves of shear stress versus shear rate from the rheological measurements.

2. Research Gap

Previous studies have investigated the suitability of a multi-blend of CC and RHA for the production of the SCC, as reviewed by [20]. Most researchers focused on the use of metakaolin as CC, which is an expensive material due to its frequent use in other competing industries and is less available compared to low-kaolinitic CC [23,24]. There is a lack of knowledge when it comes to the use of low-kaolinitic CC as a sole SCM or in combination with RHA as a partial replacement for cement in SCC, as pointed out by [20]. More so, previous studies have investigated the effects of blends of metakaolin and RHA on the fresh properties of SCC up to 30 min after production. However, the effects of these materials on the flowability retention and rheological properties of SCC in terms of yield stress, plastic viscosity, shear thickening behavior, plastic shrinkage and drying shrinkage have not been reported. Therefore, current efforts are aimed at optimizing the SCC mix design using a multi-blend of low-kaolinitic CC and RHA as a partial replacement for cement. Other properties to be investigated include the rheology, flowability retention, evolution of hydrate phases of the binder, plastic and drying shrinkage, compressive strength, and rapid chloride migration. The outcome of the study shows the effects of CC and RHA on the flowability retention and durability of SCC and the potential use of these materials to replace a high proportion of Portland limestone cement (PLC) in SCC, leading to a reduction in production costs and environmental impact.

3. Materials and Methods

3.1. Research Materials

Self-compacting paste, mortar and concrete are produced using CEM I 42.5 R, conforming to DIN EN 197-1 [9]. The cement (OPC) is partially replaced by 15 vol-% LP to form a Portland limestone cement (PLC). The mineralogical compositions of OPC (according to manufacturer's data) and LP (determined by X-ray diffraction) are provided in Table 1.

Table 1. Mineralogical composition of OPC and LP.

Materials	C_3S	C_2S	C_3A	C_4AF	Calcite	Sulfates	Quartz
OPC	61.6	18.2	5.8	9.0	0.6	3.2	-
LP	-	-	-	-	99.8	-	0.2

The PLC is partially substituted with the binary and ternary blends of CC and RHA up to 40 vol-% to determine the influence of CC and RHA on the rheological properties of SCC. The raw material for CC is an Amaltheen clay from southern Germany, which was calcined on an industrial scale at 750 °C and ground with an industrial roller mill to the fineness described in Table 2. The CC contained (wt-%) 60.8 amorphous phase, 2.2 muscovite, 16.2 quartz, 4.6 illite, 0.6 calcite and 1.6 sulfates mineralogical phases as characterized previously by [37]. For the RHA, rice husks from the vicinity of Zaria in Kaduna State, Nigeria, were calcined at 650 °C for 2 h in an electric furnace and ground with a laboratory scale mill to obtain the RHA. It contained 96.8% wt.% amorphous silica as the mineral phase, measured using X-ray diffraction with an internal standard. Table 2 shows the physical properties of the research binders. The particle shape of CC and RHA was examined using Evo LS 15 (Zeiss, Jena, Germany) scanning electron microscope (SEM). Both CC and RHA were scattered on a thin adhesive layer and coated with gold before SEM images were taken.

Table 2. Physical properties of OPC, LP, CC and RHA.

Properties	Methodology	OPC	LP	CC	RHA
Specific surface area, m^2/g	DIN ISO 9277 [38]	1.0	1.6	3.9	160
Water demand, wt.%	Puntke method [39]	29	20	38	96
Particle density, g/cm^3	DIN EN ISO 17892-3 [40]	3.29	2.81	2.65	2.4
d_{10}, µm	Bettersizer 3D instrument [26]	2.6	0.8	1.9	5.4
d_{50}, µm		16.0	4.6	12.7	23.7
d_{90}, µm		42.8	20.7	33.7	56.5

The fluidity of the SCC is controlled with the use of superplasticizer (SP), which has a total solid content of 38.6 wt.%, 1390 micromoles/g anionic charge density, 25,992 g/mol molecular weight and a side chain length of n_{EO} = 31 according to the supplier's information. To complete the SCC mix design, sand with a grading of 0 to 4 mm, a particle density of 2.87 g/cm^3 and having 7.6 wt.% passing sieves 0.125 mm was used as fine aggregate (FA). While round gravels with a grading of 4 to 16 mm, a particle density of 2.68 g/cm^3 and 2.7 wt.% passing sieves 0.125 was used as CA. Figure 1 shows the particle size distribution of the research materials.

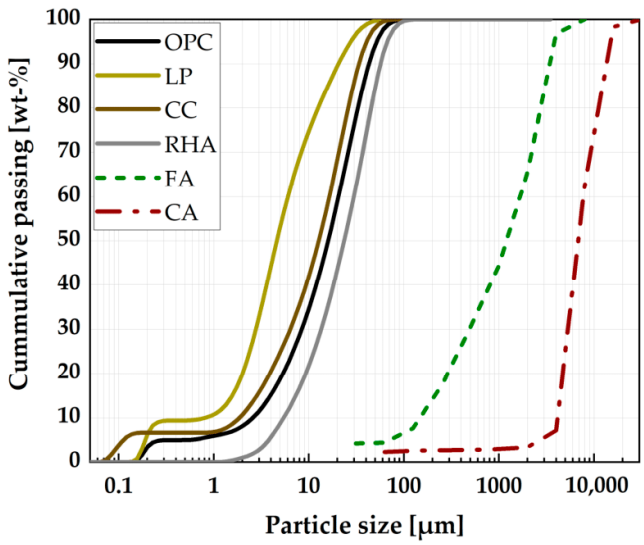

Figure 1. Particle size distribution of the research materials.

3.2. Methods

3.2.1. Self-Compacting Paste, Mortar and Concrete Mix Design

The powder type of SCC used for the study was designed using a stepwise empirical method. This implies designing the paste phase of the concrete first. The amount of water confined by the binder is determined using the spread flow method, according to [41]. At a constant volume of the powder, the volumetric water-to-powder ratio (V_w/V_p) is varied between 1 and 2 at 0.1 intervals. Four points were used for each binder system, and the relative spread is determined using Equation (1). The V_w/V_p is plotted against the relative spread, and the amount of water confined by individual binder system ($V_{w\Gamma o}$) is determined by extrapolating the points to the vertical axis [5].

$$\Gamma_{RS} = [d/d_o]^2 - 1 \quad (1)$$

where Γ_{RS} = relative spread area, $d = (d_1 + d_2)/2$, d_1 = largest flow diameter and d_2 = diameter perpendicular to d_1, and d_o = diameter of mini-slump cone, 100 mm.

The influence of CC and RHA on the amount of water confined by the PLC was determined and was used as the basis for establishing the V_w/V_p of the self-compacting paste systems (SCP) using Equation (2).

$$V_w/V_p = [0.8 \text{ to } 0.9] \cdot V_{w\Gamma o} \quad (2)$$

where $V_{w\Gamma o}$ = volume of water confined by binder in relation to its solid volume.

The amount of the SP required to deform the SCP systems was determined as the dosage of SP at which a particular binder system attained a flow diameter of 240 mm ± 20 mm —a flow diameter at which the SCP achieved deformability without segregation based on visual inspection. Self-compacting mortar (SC-M) design was achieved by considering the average V_w/V_p required to deform SCP, and the volume of the FA (V_s) is fixed at 44 vol-% of the SC-M volume, according to [41]. The amount of SP is adjusted until the individual SC-M system's self-compactability is attained. The deformability of the SC-M systems was assessed by measuring the slump flow using the mini-slump cone [5,41], and the range of 240 mm to 260 mm was used as a yardstick for indicating the deformability limit at which self-compactability is achieved. The viscosity of SC-M was monitored by measuring the mini V-funnel time [42], while visual inspection was used to evaluate the segregation resistance of the SC-M. To complete the SCC mix design, the volume of the CA was adjusted by intense testing together with varying the dosages of the SP until it was kept at 33% of the total SCC volume. The air content was also fixed at 2 vol.% of total SCC volume, according to [41].

3.2.2. Batching and Mixing of Self-Compacting Paste, Mortar and Concrete Constituents

SCP mixes were produced according to DIN EN 196-1 [43]. The binder, mixing water and SP were added together and mixed for 4 min in a mortar mixer produced by Bluhm and Feuerherdt GmbH, Berlin, Germany. SC-M was produced by mixing the constituents for 8 min in the same mixer described above. The binder materials, FA and two-thirds of the mixing water were mixed for 2 min, followed by a break of 1 min to enable the addition of the remaining water and the SP. The entire mixture was then mixed for an additional 5 min. The mixing sequence of SCC started with mixing the binder, FA and CA for 1 min in a UEZ ZM 50 concrete mixer (UEZ-MISCHTECHNIK), with a capacity of 60 L and a mixing speed of 48 rpm. Two-thirds of the mixing water was then added while the mixer was running and mixed for 2 min. The SP and the remaining mixing water were then added, and the whole constituents mix for another 7 min.

3.2.3. Fresh SCC Properties and Segregation Resistance

The deformability of the SCC in absence of obstacles was evaluated using the slump flow according to [33], while the J-ring test was employed to assess the passing ability of the SCC through an obstacle according to [35]. The viscosity of the SCC systems was

assessed using both the T_{500} time and the V-funnel test, according to [34]. The stability of the SCC was evaluated in two ways. First, using the sieve stability assessment method according to [44] and the washing test according to [45] where the fresh SCC was poured into a plastic cylinder 150 × 500 mm (with a solid base and cut at third points up to half of the circumference to accommodate metal dividers). The cut points for receiving the metal dividers were sealed with adhesive tape before pouring the SCC. Immediately after mixing, the SCC was poured into the cylinder and stored vibration-free for 30 min until the time of testing. After 30 min, the adhesive tape is removed, and the metal dividers are inserted. The SCC is then poured into vessels in segments and washed through 4 mm aperture sieve. The sieve residue was dried in a ventilated oven at 105 °C and weighed.

3.2.4. Rheology and Flowability Retention Assessment

The uniform distribution of the CA in the SCC mixtures is monitored over time using a plunger method [36]. SCC is poured into a hollow cylinder with an internal diameter of 150 mm and a height of 600 mm. A 900 g steel plunger with a diameter of 14 mm and a height of 750 mm is then guided through the guide tube (with 3 openings) to the surface of the SCC and released to penetrate into the SCC. The depth of immersion of the steel plunger is measured, and the sedimentation height (h_s) is calculated as the difference between the steel plunger height (h_0) and the immersion depth (h_T) in mm. The steel plunger and the guide tube are withdrawn, cleaned and dried for the next measurement. Previous immersion holes were avoided by changing the position of the guide tube after the whole available guide holes had been exhausted.

Rheology of the SCC in terms of the shear stress (τ), plastic viscosity (μ) and flow resistance were determined using a rotational rheometer, viskomat XL (Schleibinger Geräte, Buchbach, Germany), with a vane probe testing paddle at a constant temperature of 20 °C. The measurement started with the maximum rotational speed of 12 rpm for 80 s and decreased in 14 steps of 20 s each until the end of the measurement [46]. The recorded torque was used to estimate the yield stress (τ_0) and plastic viscosity (η) of the SCC according to the Bingham model [47,48] using Equation (3). The flowability retention of the SCC is monitored by calculating flow resistance of the SCC mixtures over time (area under curve) obtained by plotting the torque against the velocity as described previously by [26].

$$T = G + N \cdot H \tag{3}$$

where T = torque ≈ τ; G = y-intercept of the flow curve ≈ τ_0; N = velocity ≈ $\dot{\gamma}$; and H = the slope of the curve ≈ η.

3.2.5. Portlandite Consumption, Plastic and Drying Shrinkage of Self-Compacting Paste, and Mortar

The plastic shrinkage of SC-M at an early age was measured contactless using a shrinkage cone (Schleibinger Testing Systems, Buchbach, Germany), according to [49]. The measurement started 15 min after water addition and lasted for up to 48 h. Polypropylene foil was used to prevent the friction effect between the fresh SCC surface and the shrinkage cone. The SC-M drying shrinkage was measured on 40 × 40 × 160 mm^3 prisms, according to [50]. The portlandite (CH) consumption by the CC and RHA and hydrate phases formed at 2, 7 and 28 days of curing were investigated by thermogravimetric measurements (TG) conducted in Netzsch STA 449 F3 Jupiter apparatus. The constituents of the SCP were mixed according to [43], poured into 40 × 40 × 160 mm^3 steel molds and stored moist for 48 h, and then cured under water until testing. At the time of testing, a representative portion of the sample is manually chipped out from the inner part of the prisms and crushed to <1 mm size using the laboratory pestle and mortar. Hydration of the pulverized binder was stopped by solvent exchange, as described in [51]. Approximately 300 mg of the pulverized binder was placed in alumina crucibles and heated to 1000 °C at a heating rate of 2 °C/min under a nitrogen atmosphere. The CH content of the SCP was quantified by the tangent method from the weight loss between 400 °C and 490 °C.

3.2.6. Compressive Strength and Chloride Migration Resistance of SCC

For the compressive strength measurement, SCC was cast in 150 × 150 × 150 mm^3 steel molds and stored moist for 48 h and then cured underwater until the test date. The measurement was conducted according to [52] at 2, 7 and 28 days of curing on the Form + Test Prüfsysteme Alpha 1–3000 strength testing equipment with an increasing uniform loading rate of 2400 ± 200 N/s until failure. The influence of CC and RHA on chloride resistance of SCC was investigated using a rapid chloride migration by applying an electric field axially to the test specimen to accelerate the chloride penetration, according to [53]. The depth of chloride penetration was determined on 100 × 50 mm^3 cores drilled and subsequently sliced from 150 × 150 × 150 mm^3 SCC specimens at day 28 of curing.

4. Results and Discussion

4.1. Optimization of SCC Mix Design with the Blend of CC and RHA

To optimize the blend of CC and RHA as a partial replacement for PLC in SCC, the influence of CC and RHA on the amount of water confined by the binder was first considered. PLC without CC and RHA partial replacement confined approximately a volume of water equal to the volume of solid. A substitution by 10 vol-% CC showed no significant effect on the volume of water confined and increased to 11 vol-% of water at a substitution ratio of 40 vol-%. RHA at 10 vol-% PLC substitution confined 20 vol-% additional water compared to the PLC, and the volume of water confined increased to 43 vol-% at an RHA substitution ratio of 40 vol-%. Figure 2 shows the ratio of confined water (vol-%) by PLC, CC, RHA and the ternary blends of CC and RHA.

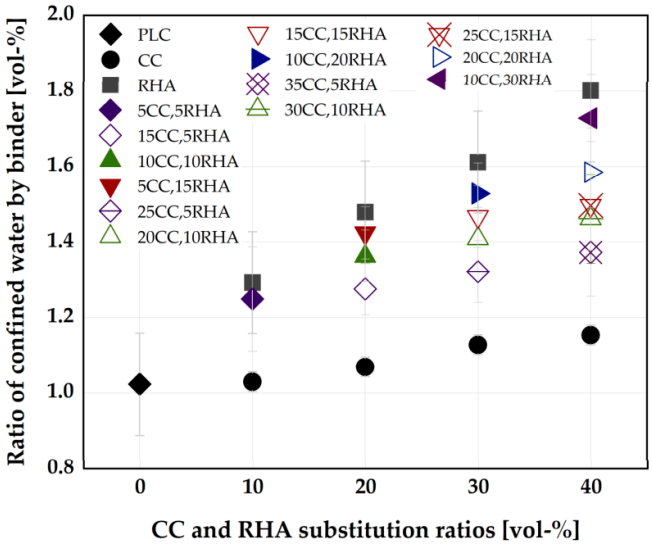

Figure 2. Influence of CC and RHA on the ratio of confined water by PLC.

However, the ternary blends of CC and RHA yielded no reduction in the $V_{w\Gamma o}$ due to the high-water demand of RHA. For instance, the $V_{w\Gamma o}$ for 40 vol-% CC replacement is 1.15 and increased drastically to 1.37 when 5 vol-% of CC is replaced by RHA in the blend (35CC, 5RHA). Figure 3 shows the relationship between the water demand and the ratio of confined water by the binder systems. The ternary blends of CC and RHA appeared above the line of best fit, while the binary blends appeared on the line or below.

A possible explanation for this behavior of the ternary blends is the dominating influence of RHA on the properties of the blended binder. Even a small amount of RHA in the ternary blend leads to an increase in both the water demand and the amount of water trapped by the binder compared to the binary CC mixes. It could also be due to improper

mixing of the two materials since CC has a heterogeneous surface morphology, while RHA contains an irregular, granular surface of isolated plate morphology, as shown in Figure 4, so the presence of CC in the mixture does not have a significant effect on reducing the water demand of ternary mixtures.

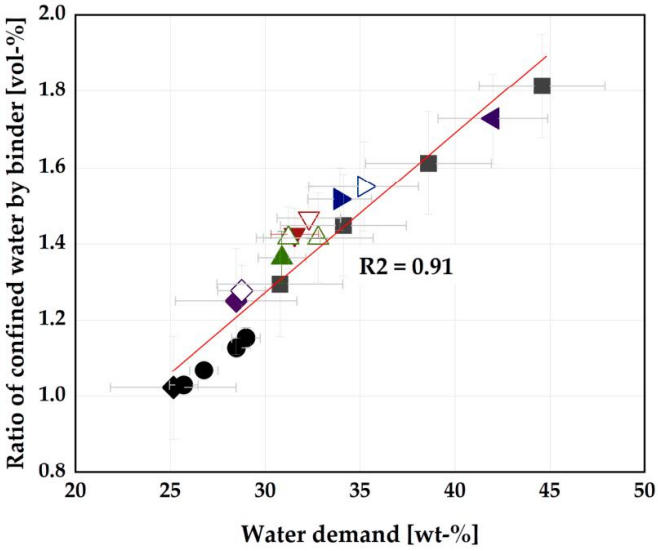

Figure 3. Relationship between the water demand and the ratio of water confined by the binder; the same legend used in Figure 2 is applicable here.

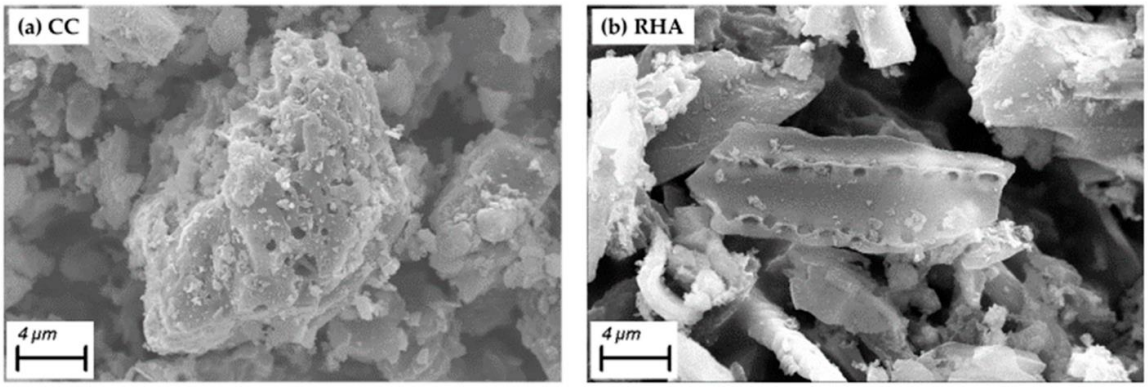

Figure 4. Particle morphology of (**a**) heterogeneous CC and (**b**) granular irregular RHA.

The design of SCC starts with the determination of the V_w/V_p required to impart on-paste self-compactability. This V_w/V_p is calculated from the volume of water confined by the individual binder system, and the average of these values for the individual binder systems is shown in Table 3. PLC requires an average of 0.87 V_w/V_p to achieve self-compactability. Partial substitution of CC up to 20 vol-% has a minor effect on this value; CC partial substitution beyond 20 vol-% requires an adjustment of this value or an increase of the SP dosage to achieve a similar deformability class as the PLC system, as a previous investigation by [54] achieved self-compactability using the same V_w/V_p and increasing SP dosage, with up to 40 vol-% CC in SC-M. On the other hand, the partial substitution of PLC with RHA requires a significant increase of V_w/V_p to achieve self-compactability. At 10 vol-% RHA partial replacement, V_w/V_p already increased to 1.1, which is 21% higher

than the value required for PLC. At 40 vol-% RHA partial replacement, the V_w/V_p increased by 42%. In this case, the SP adjustment is not sufficient to achieve the required degree of deformability because of the higher water demand and specific surface area of the RHA compared to PLC. Therefore, urgent adjustment of the V_w/V_p of the RHA and the ternary blend of CC and RHA systems is required to achieve a deformability characteristic similar to that of PLC.

Table 3. Average V_w/V_p required by individual binder system to achieve self-compactability.

RHA \ CC	0	5	10	15	20	25	30	35	40
0	0.87		0.87		0.91		0.94		0.98
5		1.1		1.08		1.12		1.17	
10	1.10		1.16		1.2		1.24		
15		1.21		1.25		1.27			
20	1.26		1.3		1.35				
25		1.34		1.42					
30	1.37		1.47						
35		1.50							
40	1.51								

The SCP design in this section will later be used as a binder in SC-M and SCC. Therefore, the selection of the V_w/V_p will be carried out considering the intended final use of SCC. The following outlook is considered to justify the selection of V_w/V_p for the SCP design. In practice, the water-to-binder (w/b) and the strength of the binder determined the strength and durability class of the concrete and, thus, its application as provided in the concrete design standards [55,56]. To achieve SCC with PLC, a V_w/V_p = 0.87 is required, corresponding to a w/b = 0.29; for CC replacement, up to 40 vol-%, a w/b = 0.32 is required. For 10 vol-% RHA, w/p = 0.36 is required, increasing to 0.42, 0.45 and 0.50 for 20, 30 and 40 vol-% partial replacement, respectively. When using a macro-mesoporous RHA as a partial replacement to cement in SC-M, Le et al. [57] achieved self-compactability using a w/b = 0.26 with up to 20 wt.% RHA as a partial replacement for cement, and despite increasing dosages of SP, RHA increased the viscosity of the SC-M. It should be noted at this point that the deformability of the SC-M does not necessarily indicate the deformability of SCC because SCC contains a large volume of coarser aggregate in addition to SC-M, which has a significant impact on its deformability characteristics. By ternary blending residual RHA and LP as partial replacement to OPC, Sua-iam et al. [58] achieved self-compactability using a low w/b = 0.28 and the same dosage of high-range water reducers with RHA substation up to 20 wt.%, but the viscosity of 20 wt.% RHA binary blended SCC was 63% higher than the control (viscosity = V-funnel time). Therefore, a lower w/b value ($\leq$0.3) does not provide the degree of deformability required when $\geq$20 vol-% RHA is used as a partial replacement for cement. The same deformability characteristic as the reference systems with higher RHA replacement ratios ($\geq$20 wt.%) were achieved by increasing the w/b to 0.44 and above [27,30,59]; similar values of w/b are assumed for this investigation as the PLC partial replacement level is kept at $\geq$20 wt.%. Another factor that governs the selection of the w/b is the expected performance of the SCC after hardening. For chloride exposure under alternating wet and dry conditions, the maximum allowable w/b is 0.45 [55].

Partial replacement of PLC with CC, even up to 40 vol-%, yields the required deformability characteristics and has wide applicability in different durability exposure classes, as previously reported by [54,60], while providing significant savings in production cost and reducing CO_2 emission. Higher PLC partial substitution with RHA up to 40 vol-% is also possible using a higher w/b of $\geq$0.5; this concrete could also have a wide range of applications, for instance, in exposure classes X0, XC, and some classes of XD and XS exposure, according to [55]. Considering that RHA poses a challenge to deformability at higher PLC partial substitution due to its high WD, this study will limit the RHA replacement ratio to 20 vol-%. For comparison, the binary blend with CC will also be kept at 20 vol-%, and the

ternary blend will use 10 vol-%CC + 10 vol-%RHA. Therefore, V_w/V_p = 1.275 required to impart self-compactability to the 20 vol-% RHA binder system is considered as the V_w/V_p in the following sections of this paper and is used to establish the SP dosages required to deform the SCP systems, as depicted in Figure 5.

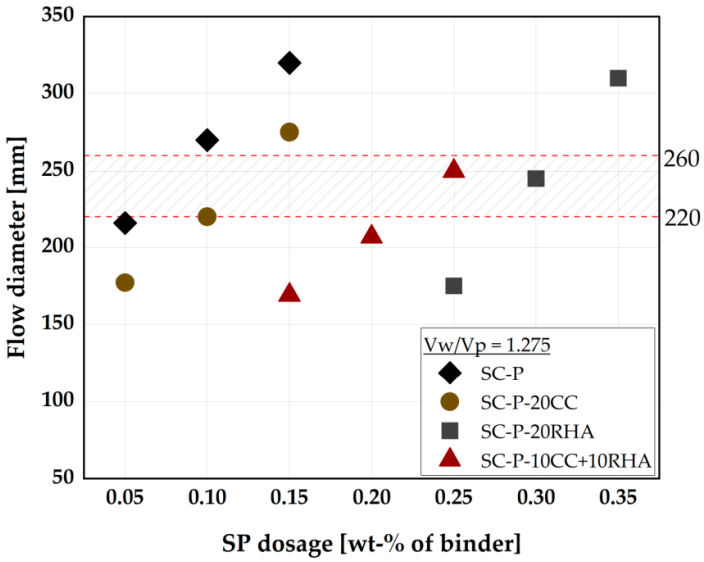

Figure 5. SP dosages required to deform SCP systems.

Based on the visual inspection, SCP achieved deformability without segregation at a flow diameter of 220 to 260 mm. Therefore, the dosage of SP is established, which is necessary for the individual binder systems to achieve a flow diameter of 240 mm ± 20 without segregation. The latter is assessed visually. PLC binder system (SC-P) requires an SP dosage of between 0.05 to 0.1 wt.% to achieve self-compactability. SC-P-20CC demands a slightly higher SP dosage than SC-P, while for the SC-P-20RHA system, the SP dosage already increases drastically to 0.3 wt.%, although this is reduced to 0.25 with the SC-P-10CC+10RHA blend. The increase in the SP demand is due to the higher WD of RHA, which continues to trap water in its structure and requires more SP to achieve the required degree of deformability. The final SCP mix design is shown in Table 4 and was used as the basis for SC-M design and to measure the influence of CC and RHA on the formation of hydrate phases over the period of 28 days of curing.

Table 4. SCP mix designation.

Mix Designation	Constituent (Measured in dm^3/m^3)							Constituent (Measured in kg/m^3)					
	V_w/V_p	OPC	LP	CC	RHA	Water	w/b	OPC	LP	CC	RHA	Water	SP [wt-%]
SC-P	1.275	374	66	-	-	560	0.4	1231	185	-	-	560	0.05
SC-P-20CC	1.275	299	53	88	-	560	0.4	984	148	233	-	560	0.1
SC-P-20RHA	1.275	299	53	-	88	560	0.4	984	148	-	211	560	0.3
SC-P-10CC+10RHA	1.275	299	53	44	44	560	0.4	984	148	116	106	560	0.2

The SCP designed above were used in the next step as media to deform the SC-M and bind the fine aggregate. The SC-M mix designs are achieved by fixing V_s at 44 vol-% of the total SC-M volume, based on the recommendation of [41]. SP dosages are adjusted to

achieve the required degree of deformability. Figure 6 shows the deformability and the rate of deformability of the individual SC-M systems.

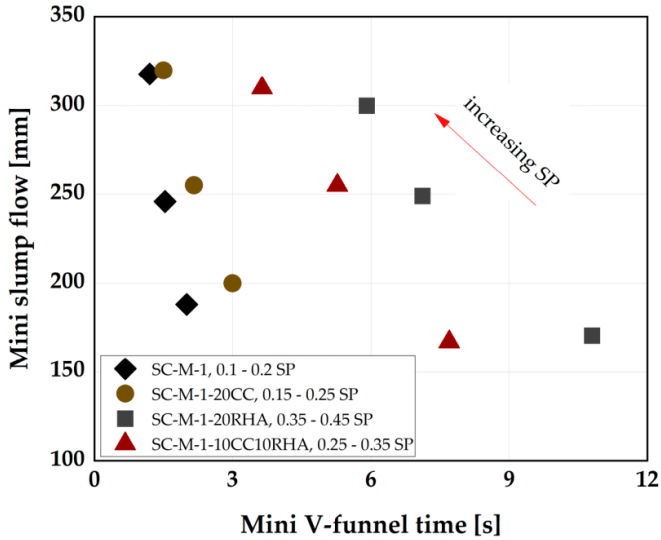

Figure 6. Influence of CC, RHA and SP dosage on the deformability characteristics of SC-M.

With a slight adjustment of the SP dosage, SC-M-1-20CC achieved a similar deformability to SC-M-1, SC-M-1-20RHA, and the blend SC-M-1-10CC+10RHA could achieve a similar deformability class to SC-M-1 but with an increased viscosity and higher SP dosages. For deformability assessment, EFNARC's [41] guidelines were adopted. A range of 240 mm to 260 mm flow diameter and a viscosity class (V-funnel time) of 7 s to 11 s were used. Only SC-M-20RHA falls under these limits. The remaining mixtures exhibited a higher flow rate, indicating low viscosity. Therefore, mixtures that are stable (judged by visual assessment) between the flow diameter = 240 mm to 260 mm were considered for the production of the SC-M specimens. Table 5 provides the final SC-M mix designs, which were used to monitor the influence of CC and RHA on plastic and dry shrinkage strains.

Table 5. SC-M mix designation.

Mix Designation	Constituent (Measured in dm^3/m^3)								Constituent (Measured in kg/m^3)						
	V_w/V_p	OPC	LP	CC	RHA	Water	FA	w/b	OPC	LP	CC	RHA	FA	Water	SP [wt-%]
SC-M-1	1.275	224	40	-	-	336	400	0.4	738	111	-	-	1104	336	0.15
SC-M-1-20CC	1.275	179	32	53	-	336	400	0.4	591	89	140	-	1104	336	0.2
SC-M-1-20RHA	1.275	179	32	-	53	336	400	0.4	591	89	-	127	1104	336	0.4
SC-M-1-10CC+10RHA	1.275	179	32	26	26	336	400	0.4	591	89	70	63	1104	336	0.3

The final SCC mix design is achieved with a fixed CA content of 33 vol-% and assuming an air content (V_a) of 2 vol-% of the total SCC volume according to EFNARC [41], while the SC-M designed above complete the remaining SCC volume. The SP dosages were adjusted until an acceptable deformability was achieved, as shown in Figure 7a. The criteria for assessing the deformability of SCC in the absence of obstacles (filling ability) include the slump flow, V-funnel and t_{500} times as an indication of viscosity, while the use of J-ring can give an estimation of the deformability in the presence of an obstacle (passing ability). The combination of these assessments was used as the basis for selecting the appropriate mixes to produce the final SCC. By adjusting the SP dosages, SCC-1 achieved a deformability class SF2 and viscosity class VS1 and VF1, according to [56]. With a slight increase in

the SP dosage, SCC-1-20CC achieved similar deformability to the SCC-1, with viscosity classes of VS2 and VF1. SCC-1-20RHA exhibited higher viscosity than SCC-1 and requires an increased SP dosage to attain deformability class SF2 and viscosity classes VS2 and VF1. The ternary blend, SCC-1-10CC+10RHA, exhibited a deformability and viscosity behavior somewhat in-between that of binary CC and RHA SCC. The increased viscosity with RHA substitution is due to the higher water demand of RHA compared to PLC and CC, as depicted in Table 2. A relationship between the V-funnel time (VF) and the t_{500} (VS) measured together with the slump flow is observed with a high correlation [61], as shown in Figure 7b.

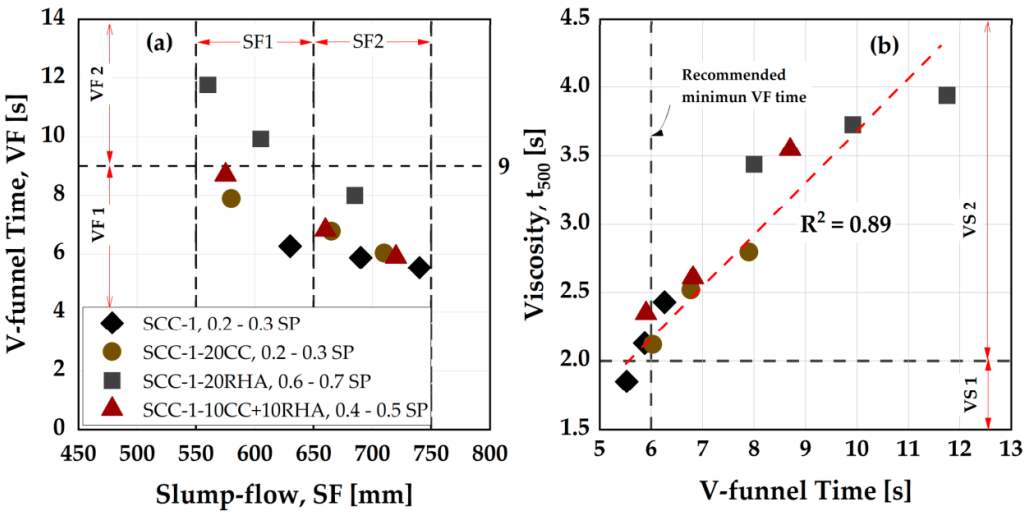

Figure 7. (**a**) Influence of CC, RHA and varying SP dosages on the deformability characteristics of SCC. (**b**) Relationship between the VF and t_{500}. Explanations for the symbols are provided in (**a**).

Similarly, by adjusting the SP dosages, the blocking tendency of the SCC decreases, and it is possible to bring all the SCC mixtures to a passing ability class PJ2, classified according to [56] (Figure 8).

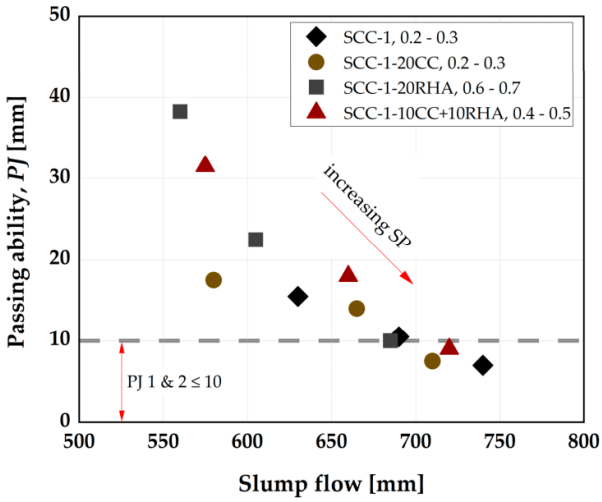

Figure 8. Influence of CC, RHA and varying SP dosage on the blocking tendency of SCC.

The reference mixture (SCC-1) exhibits good passing ability using an SP dosage of 0.3 wt.%, but the viscosity (V-funnel time) falls below 6 s, the minimum recommended by [41] (Figure 7b). The tendency of segregation is high with this mixture, and therefore it was not considered for the production of the final SCC. The viscosity of the SCC depends largely on the w/b: The higher the w/b, the higher the rate at which the SCC will flow, as previous investigations obtained VF time $\leq$ 6 s using w/b $\geq$ 0.5 [4,62]. When the w/b is <0.4, SCC have a VF time $\geq$ 6 s [30,60]. SCC-1 with 0.25 SP dosage is at the limit for both the filling and passing ability values but is considered suitable for the final SCC mix design. The selection criterion for the final SCC mix design is therefore based on SF $\geq$ 650 mm, VF $\geq$ 6 s and PJ $\leq$ 10 mm and the proportions of the final SCC mix designations are presented in Tables 6 and 7 and are used to determine the influence of CC and RHA on the segregation resistance, rheology, flowability retention, compressive strength and chloride migration resistance of SCC.

Table 6. SCC mix designation (dm^3/m^3).

Mix Designation	Constituent (Measured in dm^3/m^3)								
	V_w/V_p	OPC	LP	CC	RHA	Water	FA	CA	V_a
SCC-1	1.275	137	24	-	-	206	289	323	20
SCC-1-20CC	1.275	110	19	32	-	206	289	323	20
SCC-1-20RHA	1.275	110	19	-	32	206	289	323	20
SCC-1-10CC+10RHA	1.275	110	19	16	16	206	289	323	20

Table 7. SCC mix designation (kg/m^3).

Mix Designation	Constituent (Measured in kg/m^3)								
	w/b	OPC	LP	CC	RHA	Water	FA	CA	SP [wt-%]
SCC-1	0.4	452	68	-	-	206	798	867	0.25
SCC-1-20CC	0.4	362	54	86	-	206	798	867	0.3
SCC-1-20RHA	0.4	362	54	-	78	206	798	867	0.7
SCC-1-10CC+10RHA	0.4	362	54	43	39	206	798	867	0.5

The reference system (SCC-1) required a V_w/V_p = 0.87, corresponding to w/b = 0.29, for self-compactibality, similar to that previously used by [54,58] to achieve high-strength SCC. Both CC and RHA have a WD greater than that of PLC. The WD of CC is one-third higher than that of PLC (see Table 2) but requires only an adjustment of SP to achieve a degree of deformability comparable to SCC-1, although with increased viscosity and SP demand as previously investigated by [29,54], when high volume of CC was used as partial replacement to cement. The increase in viscosity is not only due to the higher WD of the CC compared to PLC but also due to its different particle shape, as reported by [26,63], leading to an increased resistance to flow and hence higher SP demand to deform the SCC-1-20CC system. The use of RHA as a partial replacement for PLC in SCC is more critical due to its more than three times high WD (see Table 2). Unlike the SCC-1-20CC system, SP adjustment is not sufficient to deform SCC-1-20RHA and even the SCC-1-10CC+10RHA system. Therefore, V_w/V_p adjustment is urgently needed to achieve self-compactability. When substituting a high proportion of PLC with RHA (20% and above), higher w/b, from 0.44 and above, will be required to properly deform the RHA-SCC system. This affects the concrete porosity and limits its application possibilities since the durability classes of concrete are determined on the basis of the w/p value, as already described in [55]. Therefore, this study limits the content of RHA to 20 vol-% and uses a Vw/Vp = 1.275 (0.42 w/b equivalent) for all PLC-, CC-, and RHA-SCC systems.

4.2. Influence of CC and RHA on the Segregation Resistance of SCC

Both short-term and flowability retention assessments are conducted to establish the influence of CC and RHA on the stability of the SCC. For the short-term assessment of segregation resistance, sieve stability and washing tests are conducted after the fresh SCC has settled 30 min after mixing. Figure 9a shows the segregated portion of the SCC specimens determined by sieve stability. The segregated portion of all the SCC specimens is less than 11 wt.%, which is within the limit specified by [56], standard specification for SCC performance and conformity requirements.

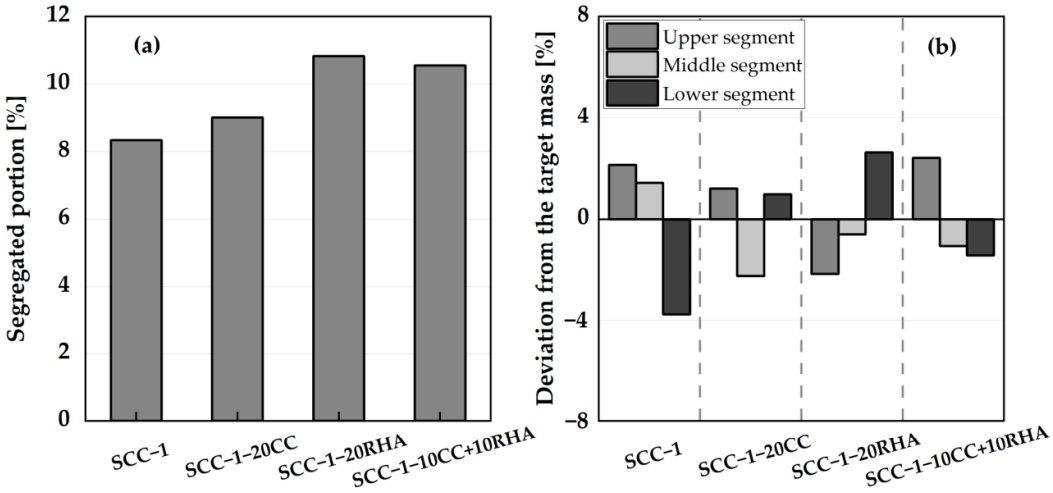

Figure 9. Sieve stability segregation resistance (**a**) and aggregate wash test (**b**) of SCC.

The proportions of the CA from the three segments of the cross-section of the fresh SCC evaluated by aggregate washing test are shown in Figure 9b. The mass deviation of the coarse aggregates from the three segments of all four test specimens is less than 4 wt.% and thus significantly below the limit (15 wt.%) specified in [45].

The flowability retention of SCC specimens is monitored for the first 90 min by sedimentation analysis using a plunger method. SCC-1 and SCC-1-20CC remain stable until 75 min, indicated by the plunger almost reaching the bottom of the cylinder. At 90 min, the immersion depths decrease, indicating that the setting has started. SCC-1-20RHA and the ternary blend SCC-10CC+10RHA also showed similar sedimentation tendencies. In this case, the flowability retention lasts up to 30 min, beyond which the plunger only sinks halfway down the cylinder and at 60 min, penetration is virtually not possible due to the stiffening of the SCC surface (Figure 10).

The short-term stability of all SCC mixes is within the specified limits by [45,56], and even SCC-1-20RHA retains its flowability up to 30 min after mixing. While for the flowability retention assessment, the use of RHA as a partial replacement for PLC is considered critical because the mixing water was absorbed after 30 min of mixing, making the mix stiffer and rapidly losing its self-compactability. The flowability retention assessment using the plunger method assumed the free sinking of the plunger down to the bottom of the concrete anytime it was guided until setting and hardening occur, which is about 90 min, depending on the type of cement used [36]. Excessive settlement of the CA during the early time of the SCC is considered to hinder the sinking of the plunger, signifying segregation had occurred. In this regard, SCC-1 and SCC-1-20CC behaved apparently stable and maintained their flowability until 75 min after mixing. For SCC-1-20RHA and SCC-1-10CC+10RHA, a rapid loss of flowability was observed after 30 min of mixing, which is attributed to the continued suction of the mixing water by RHA and not to the

settlement of the CA since the hardened SCC with RHA as PLC partial replacement still exhibited a uniform distribution of the CA across its section, as shown in Figure 11c,d.

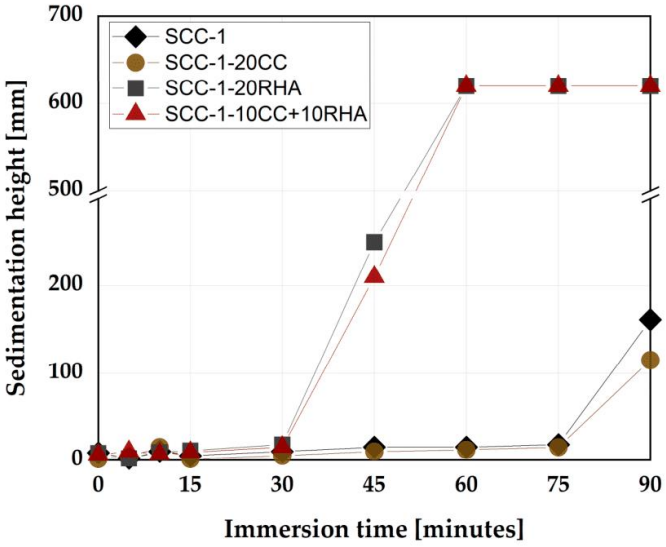

Figure 10. Flowability retention assessment of SCC.

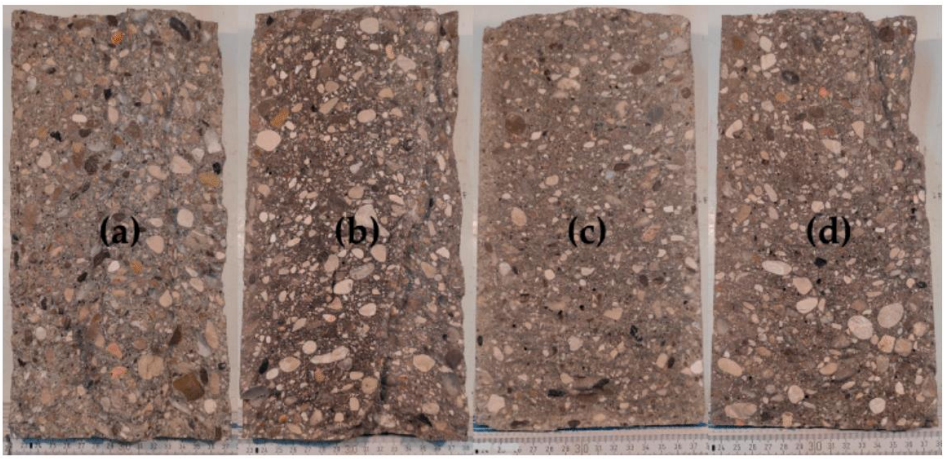

Figure 11. Cross-section of hardened SCC showing uniform distribution of FA and CA across (**a**) SCC-1, (**b**) SCC-1-20CC, (**c**) SCC-1-20RHA and (**d**) SCC-1-10CC+10RHA.

Segregation resistance is an important attribute that determines the acceptability of SCC. It can be measured by sieve stability, which measures the bleeding of SCC after 30 min of resting. The SCC-1 system has a sieve stability value similar to what was obtained by [64], signifying that the result is similar to what is obtainable in the literature, and all the SCC systems meet the requirements of [56] for segregation resistance acceptance and can therefore be used in practice, especially when flowability retention beyond 30 min is not important (RHA-SCC mixes). The wash test was also used to measure the uniform distribution of the coarse aggregate over the fresh SCC section after 30 min of settlement, and all SCC specimens retained the coarse aggregate in suspension during the test period. The only flowability issue observed is the stiffening of the RHA-SCC systems, which is critical after 30 min of production due to the continuous suction of the mixing water by RHA, which may limit applications where longer retention of flowability is required.

4.3. Rheological and Flowability Retention of SCC

The time-dependent rheological assessment of SCC begins with determining the influence of CC and RHA on the torque required to initiate and maintain displacement of SCC based on the applied shear rate measured with a viscometer, as depicted in Figure 12. At 15 min of testing, SCC-1 recorded a torque of 66 Nmm at a lower velocity of 1 rpm and 109 Nmm at the maximum applied velocity of 12 rpm. After 75 min of testing, the torque increased to 120 and 209 Nmm, respectively. SCC-1-20CC required lower torque to achieve and maintain displacement compared to SCC-1, both at lower and higher velocities and at all test times. Although CC has a higher water demand than PLC, the decreased torque could be due to the higher dosage of SP applied to deform the SCC-1-20CC system, despite both binder systems requiring almost similar V_w/V_p to achieve self-compactability, as shown in Table 3. For the RHA binder system, on the other hand, at 15 min of testing, a torque of 102 Nmm was measured at lower velocity and 180 Nmm at higher velocity. These values increased significantly after 30 min of testing due to the stiffening of the SCC-1-20RHA mixture as a result of higher water demand of RHA (see Figure 10). The ternary blend with CC and RHA behaved somewhat in between the SCC-1-20CC and SCC-1-20RHA; the presence of the CC in the blend decreased the torque required to achieve displacement at 75 min of testing by 49 and 57% at lower and higher velocities, respectively, compared to RHA-SCC system.

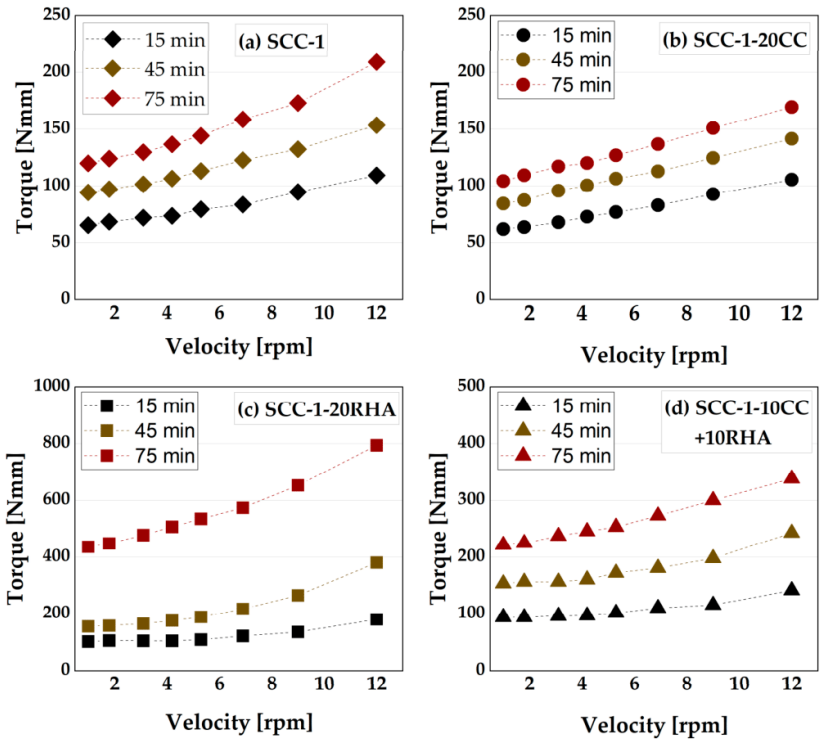

Figure 12. Influence CC and RHA on the time-dependent displacement of SCC-1 (**a**), SCC-1-20CC (**b**), SCC-1-20RHA (**c**) and SCC-1-10CC+10RHA (**d**).

Establishing the dynamic yield stress of SCC is important to determine the extent of energy required to maintain SCC flow; this is important to ensure uniform deformability of SCC across formwork sections. The time-dependent yield stress and plastic viscosity of SCC were established from the measured torque values induced by the applied velocity using a Bingham model, as presented in Figure 13. SCC-1 has a yield stress of 60 Nmm and a plastic viscosity of 3.9 Nmm*min at 15 min of testing, which gradually increased to

Materials **2023**, *16*, 5513

120 Nmm and 8.2 Nmm*min, respectively, after 90 min of testing. SCC-1-20CC showed a similar increasing tendency in yield and viscosity values as SCC-1. The gradual increase of the yield stress and plastic viscosity could be due to the loss of water from the surfaces of SCC caused by evaporation or due to the chemical reaction between the binder and mixing water leading to the initial formation of ettringite, as explained previously in [65]. SCC-1-20RHA had a yield stress of 88.5 Nmm and a plastic viscosity of 6.2 at 15 min of testing, which are 47 and 59% higher than SCC-1, respectively. This yield stress and plastic viscosity values increased rapidly up to 90 min of testing, unlike the SCC-1 and SCC-1-20CC systems. The rapid increase of both yield stress and plastic viscosity values is due to the increased plastic stiffening caused by the continued absorption of the mixing water by the RHA particles. The ternary blend of CC and RHA had both lower dynamic yield, plastic viscosity values and a lower rate at which they increased compared to SCC-1-20RHA. In all cases, SCC mixtures containing RHA exhibited higher yield stress and plastic viscosity values due to their higher water demand.

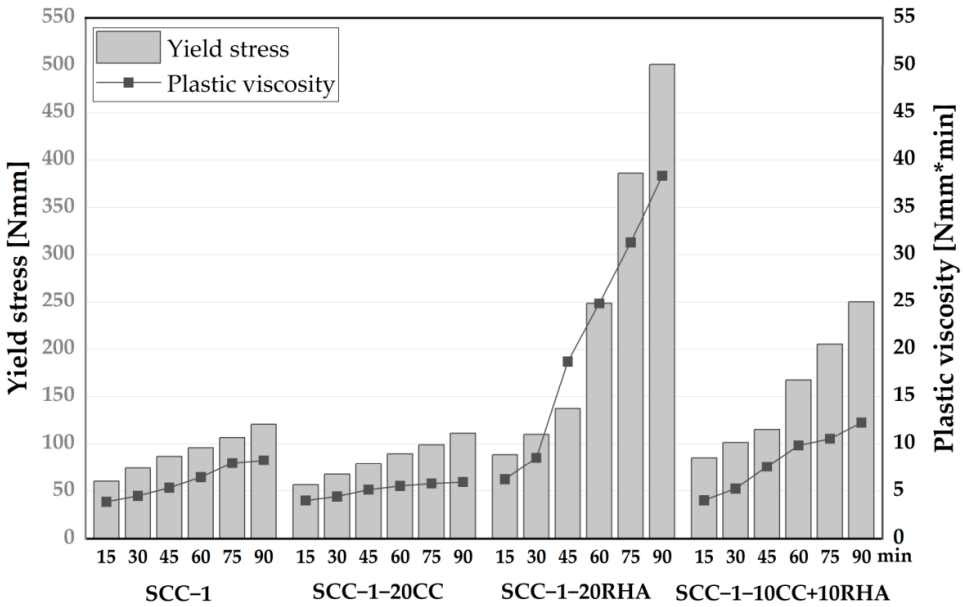

Figure 13. Time-dependent dynamic yield stress and viscosity values of SCC measured up to 90 min after water addition.

The flowability retention of SCC is monitored by comparing the flow resistance of the SCC mixes over a period of 90 min. The flow resistance is determined as the area under the curve of the torque plotted against the velocity values from Figure 12. The flow resistance of SCC-1 measured 15 min after water addition is 933 Nmm/min and increases to 1900 Nmm/min after 90 min (Figure 14). SCC-1-20CC mixture exhibits similar flow resistance to SCC-1 up to 90 min of testing. SCC-1-20RHA, on the other hand, had a flow resistance value of 1388 Nmm/min at 15 min, which is 30% higher than SCC-1, and increased to 8205 Nmm/min at 90 min of testing. SCC-1-10CC+10RHA showed similar flow resistance to SCC-1-20RHA up to 30 min of testing, after which it increased less compared to SCC-1-20RHA. The decrease in flow resistance of SCC-1-10CC+10RHA is due to the presence of CC in the blend, which reduces the water demand and SSA of the system.

Generally, by increasing the SP dosage, PLC partial replacement with 20 vol-% CC has no effect on flowability retention of SCC up to 90 min and therefore, SCC-1-20CC can be used to produce both in situ, precast and ready-mix SCC. However, the use of 20 vol-% RHA and the ternary blend 10CC+10RHA developed high flow resistance and exhibited

rapid loss of flowability after 30 min of mixing. Therefore, their flowability retention needs to be improved for applications beyond 30 min.

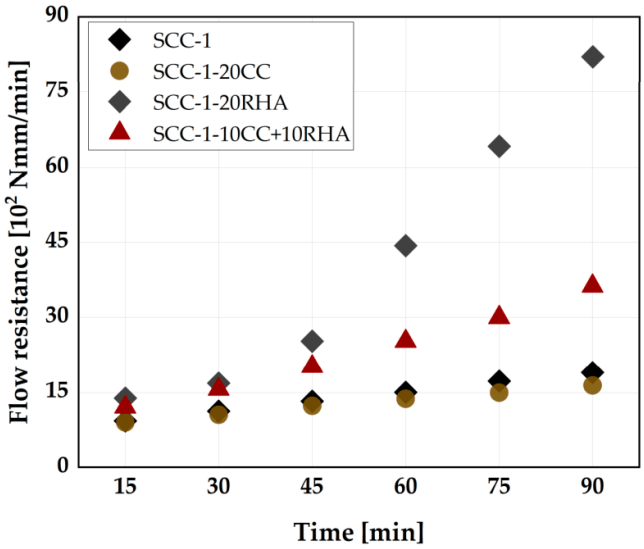

Figure 14. Effect of RHA and CC on the flow resistance of SCC.

The relationship between the flow resistance measurement and the sedimentation analysis conducted by the plunger method is valid in the case of SCC-1 and SCC-1-20CC up to 75 min of testing, while for the SCC-1-20RHA and SCC-1-10CC+10RHA, the relationship is valid only up to 30 min of testing (Figure 15). The penetration of the plunger is not possible in the SCC mixes containing RHA after 45 min of testing due to the stiffening of the SCC surface, which hinders the plunger penetration.

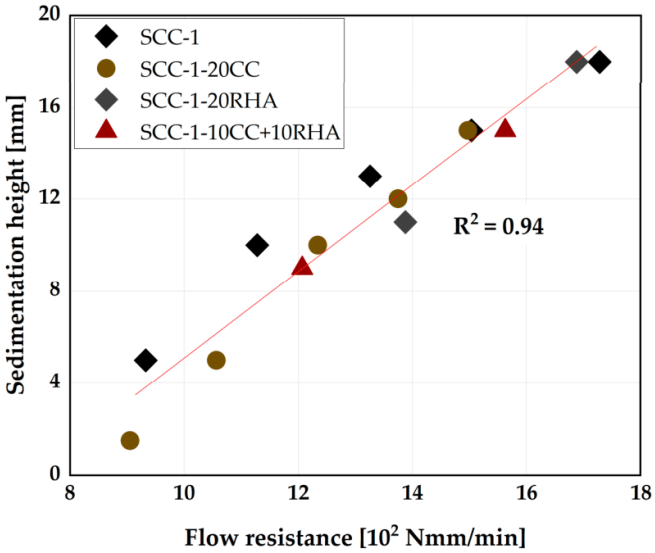

Figure 15. Relationship between the flow resistance and stability of SCC.

The differences between the two methods of flowability retention assessment could be explained by the mechanism of flowability loss due to structural build-up (thixotropy), which can easily be reversed during the viscometer rotation in the flow resistance assess-

ment method, while for the sedimentation analysis, the plunger is only guided and allowed to penetrate the concrete on its own weight, the SCC remained undisturbed and structural build ups unreversed.

4.4. Formation of Hydrate Phases from the Hardened SCP

The formation of SCP hydrates phases was determined at 2, 7 and 28 days of hydration (Figure 16). The mass loss between 50 °C and 140 °C is due to dehydration of the ettringite (E) and calcium silicate hydrates (C-S-H), as observed previously by [66], and increases with an increase in the hydration time for all the SCP specimens. The second mass loss is observed between 140 °C and 190 °C due to the dehydration of the monophases (AFm), similar to what was observed by [67], and is more pronounced in the SCP with RHA partial replacement in all hydration stages. Portlandite decomposition occurs between 400 °C and 450 °C for all SCP specimens, while calcium carbonate ($CaCO_3$) decomposition takes place between 600 °C and 800 °C (Figure 16). The pattern of the formation of the hydrate phases is similar to what was observed previously by [54] when CC was used as a partial replacement for PLC in SCP.

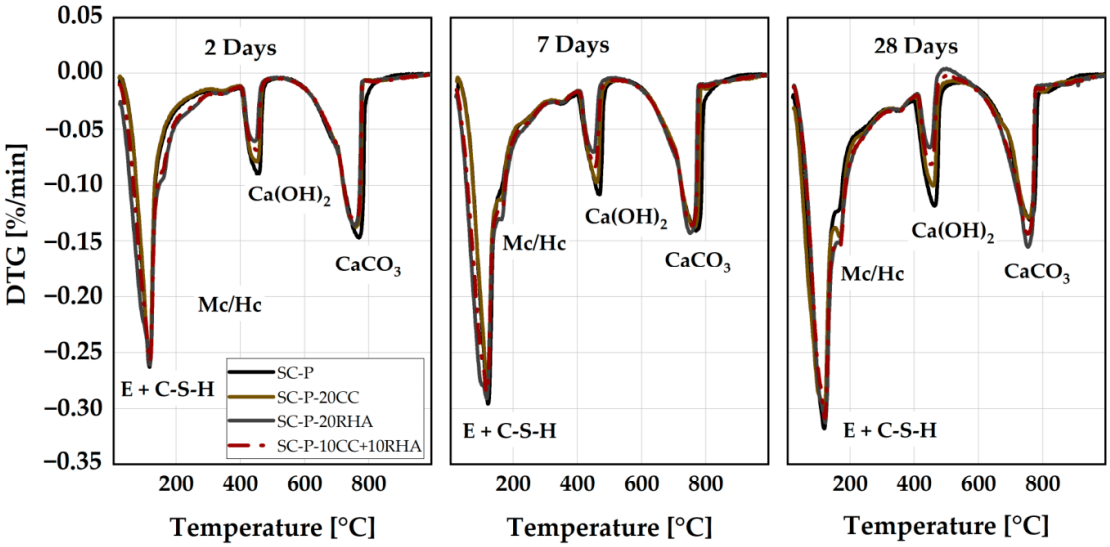

Figure 16. Differential thermal analysis of SCP specimens.

The partial replacement of PLC by CC and RHA has a noticeable effect on the formation of hydrate phases, especially in the ranges of mass loss between 140 °C and 190 °C and between 400 °C and 450 °C. At 2 days of hydration, the DTA peak due to the dehydration of carbonate AFm phases is not evident in the SC-P and SC-P-20CC systems by TG measurements due to the increase of the Vw/Vp ratio used in this study, as the previous study by [54] noticed the formation of these phases in SC-P and SC-P-CC systems at the same time of hydration using a $V_w/V_p = 0.875$. The reaction between the LP and CC enhanced the formation of the carbonate AFm phases at 7 and 28 days of hydration. This increased the volume of the hydration products in the SCP-CC system and densified its microstructure, as previously reported by [54]. RHA and the ternary blend of CC and RHA enhanced the precipitation of these phases even at 2 days of hydration and continued to increase up to 28 days of hydration.

Figure 17 shows the influence of CC and RHA on portlandite consumption. SC-P has the highest CH content at each test time, while SC-P-20RHA exhibits the lowest CH content. SC-P had a CH content of 9.4 g at 2 days, 12.3 g at 7 days and 14 g at 28 days. The CH content of SC-P-20CC at 2 days was 7.9 g and increased to 10.2 g and 10.6 g at 7 and 28 days, respectively. SC-P-20RHA had a CH content of 5.8 g at 2 days, which increased to

6.8 g at 7 days and decreased to 5.8 g at 28 days. The CH content of SC-P-10CC+10RHA is halfway between that of SC-P-20CC and SC-P-20RHA at all test times.

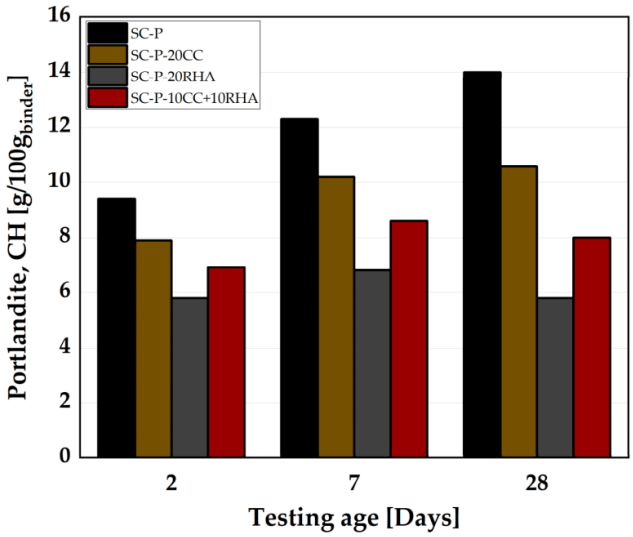

Figure 17. Influence of CC and RHA on portlandite (CH) consumption.

The CH content of SC-P increases over the experimental period due to the continued hydration of C_3S and C_2S in the clinker portion of PLC. The use of CC and RHA as SCM reduced at 2 days of hydration the CH content, mainly due to the dilution effect. Simultaneously, CC and RHA provide more nucleation sites for the precipitation of hydration products at this stage of hydration, as previously observed by [54,68]. The relative decrease in CH content at 7 days of hydration is due to the dilution effect and the initiation of the pozzolanic reaction of CC and RHA, which consumes CH. At 28 days of hydration, CH consumption is significant, especially in SCPs with RHA as a partial substitute for PLC. This is indeed expected and attributed to the pozzolanic effect of CC and RHA, which consumed the CH and produced more C-S-H, which densified the SCP microstructure and thus increased the strength of the SCC, as can be seen later in Section 4.5.2.

4.5. Plastic and Hardened Properties of Self-Compacting Mortar and Concrete

4.5.1. Effect of CC and RHA on Plastic and Total Shrinkage of Self-Compacting Mortar

The mechanism of SC-M shrinkage during early hydration can be explained in three stages. First, plastic shrinkage, during the very early hydration phase, from water addition to about 7 h. The SC-M experiences a transition from fluid to a plastic material. During this period, the rate of plastic shrinkage of SC-M-1 and SC-M-1-20CC is high, reaching up to −7.0 mm/m (Figure 18). This value is somewhat lower to −5.2 and −6.5 mm/m in SC-M-1-20RHA and SC-M-1-10CC+10RHA, respectively. This high plastic shrinkage value of SC-M at this stage is due to the particles settlement caused by gravity leading to an increased packing density of the SC-M and forcing the free water to rise to the surface of the SC-M, resulting in bleeding, as previously explained by [69], and evaporation of moisture from the surfaces of the SC-M leading to the formation of water menisci, which eventually create a negative capillary pressure that contracts the SC-M particles and consequently causes volumetric contraction, similar to was reported by [70,71]. It has been reported that the use of shrinkage-reducing admixtures (SRA) reduced the plastic shrinkage of SCC at this stage of hydration by reducing the internal friction angle between SCC particles due to their high fluidity and delaying the setting time of SCC [69]. RHA is expected to behave similarly to the SRA in reducing the plastic shrinkage of the SC-M because it delays the initial setting time of the blended cement [72]. The second stage lasts from 7 to 16 h after

water addition. Here, the plastic shrinkage rate of SC-M-1 decreases and yields a shrinkage value of −7.3 mm/m, while SC-M-20CC exhibits no further plastic shrinkage. Plastic shrinkage increases for the two other SC-M yielding −5.5 mm/m for SC-M-20RHA and −6.6 mm/m for SC-M-10CC+10RHA. Finally, after 16 h of hydration, the plastic shrinkage remains constant until the end of the measurement. The reason for the plastic shrinkage of the SC-M beyond 7 h of hydration could be due to the continuous evaporation of moisture from the SC-M surfaces and volume reduction due to water consumption by the hydration process, as previously observed by [54,70,71]. In general, the reduction in plastic shrinkage after 7 h of hydration due to the partial replacement of CC and RHA in SC-M could be attributed to the fact that both act as nuclei for the formation of hydration products at an early time of hydration, thereby increasing the volume of hydration product and densifying the SC-M microstructure, as observed previously by [73] when studying the dominant factors on the early hydration of metakaolin-cement paste. And for the RHA and ternary blend of CC and RHA, the reduction in plastic shrinkage could also be due to the release of the early absorbed water by the RHA particles, thereby increasing the internal relative humidity of the SC-M and reducing the autogenous shrinkage at an early time of the SC-M, as RHA was used previously by [74] to mitigate the autogenous shrinkage of cement paste.

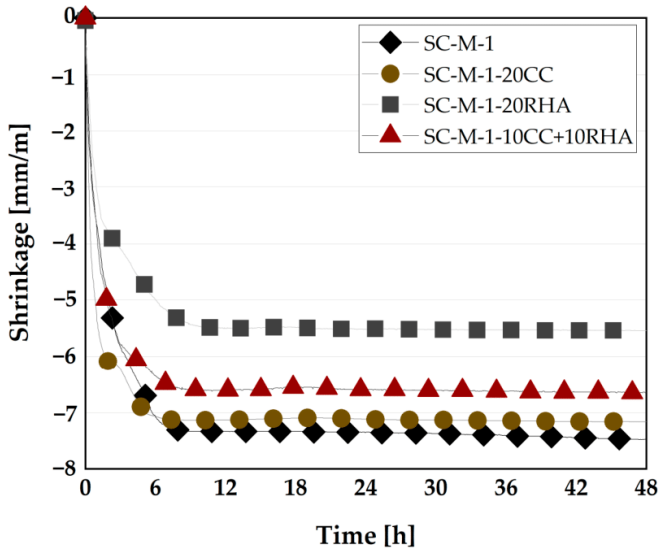

Figure 18. Effect of CC and RHA on plastic shrinkage of SC-M.

The effect of the partial replacement of PLC with CC and RHA on the total shrinkage of SC-M was measured on 40 × 40 × 160 mm^3 prisms, as presented in Figure 19. SC-M-1 and SC-M-1-20CC exhibited the same drying shrinkage values at all test times up to 14 days, after which SC-M-1-20CC shrank less than SC-M-1. SC-M-1-20RHA had the highest initial drying shrinkage of all SC-M specimens until about 14 days, when it decreased, yielding shrinkage values similar to SC-M-1 at 56 days. From 21 days and beyond, SC-M-1-10CC+10RHA shrank more than the other specimens.

The total shrinkage of SC-M specimens is a combination of drying shrinkage caused by the continuous loss of water from the capillary pores of the SC-M to equilibrate the relative humidity of the surrounding environment and autogenous shrinkage due to the reduction of water by the hydration process. SC-M-1 and SC-M-1-20CC have the same total shrinkage tendency up to 28 days of testing; beyond 28 days of testing, CC decreased the total shrinkage of the SC-M partly due to the volume increase of hydration product from the formation of more carboaluminate AFm phases, as shown previously in Figure 16, and or due to lower amount of evaporable water because of the pozzolanic reaction of the CC, which consumes more water, as previously reported by [75] in the case of using metakaolin

as partial replacement for cement. RHA and the ternary blend of CC and RHA in SC-M specimens exhibit a different pattern of total shrinkage. RHA-SC-M specimens shrank more than other specimens up to 7 days of testing due to rapid evaporation of the absorbed water from the surfaces of the RHA-SC-M specimens, as the absorbed water was reported by [76] as having higher mobility than the water in the capillary pores and could evaporate easily, and thus an increase of the drying shrinkage. Beyond 7 days of testing, the total shrinkage of RHA-SC-M decreased and was equal to that of PLC-SC-M from 56 days and 91 days. The improvement of the total shrinkage could be due to the further release of absorbed water by RHA to restrain the decrease of the internal relative humidity of SC-M and, thus, a decrease in the total shrinkage. This phenomenon was explained previously by [74] when RHA was used as an internal curing agent in cement paste. From 21 days of testing and beyond, SC-M-1-10CC+10RHA shrank more than any other specimen due to continuous evaporation of the absorbed water from its surfaces.

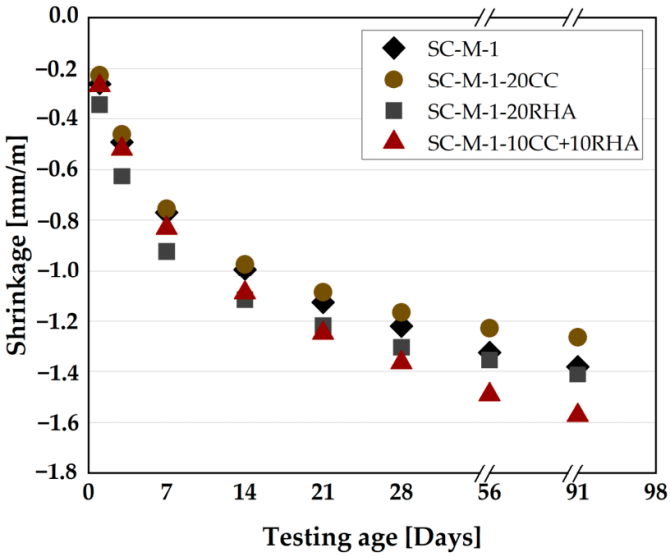

Figure 19. Effect of CC and RHA on drying shrinkage of SC-M.

4.5.2. Compressive Strength and Rapid Chloride Migration Assessment of SCC

The impact of the CC and RHA on the development of compressive strength of SCC up to 28 days is shown in Figure 20. SCC-1 achieved higher values of compressive strength at 2 and 7 days. All the remaining specimens exhibited similar compressive strength values at 2 and 7 days, which are 8% and 21% lower than SCC-1, respectively. At this stage of curing, CC and RHA behaved similarly, and their physical presence resulted in a dilution effect and, thus, a reduction of the compressive strength, as observed previously by [54] when CC was used as a partial replacement for PLC in SC-M. At 28 days, SCC-1 and SCC-1-20CC reach similar compressive strength values while a slight increase of 6% is observed compared to SCC-1 for SCC-1-20RHA and SCC-1-10CC+10RHA due to the pozzolanic reactive of CC and RHA. The use of RHA and the blend of CC and RHA at 28 days of curing behaved similarly to silica fume in improving the compressive strength of SCC beyond the level of the pure cement, as previously observed by [77,78]. Another explanation for the increase of the compressive strength of RHA and the ternary blend of CC and RHA specimens is the continuous transition of Ca^{2+} from the PLC matrix to RHA, which enhances the pozzolanic reactivity of the RHA blended SCC and improves its compressive strength as explained by [79].

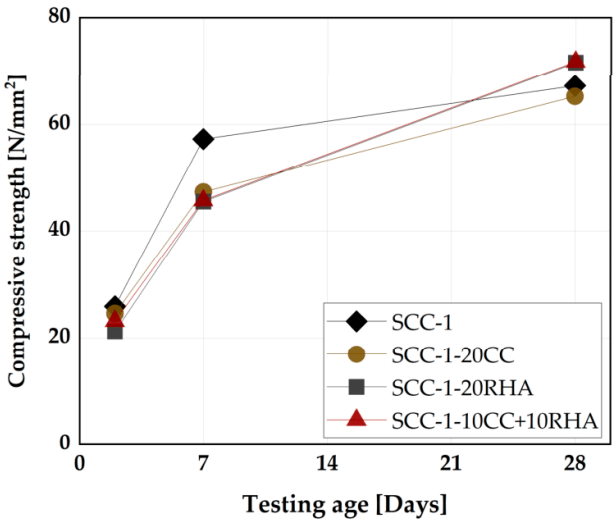

Figure 20. Compressive strength development of SCC specimens.

4.6. Rapid Chloride Resistance of SCC

The depth of chloride penetration and migration coefficient of all SCC specimens are shown in Figure 21. The depth of chloride penetration of SCC-1 is 26 mm and increases to 30 mm for SCC-1-20CC. SCC-1-20RHA had the lowest chloride penetration depth of 13 mm, while that of SCC-1-10CC+10RHA was 19 mm. There is no significant difference between the chloride migration coefficient of SCC-1 and SCC-1-20CC, 16 × 10^{-12}. SCC-1-20RHA had a chloride migration coefficient of 4.5 × 10^{-12} and increased to 8.2 × 10^{-12} for SCC-1-10CC+10RHA.

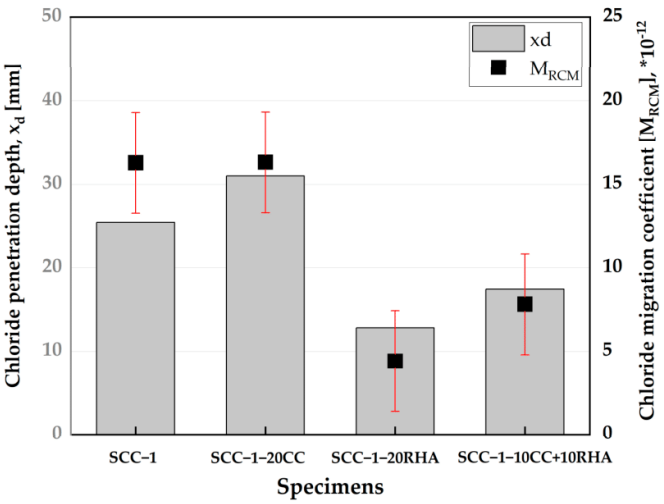

Figure 21. Influence of CC and RHA on the chloride resistance of SCC.

SCC-1-20CC achieved similar performance to SCC-1 in terms of chloride migration resistance; although the chloride penetration depth of SCC-1-20CC is greater than that of SCC-1, the determination of chloride migration resistance according to [53] considers other factors, such as the duration of the test and the voltage used, which give an indication for the density of a concrete microstructure. Both SCC-1 and SCC-1-20CC can be classified as having "Normal" SCC quality—8–16 × 10^2 m^2/s—according to non-steady state chloride migration resistance concrete classification by [80,81]. SCC-1-20RHA and

SCC-1-10CC+10RHA achieved a "Good" SCC quality due to the pozzolanic reactivity of RHA that consumed CH from PLC hydration and produced more C-S-H, which densified the concrete microstructure and improved its chloride resistance.

5. Summary and Conclusions

- The study investigated the potential use of up to 40 vol-% CC and RHA as a partial replacement for PLC in SCP. Partial replacement of PLC with CC, as used in this study, is possible up to 40 vol-% and can be achieved with the same V_w/V_p used for the PLC system, with an increase in SP dosages. The use of RHA as a partial replacement for PLC, on the other hand, requires urgent adjustment of the V_w/V_p even at a lower replacement level of 5 vol-% to achieve similar deformability to the PLC systems; SP adjustment alone cannot provide the required degree of deformability. Therefore, for the application in SCC, the partial replacement of PLC by RHA should be kept at 20 vol-%;
- By adjusting the SP dosages, self-compactability can be achieved with PLC partial replacement with 20 vol-%CC, 20 vol-% RHA and 10 vol-% CC + 10 vol-% RHA, using a $V_w/V_p = 1.275$;
- The deformability and short-term segregation resistance of the binary and ternary mix design with 20 vol-% CC, 20 vol-% RHA and 10 vol-% CC + 10 vol-% RHA are within acceptable limits, and therefore, the binary and ternary blends of CC and RHA could use in practice up to 20 vol-% as PLC partial replacement;
- At an increased SP dosage, PLC partial replacement with 20 vol-% CC has less impact than the binary and ternary blend of 20 vol-% RHA and 10 vol-% CC + 10 vol-% RHA on flowability retention of SCC up to 60 min, and therefore, SCC-1-20CC can be used to produce both precast and ready-mix SCC. However, the use of 20 vol-% RHA and the ternary blend 10CC+10RHA developed high flow resistance and showed rapid loss of flowability after 30 min of mixing. Therefore, their flowability retention needs to be improved for applications beyond 30 min. SCC with high content of RHA, 20 vol-% and above, is recommended for the production of precast SCC elements only due to the short flowability retention window required by precast SCC compared to ready-mix SCC. Although additional treatment may be required to improve the early strength development of RHA SCC;
- SCC produced with RHA as PLC partial replacement showed higher flow resistance and viscosity and increased both the static and dynamic yield stress of SCC. This effect is reduced to some extent by ternary blending CC and RHA. Therefore, the proportion of RHA shall always be kept low, perhaps at 5 vol-%, in the binary and ternary blended SCC mixture, when flowability retention beyond 30 min is required, for example, in the ready-mix concrete;
- Partial replacement of PLC with 20 vol-% CC reduced the plastic shrinkage of SC-M by 4%, 20 vol-% RHA reduced the plastic shrinkage of SC-M by 26%, while the ternary blend of 10 vol-% CC+10 vol-% RHA reduced the plastic shrinkage by 11%. Partial replacement of PLC with 20 vol-% CC had no effect on the total shrinkage of SC-M at 28 days of curing, while the binary and ternary blends of RHA, CC and RHA increased the total shrinkage of SC-M by 8 and 16%, respectively. Therefore, RHA could be an effective SCM to reduce hairline cracking that occurs at an early time in concrete due to the use of a high amount of cement per m^3 of concrete;
- Both CC and RHA consumed CH due to their pozzolanic reactivity. Partial replacement of 20 vol-% PLC with CC had no significant effect on the 28-day compressive strength and chloride migration resistance of SCC. While the SCC produced with RHA and the blend of CC and RHA increased the 28-day compressive strength of SCC by 5%. The chloride migration resistance of 20 vol-% RHA is 3 times that of SCC produced with only PLC, while that of the ternary blend 10 vol-% CC + 10 vol-% RHA is 2 times that of SCC produced with only PLC. RHA is capable of improving the chloride migration resistance of SCC and should be used to improve the microstructural densification of SCC produced with only PLC.

Author Contributions: Conceptualization, A.M.; writing—original draft preparation, A.M.; writing—review and editing, A.M. and K.-C.T.; supervision, K.-C.T. All authors have read and agreed to the published version of the manuscript.

Funding: The first author was funded by the German Academic Exchange Service (DAAD) and the Nigerian Petroleum Technology Development Fund (PTDF). We acknowledge financial support from Universität der Bundeswehr München.

Institutional Review Board Statement: Not applicable.

Informed Consent Statement: Not applicable.

Data Availability Statement: Not applicable.

Conflicts of Interest: The authors declare no conflict of interest.

References

1. Aïtcin, P.-C. Cements of yesterday and today: Concrete of tomorrow. *Cem. Concr. Res.* **2000**, *30*, 1349–1359. [CrossRef]
2. Al-Akhras, N.M. Durability of metakaolin concrete to sulfate attack. *Cem. Concr. Res.* **2006**, *36*, 1727–1734. [CrossRef]
3. Kavitha, O.; Shanthi, V.; Arulraj, G.P.; Sivakumar, V. Microstructural studies on eco-friendly and durable Self-compacting concrete blended with metakaolin. *Appl. Clay Sci.* **2016**, *124*, 143–149. [CrossRef]
4. Kannan, V. Strength and durability performance of self compacting concrete containing self-combusted rice husk ash and metakaolin. *Constr. Build. Mater.* **2018**, *160*, 169–179. [CrossRef]
5. Okamura, H.; Ozawa, K. Mix-design for self-compacting concrete. *Concr. Libr. JSCE* **1995**, *25*, 107–120.
6. Okamura, H. Self-Compacting High-Performance Concrete. *Concr. Int.* **1997**, *19*, 50–54.
7. Su, N.; Hsu, K.-C.; Chai, H.-W. A simple mix design method for self-compacting concrete. *Cem. Concr. Res.* **2001**, *31*, 1799–1807. [CrossRef]
8. Ramanathan, P.; Baskar, I.; Muthupriya, P.; Venkatasubramani, R. Performance of self-compacting concrete containing different mineral admixtures. *KSCE J. Civ. Eng.* **2013**, *17*, 465–472. [CrossRef]
9. *DIN EN 197-1*; Zement—Teil 1: Zusammensetzung, Anforderungen und Konformitätskriterien von Normalzement (Cement—Part 1: Composition, Specifications and Conformity Criteria for Common Cements). Beuth-Verlag: Berlin, Germany, 2011; p. 8.
10. Uysal, M.; Sumer, M. Performance of self-compacting concrete containing different mineral admixtures. *Constr. Build. Mater.* **2011**, *25*, 4112–4120. [CrossRef]
11. Yahia, A.; Tanimura, M.; Shimoyama, Y. Rheological properties of highly flowable mortar containing limestone filler-effect of powder content and W/C ratio. *Cem. Concr. Res.* **2005**, *35*, 532–539. [CrossRef]
12. Avet, F.; Scrivener, K. Hydration Study of Limestone Calcined Clay Cement (LC3) Using Various Grades of Calcined Kaolinitic Clays. In *Calcined Clays for Sustainable Concrete, Proceedings of the 2nd International Conference on Calcined Clays for Sustainable Concrete, La Havana, Cuba, 5–7 December 2017*; Martirena, F., Favier, A., Scrivener, K., Eds.; Springer Nature: La Havanna, Cuba, 2018; pp. 35–40.
13. Scrivener, K.; Martirena, F.; Bishnoi, S.; Maity, S. Calcined clay limestone cements (LC3). *Cem. Concr. Res.* **2018**, *114*, 49–56. [CrossRef]
14. Khatib, J. Performance of self-compacting concrete containing fly ash. *Constr. Build. Mater.* **2008**, *22*, 1963–1971. [CrossRef]
15. Gesoğlu, M.; Güneyisi, E.; Kocabağ, M.E.; Bayram, V.; Mermerdaş, K. Fresh and hardened characteristics of self compacting concretes made with combined use of marble powder, limestone filler, and fly ash. *Constr. Build. Mater.* **2012**, *37*, 160–170. [CrossRef]
16. Yazıcı, H. The effect of silica fume and high-volume Class C fly ash on mechanical properties, chloride penetration and freeze–thaw resistance of self-compacting concrete. *Constr. Build. Mater.* **2008**, *22*, 456–462. [CrossRef]
17. Bingöl, A.F.; Tohumcu, T. Effects of different curing regimes on the compressive strength properties of self compacting concrete incorporating fly ash and silica fume. *Mater. Des.* **2013**, *51*, 12–18. [CrossRef]
18. Parande, A.K.; Babu, B.R.; Karthik, M.A.; Kumaar, K.D.; Palaniswamy, N. Study on strength and corrosion performance for steel embedded in metakaolin blended concrete/mortar. *Constr. Build. Mater.* **2008**, *22*, 127–134. [CrossRef]
19. Said-Mansour, M.; Kadri, E.-H.; Kenai, S.; Ghrici, M.; Bennaceur, R. Influence of calcined kaolin on mortar properties. *Constr. Build. Mater.* **2010**, *25*, 2275–2282. [CrossRef]
20. Muhammad, A.; Thienel, K.-C.; Sposito, R. Suitability of Blending Rice Husk Ash and Calcined Clay for the Production of Self-Compacting Concrete: A Review. *Materials* **2021**, *14*, 6252. [CrossRef]
21. Dhandapani, Y.; Sakthivel, T.; Santhanam, M.; Gettu, R.; Pillai, R.G. Mechanical properties and durability performance of concretes with Limestone Calcined Clay Cement (LC^3). *Cem. Concr. Res.* **2018**, *107*, 136–151. [CrossRef]
22. Beuntner, N.; Kustermann, A.; Thienel, K.-C. Pozzolanic potential of calcined clay in high-performance concrete. In Proceedings of the International Conference on Sustainable Materials, Systems and Structures—SMSS 2019 New Generation of Construction Materials, Rovinj, Croatia, 20–22 March 2019; Serdar, M., Štirmer, N., Provis, J., Eds.; RILEM Publications S.A.R.L.: Rovinj, Croatia, 2019; pp. 470–477.
23. Kannan, V.; Ganesan, K. Chloride and chemical resistance of self compacting concrete containing rice husk ash and metakaolin. *Constr. Build. Mater.* **2014**, *51*, 225–234. [CrossRef]

24. Gill, A.S.; Siddique, R. Durability properties of self-compacting concrete incorporating metakaolin and rice husk ash. *Constr. Build. Mater.* **2018**, *176*, 323–332. [CrossRef]
25. Memon, S.A.; Shaikh, M.A.; Akbar, H. Utilization of Rice Husk Ash as viscosity modifying agent in Self Compacting Concrete. *Constr. Build. Mater.* **2010**, *25*, 1044–1048. [CrossRef]
26. Sposito, R.; Maier, M.; Beuntner, N.; Thienel, K.-C. Physical and mineralogical properties of calcined common clays as SCM and their impact on flow resistance and demand for superplasticizer. *Cem. Concr. Res.* **2022**, *154*, 106743. [CrossRef]
27. Kannan, V. Relationship between ultrasonic pulse velocity and compressive strength of self compacting concrete incorporate rice husk ash and metakaolin. *Asian J. Civ. Eng.* **2015**, *16*, 1077–1088.
28. Chopra, D.; Siddique, R. Strength, permeability and microstructure of self-compacting concrete containing rice husk ash. *Biosyst. Eng.* **2015**, *30*, 72–80. [CrossRef]
29. Madandoust, R.; Mousavi, S.Y. Fresh and hardened properties of self-compacting concrete containing metakaolin. *Constr. Build. Mater.* **2012**, *35*, 752–760. [CrossRef]
30. Gill, A.S.; Siddique, R. Strength and micro-structural properties of self-compacting concrete containing metakaolin and rice husk ash. *Constr. Build. Mater.* **2017**, *157*, 51–64. [CrossRef]
31. Rahman, M.E.; Muntohar, A.S.; Pakrashi, V.; Nagaratnam, B.H.; Sujan, D. Self compacting concrete from uncontrolled burning of rice husk and blended fine aggregate. *Mater. Des.* **2014**, *55*, 410–415. [CrossRef]
32. Kordts, S.; Grube, H. Steuerung der Verarbeitbarkeitseigenschaften von Selbstverdichtendem Beton als Transportbeton (Controlling the workability properties of self compacting concrete used as ready-mixed concrete). *Beton* **2002**, *52*, 217–223.
33. *DIN EN 12350-8*; Prüfung von Frischbeton—Teil 8: Selbstverdichtender Beton—Setzfließversuch (Testing Fresh Concrete—Part 8: Self-Compacting Concrete—Slump-Flow Test). Beuth-Verlag: Berlin, Germany, 2019; p. 8.
34. *DIN EN 12350-9*; Prüfung von Frischbeton—Teil 9: Selbstverdichtender Beton—Auslauftrichterversuch (Testing Fresh Concrete—Part 9: Self-Compacting Concrete—V-Funnel Test). Beuth-Verlag: Berlin, Germany, 2010; p. 8.
35. *DIN EN 12350-12*; Prüfung von Frischbeton—Teil 12: Selbstverdichtender Beton—Blockierring-Versuch (Testing Fresh Concrete—Part 12: Self-Compacting Concrete—J-Ring Test). Beuth-Verlag: Berlin, Germany, 2010; p. 11.
36. Kordts, S.; Breit, W. Beurteilung der Frischbetoneigenschaften von Selbstverdichtendem Beton (Assessment of the fresh concrete properties of self compacting concrete). *Beton* **2003**, *53*, 565–571.
37. Beuntner, N.; Thienel, K.-C. Properties of Calcined Lias Delta Clay—Technological Effects, Physical Characteristics and Reactivity in Cement. In *Calcined Clays for Sustainable Concrete, Proceedings of the 1st International Conference on Calcined Clays for Sustainable Concrete, Ecublens, Switzerland, 23–25 June 2015*; Scrivener, K., Favier, A., Eds.; Springer: Dordrecht, The Netherlands, 2015; pp. 43–50.
38. *DIN ISO 9277*; Determination of the Specific Surface Area of Solids by Gas Adsorption—BET Method. Beuth-Verlag: Berlin, Germany, 2003; p. 19.
39. Puntke, W. Wasseranspruch von feinen Kornhaufwerken. *Beton* **2002**, *52*, 242–248.
40. *DIN EN ISO 17892-3*; Geotechnical Investigation and Testing—Laboratory Testing of Soil—Part 3: Determination of Particle Density. Beuth-Verlag: Berlin, Germany, 2015; p. 21.
41. EFNARC. Specification and Guidelines for Self-Compacting Concrete. In *Specification and Guidelines*; EFNARC: Farnham, UK, 2002.
42. Okamura, H.; Ouchi, M. Self-Compacting Concrete. *J. Adv. Concr. Technol.* **2003**, *1*, 5–15. [CrossRef]
43. *DIN EN 196-1*; Prüfverfahren für Zement—Teil 1: Bestimmung der Festigkeit (Methods of Testing Cement—Part 1: Determination of Strength). Beuth-Verlag: Berlin, Germany, 2016; p. 31.
44. *DIN EN 12350-11*; Prüfung von Frischbeton—Teil 11: Selbstverdichtender Beton—Bestimmung der Sedimentationsstabilität im Siebversuch (Testing Fresh Concrete—Part 11: Self-Compacting Concrete—Sieve Segregation Test). Beuth-Verlag: Berlin, Germany, 2010; p. 11.
45. Brameshuber, W.; Uebachs, S. Sedimentationsstabilität von Selbstverdichtenden Betonen (Sedimentation Stability of self-Compacting Concretes). In *Rheologische Messungen an mineralischen Baustoffen—Workshop 2003*; Kusterle, W., Ed.; Schleibinger: Regensburg, Germany, 2003; p. 10.
46. Feys, D.; Verhoeven, R.; De Schutter, G. Fresh self compacting concrete, a shear thickening material. *Cem. Concr. Res.* **2008**, *38*, 920–929. [CrossRef]
47. Barnes, H.A.; Walters, K. The yield stress myth? *Rheol. Acta* **1985**, *24*, 323–326. [CrossRef]
48. Hackley, V.A.; Ferraris, C.F. *Guide to Rheological Nomenclature—Measurements in Ceramic Particulate Systems*; National Institute of Standards and Technology (NIST): Gaithersburg, MD, USA, 2001; pp. III, 29.
49. *DIN EN 60825-1*; Sicherheit von Lasereinrichtungen—Teil 1: Klassifizierung von Anlagen und Anforderungen (Safety of laser products—Part 1: Equipment Classification and Requirements). Beuth-Verlag: Berlin, Germany, 2015; p. 115.
50. *DIN EN 12617-4*; Produkte und Systeme für den Schutz und die Instandsetzung von Betontragwerken Prüfverfahren Teil 4: Bestimmung des Schwindens und Quellens (Products and Systems for the Protection and Repair of Concrete Structures—Test Methods—Part 4: Determination of Shrinkage and Expansion). Beuth-Verlag: Berlin, Germany, 2002; p. 14.
51. Snellings, R.; Chwast, J.; Cizer, Ö.; De Belie, N.; Dhandapani, Y.; Durdzinski, P.; Elsen, J.; Haufe, J.; Hooton, D.; Patapy, C.; et al. Report of TC 238-SCM: Hydration stoppage methods for phase assemblage studies of blended cements—Results of a round robin test. *Mater. Struct.* **2018**, *51*, 111. [CrossRef]
52. *DIN EN 12390-3*; Prüfung von Festbeton—Teil 3: Druckfestigkeit von Probekörpern (Testing Hardened Concrete—Part 3: Compressive Strength of Test Specimens). Beuth-Verlag: Berlin, Germany, 2019; p. 20.

53. *DIN EN 12390-18*; Prüfung von Festbeton—Teil 18: Bestimmung des Chloridmigrationskoeffizienten (Testing Hardened Concrete Part 18: Determination of the Chloride Migration Coefficient). Beuth-Verlag: Berlin, Germany, 2021; p. 20.
54. Muhammad, A.; Thienel, K.-C.; Sposito, R. Suitability of Clinker Replacement by a Calcined Common Clay in Self-Consolidating Mortar—Impact on Rheology and Early Age Properties. *Minerals* **2022**, *12*, 625. [CrossRef]
55. *DIN 1045-2*; Tragwerke aus Beton, Stahlbeton und Spannbeton—Teil 2: Beton—Festlegung, Eigenschaften, Herstellung und Konformität—Anwendungsregeln zu DIN EN 206-1 (Concrete, Reinforced and Prestressed Concrete Structures—Part 2: Concrete—Specification, Properties, Production and Conformity—Application Rules for DIN EN 206-1). Beuth-Verlag: Berlin, Germany, 2008; p. 62.
56. *DIN EN 206*; Beton—Festlegung, Eigenschaften, Herstellung und Konformität (Concrete—Specification, Performance, Production and Conformity). Beuth Verlag GmbH: Berlin, Germany, 2021; p. 105.
57. Le, H.T.; Kraus, M.; Siewert, K.; Ludwig, H.-M. Effect of macro-mesoporous rice husk ash on rheological properties of mortar formulated from self-compacting high performance concrete. *Constr. Build. Mater.* **2015**, *80*, 225–235. [CrossRef]
58. Sua-Iam, G.; Sokrai, P.; Makul, N. Novel ternary blends of Type 1 Portland cement, residual rice husk ash, and limestone powder to improve the properties of self-compacting concrete. *Constr. Build. Mater.* **2016**, *125*, 1028–1034. [CrossRef]
59. Raisi, E.M.; Amiri, J.V.; Davoodi, M.R. Mechanical performance of self-compacting concrete incorporating rice husk ash. *Constr. Build. Mater.* **2018**, *177*, 148–157. [CrossRef]
60. Muhammad, A.; Thienel, K.-C. Performance of Calcined Common Clay as Partial Replacement to Cement in Selfcompacting Concrete. In Proceedings of the International Conference on Calcined Clays for Sustainable Concrete, Lausanne, Switzerland, 5–7 July 2022; Sharma, M., Hafez, H., Eds.; Springer: Berlin/Heidelberg, Germany, 2022; pp. 102–103.
61. Kundt, G.; Krentz, H.; Glass, Ä. *Epidemiologie und Medizinische Biometrie (Epidemiology and Medical Biometry). Berichte aus der Statistik*; Shaker Verlag: Aachen, Germany, 2011; p. 246.
62. Diniz, H.A.; dos Anjos, M.A.; Rocha, A.K.; Ferreira, R.L. Effects of the use of agricultural ashes, metakaolin and hydrated-lime on the behavior of self-compacting concretes. *Constr. Build. Mater.* **2021**, *319*, 126087. [CrossRef]
63. Sposito, R.; Beuntner, N.; Thienel, K.-C. Characteristics of components in calcined clays and their influence on the efficiency of superplasticizers. *Cem. Concr. Compos.* **2020**, *110*, 103594. [CrossRef]
64. Belaidi, A.; Azzouz, L.; Kadri, E.; Kenai, S. Effect of natural pozzolana and marble powder on the properties of self-compacting concrete. *Constr. Build. Mater.* **2012**, *31*, 251–257. [CrossRef]
65. Brooks, J.; Johari, M.M. Effect of metakaolin on creep and shrinkage of concrete. *Cem. Concr. Compos.* **2001**, *23*, 495–502. [CrossRef]
66. Palou, M.; Boháč, M.; Kuzielová, E.; Novotný, R.; Žemlička, M.; Dragomirová, J. Use of calorimetry and thermal analysis to assess the heat of supplementary cementitious materials during the hydration of composite cementitious binders. *J. Therm. Anal. Calorim.* **2020**, *142*, 97–117. [CrossRef]
67. Boháč, M.; Palou, M.; Novotný, R.; Másilko, J.; Všianský, D.; Staněk, T. Investigation on early hydration of ternary Portland cement-blast-furnace slag–metakaolin blends. *Constr. Build. Mater.* **2014**, *64*, 333–341. [CrossRef]
68. Berodier, E.; Scrivener, K. Understanding the Filler Effect on the Nucleation and Growth of C-S-H. *J. Am. Ceram. Soc.* **2014**, *97*, 3764–3773. [CrossRef]
69. Saliba, J.; Rozière, E.; Grondin, F.; Loukili, A. Influence of shrinkage-reducing admixtures on plastic and long-term shrinkage. *Cem. Concr. Compos.* **2010**, *33*, 209–217. [CrossRef]
70. Turcry, P.; Loukil, A. Evaluation of plastic shrinkage cracking of self-consolidating concrete. *ACI Mater. J.* **2006**, *103*, 272–279.
71. Sayahi, F.; Emborg, M.; Hedlund, H.; Cwirzen, A. Plastic Shrinkage Cracking of Self-compacting Concrete: Influence of Capillary Pressure and Dormant Period. *Nord. Concr. Res.* **2019**, *60*, 67–88. [CrossRef]
72. Ganesan, K.; Rajagopal, K.; Thangavel, K. Rice husk ash blended cement: Assessment of optimal level of replacement for strength and permeability properties of concrete. *Constr. Build. Mater.* **2008**, *22*, 1675–1683. [CrossRef]
73. Shui, Z.; Sun, T.; Fu, Z.; Wang, G. Dominant factors on the early hydration of metakaolin-cement paste. *J. Wuhan Univ. Technol. Sci. Ed.* **2010**, *25*, 849–852. [CrossRef]
74. Huang, H.; Ye, G.; Fehling, E.; Middendorf, B.; Thiemicke, J. Use of rice husk ash for mitigating the autogenous shrinkage of cement pastes at low water cement ratio. In Proceedings of the HiPerMat 2016 4th International Symposium on Ultra-High Performance Concrete and High Performance Construction Materials, Kassel, Germany, 9–11 March 2016.
75. Güneyisi, E.; Gesoğlu, M.; Özbay, E. Strength and drying shrinkage properties of self-compacting concretes incorporating multi-system blended mineral admixtures. *Constr. Build. Mater.* **2010**, *24*, 1878–1887. [CrossRef]
76. Mechtcherine, V.; Gorges, M.; Schroefl, C.; Assmann, A.; Brameshuber, W.; Ribeiro, A.B.; Cusson, D.; Custódio, J.; da Silva, E.F.; Ichimiya, K.; et al. Effect of internal curing by using superabsorbent polymers (SAP) on autogenous shrinkage and other properties of a high-performance fine-grained concrete: Results of a RILEM round-robin test. *Mater. Struct.* **2013**, *47*, 541–562. [CrossRef]
77. Zhao, H.; Sun, W.; Wu, X.; Gao, B. The properties of the self-compacting concrete with fly ash and ground granulated blast furnace slag mineral admixtures. *J. Clean. Prod.* **2015**, *95*, 66–74. [CrossRef]
78. Wongkeo, W.; Thongsanitgarn, P.; Ngamjarurojana, A.; Chaipanich, A. Compressive strength and chloride resistance of self-compacting concrete containing high level fly ash and silica fume. *Mater. Des.* **2014**, *64*, 261–269. [CrossRef]
79. Van, V.-T.; Rößler, C.; Bui, D.-D.; Ludwig, H.-M. Mesoporous structure and pozzolanic reactivity of rice husk ash in cementitious system. *Constr. Build. Mater.* **2013**, *43*, 208–216. [CrossRef]

80. *ASTM C1202—19*; Standard Test Method for Electrical Indication of Concrete's Ability to Resist Chloride Ion Penetration. ASTM International: West Conshohocken, PA, USA, 2019; p. 8.
81. Bjegović, D.; Serdar, M.; Oslaković, I.S.; Jacobs, F.; Beushausen, H.; Andrade, C.; Monteiro, A.V.; Paulini, P.; Nanukuttan, S. Test methods for concrete durability indicators. In *Performance-Based Specifications and Control of Concrete Durability: State-of-the-Art Report RILEM TC 230-PSC*; Beushausen, H., Fernandez Luco, L., Eds.; Springer: Dordrecht, The Netherlands, 2016; pp. 51–105.

9 Curriculum Vitae

Name:	Abubakar Muhammad
Birth:	March 15, 1984 in Gombe, Nigeria

Education:

05/2005 – 09/2010	Abubakar Tafawa Balewa University Bauchi, Nigeria Graduated as *Bachelor of Technology* in Building Construction
05/2016 – 10/2018	Ahmadu Bello University Zaria, Nigeria Graduated as *Master of Science* in Construction Technology – with specialization in Concrete Structures

Work experience:

03/2011 – 12/2013	*Construction Site Engineer* at Lubell Nigerian limited
01/2014 – 12/2014	*University Building Officer* at Gombe State, Nigeria
01/2015 – 12/2019	*Lecturer* at Abubakar Tafawa Balewa University Bauchi, Nigeria

Journal Publications:

Muhammad, A., & Thienel, K. C. (2023). Properties of Self-Compacting Concrete Produced with Optimized Volumes of Calcined Clay and Rice Husk Ash—Emphasis on Rheology, Flowability Retention and Durability. *Materials*, *16*(16), 5513. (**https://doi.org/10.3390/ma16165513**)

Muhammad, A., Thienel, K. C., & Scherb, S. (2023). Calcined Clays from Nigeria—Properties and Performance of Supplementary Cementitious Materials Suitable for Producing Level 1 Concrete. *Materials*, *16*(7), 2684. **(https://doi.org/10.3390/ma16072684)**

Muhammad, A., Thienel, K. C., & Sposito, R. (2022). Suitability of Clinker Replacement by a Calcined Common Clay in Self-Consolidating Mortar—Impact on Rheology and Early Age Properties. *Minerals*, *12*(5), 625. (**https://doi.org/10.3390/min12050625**)

Mohammed, M., Shafiq, N., Al-Mekhlafi, A.B.A., Rashed, E.F., Khalil, M.H., Zawawi, N.A., **Muhammad, A.** and Sadis, A.M. (2022). The mediating role of policy-related factors in the relationship between practice of waste generation and sustainable construction waste minimisation: PLS-SEM. *Sustainability*, *14*(2), p.656. (**https://doi.org/10.3390/su14020656**)

Muhammad, A., Thienel, K. C., & Sposito, R. (2021). Suitability of blending rice husk ash and calcined clay for the production of self-compacting concrete: A review. *Materials*, *14*(21), 6252. (**https://doi.org/10.3390/ma14216252**)

Muhammad, A., Garba, M. M., Nafi'u, Z. A., & Mohammed, M. (2021). Mechanical Properties of Self-Compacting Concrete Subjected to Elevated Temperature. *International Journal of Integrated Engineering*, *13*(7), 119-127. (**https://publisher.uthm.edu.my/ojs/index.php/ijie/article/view/9535**)

Muhammad, A., Usman, N., & Gambo, N. (2020). Effect of binary blended pozzolanic materials on properties of self-compacting concrete. *International Journal of Construction Management*, *22*(7), 1323-1332. (**https://doi.org/10.1080/15623599.2019.1707500**)

Usman, N., **Abubakar, M**., & Ibrahim, M. A. (2016). Assessment of some key issues that affect the acceptance of Building Information Modelling (BIM). *ATBU Journal of Environmental Technology*, *9*(2), 40-52. (**https://www.ajol.info/index.php/atbu/article/view**

/150300)

Conference publications:

Muhammad, A., and Thienel, K. C. (2022). Performance of calcined common clay as partial replacement to cement in self-compacting concrete. International conference on calcined clay for sustainable concrete. (**https://www.researchgate.net/publication/362067185**)

Abubakar, M. and Usman, N. (2018): Influence of Rice Husk Ash on Properties of Self Compacting Concrete. Proceedings of NBRRI International Conf. on Sustainable Development Goal and Nigerian Construction Industry. **ISBN 978-978-521-470-3**

Abubakar, M. and Usman, M. Nafi'u and M. Sha'aya'u (2018): Suitability of Soaked Sesame Leaf Extract (Sesamum Indicum) As Stabilizer in Concrete Production. Proceedings of NBRRI International Conf. on Sustainable Development Goal and Nigerian Construction Industry. **ISBN 978-978-521-470-3**